Technical Note of the National Research Institute for Earth Science and Disaster Prevention, No. 204 ; March, 2000

An Anomalous Electric Field Variation Associated with the Seismic Swarm (1)

—Underground Electric Field Observation at Hodaka Station— (1993-1999)

By

Kozo TAKAHASHI*, Yukio FUJINAWA, Takumi MATSUMOTO**, Takeshi NAKAYAMA***, Toyoaki SAWADA***, Hideo SAKAI**** and Hiroshi IITAKA*****

Commucations Research Laboratory

**National Research Institute for Earth Science and Disaster Prevention*

***Disaster Prevention Research Institute, Kyoto University*

****Toyama University*

*****Electrotechnical Laboratory*

Abstract

Electric field observation data at Hodaka, near Mt. Yake in Gifu Prefecture in central Japan, has been conducted since 1994 in order to develop a method of detecting anomalous electromagnetic anomalies related to earthquakes and volcanic eruption occurrences. The ultra-long electrode measurement (ULEM) method was adopted by means of a very long electrode of approximately 400 m. Here the monitoring data acquired by the digital equipment are presented in order to provide basic data for assessment of the anomalous electric field phenomena detected at the time of the seismic swarm which occurred at the border of Gifu-Nagano Prefectures in August 1998. The anomaly is shown to be closely correlated with the seismic activity that occurred near the Hodaka site. It is suggested that the electromagnetic anomalies were induced by electro-kinetic effects through changes in the confined water pressure. This paper is one of a series of papers providing detailed evidence to show electric field changes are plausible precursors of earthquakes in terms of reproductivity and statistical relations. It is found that the anomalies is generally so small that they can be only detected using a special electrodes immersed deep in the ground near the source.

Key words: Earthquake prediction, Precursor, Evaluation, Electromagnetism

1. Introduction

One of the most dangerous natural hazards is induced by earthquakes, as recently experienced in Kobe in 1995, in both Turkey and Taiwan in 1999. In the case of the Kobe earthquake there were more than 6,500 victims and economic losses totaling several hundred billion US dollars. The impact of such a large earthquake could be reduced by appropriate counter measures. We already have example experience of earthquake-induced-disasters throughout the world and know what types of counter-measures are useful to reduce the disasters. We should continue to develop methods for disaster mitigation using the resources available in the community.

There are many phases in the efforts of disaster mitigation; broadly speaking, these can be divided into hardware and software responses. Hardware responses include risk assessment for the specific cause of a disaster in a particular area, increasing the resistive force of buildings and infrastructure, for instance, strengthening houses on the basis of the established building code, and predicting or forecasting when or with what frequency specific large-scale natural phenomenon might occur. Software responses include land use plans, preparedness programs, public awareness campaigns, and insurance disaster diffusion and so on (White and Haas, 1975). Accordingly, we need to develop a well-balanced system of disaster mitigation in any given community.

The types of counter-measures to be implemented

and the percentage of total expenses which will be allocated are decided on the governmental level. In the course of the decision-making process, however, the scientific community can provide important suggestions based on scientific knowledge. The scientific community is expected to propose new techniques to mitigate disasters as well as to develop the necessary resources to realize them. Earthquake prediction is one of the important factors in earthquake disaster mitigation, although appropriate techniques have yet to be sufficiently developed. If the community reaches the conclusion that a particular approach is impossible, it is important to tell the truth to the community (Geller, 1996). If communities conclude any technique, for example, earthquake prediction, has not been fully developed, but needs further research such as the SES signals of VAN group (Varotsos *et al.*, 1996, Park *et al.*, 1993), it is also important to state that a method is not intrinsically impossible. We believe that the feasibility study on the earthquake prediction research should be further conducted.

Definition of Earthquake Prediction

Earthquake prediction is generally assumed to be concerned with the estimation of the parameters for future earthquake sources: their location, time and size (Allen, 1982). The ultimate goal of the prediction method is to be quantitative. More accurate information is assumed to be more useful. The quantitative approach deals with definite statements of parameters with narrow and well-defined error boundaries (Wood and Gutenburg, 1935), and to be above the level of random chance or of a time independent seismic hazard (Main, 1996). The approaches can further be divided into one based on a physical model and one based on an empirical approach.

The research on the earthquake prediction should follow several steps from model formulation to testing (Rhoades and Evison, 1989). The procedures contain learning steps, which more or less involve the subjective selection of precursory candidates. And the primary objective of the testing is to evaluate performance of the proposed method. In the course of developing of the prediction technique, we should use up-to-date knowledge concerning the physical process in the preparatory stage of earthquake occurrence. Any reliable knowledge concerning the preparatory stage is more or less useful in the development of counter-measures against possible hazards, for example, to the hazard assessment and to the possible development of forecasting technology. We will be well rewarded by any well-organized investigation to establish an earthquake prediction method even if it may take a long time without resulting in significant success in the prediction.

There have been several reports from China on practical success in the earthquake prediction including public announcements to recommend the evacuation of several hundreds thousands of people. These reported successes in China are said to have relied on an empirical approach utilizing various anomalous phenomena inferred by experienced scientists. It could neither have been possible for the involved persons to infer on the basis of strict quantitative knowledge of the probability relations between earthquakes and precursory phenomena nor on well-founded physical model.

From those experiences we can build a strategy for the earthquake prediction. At this stage of development we need to take a practical standpoint as to the usefulness of the empirical approach. Under the situation of impossibility of programmed application of counter-measures such as evacuation based on a highly reliable forecast (Wood and Gutenberg, 1935; Main, 1997), ambiguous information about the possibility of earthquake occurrence should be properly used. These prediction information could be utilized by some (not whole) part of the community on their own responsibility. Flexible and practical attitude is necessary to make a decision in which direction the research and development in the earthquake disaster mitigation is to be conducted. It is necessary for scientific community to publish all types of data and interpretation concerning crustal activities for more fruitful discussion in the community.

Present Status of Earthquake Prediction

As a part of earthquake prediction program in Japan a systematic research effort was started from the Blue Print in the 1960's (e. g., Geller, 1991, 1996). The seventh five-year research plan aimed at the development of prediction technology has been underway in Japan since 1994. No earthquakes have been officially predicted in this time period of the previous three decades. But a large volume of data have been collected by the earthquake prediction community, and analyzed with the results of extensive progress in the research on crustal activities (e. g., Hamada, 1991). The progress of the research on seismic activities and seismo-tectonics is so substantial as to provide profound knowledge on the preparatory stage of earthquake occurrence. But it should be noted that these data have not been collected and fully analyzed for the purpose of second-stage earthquake prediction

research, as proposed by Rhoades and Evison (1989)

A compilation of observation of earthquake precursory phenomena have indicated that there are approximately 15 more or less independent phenomena, including seismic activity, ground water level change, radon content, electromagnetic phenomena and so on (Rikitake, 1976). Analysis of those precursory phenomena suggests several general properties, for instance, the relation between the preceding time and the magnitude of earthquakes indicating a log-linear relationship for the so-called first type precursors and another relationship for the second type of precursors (Rikitake, 1976). The Rikitake relationship might suggest the existence of meaningful precursors, though none of the claimed precursors has passed the strict guidelines of the IASPEI subcommittee to be approved as a precursor (Wyss, 1991). The Rikitake relationship was not based on the established criterion of anomalous phenomena, but relied on the subjective judgement of individual scientists. Despite this ambiguity, the knowledge would be useful at least in the estimation of the occurrence time and the magnitude of future earthquakes if the large confidence limit is taken into account.

The claimed precursors have been assessed by the IASPEI subcommittee (Wyss, 1991 ; Wyss and Booth, 1997) in an issue for the International Decade for International Disaster Reduction (IDNDR) for the sake of more objective evaluation. The evaluation was performed using a kind of the so-called passive assessment on the submitted reports of individual groups following the proposed guidelines, because of the difficulty of independent verification on the claimed precursory phenomena at the time of strong earthquakes.

The IASPEI evaluation is a major milestone in the development of earthquake prediction technology because it proposes an example of guidelines for the evaluation of the claimed precursor, and the efforts could contribute to establishing a consensus for the quantitative evaluation procedure. Evaluation procedures such as this, however, would not be particularly useful outside the scientific community. Because of the adopted way of the peer review using only submitted materials, it would be difficult to provide confirmative output. In order for the result to be accepted independent experimentations on the phenomenon seems indispensable.

We should stress here the necessity of an evaluation of precursors through more systematic research and development, as proposed by Rhoades and Evison (1989). In particular, an objective experimentation should be included in the evaluation program to ascertain the intrinsic relationship of plausible precursory phenomena. Experiments should be conducted by several independent groups for verification. Any assessment without such verification would be insufficient to answer the serious question as to the possibility of the earthquake prediction. Small scientific group could find plausible phenomena and choose some useful characteristics. However, a formulation model of the prediction (Rhoades and Evison, 1989) can only be condstructed with systematic efforts, which will require a considerable amount of resources.

Here we will present an trial of evaluation of precursory phenomena by taking electromagnetic field changes as an example. In many electric, magnetic and electromagnetic phenomena that are seemingly useful to earthquake prediction (Park *et al.*, 1993), the ULF, the VLF band signals have been reported before major earthquakes (Gokhberg *et al.*, 1987 ; Oike and Yamada, 1994 ; Yamada and Oike, 1996, Fujinawa and Takahashi, 1998). We have been investigating electromagnetic field changes focusing on the search for useful phenomena for the prediction as well as their efficient characteristics (Fujinawa and Takahashi, 1990, 1996, 1998 ; Fujinawa *et al.*, 1997). In the course of the evaluation, the guidelines of IASPEI (Wyss, 1991) have been taken into account as far as possible.

2. Measurement Method

The construction of electromagnetic field observation stations in central Japan has been underway since 1988, and now ten observation sites are in operation (Fig. 1). The borehole antenna (Fujinawa and Takahashi, 1990) is used to measure the vertical electric field by means of a casing pipe in deep boreholes on the basis of the original idea of Takahashi and Takahashi (1989) (Fig. 2). The so-called borehole antenna has been proved to be very efficient for detecting small signals possibly related with earthquakes induced underground even in the circumstance of large urban noise (Fujinawa *et al.*, 1992, Fujinawa and Takahashi, 1996). The steel casing pipe functions as a monopole of the antenna in the conductive substance, and the copper wire buried underground surrounding the casing pipe as the reflector of the antenna. The antenna, using a very long vertical casing pipe in the borehole, senses the vertical components of underground electric fields. In the low frequency limit, the borehole can be taken as an ultra-long electrode (ULE) immersed in the earth (Fig. 3). The input voltage V_i in the detector can be expressed as the weighted average of

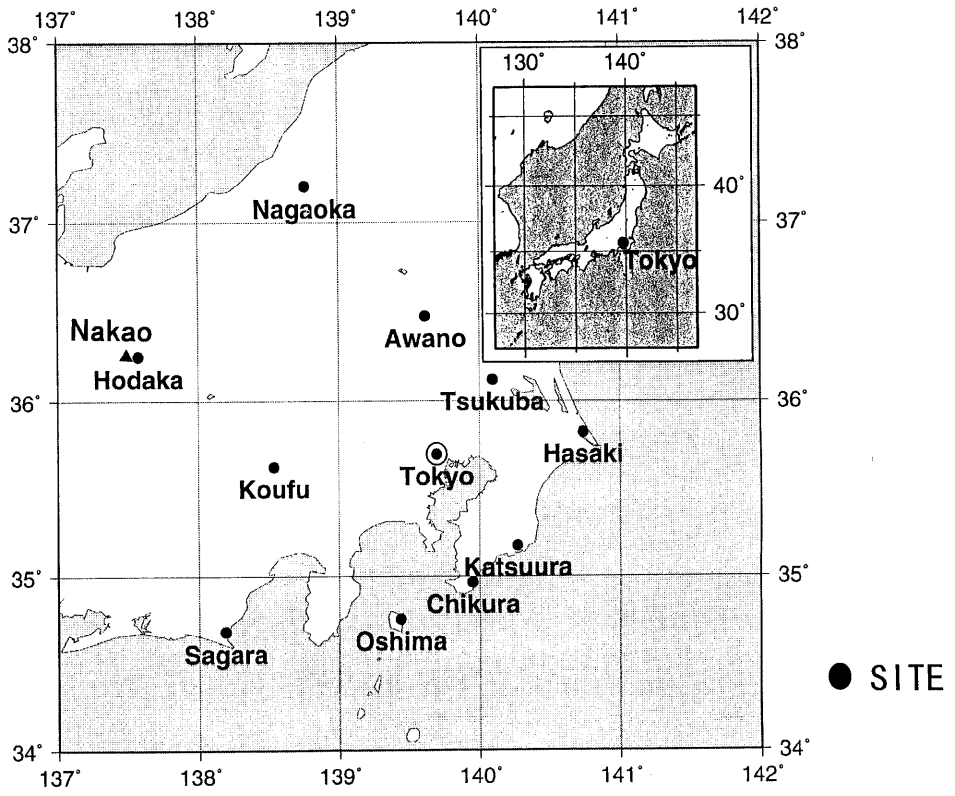

Fig. 1 Locations of the electro-magnetic field observation sites in central Japan utilizing borehole antenna 150-1200 m long as the principal sensor. For the horizontal component of the electric field mutually perpendicular short dipoles of 20~60 m long were used together with induction type magnetometers for the five sites (Hasaki, Chikura, Koufu, Nagaoka and Sagara). The network has been in operation since 1988, and the sites were selected on the basis of several geological conditions. Specifically, Hodaka and Oshima are in a geothermal region with volcanos.

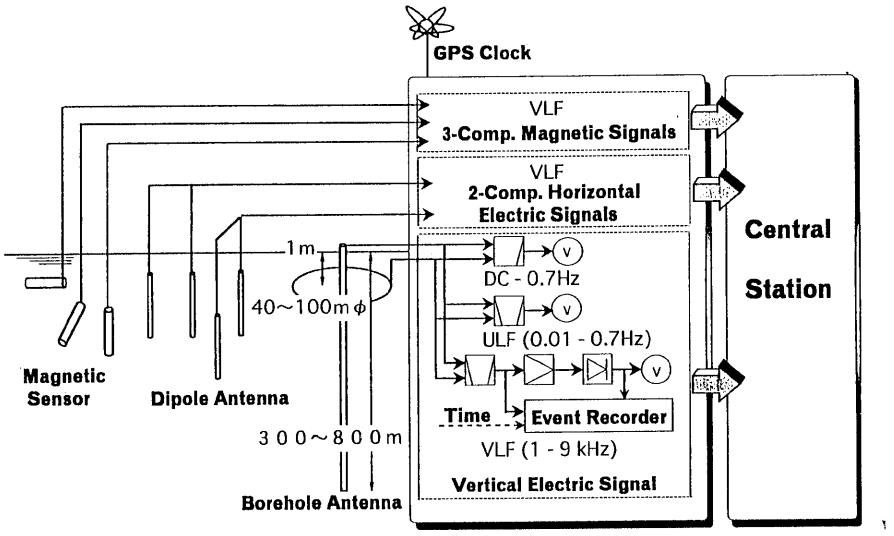

Fig. 2 Schematic diagram of multiple component electromagnetic field observations. The electric field is measured by a pair of horizontal dipoles of 8 m in length with a span of 20~50 m and using a vertical mono-pole of 300-800 m surrounded by wire with a radius about 10-20 m buried at a depth of about 1 m. The magnetic field is measured by three induction-type magnetometers (BF-6, EMI) installed perpendicularly to each other. Triggered data in three electrical and magnetic fields component are transmitted to a central station once a night.

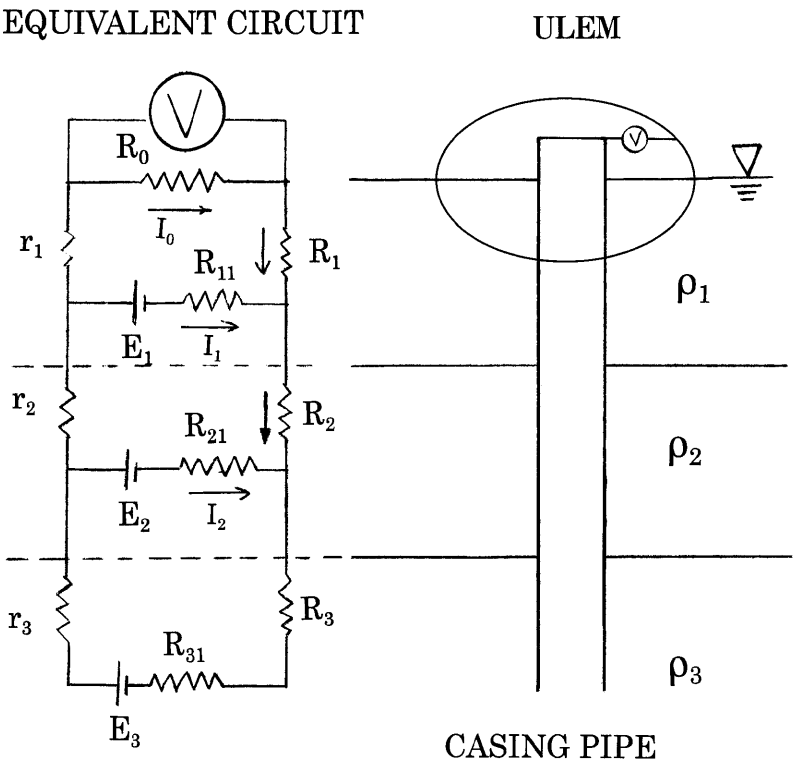

Fig. 3 Equivalent circuit of the ULEM for the dc component

potential along the casing pipe,

$$V_i = \sum a_i E_i$$

where E_i is potential at the i-th layer. The coefficient a_i is expressed by the resistivity of each layer R_i and of the casing pipe r_i. For instance, if there is an electric field change in a certain layer in contact with the pipe, the change can be sensed by the sensor system. Any electric field change along the pipe can be easily detected by this tensor. However it is difficult to ascertain the layer at which the change is occurring. This type of measurement (ULEM : Ultra Long Electrical Measurement) has been shown to be a highly efficient method for detecting underground anomalous signal under the situation of large urban noises (Fujinawa and Takahashi, 1996).

We selected three specific frequency bands : the dc (dc~0.7 Hz), the ULF (0.01~0.7Hz), and the ELF/VLF (1kHz~9kHz) for our observation (Fujinawa and Takahashi, 1990 ; Fujinawa *et al.*, 1992). These frequency bands were selected in consideration of regulations governing radio frequency in Japan, and reported anomalous changes (e. g. Gokhberg *et al.*, 1987 ; Park *et al.*, 1993 ; Popov *et al.*, 1989 ; Parrot *et al.*, 1993).

Raw signals have been recorded for the dc and the ULF bands, and an envelope of the amplitude for the ELF/VLF bands using strip-chart on sites. A few years after the initial stage of the development of the system, digitized data for those signals were also transmitted to Tsukuba, central station (Fig. 1). At Hodaka the observation started in October 1994, and digital equipment was supplemented in January 1995. In this report all digitized data at Hodaka are used.

The five sites in the network were additionally equipped with the waveform recording system for the ELF/VLF bands signals with a sampling interval of 50 kHz (Fujinawa *et al.*, 1997 ; Fujinawa and Takahashi, 1998). At those sites time synchronization is accomplished to the level of 1μsec by using the GPS clock. The arrival time data of the pulse-like signals in the ELF/VLF bands enable us to determine the source position of the signals in the same way as the hypocenter determination in seismology (Fujinawa *et al.*, 1997). In this paper, however, we will predominantly use the field strength data because of the particular emphasis investigating anomalous signals at the time of seismic activity.

Fig. 4 shows a schematic map for the observation site at Hodaka situated in Nakao about 4 km west of Mt. Yake. The site is in a geothermal zone, which is the location of a famous resort, "Kamikouchi" having many hot springs. The antenna configuration is shown in Fig. 4-2. The borehole, approximately 400 m in length, is used to gather hot water vapor. The surrounding copper wires are buried in the cedar

HOT SPRINGS AROUND MT. YAKE

⑤源　泉

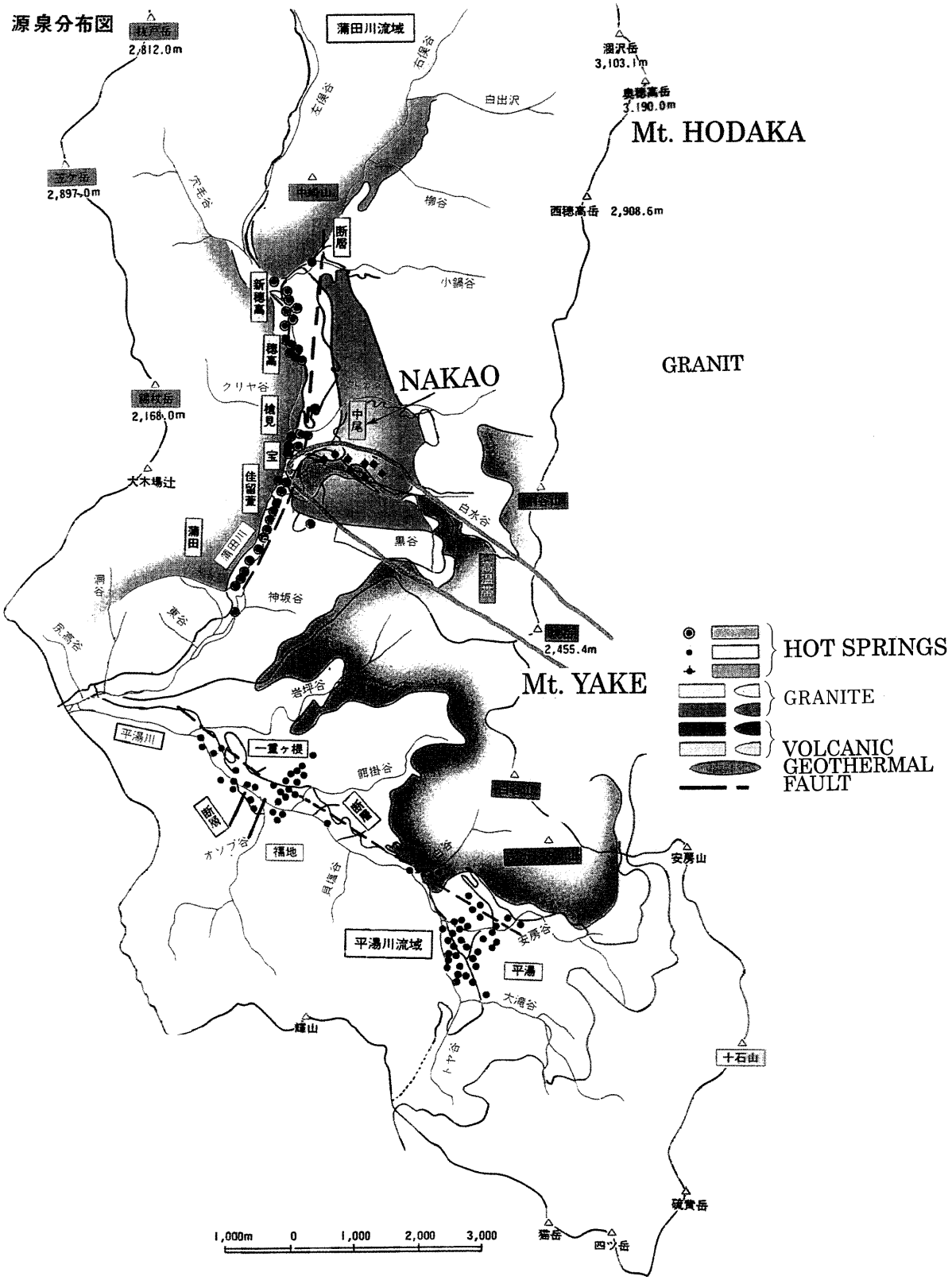

Fig. 4-1 Map around the observation site at Hodaka. The site Hodaka is about 4 km west of Mt. Yake, one of the active volcanoes in central Japan.

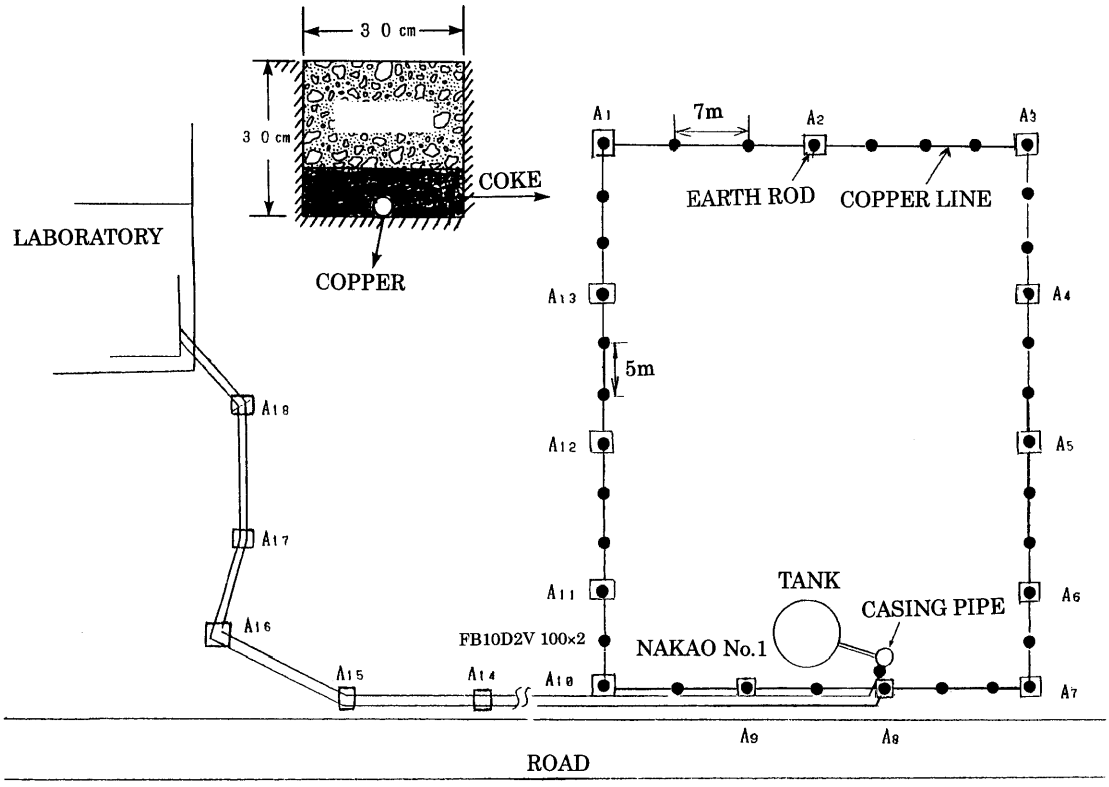

Fig. 4-2 Schematic diagram of the ultra-long electrode measurement (ULEM) at Hodaka.

Fig. 4-3 A casing pipe (right of the tank) of 400m leingth for taking water vapor is used as a monopole of ULEM (see also Fig. 4-2).

forest. The wire was in the midst of coke on the bottom of ditch as is seen in Fig. 4-2. And the wire was attached by an earth rod 3 m long every 7 m. The borehole is not in the center of the reflector because of an official road near the borehole.

Fig. 4-3 shows the water tank and part of the casing pipe appeared on the ground. The signal transmitting cable was buried beside the road, and electrical equipment is housed in a laboratory at the Hodaka Sedimentation Observatory, Disaster Prevention Research Institute of Kyoto University. Electrical resistivity R_0 between the borehole and surrounding wires is 55Ω. The site is relatively calm in terms of urban noises, as it is located in a mountainous area with a small population at a distance of about 30 km from the nearest railroad. However, noises were also generated in resort hotels, and the noise level was not constant. For instance, circumstantial noise changed from February 1997 in the ELF/VLF bands inducing nearly constant amplitude noises continuing for several hours, probably due to an air-conditioner installed nearby.

3. Observation

Except for an occasional trouble of electrical equipments caused by severe lightning strikes the systems have been continuously providing high-quality data. The system has been progressively refined to reduce malfunctions due to lightning. Calibration has been conducted nearly every 6 weeks since the installation of the system. The calibration includes input impedance for the antenna and amplification factors. The input inpedance is found to be highly constant. The paper recording chart is changed at the time of calibration. Strip chart recording has been used in order to produce back-up data. Even if it is not convenient for quantitative analysis, the analog recording has its own merits such as a fine resolving power. Accordingly this type of recording has been continuing.

4. Typical Pattern of Record

4.1 Normal State

The recording parameters are determined after an experimental observational period of about one month so as that the background noise level for the dc channel is almost a flatline, and about one-tenth of saturation level for the ULF and the ELF/VLF bands in the monitoring record.

An example of a record of a normal state is shown in Fig. 5 for 5 August 1998, which is two days before the start of the seismic swarm. The swarm occurred near the site Hodaka in 1998, as will be described in more detail later. The noise level for each frequency band is :

$$N_{dc} \sim 0.1 \text{ mV}$$
$$N_{ULF} \sim 0.1 \text{ mV}$$
$$N_{VLF} \sim 0.7 \text{ mV}$$

The noise levels for the dc and the VLF band have remained virtually constant since the beginning of the observations. But the background noise level of the VLF component has increased abruptly since February 1997, as can be seen from the Figures in the Appendix. Before the increase the noise level was about 0.2 mV in the ELF/VLF bands. The contaminated noise in the ELF/VLF bands is almost constant amplitude for a while. Detection of anomalies has not been difficult because of the property of the noise.

4.2 Noise Pattern at the Time of Lightning Discharge

At the time of a lightning return stroke a strong surge current flows underground generally causing large signals in the record. An example of the record at the time of lightning discharges is shown in Fig. 6. The large input voltage occasionally causes the destruction of electronic instruments. The "noises" induced by the lightning discharges have general features in terms of duration of a few hours, and the evolution of amplitude change, as is illustrated in Fig. 6.

Consequently, it is not difficult to determine whether or not the signals are related to atmospheric discharge. Smaller amplitude VLF signals of inter-cloud discharge and remote return stroke which comprise a large part of signals in the ELF/VLF bands (Fujinawa *et al.*, 1997) are almost buried in the background noise level. And those do not appear in either the ULF or the dc bands.

4.3 Noise Associated with Geomagnetic Disturbances

Even very large geo magnetic disturbances appear only slightly in the monitoring records in our choice of recording parameters for the ULEM. The extent of the effect of geomagnetic disturbances can be seen in Fig. 7. Electric field changes at around 16:30 on 6 August 1998 corresponded to severe geomagnetic disturbances amounting to some 200 nT. The induced variations of the electric field signals in the dc, the ULF, the ELF/VLF records were negligibly small : 0.2 mV for the ULF band (Fujinawa *et al.*, 2000b).

So the geomagnetic effects on these measurements did not appear to be large. But we need to take the

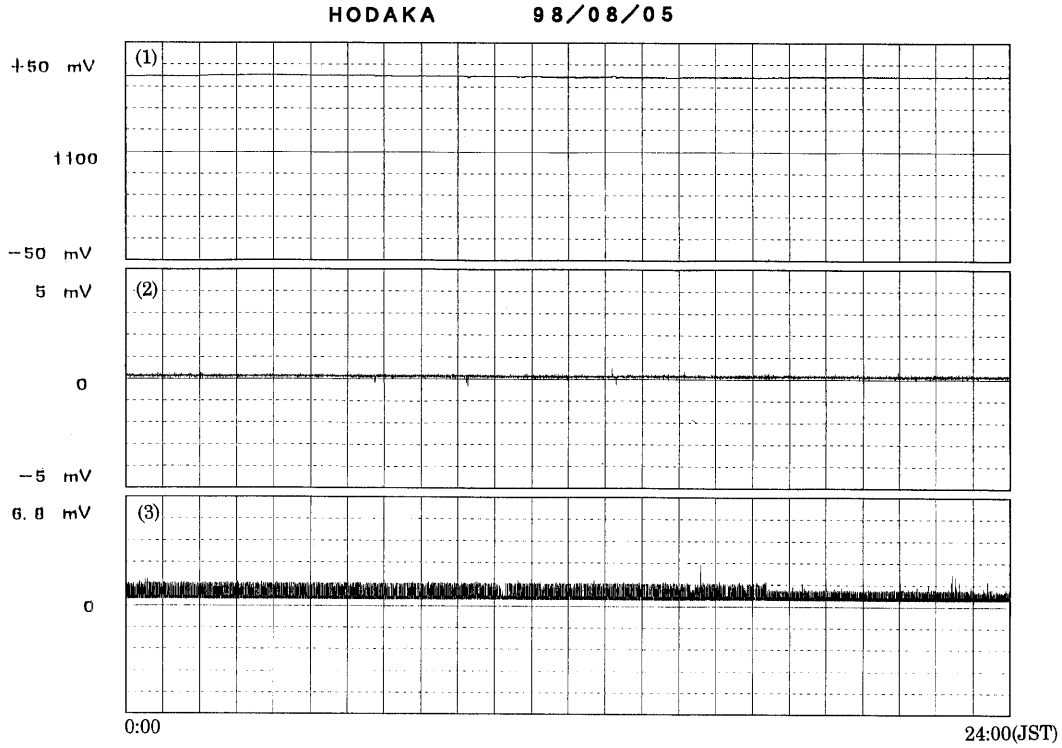

Fig. 5 An example of monitoring records at a normal state of the vertical electric field observation on 5 August 1998 at Hodaka. The dc component has an almost flat curve for the selected recording parameters of the dc (0～0.7 Hz, upper) and less than 1/50 in full scale in the ULF band (0.01～0.7 Hz, middle) showing waveforms, and 1/20 in the ELF/VLF bands (1～kHz 9kHz, lower) showing an amplitude envelope. Almost constant level signals of about 1 mV in the ELF/VLF channels (lower) are due to urban noises with background noise evident from December 1997.

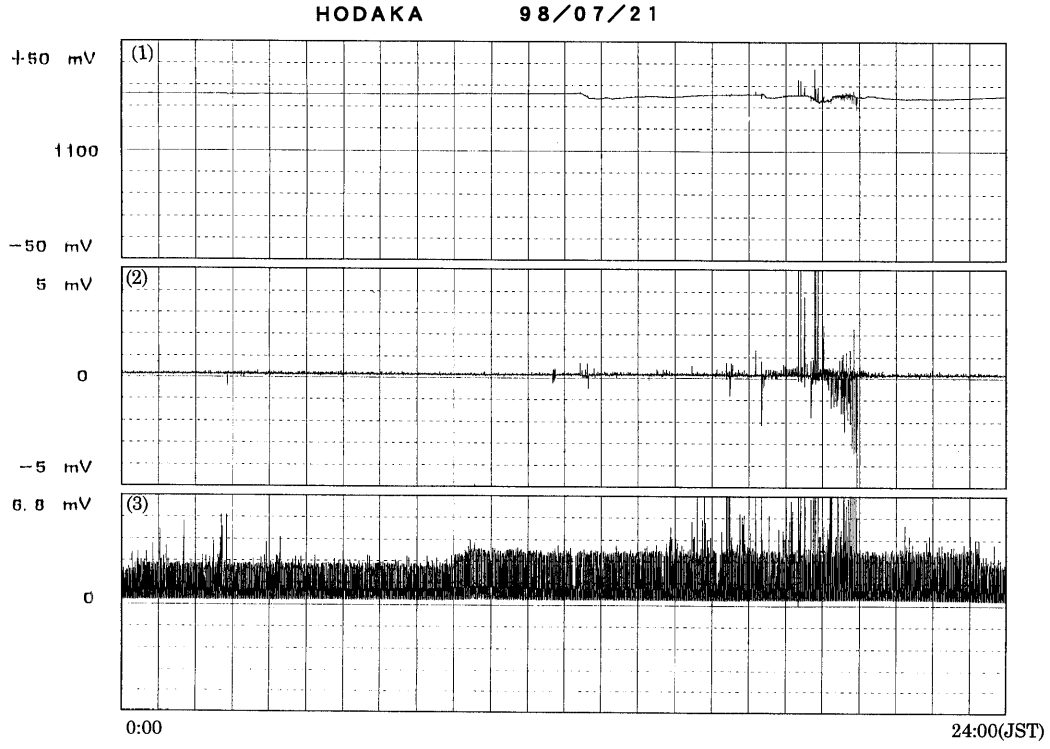

Fig. 6 Typical examples of records at the time of severe lightning discharge at around 18 : 00 ～20 : 00.

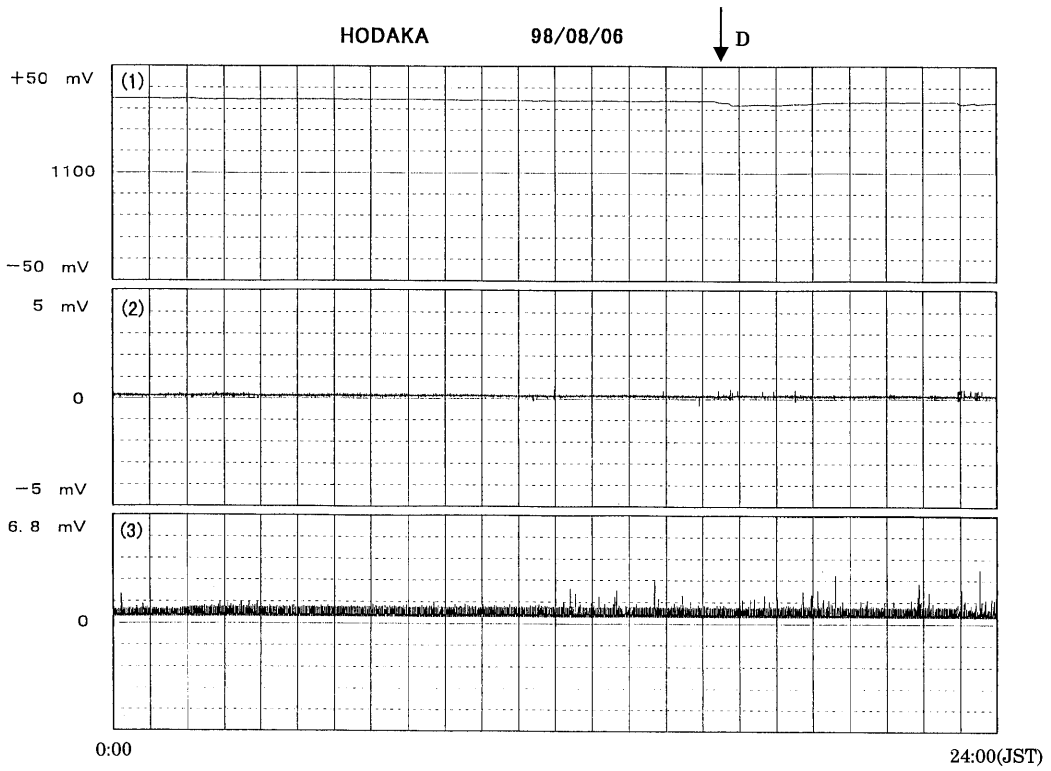

Fig. 7 An example of ULEM records at the time of strong geomagnetic disturbances amounting to 200 nT at around 16 : 30 (D in the Figue).

geomagnetic data for reference into account when we check anomalous signals of similar duration as of geomagnetic disturbances in the effect to identifying precursory phenomena.

5. Prominent Anomalies

5.1 Vapor Ejection in 1996

Sudden and sharp increases in electric field strength were detected preceding a vapor ejection on 14 July 1996. The ejection occurred in the course of drilling a hole for another hot spring about 400 m north of the Hodaka site (photo. 1). An abnormal increase in the electric field started about three hours before the onset of the vapor ejection (Nakayama *et al.*, 1997). The increase was detected at dc-0.7 Hz and 1-9 kHz frequency bands with the vertical electrodes, and at dc -0.7 Hz band by the horizontal electrodes belonging to Kyoto University. The perpendicular horizontal fields were measured with the four electrodes consisting of vertical lead pipes. Each pipe was 2 cm in diameter, and the underground length is 50 cm. Both pairs of N -S electrodes and E-W electrodes had spaces of 50 m between their electrodes. The horizontal fields were measured at the dc-0.7 Hz frequency band only.

The ejection started at about 16 JST (Japan Standard Time), that is equivalent to 7 UT, 14 July 1996, at the foot of Mt. Yake. Mt. Yake been dormant for 34

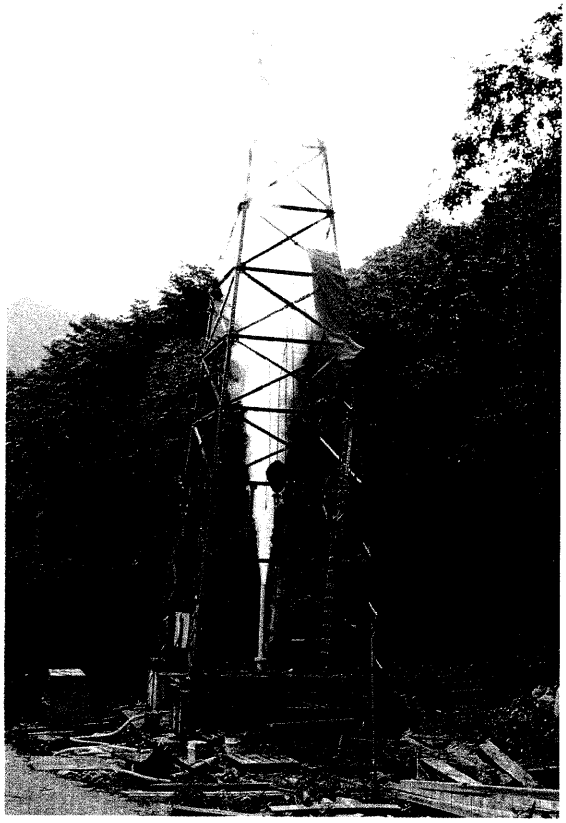

Photo 1 Vapor ejection on 22 July 1996 from the borehole in the course of searching for hot water to be used for hot spring.

years since the last ejection in 1962. Photo 1 shows the vapor ejection from the borehole. There was no particular increase of seismicity around the event as seen later (Fig. 14-1).

Figure 8 shows the records for vertical electric fields at the dc~0.7 Hz, 0.01-0.7 H, and 1-9 kHz bands, together with the records of horizontal fields at dc-0.7 Hz on 14 July when the vapor ejection started. Anomalous signals are seen in the three whole bands in the ULEM, and in the dc channels in the horizontal electrode. Higher frequency components of the ULF band are observed only the ULEM. The ELF/VLF band anomalies were seen to appear intermittently as in the case of the submarine volcanic ejection east of the Izu-peninsula in 1989 (Fujinawa and Takahashi, 1990).

Figure 9 and Figure 10 show the records for vertical electric fields at dc-0.7 Hz, 0.01-0.7 Hz, and 1-9 kHz bands, one day before and two days after the onset of the ejection, respectively, for the sake of contrasting the anomalous signals shown in Fig. 8. Figure 10 shows a part of Fig. 8 with an expanded time axis with the center of the figure being located at the onset time for the ejection. The records for horizontal electric fields show small variations during these days as shown in Fig. 8 and Fig. 11.

Here we can compare anomalous signal strength detected by the vertical electrode with that by the horizontal electrodes using the records shown in Fig. 8 and Fig. 11. The vertical component in the dc band indicates a decrease of about 2 mV (casing pipe potential increases) and an increase of about 1 mV in the horizontal component. Larger fluctuations in horizontal (NS, EW) and vertical (dc, VLF) components are found to correspond closely with each other. A prominent fluctuation starting at about 12:50 (IST) on July 14 1996, was recorded as 1.3 mV in NS, and about 2.5 mV in the dc band of the vertical electrode. As a

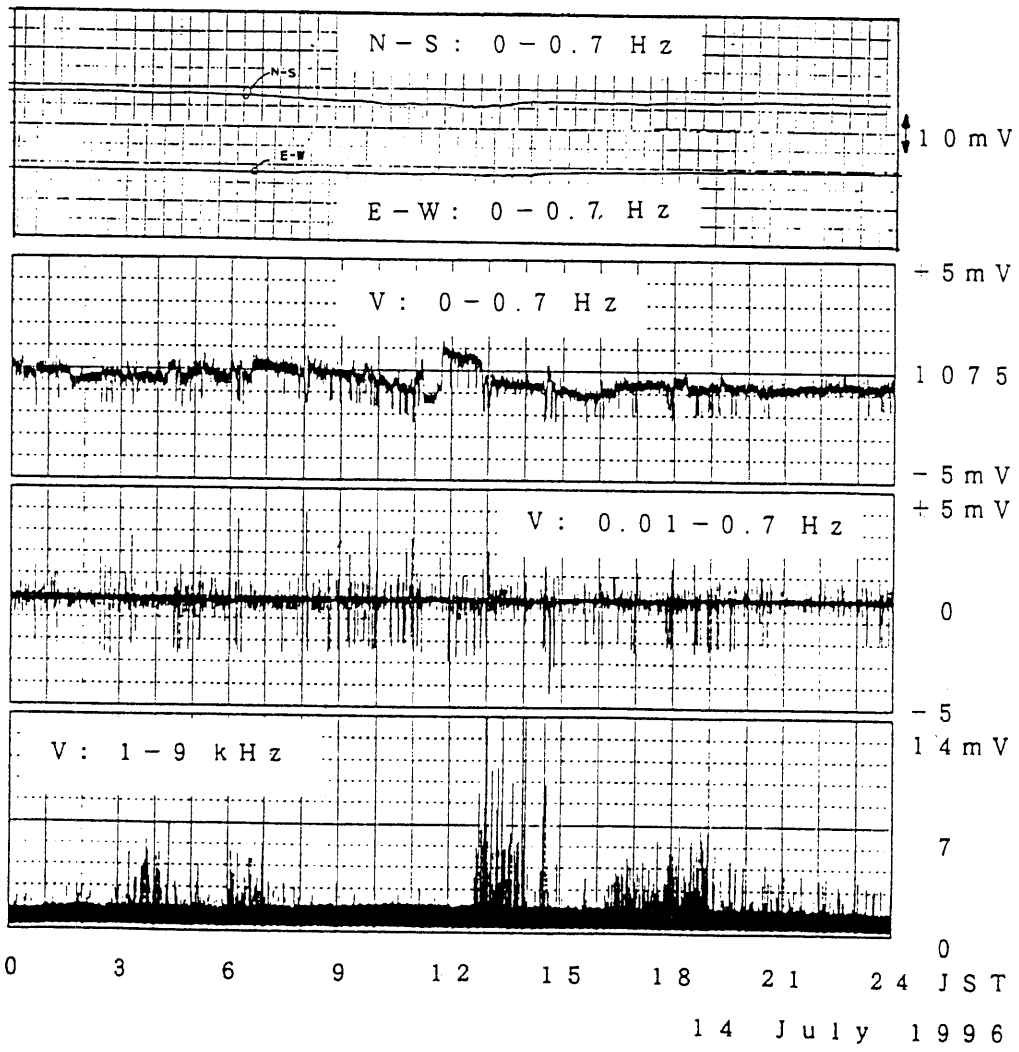

Fig. 8 Records of vertical electric fields at the DC-0.7 Hz, 0.01-0.7 Hz, and 1-9 kHz bands, and of horizontal fields at the DC-0.7 Hz band, on 14 July 1996, the day of the vapor eruption.

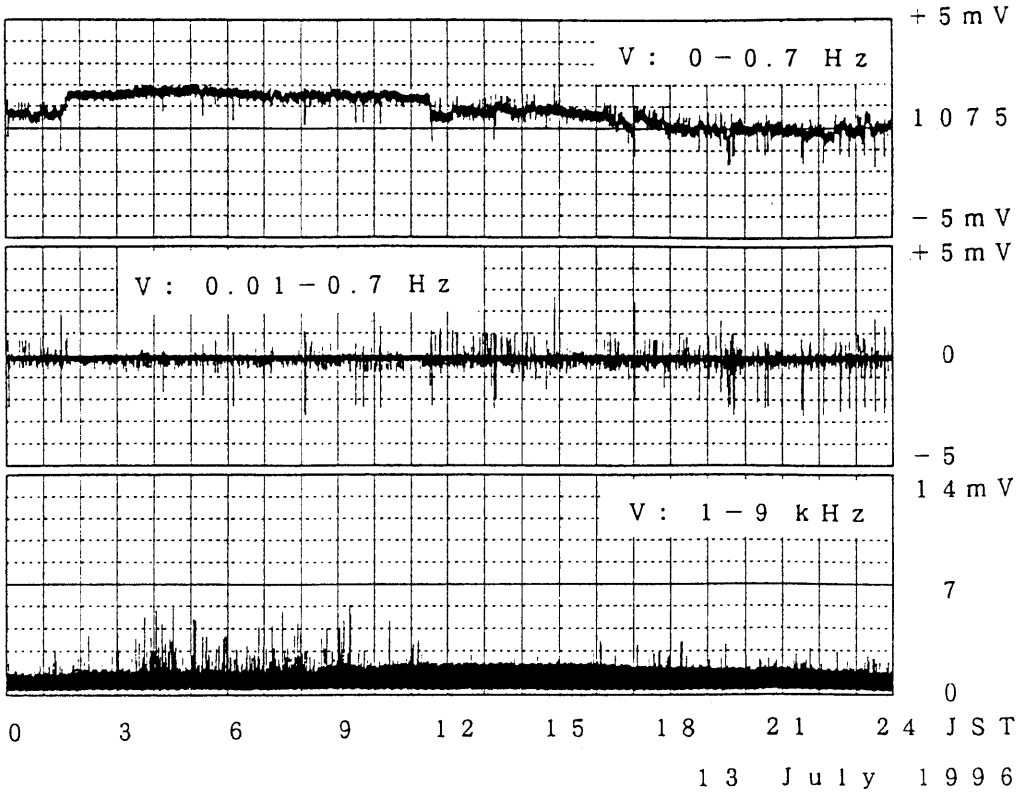

Fig. 9 Records of vertical electric field obsevation be ULEM, on 13 July 1996 (JST), one day before the onset of the vapor eruption.

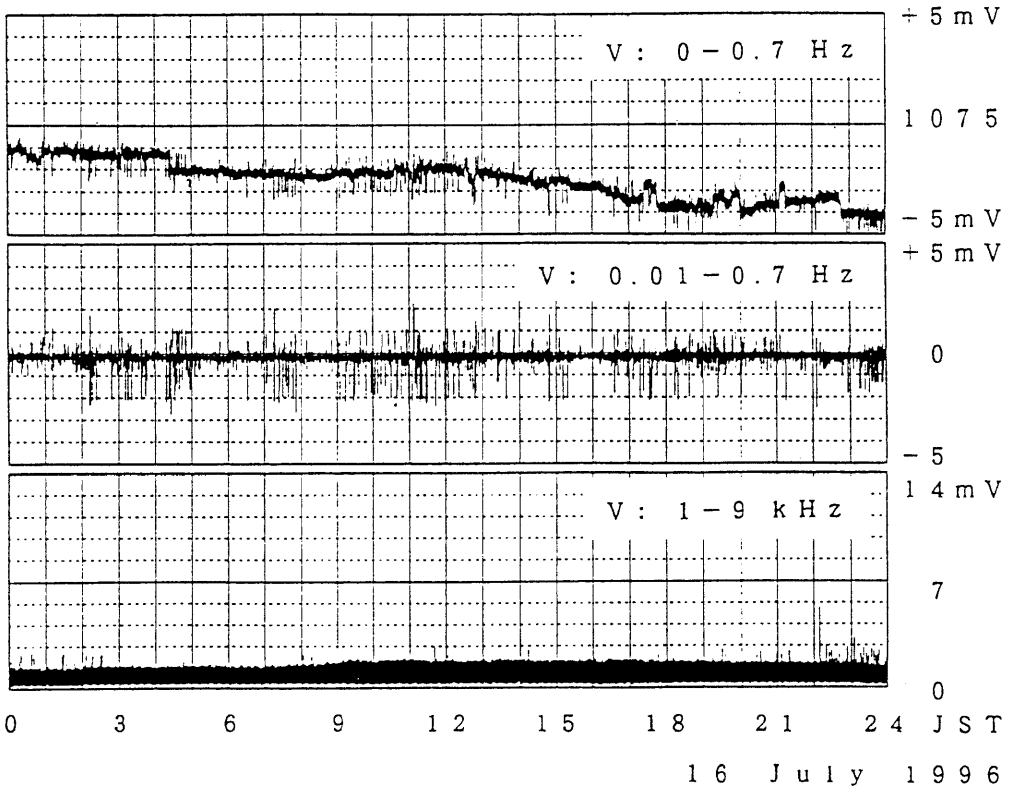

Fig. 10 Records of vertical field obsevation be ULEM, on 16 July 1996, two day after the onset of the vapor ejection. They are very similar to typical records on usual days.

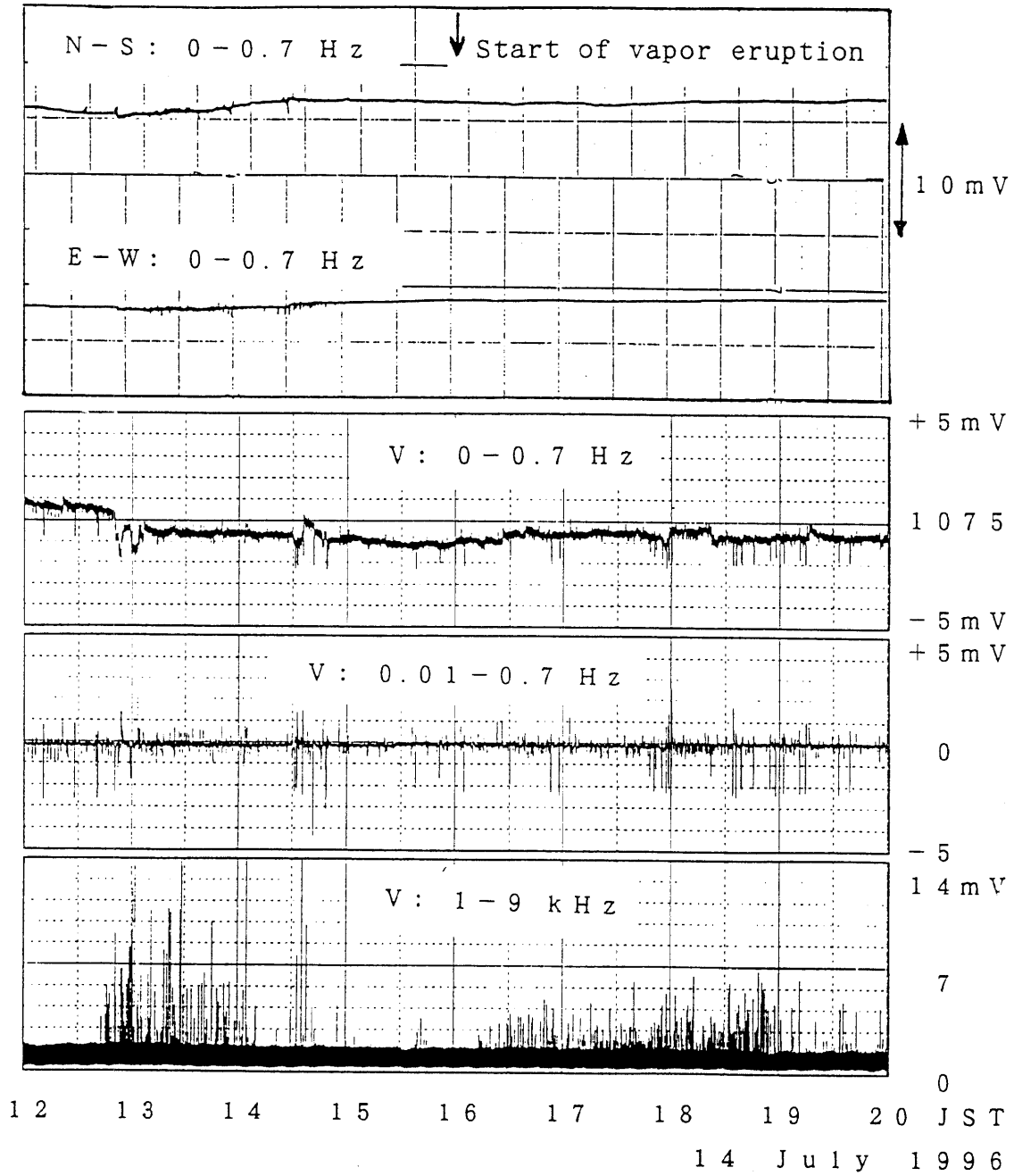

Fig. 11 Records of vertical electric fields at the DC-0.7 Hz, 0.01-0.7 Hz, and 1-9 kHz bands, and of horizontal fields at the DC-0.7 Hz band, on 14 July 1996, from four hours before to four hours after the onset of the vapor ejection.

matter of fact, the dc band anomaly could not have been detected in the monitoring records of ordinary full-scale(±50 mV), about 10 times larger compared with those shown in Fig. 9 and Fig. 10. Larger dynamic range in monitoning record is necessary.

Anomalies are more clearly seen in ULF bands, and most clearly in the ELF/ VLF bands. The extent of the anomaly can be seen from the monitored records (Fig. A-95-1-0～A-99-12-2). Here A-95-1-0, for instance, refers to the monitoring records for a month period for channel 0 (dc component) in January 1995. From Figures A-96-6-0～A-96-8-2 we can know that anomalies appeared from the beginning of June 1996 to the end of August in the ULF band. The dc component was very small, and ELF/VLF components were minimal.

The anomalies at 1-9 kHz on 14 July were larger than 14 mV, and such large anomalies belong to the most conspicuous signals in the record , except those for the seismic swarm in 1998 and for anomalies caused by lightning discharge near the observation site. The ELF/VLF bands became very anomalous at

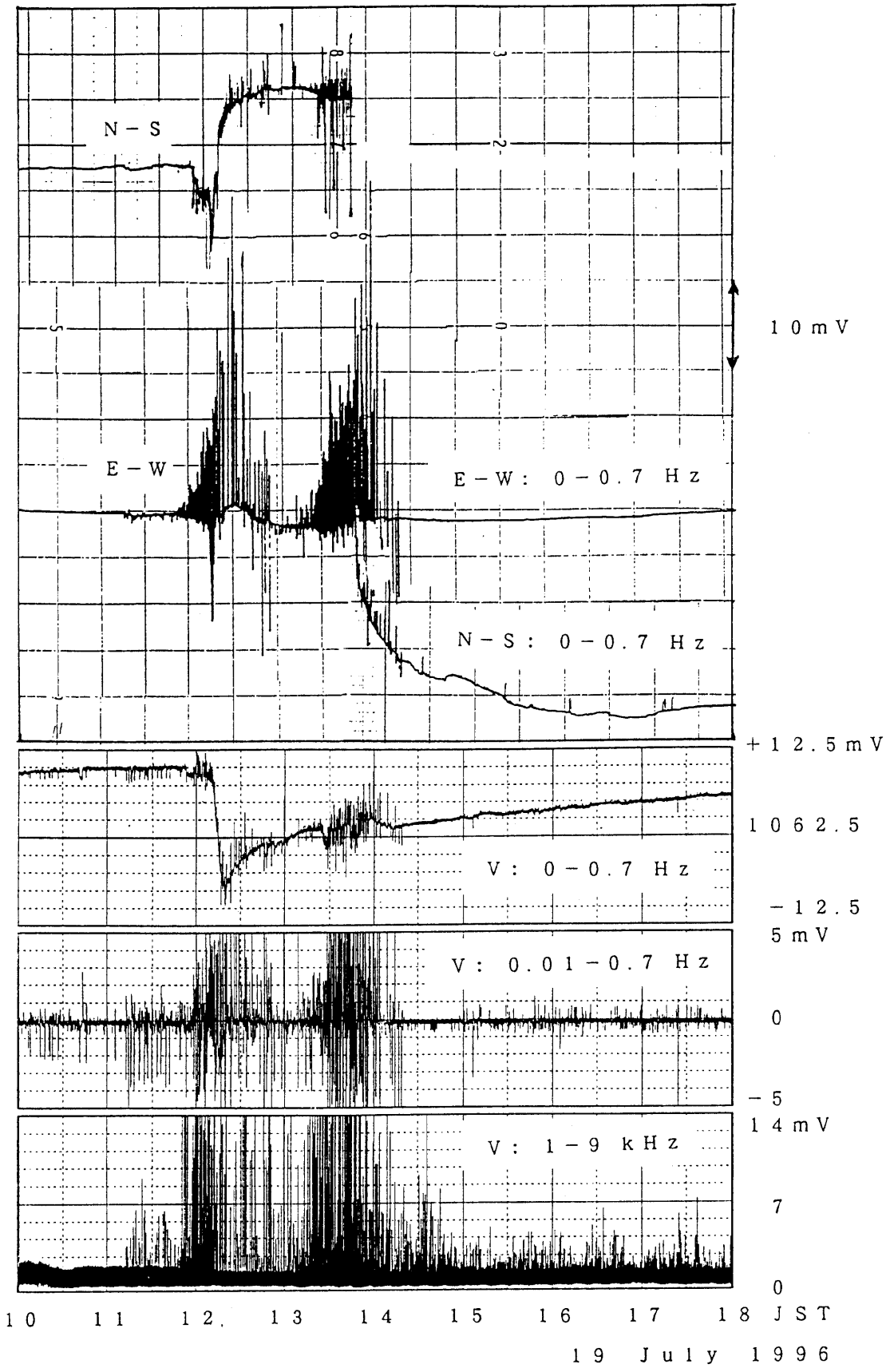

Fig. 12 Records during lightning discharges near the observation site.

about 12:40 some 10 minutes earlier than the ULF and dc bands (Fig. 11). From the example record at the time of lightning discharge, we can think that the anomalous electric signals were not induced by a lightning discharge.

Electric surge signals caused by lightning are shown in Fig. 12 to show the difference between anomalies preceding a vapor ejection and anomalies caused by lightning in the vicinity. The amplitudes of the signals are about 17 mV, >5 mV, and >14 mV in the dc, the ULF, and the VLF band in ULEM and 100 mV, 60 mV in the horizontal components, respectively, providing further evidence of the high performance level of the ULEM to reduce extreneous underground noises.

A larger vapor ejection occurred at Nakanoyu about 4 km south-east of Mt. Yake (Fig. 4-1) on 1 February 1995 causing several casualties. The eruption did not induce any discernible electric anomalies at the Hodaka site. The signal detectability difference will be touched in more detail later when the anomalies at the time of the seismic swarm in 1998 is disccussed.

5.2 Anomalies Associated with Seismic Swarm

(1) Summary of the sub-section

Anomalous signals were found to be in good correlation with the swarm activity that occurred in central Japan starting in August 1998. The anomaly is discriminated in terms of duration and field strength on the basis of almost continuous observational records from 1993. This second anomaly in the observation is far larger compared with the first anomaly detected in 1996 in relation witi the vaper ejection. Anomalies were found across all frequency bands of the dc, the ULF and the ELF/VLF bands in the adopted recording parameters with persistent occurrences in the dc and the ULF bands. But the ELF/VLF bands appeared to be anomalous only around the periods of huge anomalies in the dc and the ULF bands at the time of high seismic activities.

The anomalies were detected only at the nearest site from the swarm activity zone in all networks at a maximum distance of about 300 km (Figure 1). A sharp detectability difference of the anomaly responding to different seismic swarm activities can be attributed to the geological setting around the area. It is suggested that the sources of the anomalous electric signals are deep in the ground on the basis of measurements using electrodes at different depths. A prospective method for investigating and monitoring the preparatory stage of earthquakes and/or volcanic eruptions through an electromagnetic window is suggested from these results.

(2) Characteristics of Anomalies

A seismic swarm started on 7 August 1998 at the border between the Nagano and Gifu prefectures in central Japan (Fig. 13). Seismic activity around the observation site had been very calm since 1993 around the present swarm zone (Fig. 14). An exception is a slight and spotted activity in July 1997 and a small activity near Mt. Yake from July through December 1993 with the largest earthquake having magnitude of 4.5 (Fig. 14-3). The present activity took place several kilometers distant from one of the sites (Hodaka) of the observation network (Figure 1).

The present swarm activity zone moves in NS direction during the total evolution of the activity (Fig. 14-2). At the initial stage the swarm activity was limited to the area near the Mt. Yake several kilometers east of the Hodaka site (Fig. 13). Meanwhile the dominant activity moved to the northern region crossing a clear aseismic zone. The most active period was around the middle of August 1998 (Fig. 14-4). It continued till recently (April 1999).

The electric field records on typical days of the seismic swarm activity in the three frequency bands are shown in Fig. 15. We have already shown the monitoring record corresponding to the normal state on 5 August 1998, the day before the start of the swarm (Fig. 5). Fig. 15a shows records on 7 August when the seismic swarm started. Fig. 15b is the record from 12 August when the second largest earthquake in the swarm with magnitude of 4.1 occurred, and Fig. 15c is the record on 16 August when the largest earthquake with magnitude of 5.2 occurred. Electric field changes are seen to be anomalous on the day when the swarm started (Fig. 15a), and more clearly anomalous on the days of major earthquakes (Fig. 15b and Fig. 15c) in comparison with those at the normal state of almost flat record lines (Fig. 5) for chosen recording parameters.

A slight anomaly can be seen in the dc band (Fig. 15a), moderately clear anomalous signals on the ULF band, and a clear anomaly in the VLF band from about 12 hours before the occurrence of the first earthquake with magnitude of 3.9. Abrupt coseismic electric field changes at the exact time of the first earthquake occurrence are seen on the dc band, and on the ULF channel, but not in the ELF/VLF band. The coseismic changes in the dc and the ULF bands were induced by the seismic ground movement in association with the arrival of seismic waves (Fujinawa and Takahashi, 1998; Nakayama *et al.*, 1998).

A co-fracturing pulse-like signal in the ELF/VLF bands is suggested at the time of the second largest

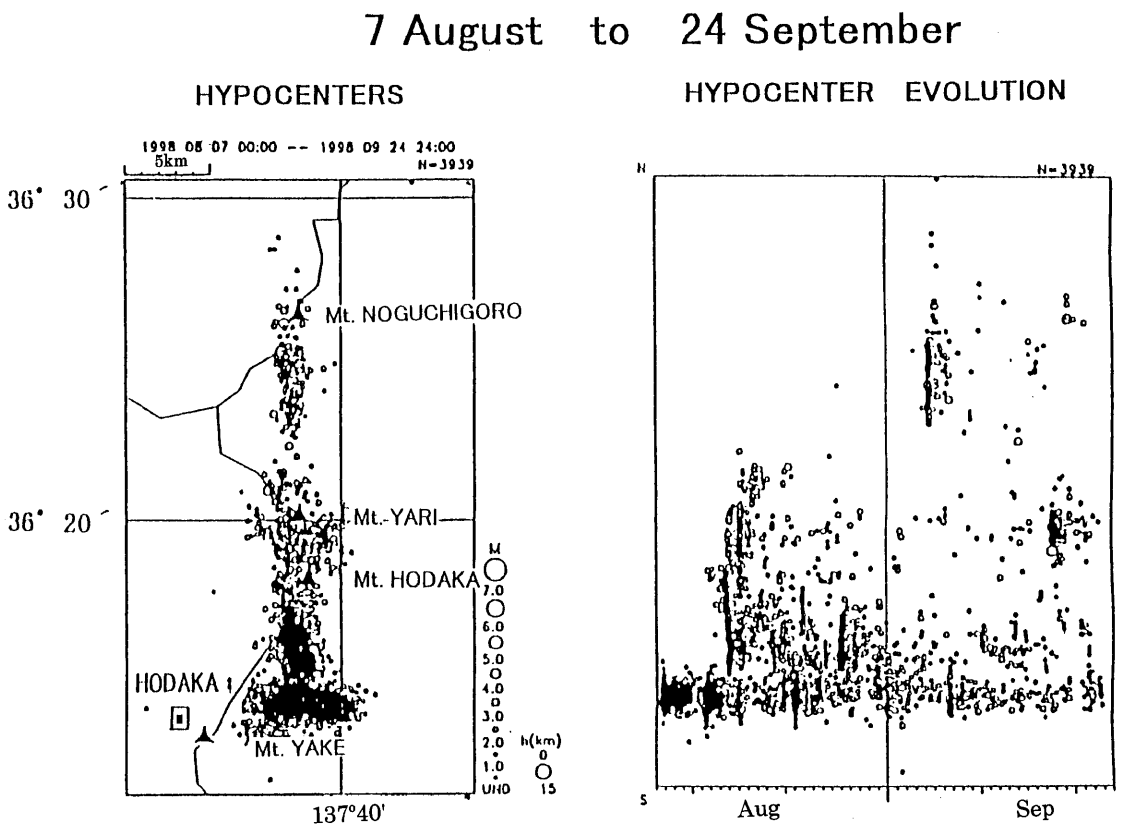

Fig. 13 A seismic swarm started on of 7 August 1998 just west of the observation site at Hodaka (●). The activity was the first since the start of the observations here in 1993. The hypocentral data (Japan Meteorological Agency ; JMA) indicate that the initial activity till 12 August was limited to the east of Mt. Yake, but extended northwards in the second stage of activity. Data from short vertical and horizontal dipoles maintained by Nagoya University about 600 m west of Hodaka site are also utilized supplementarily in this research.

earthquake with M4.1 on 12 August as in the case of the 1994 Great Kuril Earthquake (Fujinawa and Takahashi, 1998). The present co-fracturing signals were not detected at other sites contrary to the Kuril case. Therefere we could not rely on the arrival time difference between the co-fracturing signal. We suspected the existence of the co-fracturing signals by comparing the ULF band and the ELF/VLF band. Other moderate earthquakes in the swarm were not accompanied by any discernible co-fracturing signals. Strength of the signals may depend dominantly on the earthquake magnitude (Gokhberg *et al.*, 1987).

Very clear anomalies in the electric field could be seen on the records for 12 August, when the second largest earthquake with a magnitude of 4.1 in the swarm occurred (Fig. 15b). It should be noted that this earthquake marked the start of the second swarm activity extending to the north (Fig. 14). The lightning information servicing company (Franklin Japan Co., Ltd.) reported that there was slight atmospheric discharge activity on 12 August. But the activity was not noticeably large compared with that on other days in August 1998 (Fig. A-98-8-0, 1, 2). The horizontal electic freld recond suggests that the anomalous electic freld is more or less similar with that induced by return stroke (Fig. 12). We suspect the possibility that the lightning discharges were accelerated on this day. Moreover, the variations in the electric field on the day were too large to be attributed to magnetosphere disturbances, as has been noted previously.

The degree of anomaly in the present case could be confirmed by checking all data from the start of observation including the digital observation in 1995 shown in the Appendix. The strip chart records before the digital recording do not contain any anomalies except for those induced by lightning discharges or "noises" at the time of caliblation. Therefore the anomalies such as those in Fig. 15b and Fig. 15c could not be attributed to external noises. The aforementioned anomalies at the time of the vapor eruption in July 1996 (Nakayama *et al.*, 1997) were much smaller in terms of amplitude and duration compared

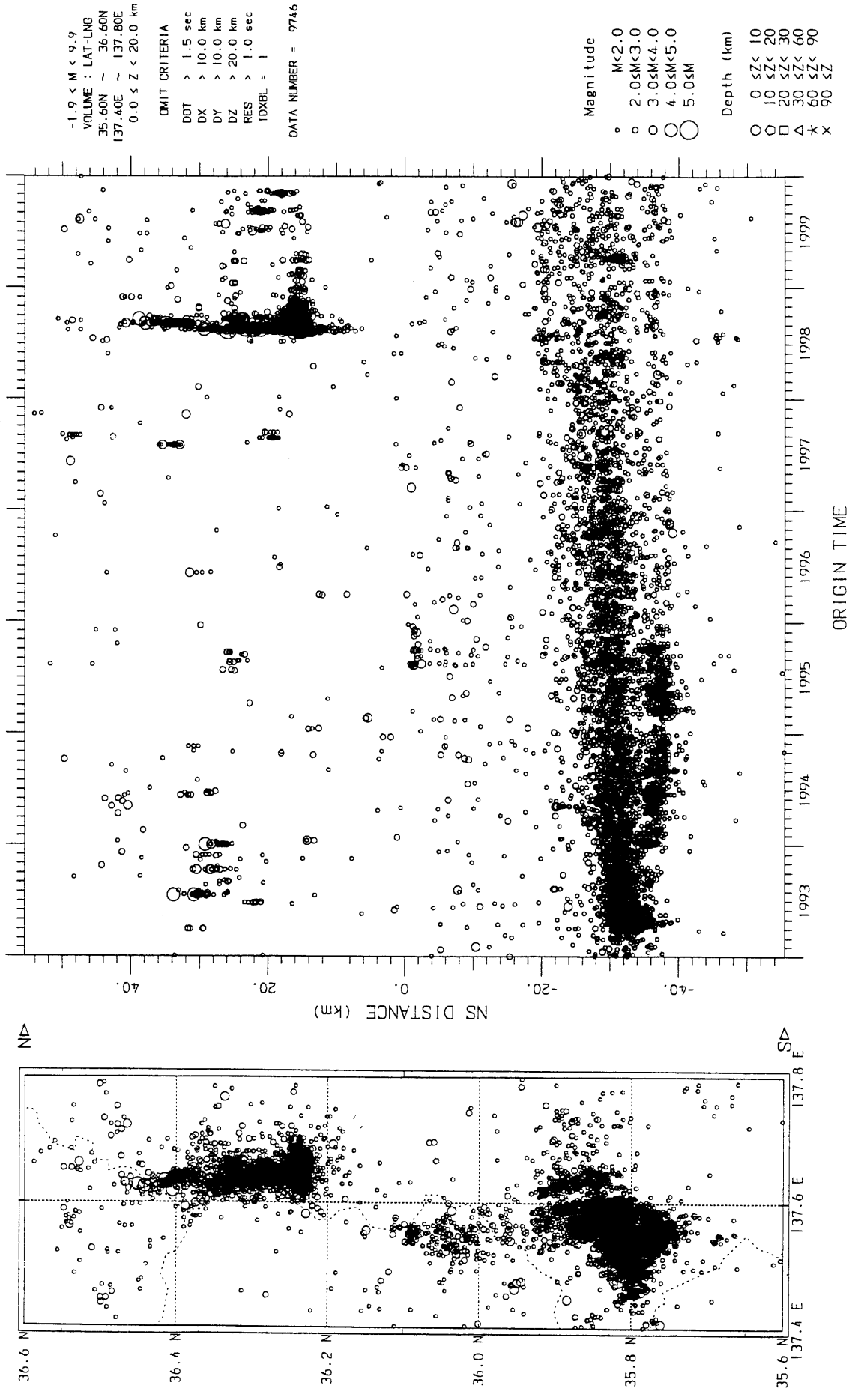

Fig. 14-1 Seismicity around the observation site Hodaka determined by the Kanto Tokai crustal observation network of NIED. Left; hypocenter distribution from January 1 1993 through 30 December 1999, right: space time distribution in the same period.

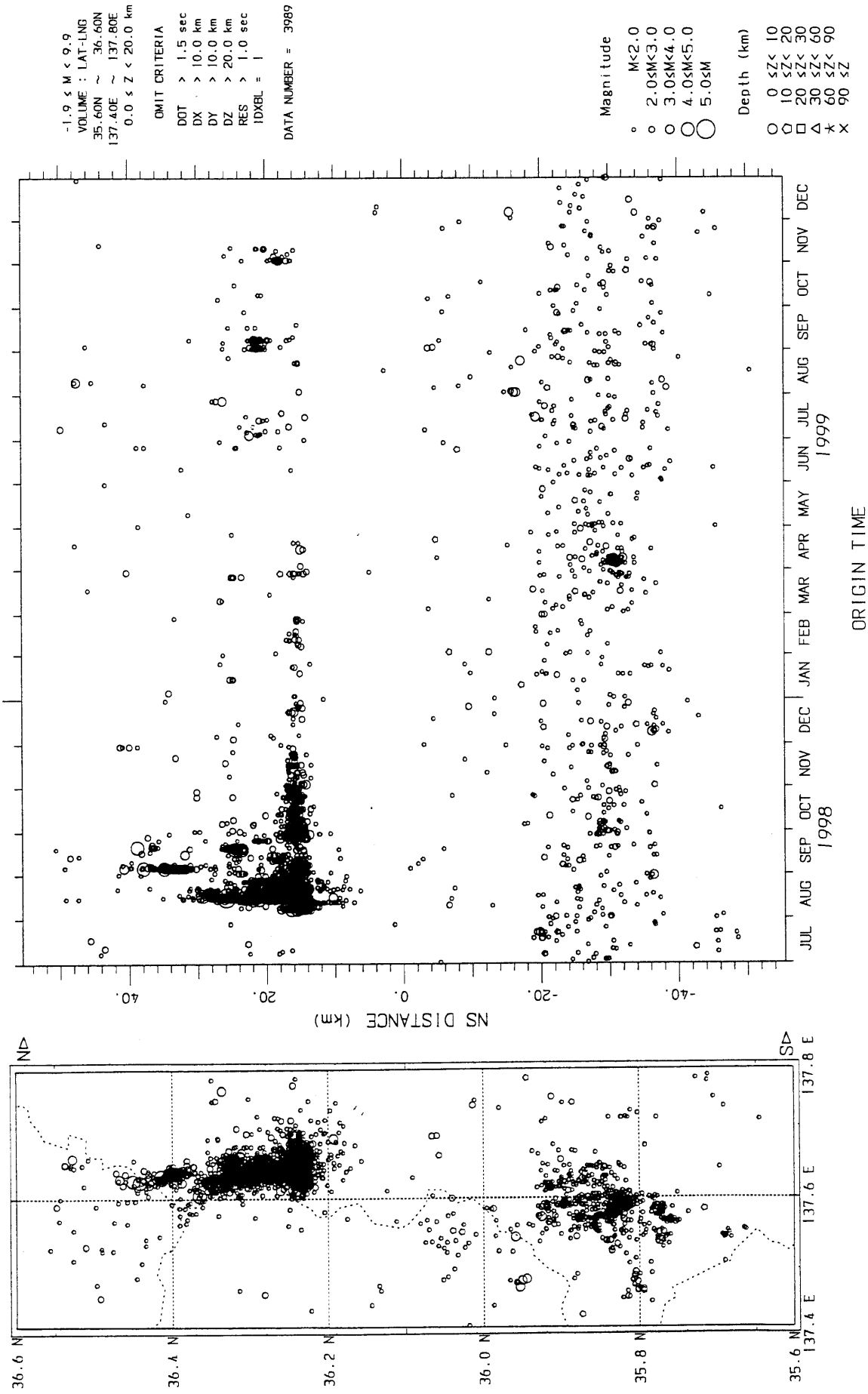

Fig. 14-2 Seismicity round the Hodaka site during the last activity from July, 1998 through Decenber, 1999.

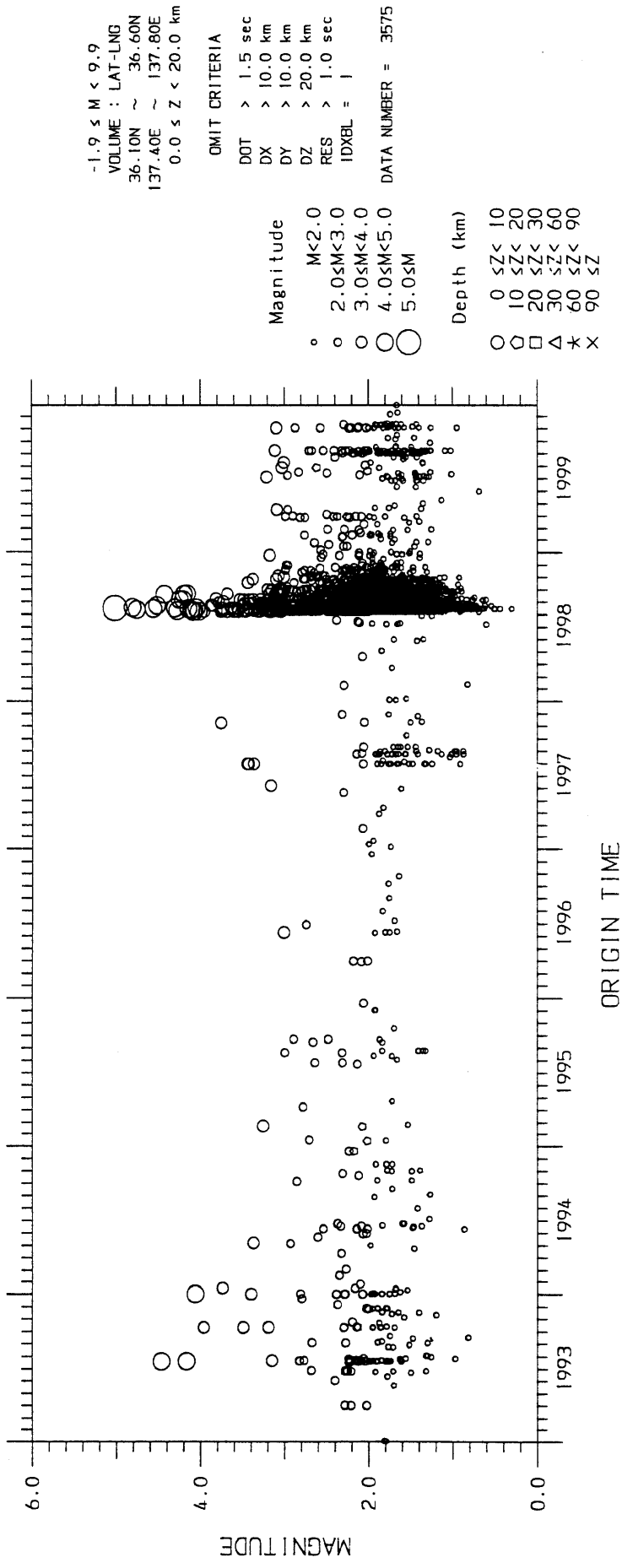

Fig. 14-3 Magnitude-time distribution in the zone of the present swarm, northern part activity shown in Fig. 14-2 for the total observation period be ULEM.

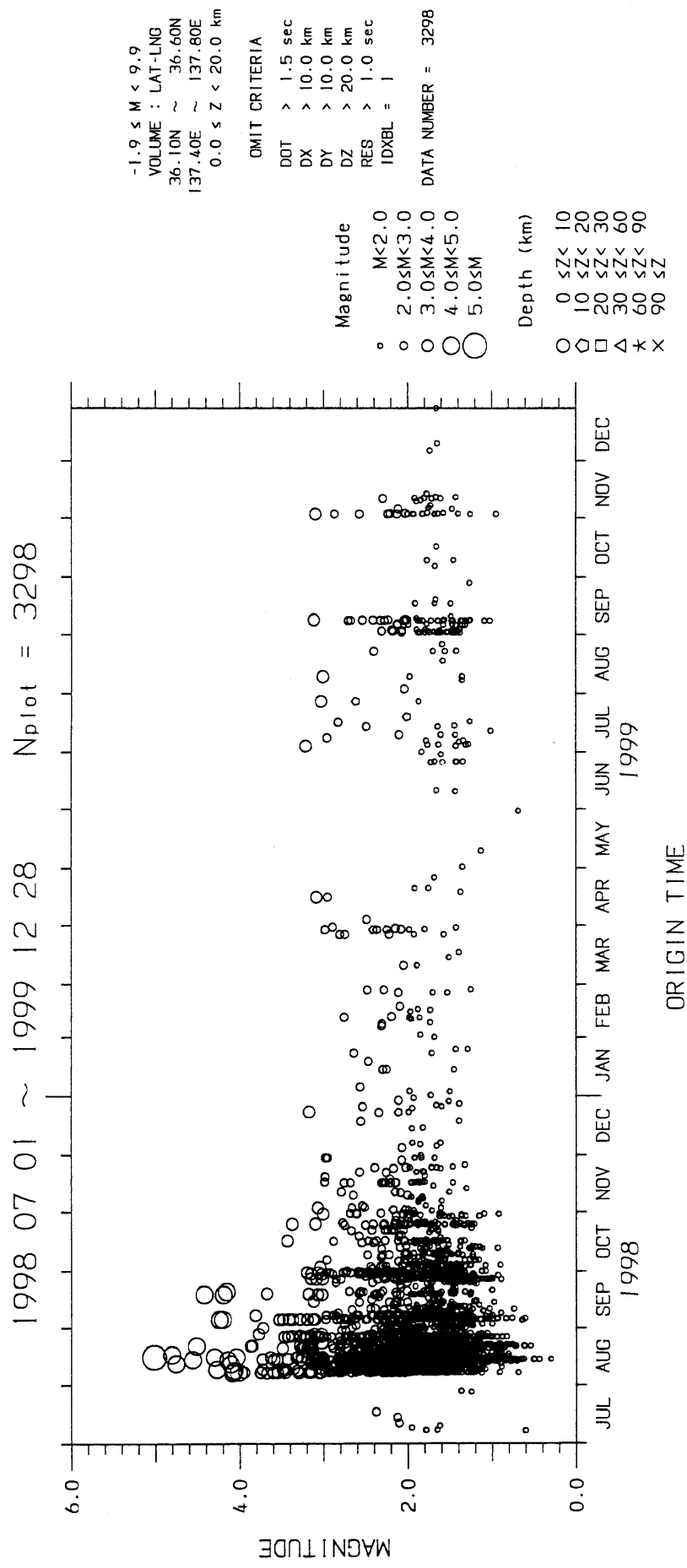

Fig. 14-4 Same as Fig. 14-3 except for the observation period.

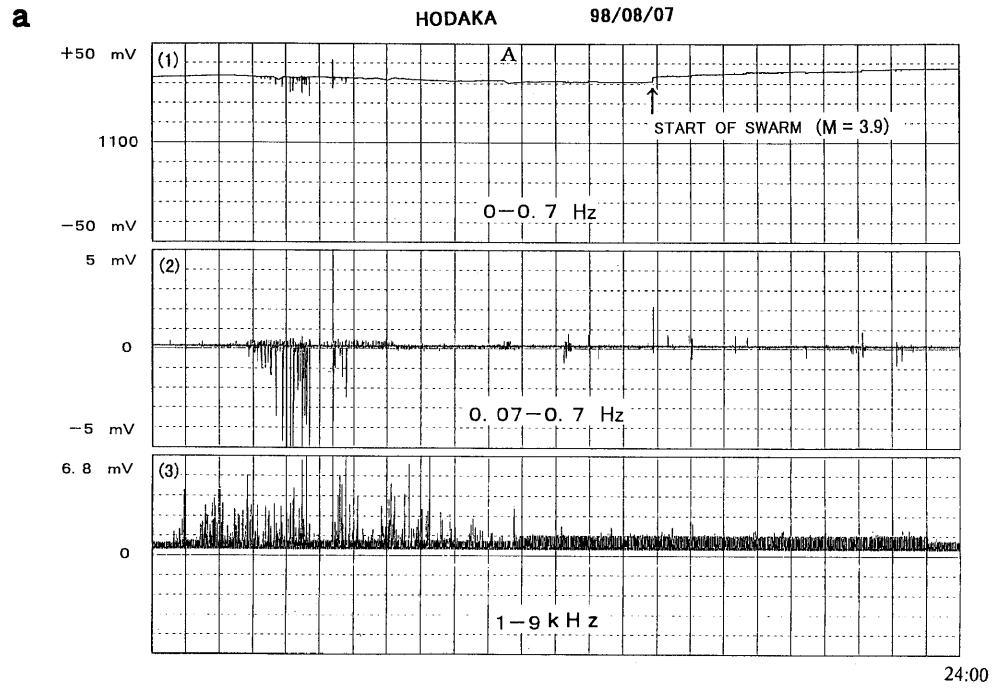

Fig. 15a Monitoring record on 7 August 1998, when the swarm activity started from about 15:00. Anomalous transient electric field changes were recorded on all three frequency bands about 10 hours before the first earthquake with a magnitude of 3.9. The starting time and duration of anomalous signals are somewhat different for the three frequency bands.

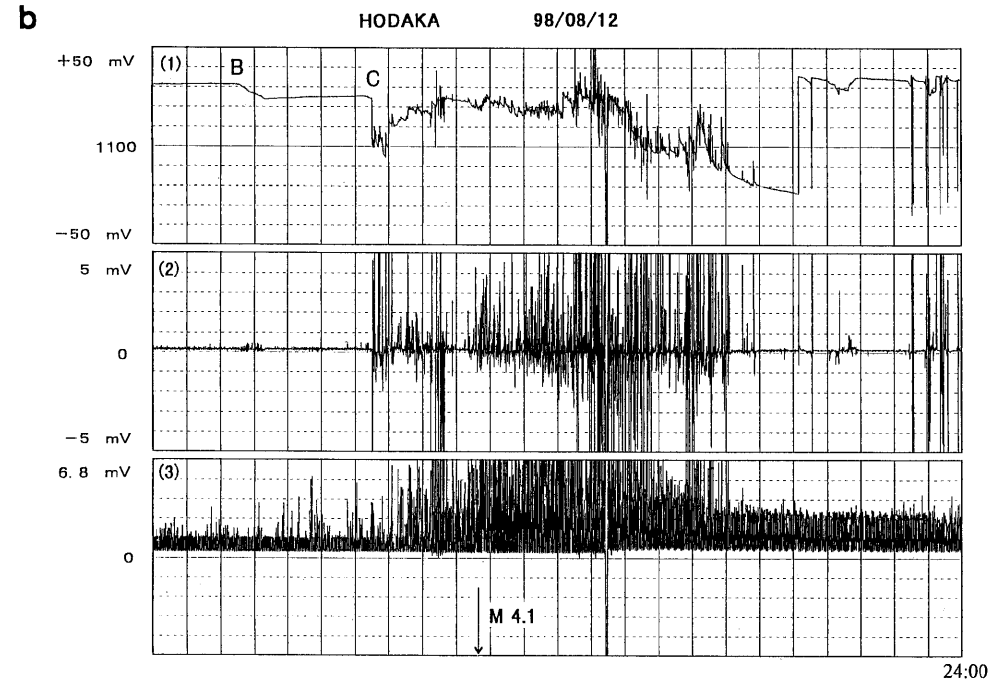

Fig. 15b A very clear anomalous transient electric field charges (SP : self-potential) were recorded about seven hours before the occurrence of the second largest earthquake (M 4.1) in the earthquake swarm, as a start event of the second stage of the seismic swarm on the dc channel (B). About four hours after the appearance of the dc component anomaly, the dc (C in(1)), ULF (2) and the ELF/VLF (3) bands also provided, almost simultaneously, large and clear anomalies. Urban noises in the ELF/VLF channels increased from about 0.8 mV to 2.4 mV during the period of the most active electric field anomaly occurrence.

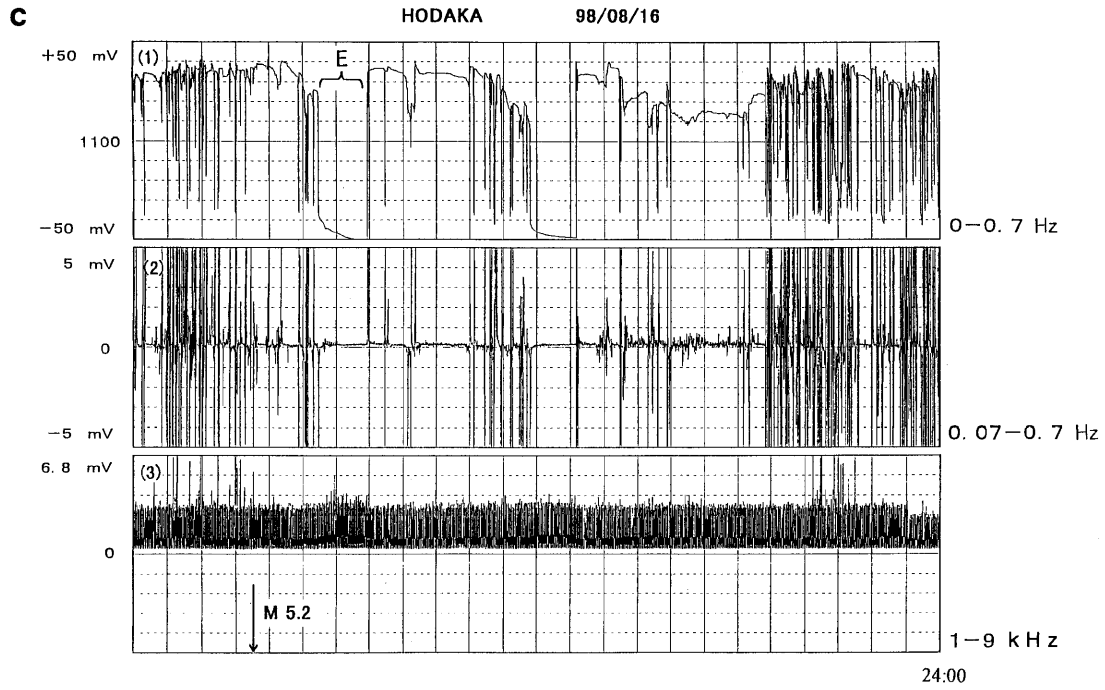

Fig. 15c The monitoring records on 16 August, 1998 when the largest earthquake with magnitude of 5.2 occurred. Transient SP anomalies consisted of a typical type of fluctuation seen as "high" frequency pulse signals of negative polarity and variable duration, from several seconds to tens of minutes. The sharp drop at the initial stage, followed by gradual decrease to saturation, and final sharp recovery is well exemplified in (1). It should be noted that these were accompanied by only minor anomalous signals in the ELF/VLF channels (3) in comparison with other channels. Digitized data for 15 August could not be recovered because of modem trouble at the time of the severe shock induced by the largest earthquake. The paper monitoring chart, however, shows that a very large increase in electric field anomalies occurred about 10 hours before the earthquake. The anomaly is several times larger compared with those on previous days, even causing a recording malfunction due to paper breakage induced by large fluid ink drainage, which indicates rapid and large signal occurrence.

with the present case.

In the dc band a slight decrease with a longer period variation of about 8 mV appeared at about 2:30 (B in Fig. 15b-(1)), around eight hours before the earthquake, and a sharp decrease of 20~30 mV at about 6:30 (C in Fig. 15b-(1)). Such dc band changes were also seen before the start of the swarm activity (A in Fig. 15a-(1)), and occasionally at a normal state in the absence of any crustal activity. We, however, have never seen this type of large event as demonstrated by 'E" in Fig. 15c-(1). The ULF band strip chart record (Fig. 15b-(2)) provides a much clearer anomaly compared with the dc component because of an amplification approximately ten times larger than the dc band, as will be shown more clearly later by color figures (Fig. 18).

The ELF/VLF bands indicate a different evolution in comparison with those of the other two bands. In general, the ELF/VLF bands signals appeared only at the time of large amplitude signals in the other two bands when seismic activity was large, such as during the day on 12 August (Fig. 15b). The feature could be interpreted in terms of frequency spectral characteristics of electomagnetic field generation by the qround water movement as will be touched later.

On 7 August 1998 severe lighting discharges around the observation site inducing large atmospheric noises were not reported, though there was a considerable rainfall around the Hodaka area (Japan Meteorological Agency : JMA). The general pattern of the electric field change, is somewhat similar to those at the time of lightning discharge. However, the extremely long duration of the increase in the electric amplitude of the ELF/VLF band such as during 1:00~11:00 on 7 August (Fig. 15a) has rarely been seen since the start of the observation in 1993.

Moreover, there were no pulse-like signals in the ELF/VLF bands (VPS) located around the seismic

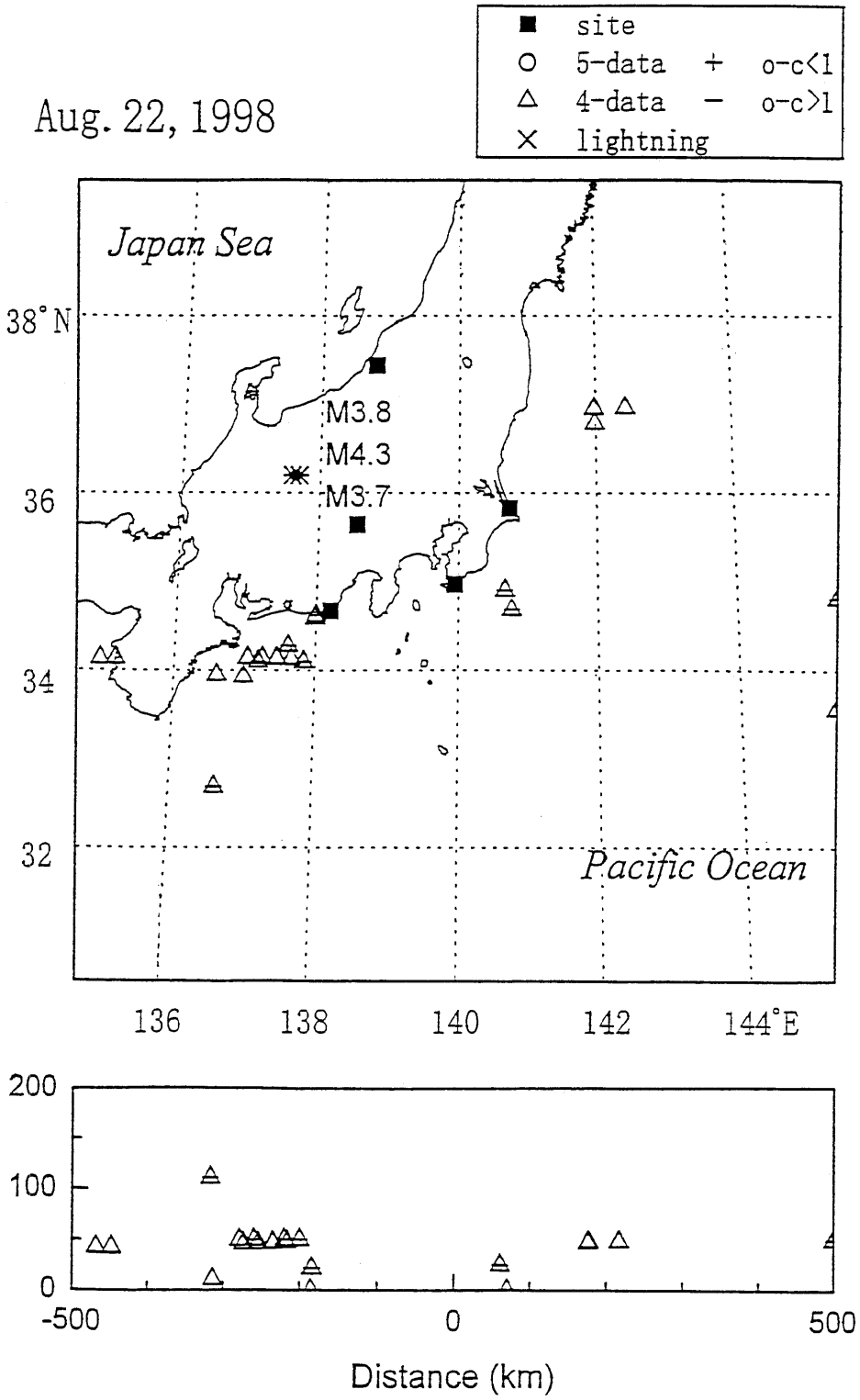

Fig. 16 VLF pulse-like source point (○, here+added denote a better determination with O-C less than 10 μs) projections in the horizontal plane (a), and in the east-west vertical plane (b) on 22 August 1998 when moderate earthquakes (*) occurred in the seismic swarm activity in central Japan. Source determination accuracy in the horizontal plane is about 10 km inside the network, but several tens of kilometers outside the network with the vertical direction being less accurate. Note that there are no pulse-like ELF/VLF signals in the vicinity of the seismic swarm activity, also that there were no lightning discharges (×) on this day even if conspicuous anomalies were detected at the Hodaka site.

swarm region by means of the signal locations determination method (Fujinawa *et al.*, 1997), as is illustrated in Fig. 16. It indicates that the ELF/VLF bands signals detected in association with the seismic swarm (Fig. 15a) were not so large as those due to the return stroke, which can usually be detected at other stations in the network because of their large strength and enabling source location determination. It might be considered that the present ELF/VLF anomalies are of local origin. It is more probable that the VLF signals are generated deep under the ground. The large dissipation of the signals could have been overcome by use of the ULEM.

In addition, the K-index reported by JMA during 4 hours period were less than 4 on 12 August 1998 (Fig. 15b), showing that those anomalous signals are not related to the geomagnetic disturbances. On the whole, the magnitude and the duration of the variations in the electric field were large enough to conclude that those electric field anomalies were originated in association with crustal activity.

The anomalous electric field changes at the time of the largest earthquake in the swarm were very large (Fig. 15c). On the other hard it is hard to make to correspond anomalies of each electric field to particular earthquake. It is mainly because of the persistent appearance of large fluctuations (Fig. 17) in contrast to the previous two cases (Fig. 15b and Fig. 15c) preceding the first earthquake at the initial stage of each swarm activity.

It is, nonetheless, also true that we can suspect conspicuous large fluctuations preceding each larger -scale earthquake. For cinstance, the strip chart record clearly indicates that there was a very large electric field variation as over-scaling in the recording chart (Fig. 18). We could not recover the digitized data on the day before the largest earthquake eccurrence, because of a malfunction of the modem for data transmission caused by the severe seismic shock. The strip chart record on a calm day is illustrated in Fig. 18-1 on 6 August 1998. The lowest blue line is for the dc component with the recording range selected from -10 mV to $+40$ mV by the use of a bias voltage of 1.100 V. The second lowest line is for atmospheric pressure, the green line for the ULF band in the range of ± 5 mV as for the digitized monitoring records (15a, 15b and 15c (2)). The uppermost line is for the ELF/VLF bands. Fig. 18-2 shows the analog recording for a part of 12 August 1998 (see Fig. 15b). We are able to see a more clear pattern in the anomalies than that using the digitized data by means of data compression procedure. One of the over-scaling pulses in the ELF/VLF bands is recorded at the time of the earthquake with a magnitude of 4.1 (VLF in Fig. 18-2). The signal was already assumed to be a co-fracturing signal.

Fig. 18-3 shows the part of the record including the time of recording breakdown probably due to excessively large and rapid fluctuations of the pens at about 18:51 on 15 August 1998. This part of the record was not covered by the digitized record owing to the malfunction of the modem at the time of the largest earthquake (M 5.2) on 16 August 1998. The fluctuation amounted to more than 50 mV. The ELF/VLF channels remained almost normal proving that the severe anomalies were not originated by lighting discharges. The recording was resumed at about 1:30 on 16 August, as is seen from Fig. 18-4 possibly because of the release of entangled ink pens for the three channel recorders.

The large anomalous signals appeared about ten hours prior to the largest earthquake. Trend-like larger period fluctuations with period of order hours (such as B, C in Fig. 15b) suggest that there were structural changes of forcing term inducing electric field anomalies. The ground water circulation change is considered to be the origin of the electric field source, as will be described in more detail later.

The anomalies were still in evidence in April 1999, and almost none of the electric field strength in January 2,000 corresponded to a decrease in the swarm activity (Fig. 14). We suspect that the source of the electric field change had existed for more than a year without having sufficient strength resulting in earthquakes of considerable magnitude. The persistence of electric anomalies over a long period is a general characteristic for cases in geothermal regions (Fujinawa *et al.*, 2000c)

Apparent flattening of the record in the dc channel starting at the end of August (Fig. 15) is caused by saturation of recording ranges and considerable fluctuating signals seen consistently in the ULF bands.

Whole digitized records for the dc component shown in the Appended Figures demonstrate how anomalous the present field changes were at the time of the conspicuous seismic activity which occurred near the observation site Hodaka. For instance, there were scarcely any anomalies throughout July 1998 before the earthquake swarm started on 7 August 1998.

Exceptions to this are large irregular signals which appeared for about one hour during calibration work, such as those seen on 12 July 1998 (Fig. A-98-7-1) and sporadic noises of very short duration on 3 July 1998 (Fig. A-98-7-1). Records for the other two frequency

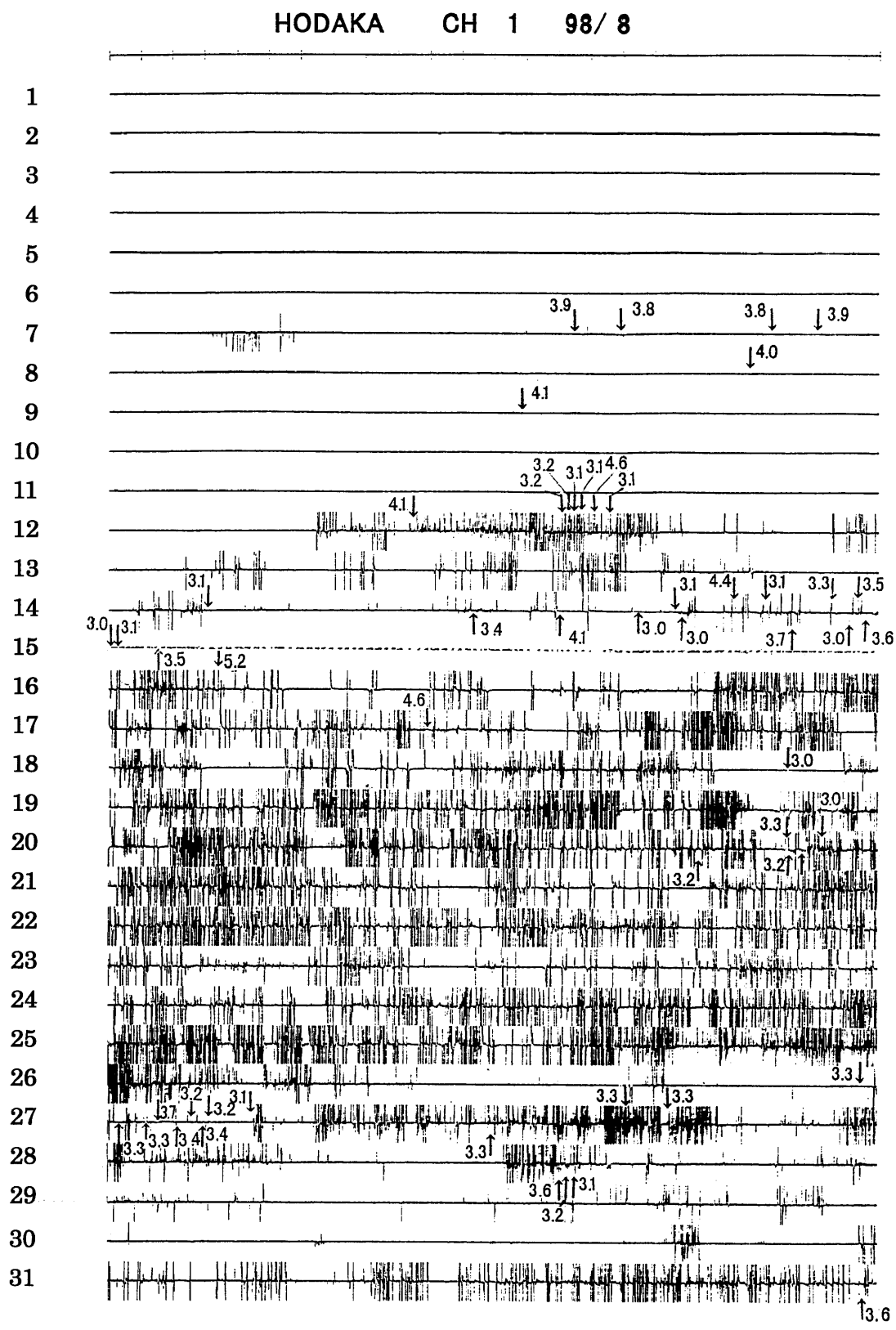

Fig. 17 Monitoring records for the dc channels for the whole of August 1998 including the normal stage till 6 August and the anomalous stage associated with the seismic swarm starting on 7 August. Earthquakes with a magnitude larger than 3.0 are indicated in the waveform trace. Correlations of individual earthquakes with transient electric field anomalies (TSP) are not clear because of the high frequency of earthquake occurrences in a swarm activity except for some special earthquakes occurring around the starting time of different stages of seismic activity.

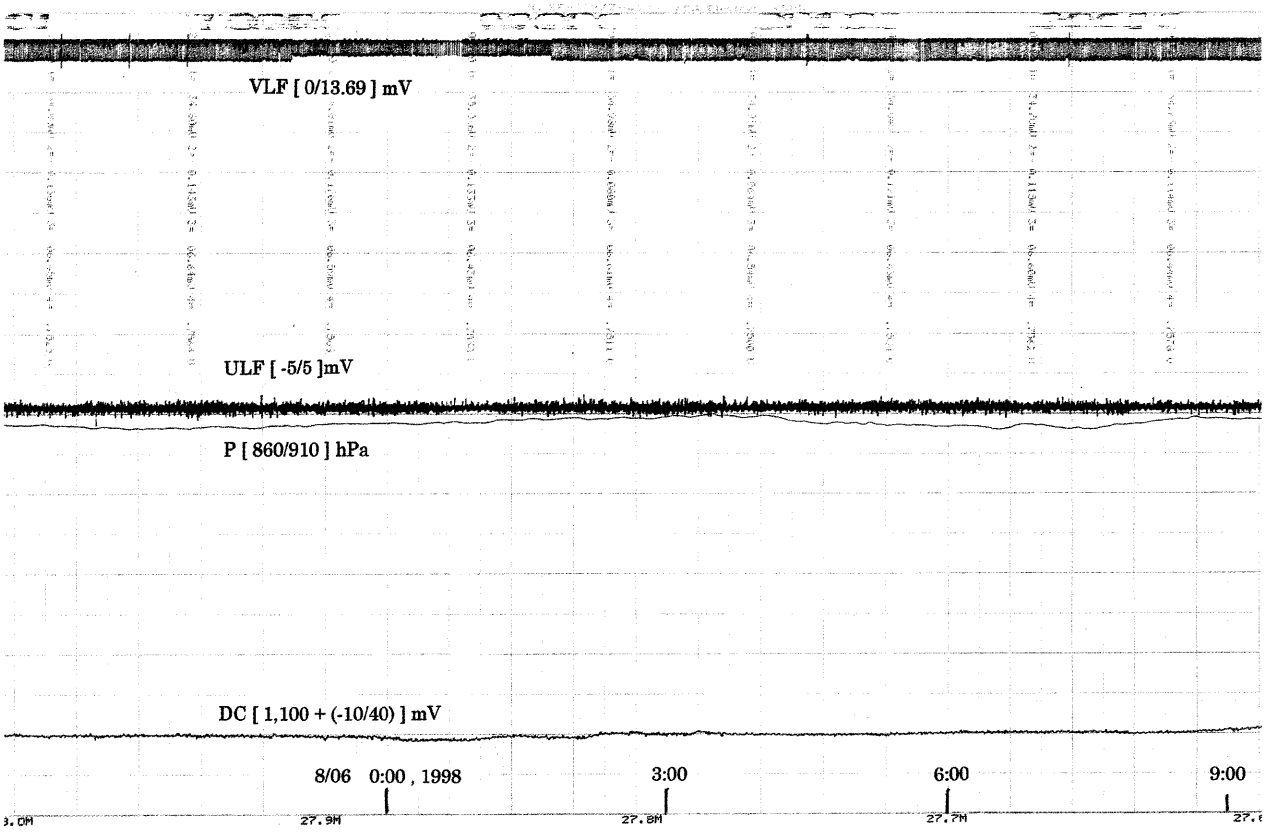

Fig. 18-1 Strip chart records for 6 August 1998 at a normal state.

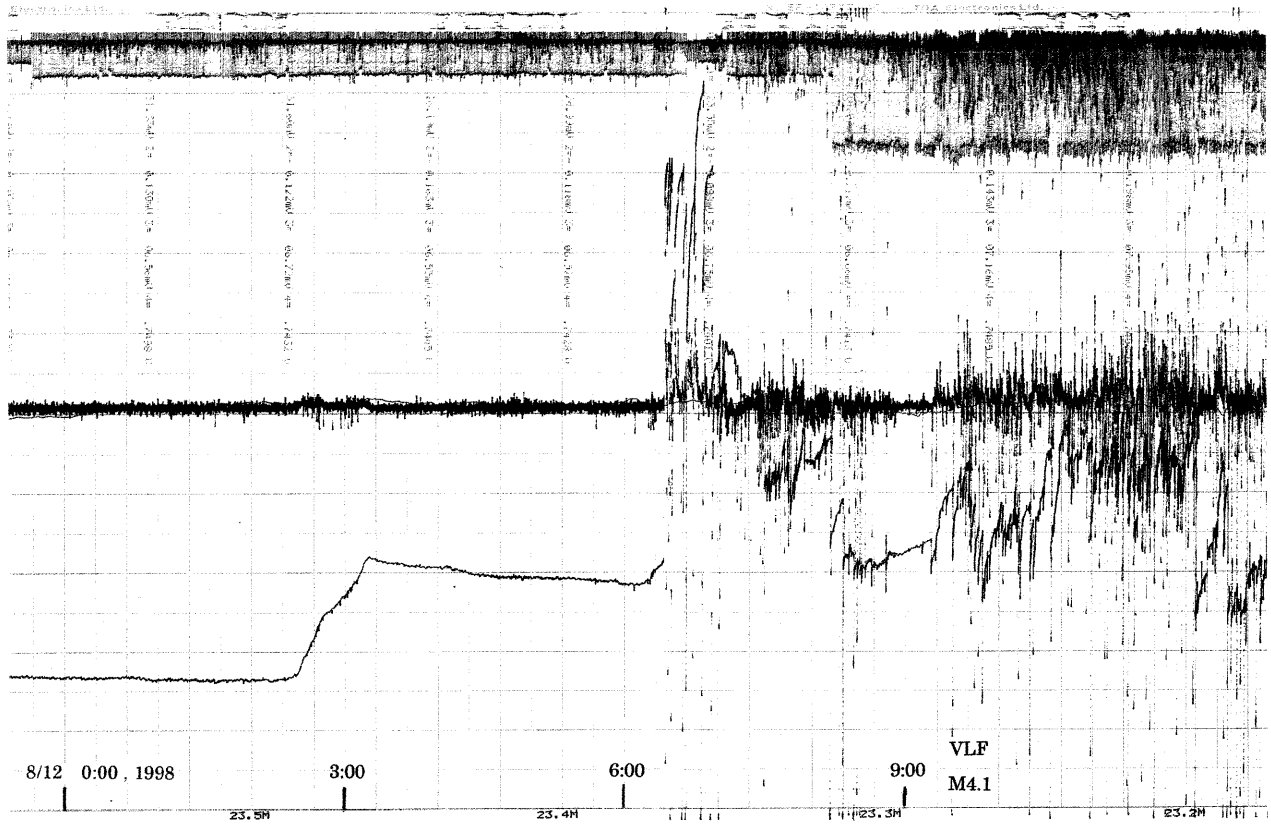

Fig. 18-2 Strip chart records for 12 August 1998 , when we had the second largest earthquake (M 4.1) of the swarm.

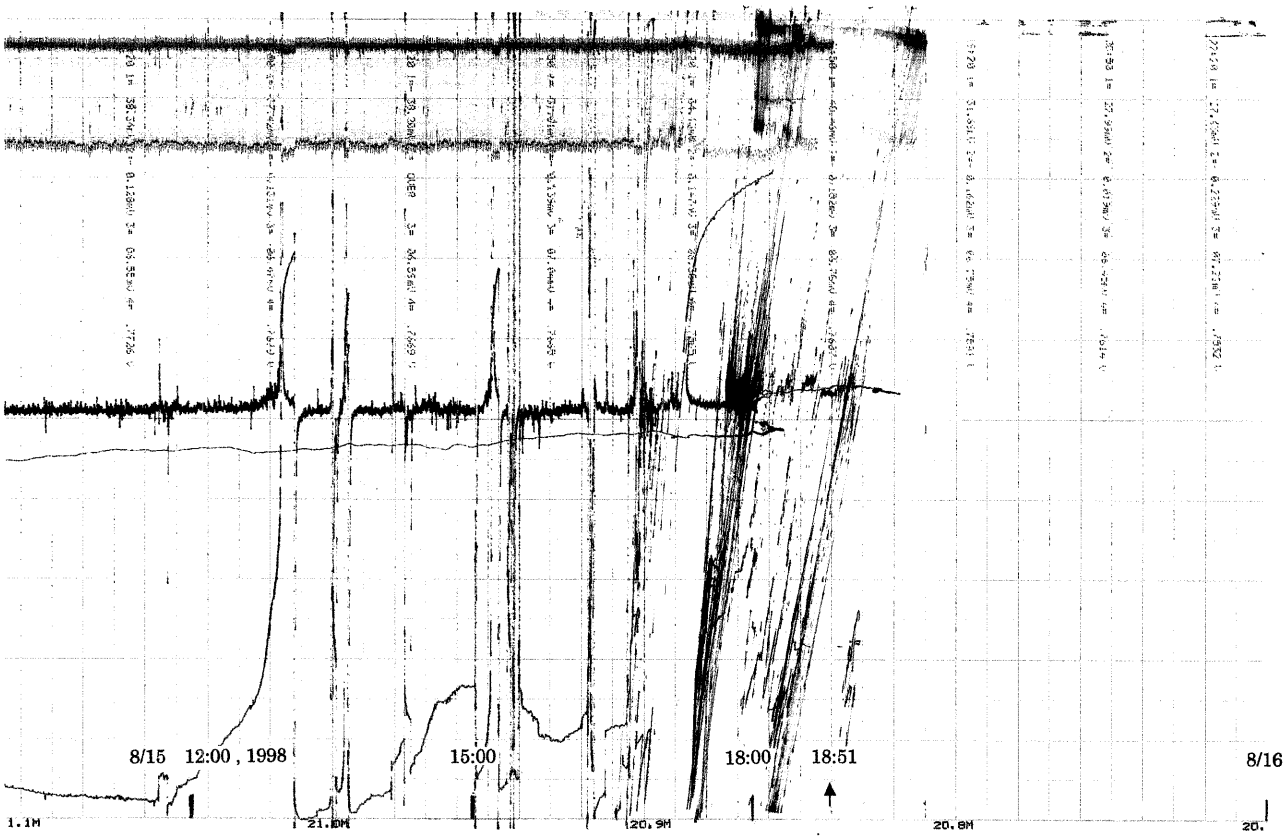

Fig. 18-3 Strip chart records for 15 August 1998, one day before the largest earthquake (M 5.2) of the swarm.

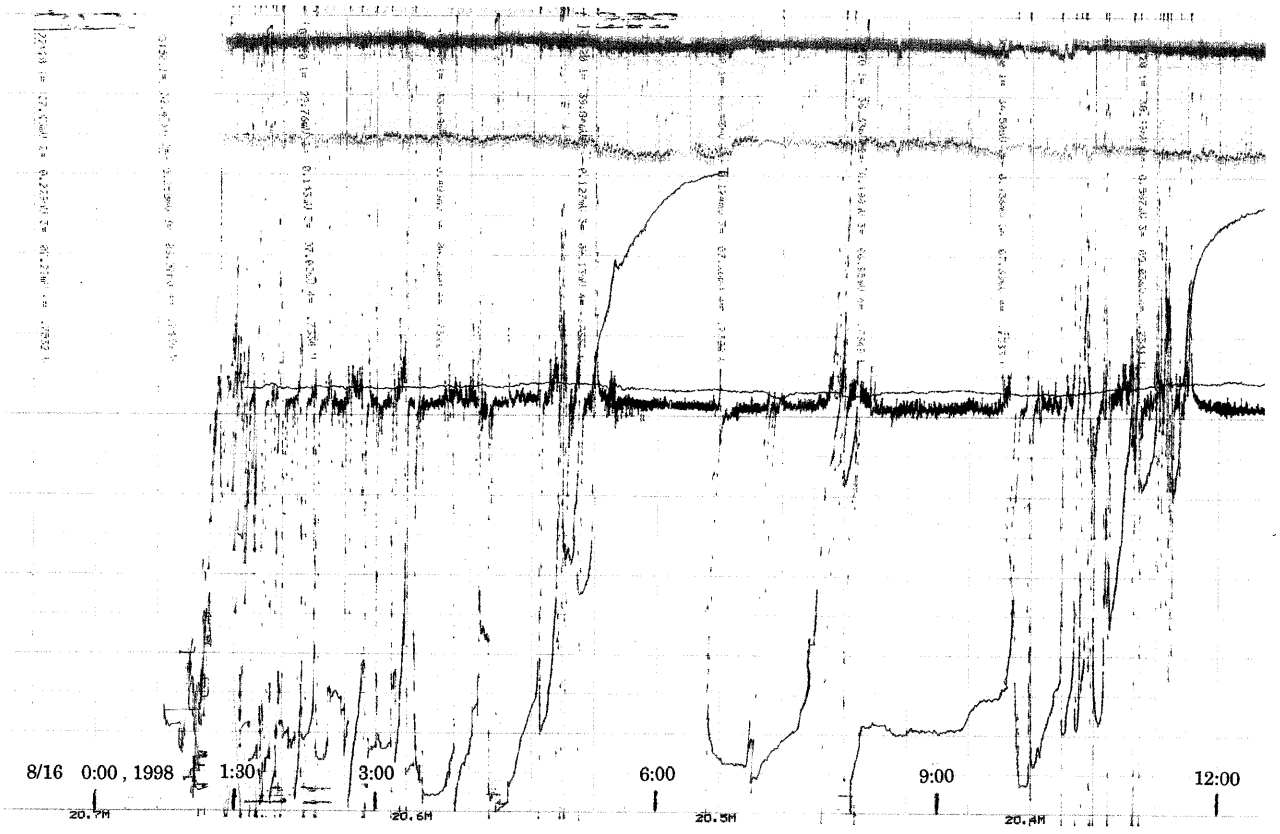

Fig. 18-4 The records resumed at almost 12 : 00, 16 August

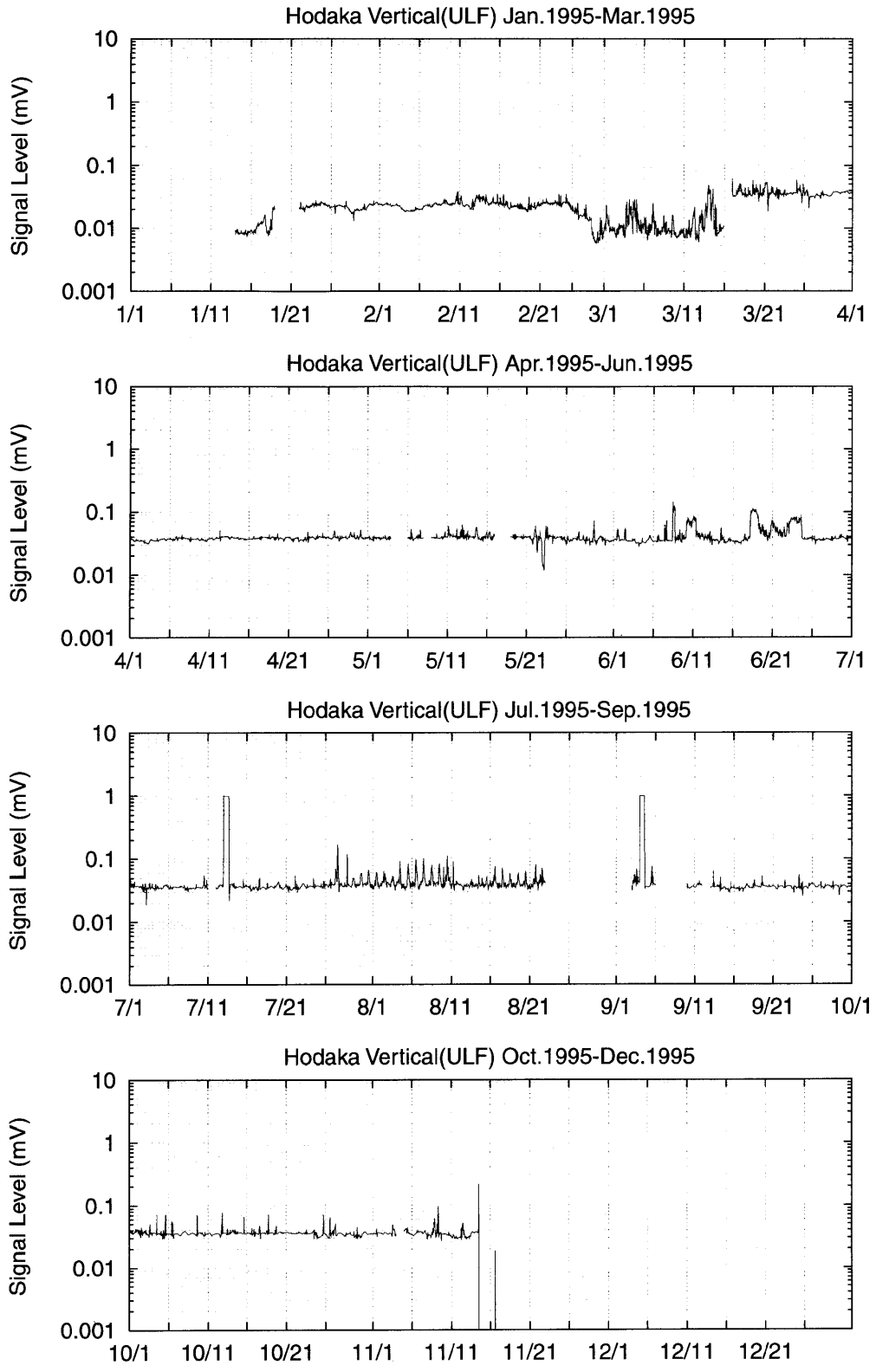

Fig. 19 Compressed monitoring record for the ULF band with the amplification gain being corrected on the basis of the parameters of the ULF band shown in Appended Table. The anomaly appeared from August 1998 is shown to be large amount about 1 mV compared with the background noise level of less than 0.1 mV. The anomaly has almost disappeared at about December 1999 with the ordinary level of less than 0.1 mV. The anomalies at the time of vapor ejection in July 1996 did not appear in this form of representation, though it was discerned clearly in the original monitors A-Fig. 96-7-2.

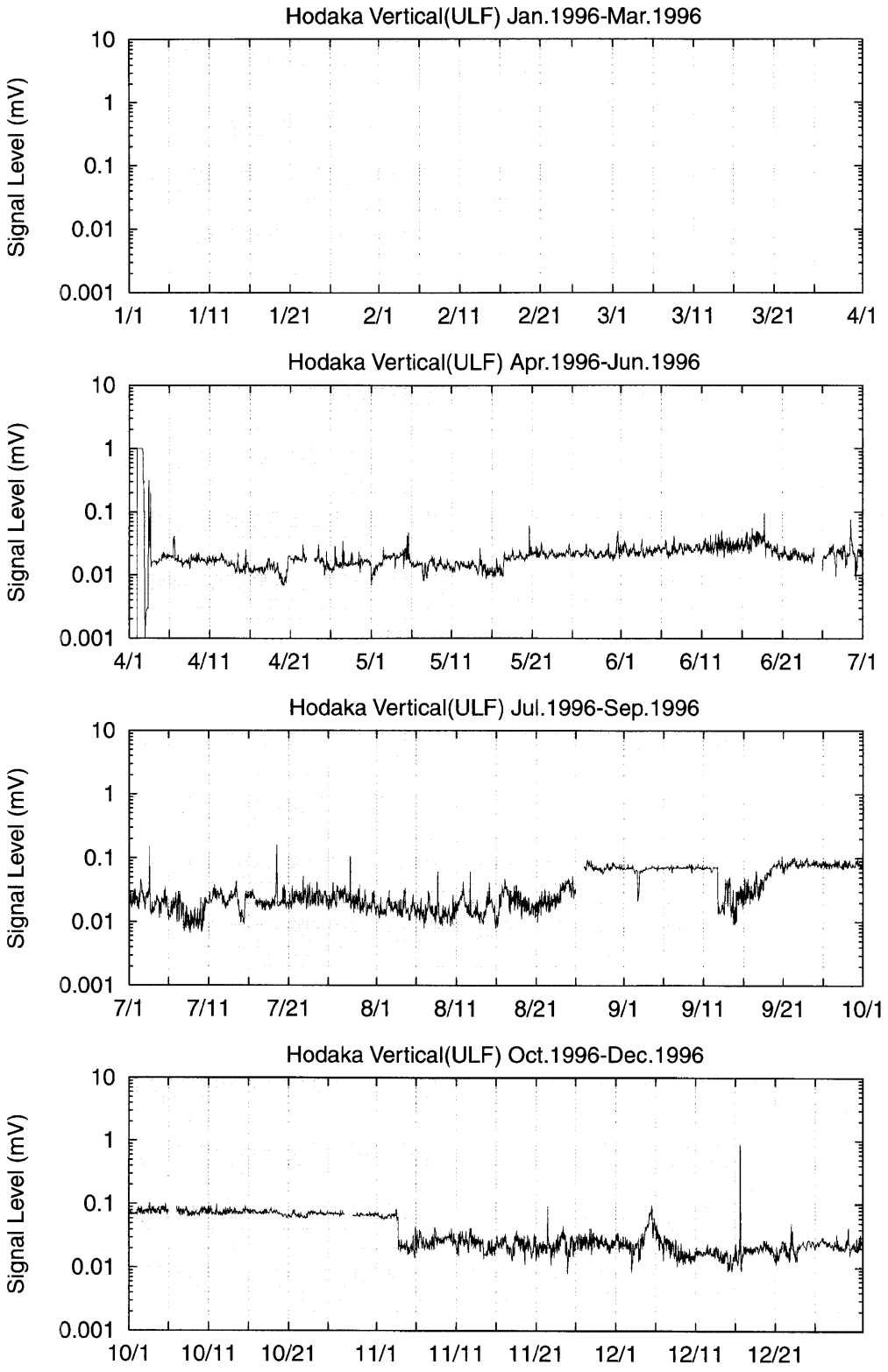

Fig. 19 (Continued)

Compressed monitoring record for the ULF band with the amplification gain being corrected on the basis of the parameters of the ULF band shown in Appended Table. The anomaly appeared from August 1998 is shown to be large amount about 1 mV compared with the background noise level of less than 0.1 mV. The anomaly has almost disappeared at about December 1999 with the ordinary level of less than 0.1 mV. The anomalies at the time of vapor ejection in July 1996 did not appear in this form of representation, though it was discerned clearly in the original monitors A-Fig. 96-7-2.

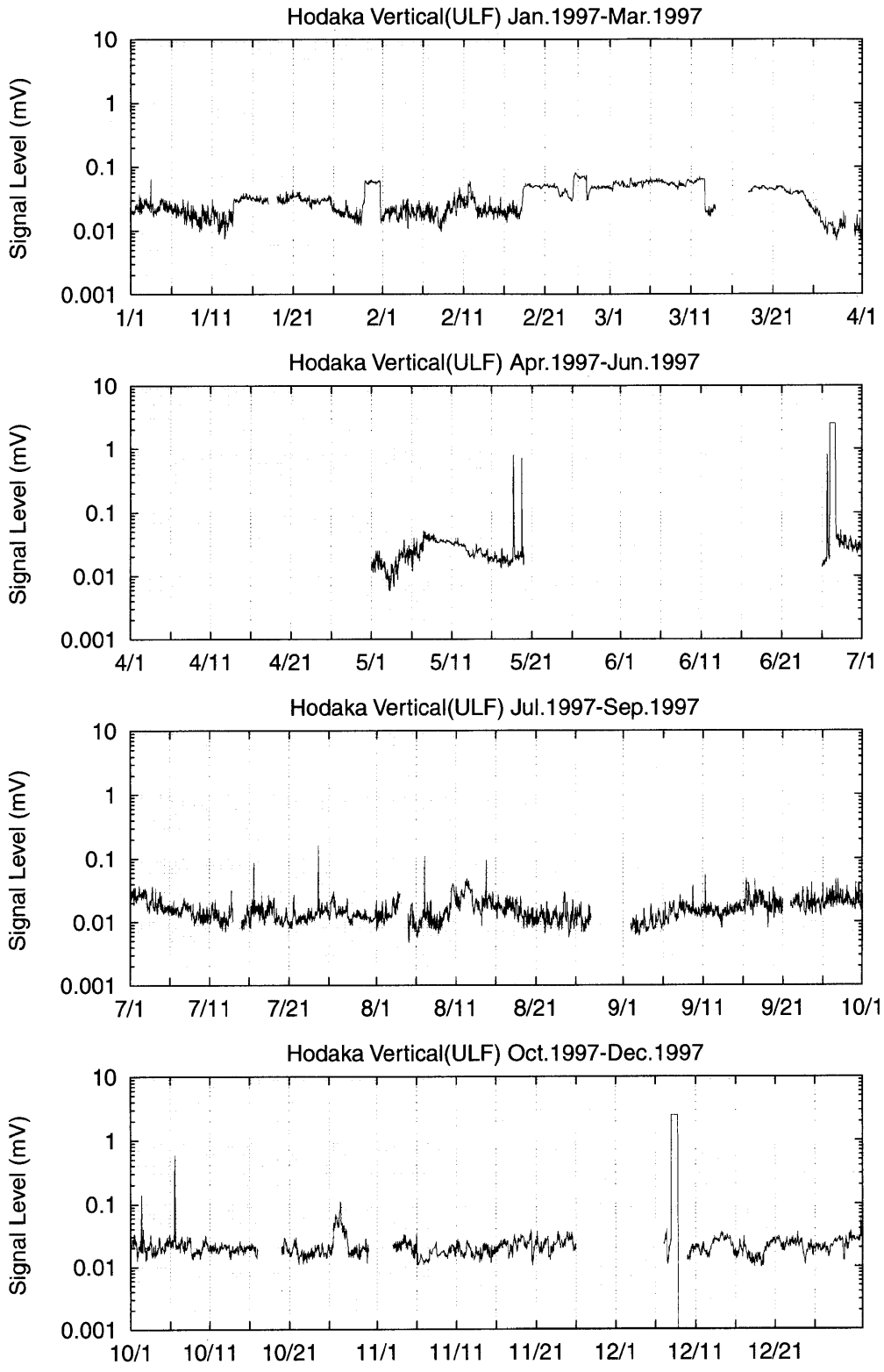

Fig. 19 (Continued)

Compressed monitoring record for the ULF band with the amplification gain being corrected on the basis of the parameters of the ULF band shown in Appended Table. The anomaly appeared from August 1998 is shown to be large amount about 1 mV compared with the background noise level of less than 0.1 mV. The anomaly has almost disappeared at about December 1999 with the ordinary level of less than 0.1 mV. The anomalies at the time of vapor ejection in July 1996 did not appear in this form of representation, though it was discerned clearly in the original monitors A-Fig. 96-7-2.

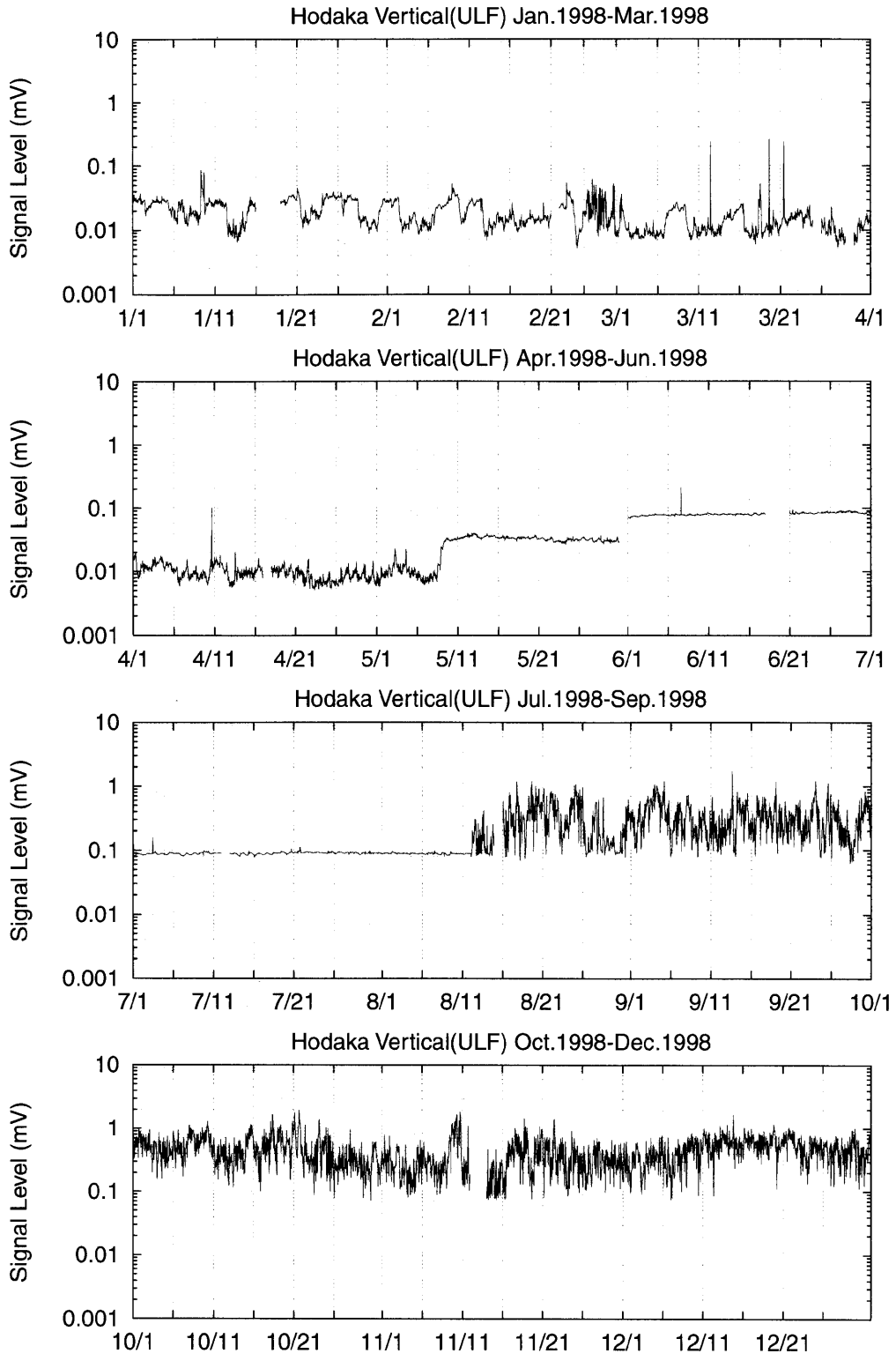

Fig. 19 (Continued)

Compressed monitoring record for the ULF band with the amplification gain being corrected on the basis of the parameters of the ULF band shown in Appended Table. The anomaly appeared from August 1998 is shown to be large amount about 1 mV compared with the background noise level of less than 0.1 mV. The anomaly has almost disappeared at about December 1999 with the ordinary level of less than 0.1 mV. The anomalies at the time of vapor ejection in July 1996 did not appear in this form of representation, though it was discerned clearly in the original monitors A-Fig. 96-7-2.

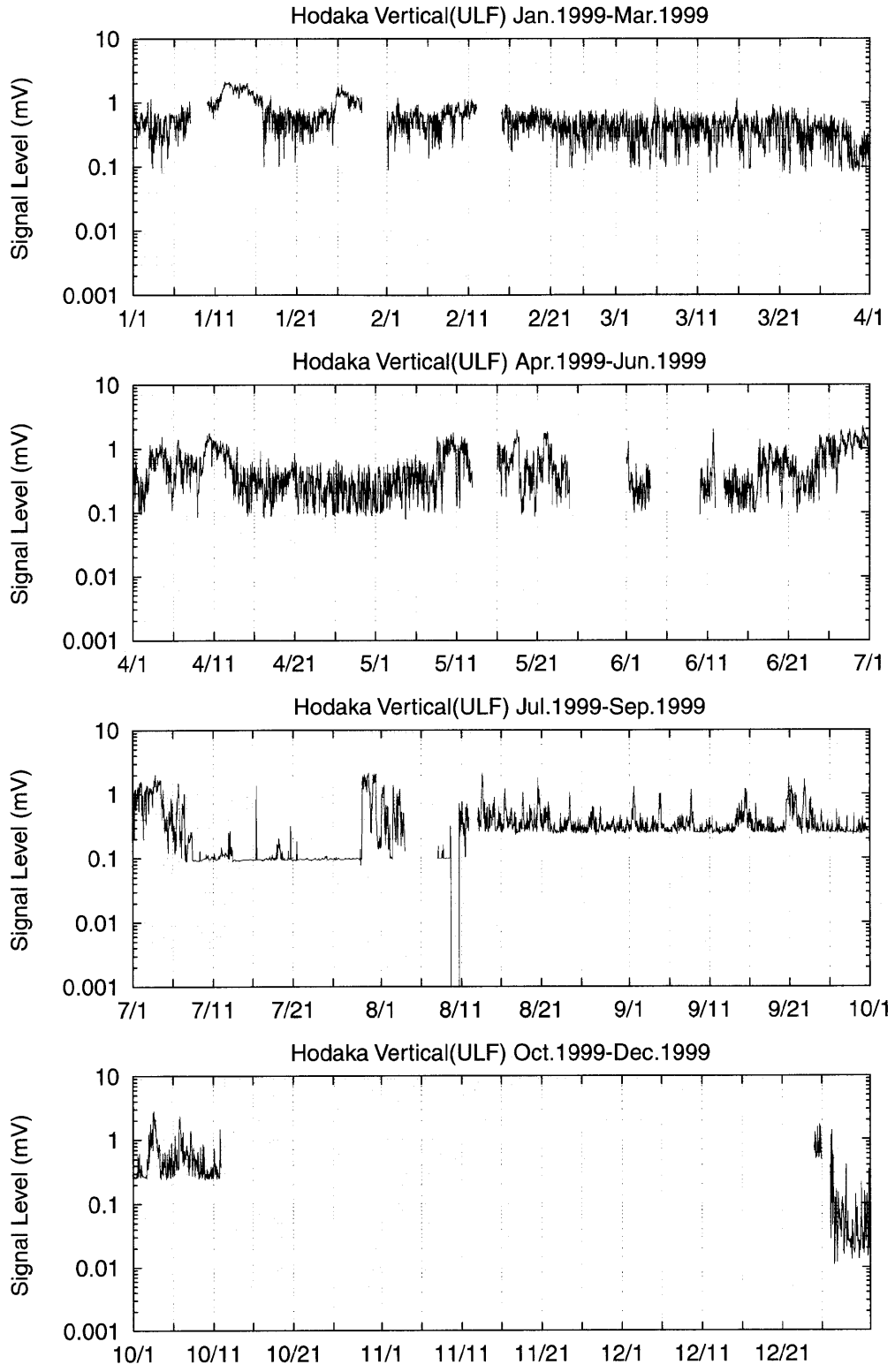

Fig. 19 (Continued)
Compressed monitoring record for the ULF band with the amplification gain being corrected on the basis of the parameters of the ULF band shown in Appended Table. The anomaly appeared from August 1998 is shown to be large amount about 1 mV compared with the background noise level of less than 0.1 mV. The anomaly has almost disappeared at about December 1999 with the ordinary level of less than 0.1 mV. The anomalies at the time of vapor ejection in July 1996 did not appear in this form of representation, though it was discerned clearly in the original monitors A-Fig. 96-7-2.

bands are more or less identical in the point that there are almost no anomalies of sufficient duration or magnitude compared with those registered during the vapor ejection in 1996 and the seismic swarm in 1998. In the ULF band slight and scattered increases of field strength occasionally appeared, which are, however, far smaller in extent compared with the anomalies already described. The appended Figures present a detailed monitoning record. The condensed presentation using the field strength in 10 min interval is phown in Fig. 19.

We may conclude that the anomalous electric field changes at Hodaka in association of the seismic activity in 1998 were related to the earthquake occurrence process, not induced by any other extraneous natural phenomena such as geomagnetic disturbances, and atmospheric disturbances including lightning, as well as by urban noises.

6. Discussion

6.1 Horizontal Selectivity

In addition to the present seismic activity there was considerable seismic activity about 50 km south of the zone during the period of observation (Fig. 14). But scarcely any anomalous signals were induced (Fig. 19, Appended Figures) in association with this activity. Further, no other sites of our observation network (Fig. 1) showed any anomalies associated with the present swarm activity. It is suggested that the signal detectability is limited within the distance of several times of the spatial dimension of seismic activity (Bernard and Le Mouel, 1996).

It is interesting that the first stage of the seismic activity from 7 August 1998 occurring in the southern part of the swarm area (Fig. 13) gave rise to only small signals at the Hokoda site (Fig. A-98-8-0 and Fig. A-98-8-1). It is suggested that there is a clear boundary of detectability of the anomalous signals at Hodaka for the whole seismic zone, divided into the earlier active zone and the later main active zone (Fig. 3). The high resolution hypocenter determination result shows that the border corresponds to geological boundary, as is shown in Fig. 20 (Yoshida *et al.*, 1998). We can assume that there is a good physical connection between the observation site at Hodaka (▣ in right sheet of Fig. 20) and the northern region of the seismic activity in terms of the signal propagation.

On the other hand, the connection with the southern region where the initial seismic activity occurred is not so strong. The conjecture is based on the field strength estimation using the electro-kinetic model (Fujinawa *et al.*, 2000c), however, we have no evidence to determine whether the apparent close connection is because of high propagation efficiency of the signals or of a favorable source location near the ULEM. There is a kind of similarity with the so-called selectivity rule of the VAN group (Varotsos and Lazaridou, 1991) though the present case concerns the near field detectability.

6.2 Vertical Selectivity

At the NKO site about 400 m west of the Hodaka site a different type of vertical electric field observation is conducted (Nakayama *et al.*, 1997). They use three pairs of vertical electrodes of 25 m, 50 m and 75 m respectively, with an electrode at the bottom of the borehole working as a common earth as well as two horizontal, mutually perpendicular dipoles of 50 m in length. Comparisons of observational data at these sites with ours provide a valuable clue to guess the source location of the anomalous electric field changes associated with earthquake swarms. The electric strength drop B on 12 August (Fig. 15b-(1)) detected by different sensors of the vertical electric field indicates that the vertical gradient of the electric field strength was predominantly concentrated in a region at a depth of more than 75 m. The same holds true for typical anomalous signals illustrated in the record section from 19:10 through 24:00 (Fig. 15c): sharp pulse-like changes with nearly the constant amplitude superimposed on the dc trend. The negative polarization means that electric field strength increases with depth. Those pulse-like signals have rarely appeared on the shallower electrodes or in the horizontal dipoles suggesting that their origins are deep in the ground.

Therefore, we can conclude that the source region of the present electric anomalies is at least deeper than about 100 m. The data is also interesting from the point of view of the detection method of development of small electromagnetic signals in the circumstance of a high rate of dissipation. Installing the sensor near the source such as using the casing pipe seems to be very profitable. For instance, the ELF/VLF signals decays very rapidly for electrical resistivity of 100Ω-m of the skin depth of 100 m. Even such small signals (Fig. 15b-(3)) could be detected using a casing pipe antenna touching or near the source of the electric field generations, for instance, confined water layer (Fujinawa *et al.*, 2000a).

6.3 Mechanisms

It is important for any precursory phenomena candidate to give a firm scientific foundation in the physico-chemical processes of earthquakes or volcanic eruptions. The step is essential in order to develop a

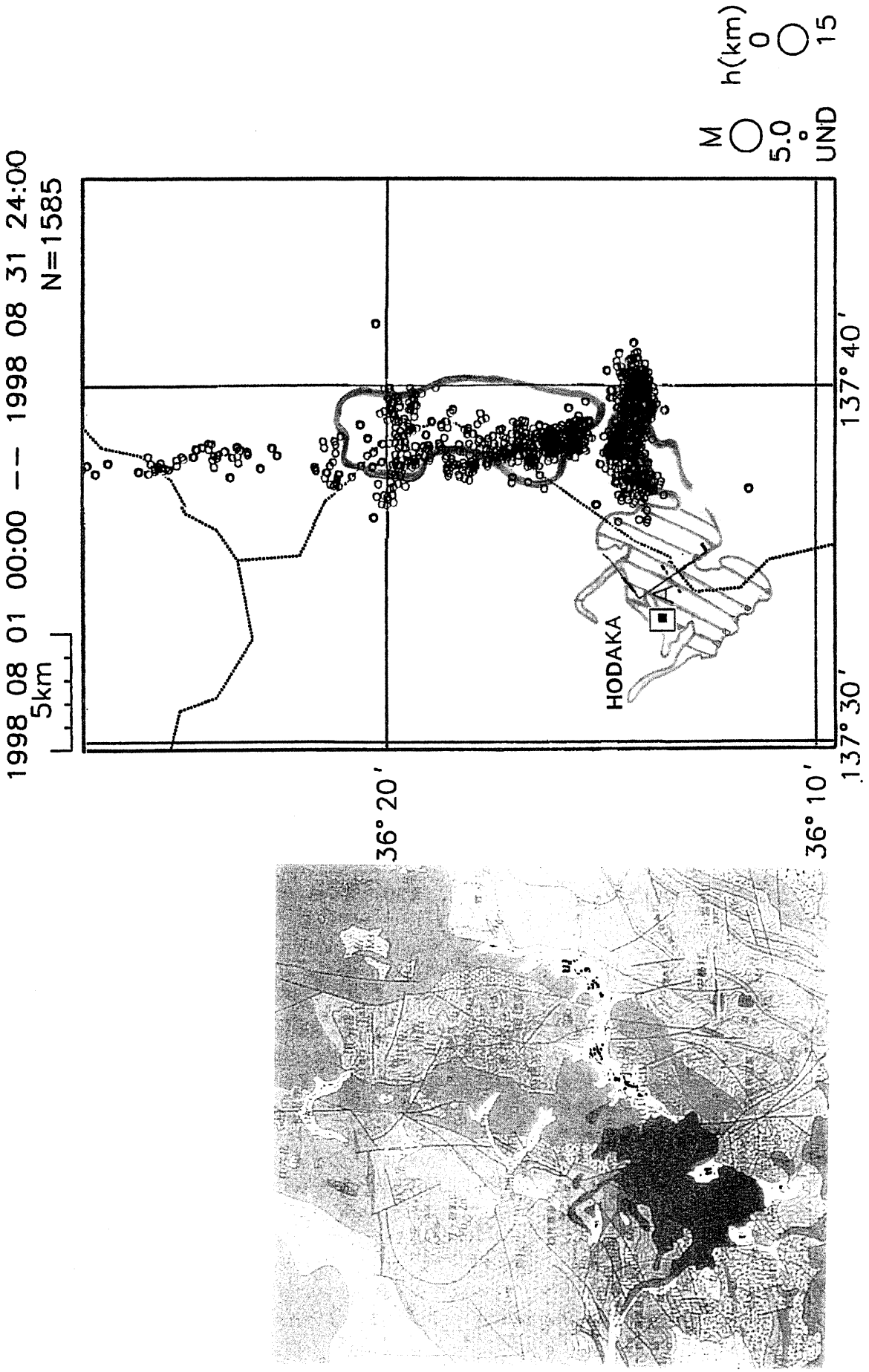

Fig. 20 Geological map overwritten with a seismic hypocenter obtained from a dense seismic network of JMA(Yoshida *et al.*, 1999).

practical and useful forecasting technique. Only in such situation we can expect a fruitful interaction between the evaluation effect of precursory phenomena from the standpoint of practical interests and investigation of generation processes from the perspective of basic scientific interests.

Anomalous electromagnetic phenomena have been predominantly studied from a more practical standpoint of prediction for a variety of physical quantities, frequency bands, and using numerous measurement techniques (e. g. Park *et al.*, 1993 : Parrot *et al.*, 1993 : Hayakawa and Fujinawa, 1994 : Hayakawa, 1999). Nonetheless, evidence of the interrelation between the phenomena and the earthquake occurrence has not been given affirmatively in this time period of the developing phase of the investigation.

Recent accumulation of field observations including the present report, laboratory experiments and theoretical analysis suggest that the ULF band phenomena could be induced in association with the occurrence of earthquakes and volcanic eruptions. In particular, seismic swarms have been found to be accompanied by electric field anomalies of the ultra-low frequency in geothermal zones (Zlotnicki and Le Mouel, 1990 : Bernard 1992, Fujinawa *et al.*, 1992 : Fujinawa *et al.*, 2000a). The analysis of data at the time when an earthquake swarm commenced in August 1998 in central Japan provided highly conclusive evidence to demonstrate that the source region was deep in the ground. And the phenomena could be explained by the electro-kinetic effect (Fujinawa *et al.*, 2000b, 2000c) in agreement with the previous inference (Bernard, 1992), based on observations around active volcanic zone. In this section we summarize the results to investigate the source mechanism of the ULF band electromagnetic field changes i. e. the confined water pressure variation inducing the anomaly.

(1) Typical Signals

We phowed that the anomalous ULF band signals observed at the time of a seismic swarm are dominated by typical pulse-like signals. In Fig. 15 we have already shown anomalous records including many such signals at the time of the seismic swarm which occurred in August 1998 in central Japan (Fujinawa *et al.*, 2000a and 2000b). Similar anomalies were also detected at Izu-Oshima in the course of almost periodical seismic swarms occurring to the east of the Izu Peninsula (Fig. 21a from Matsumoto *et al.*, 1996). At Awano site similar anomalies were detected in the case of a recent seismic swarm which occurred about 20 km northwest of the site (Fig. 21b from Fujinawa *et al.*, 2000b), and at Izu-Oshima at the time of the small volcanic eruption in 1990 (Fig. 21c. from Fujinawa *et al.*, 1992).

Those electric signals were all obtained using the ULEM (Takahashi and Takahashi, 1989 : Fujinawa and Takahashi, 1990). The fluctuating signal is schematically depicted in Fig. 22. The amplitude increased abruptly, decreased gradually till about half the peak amplitude, decreased sharply till about one -tenth of the peak, and finally returned to the gradual trend level.

The minor volcanic activity inducing anomalies in October 1990 in Izu-Oshima, an active volcanic island, followed the major eruption which occurred in 1986. Further, the seismic swarms have been occurring almost periodically since 1979 off the east coast of the Izu Peninsula, accompanying electic field anomalies. The seismic activity is possibly induced by the magma activity. The largest activity induced a submarine volcanic eruption in 1989 (e. g., Ida and Mizoue, 1991 ; Fujinawa *et al.*, 1991).

The area of the present swarm activity inducing the ULF band anomalies (Fig. 15) is known as a famous resort zone, and has numerous hot springs and geothermal resources (Fig. 4-1). It is suggested that the last swarm activities starting in August 1998 were caused by a kind of fluid movement possibly related to a change of magma chamber, though there were no volcanic tremors to suggest directly the involvement of the magma activity. The fluctuations at the time of the evaporation ejection in 1996 (Nakayama *et al.*, 1997) are different compared with the present one. At present we have no idea to explain the feature. The difference is to be taken up in future work.

Our observations in central Japan at 10 sites for more than almost 10 years clearly demonstrate that seismic swarms and volcanic eruption are preceded by conspicuous electric field changes possibly related to changes in the confined water regime in the crustal activity zone. Here we are going to introduce a quantitative discussion on the basis of governing field equations.

Mizutani *et al.*, (1976) attempted to explain the observed electromagnetic anomalies associated with the Matsushiro seismic swarm based on electro -kinetic effects. A self-potential (SP) anomaly has been provided for its generation mechanism by more evidence (Ishido, 1999 : Ishido and Mizutani, 1981 : Murakami *et al*, 1989) in comparison with other electromagnetic phenomena (e. g., Park *et al.*, 1993 : Parrot *et al.*, 1993).

Descriptions of the electromagnetic field induced by elecro-kinetic effect have been limited to stationary

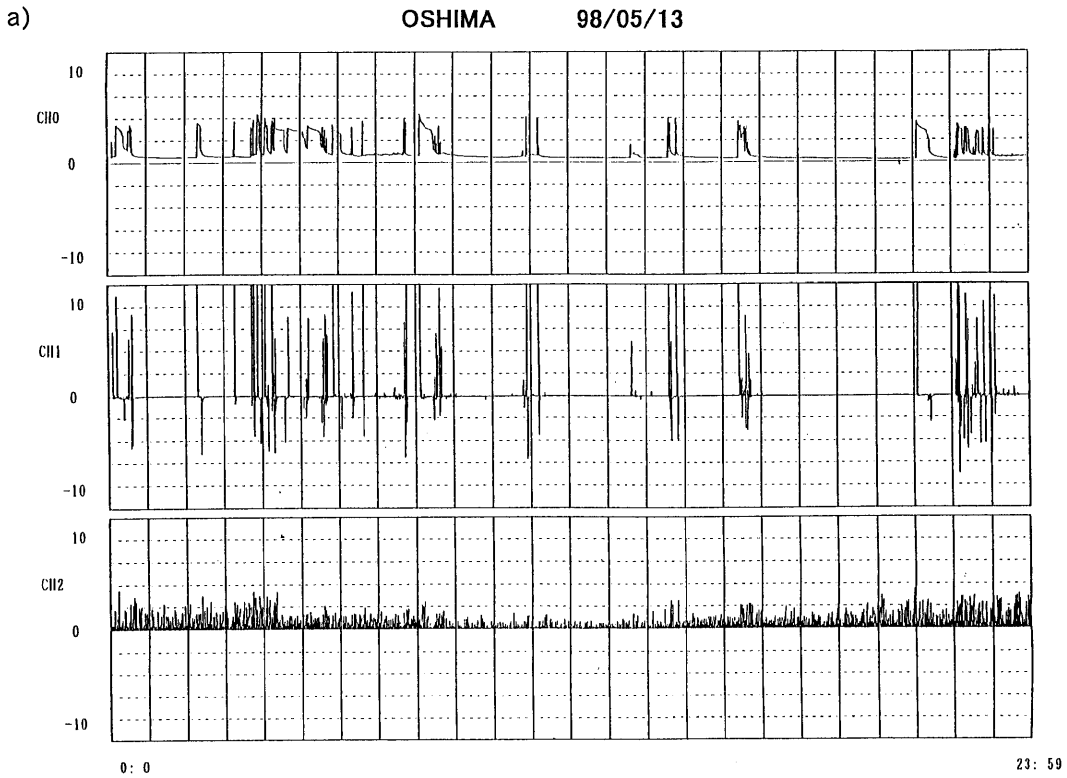

Fig. 21a Examples of ULF band anomalous signals observed by a borehole antenna at the time of seismic swarm activity. a) At Izu-Oshima in association with the swarm off the east coast of Izu peninsula.

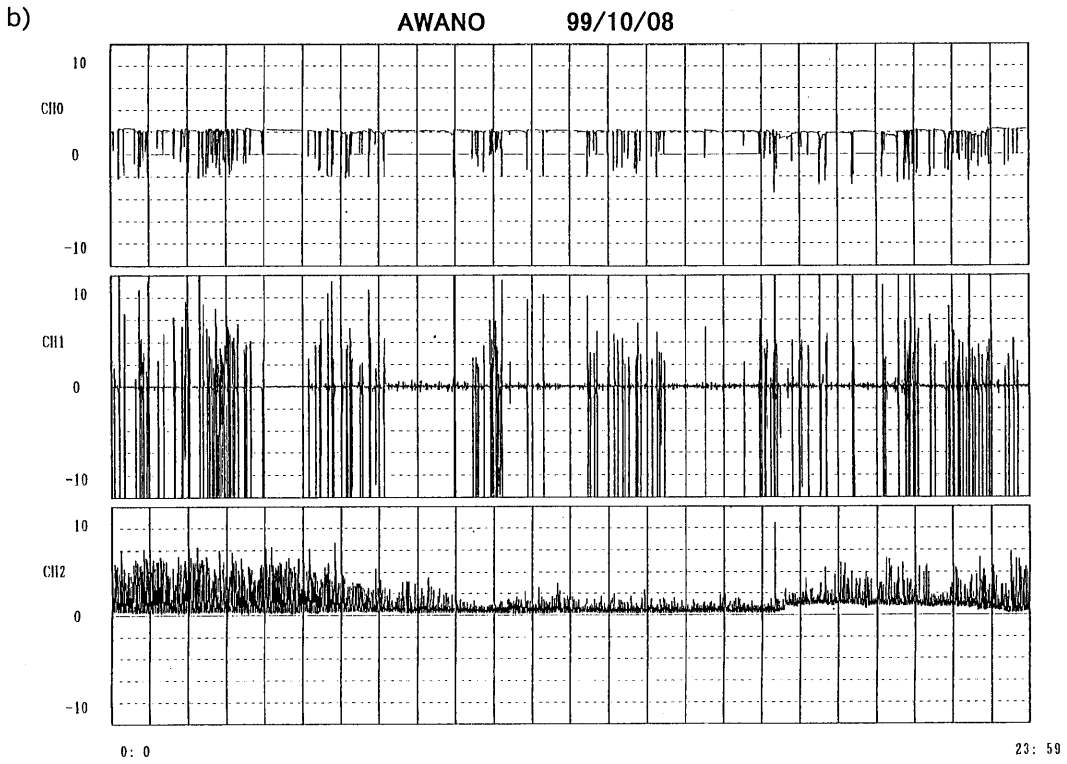

Fig. 21b Examples of ULF band anomalous signals observed by a borehole antenna at the time of seismic swarm activity. b) at Awano in association with the seismic swarm near Nikko in October 1999.

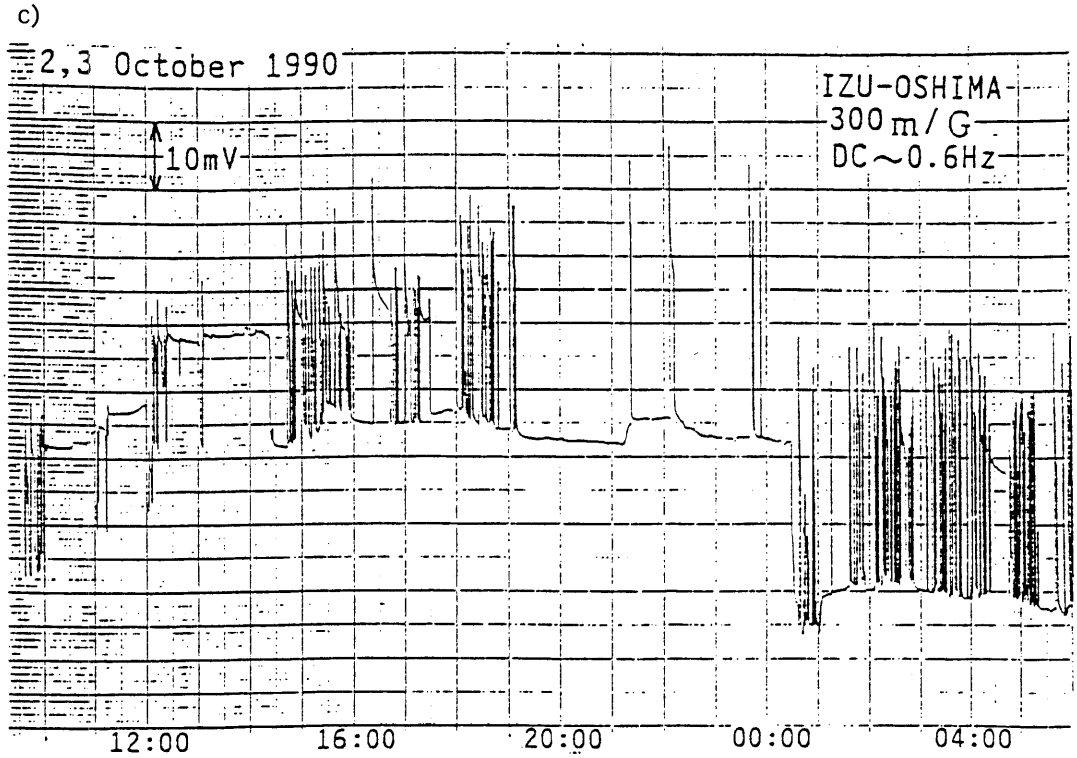

Fig. 20c Examples of ULF band anomalous signals observed by a borehole antenna at the time of seismic swarm activity. c) at Izu-Oshima in the case of a small volcanic eruption (Fujinawa *et al.*, 1992).

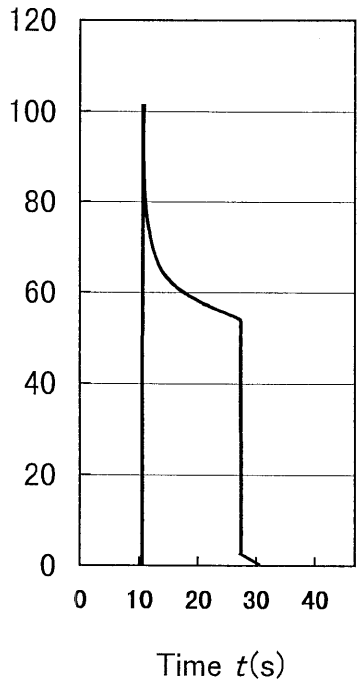

Fig. 22 A typical waveform of higher frequency electric anomalous signals at the time of a seismic swarm.

cases and the source region is limited to the boundaries of different substances (e. g., Fittermann, 1978).

An extended treatment of the field calculation for transient generating forces was first attempted by Majaeva *et al.*, (1997). A reformulation is given in the form which is more useful for a wide application (Fujinawa *et al.*, 2000c). Field strength distributions at particular distances from the source are then discussed. Thirdly, typical observed signals are used to estimate confined water pressure changes to explain the anomalous typical electric field waveform using a forward method.

(2) Formulation

Electromagnetic fields can be generated by ion transport in fluids through electro-kinetic effects with interaction between fluid motion and electric currents. The coupling has been described by the relation:

$$\begin{bmatrix} \boldsymbol{I}_e \\ \boldsymbol{I}_f \end{bmatrix} = \begin{bmatrix} L_{11} & L_{12} \\ L_{21} & L_{22} \end{bmatrix} \begin{bmatrix} -\nabla\phi \\ -\nabla P \end{bmatrix} \quad (1)$$

where $\boldsymbol{I}_e$ is electric current density, $\boldsymbol{I}_f$ fluid volume velocity, ϕ electric potential, P pore pressure, and L_{ij} the generalized coefficients of conductivity (Overbeek, 1953: Nourbehecht, 1963: Mizutani *et al.*, 1976: Ishido and Mizutani, 1981). Some of the coefficients are familiar electric coefficients: L_{11} is electrical conductivity, L_{12} fluid permeability in Darcy's law. The cross coupling term containing L_{12} or L_{21} corre-

sponds to the electro-kinetic effect with L_{12}/L_{11} being the streaming potential coefficient ($=C$), and L_{21}/L_{22} the electro-osmosis coefficient. The generalized conductivity coefficient matrix is shown to be symmetric from Onsagar's reciprocal relations (Nourbehecht, 1963)

From Equation (1) the electric current density $\boldsymbol{I}_e$ is described as,

$$\boldsymbol{I}_e = -\sigma(\nabla\phi + C\nabla P) \tag{2}$$

and the streaming potential coefficient as

$$C = \varepsilon\zeta / \sigma\mu_f \tag{3}$$

where ζ is the zeta potential in an electric double layer formed at a solid-liquid interface, ε the dielectric constant of the fluid, σ electric conductivity, and μ_f the viscosity of the fluid (Nourbehecht, 1963 : Mizutani *et al.*, 1976). This type of formulation has been adopted to explain the anomalous electromagnetic field changes at the time of earthquake occurrences (Mizutani *et al.*, 1976 : Murakami 1989 : Dobrovolsky *et al.*, 1989 : Fenoglio *et al.*, 1995) and the self-potential distribution in geothermal fields (Ishido and Pritchett, 1999).

These calculations assume the stationary state. We need a more general formulation based on Maxwell's equations for unstable electromagnetic fields as in the case where transient field changes induced by varying pore water pressure are treated (e. g., Fenoglio *et al.*, 1995). Majaeva *et al.*, (1997) attempted this kind of formulation. Under the assumption of a quasi-stationary situation with the negligible displacement current in the ordinary crustal conductive medium of the piece-wise continuous continuity, Maxwell's equations are :

$$\nabla \times \boldsymbol{E} + \frac{\partial \boldsymbol{B}}{\partial t} = 0 \tag{4a}$$

$$\nabla \times \boldsymbol{H} = \boldsymbol{I}^{(t)} \tag{4b}$$

$$\nabla \cdot \boldsymbol{B} = 0 \tag{4c}$$

$$\nabla \cdot \boldsymbol{E} = 0 \tag{4d}$$

where $\boldsymbol{E}$ is electric field intensity, $\boldsymbol{B}$ magnetic induction, $\boldsymbol{H}$ magnetic field intensity, and $\boldsymbol{I}^{(t)}$ the total electric current. It was shown by Nourbehecht (1963) that the electro-osmotic effect (term containing L_{21}/L_{22}) could be negligibly small compared with the hydrodynamical pressure term on the basis of the measurement data of Madden and his group. In that case we can think that the electric field is induced by the fluid pressure gradient ∇P as a cause (Nourbehecht, 1963).

Under this situation total electric current can be decomposed into ;

$$\boldsymbol{I}^{(t)} = \boldsymbol{I} + \boldsymbol{I}^{\mathrm{ext}} \tag{5}$$

where $\boldsymbol{I}$ is the internal current relating to electric field intensity through a constitutive relation and $\boldsymbol{I}^{\mathrm{ext}}$ is the external current generated in non-electromagnetic processes (e. g., Rokityansky, 1982) : a component induced by the electro-kinetic effect through the pore water pressure gradient in this case.

Additionally we use the constitutive equations :

$$\boldsymbol{D} = \varepsilon\boldsymbol{E}, \tag{6a}$$

$$\boldsymbol{B} = \mu\boldsymbol{H}, \tag{6b}$$

$$\boldsymbol{I} = \sigma\boldsymbol{E} \tag{6c}$$

where μ is magnetic permeability. The external electric current $\boldsymbol{I}^{\mathrm{ext}}$ can be naturally written down from Eq. (1), Eq. (2) and Eq. (5) as,

$$\boldsymbol{I}^{\mathrm{ext}} = -\sigma C\nabla P \tag{7}$$

The present formulation is general enough to make the most of resources developed in the field of the electromagnetic induction research to be used in this field to treat problems of the non-stationary state as well as any inhomogeneity in the medium.

The formulation has a limited applicability. It is because that the relationship between generalized velocity and thermodynamic force (Eq. (1)) is derived by assuming the steady state time invariant system. We can, however, expect that the formula will provide a useful tool to estimate physico-chemical states in the case of gradually varying systems of small flow densities (Nourbehecht, 1963).

In the piece-wise continuous medium, the electromagnetic field can be described by following partial differential equations, containing unique electromagnetic field quantity of interests,

$$\left(\Delta - \frac{1}{\varkappa^2}\frac{\partial}{\partial t}\right)\boldsymbol{F} = -\boldsymbol{\rho}(\boldsymbol{r}, t) \tag{8}$$

$$\frac{1}{\varkappa^2} = \sigma\mu$$

where $\boldsymbol{\rho}$ is the forcing term depending on field quantity of interests $\boldsymbol{F}$: electric field intensity $\boldsymbol{E}$, magnetic field intensity $\boldsymbol{H}$, and vector potential $\boldsymbol{A}$. The forcing term $\boldsymbol{\rho}$ are,

$$\boldsymbol{F} = \boldsymbol{E}\ ;\ \boldsymbol{\rho}_E = -\mu\partial\boldsymbol{I}^{\mathrm{ext}}/\partial t \tag{9a}$$

$$\boldsymbol{H}\ ;\ \boldsymbol{\rho}_H = \nabla \times \boldsymbol{I}^{\mathrm{ext}} \tag{9b}$$

$$\boldsymbol{A}\,;\ \boldsymbol{\rho}_A = \mu \boldsymbol{I}^{\mathrm{ext}} \tag{9c}$$

We can deduce simple characteristics of the electromagnetic field generated under the adopted assumptions from these relationships. For a homogeneous medium, the source term of the magnetic field intensity (9b) is:

$$\begin{aligned}\rho_{\mathrm{H}} &= -(\nabla C \times \nabla P + C\nabla \times \nabla P)\\ &= -\sigma \nabla C \times \nabla P\\ &= 0\end{aligned} \tag{10}$$

showing that magnetic field has not been generated in this case. It is easy to derive the source term in the case of a homogeneous medium includuing for the conductive boundary (Nourbehecht, 1963; Fitterman, 1978, 1979). There is no electric field at all for the stationary case induced by the electro-kinetic effect as is seen from (9). As to the dependence of the electric field on the medium parameters, the electric field is related to the streaming potential coefficient C itself, and the magnetic field to the degree of spatial inhomogeneity of the coefficient.

If boundary conditions on the surrounding surface of S for the domain V are specified the solution of the Eq. 8 is:

$$\begin{aligned}\psi(\boldsymbol{r}, t) = &\int_0^t \mathrm{d}t' \int_S \mathrm{d}S' \boldsymbol{n} \cdot (G\nabla'\psi - \psi\nabla' G)\\ &+ \int_0^t \mathrm{d}t' \int_V \mathrm{d}v' G\rho\\ &+ \frac{1}{\varkappa^2}\int_V \mathrm{d}v' G(\boldsymbol{r}, t; \boldsymbol{r}', 0)\,\psi(\boldsymbol{r}', 0)\end{aligned} \tag{11}$$

by the use of Green's function $G(\boldsymbol{r}, t \mid \boldsymbol{r}', t')$ satisfying the same boundary conditions:

$$\begin{aligned}&\left(\Delta - \frac{1}{\varkappa^2}\frac{\partial}{\partial t}\right) G(\boldsymbol{r}, t \mid \boldsymbol{r}', t') =\\ &\quad -\delta(\boldsymbol{r} - \boldsymbol{r}')\,\delta(t - t')\end{aligned} \tag{12}$$

(e. g., Morse and Feshbach, 1953), where $\boldsymbol{n}$ denotes the outward unit vector normal on the bounding surface, $\psi(\boldsymbol{r}', 0)$ the initial value of any related field quantities interested and ρ the corresponding forcing term denoted in Eqs. (9a, 9b and 9c).

In the case of the most simple n-dimensional homogeneous medium the Green function G^{∞} is explicitly given as,

$$\begin{aligned}G^{\infty}(\boldsymbol{r}, t; \boldsymbol{r}', t') = &\frac{1}{\varkappa^2}\left(\frac{1}{4\pi^2\varkappa^2(t - t')}\right)^{n/2}\cdot\\ &\exp\left\{-|\boldsymbol{r} - \boldsymbol{r}'|^2/(4\varkappa^2(t - t'))\right\} H(t)\end{aligned} \tag{13}$$

when the boundary condition is homogeneous at infinite boundary, and $H(t)$ is the step function:

$$\begin{aligned}H(t) = 0\,;\ t < 0\\ 1\,;\ t \geqq 0\end{aligned} \tag{14}$$

Then the solution ψ becomes a simple form:

$$\psi(\boldsymbol{r}, t) = \int_0^t \mathrm{d}t' \int_V G\rho \mathrm{d}v \tag{15}$$

in the case of zero initial value:

$$\psi(\boldsymbol{r}, 0) = 0 \tag{16}$$

In the case of layered earth the Green's function in the frequency domain can be obtained as in Raiche (1974) and Weidelt (1975). The most interesting condition is three layered earth consisting of overburden, a conductive layer and bedrock under the air of very small conductivity. The conductive layer is assumed to be the conduit of the ground water channel through which water is transmitted to the earthquake preparatory zone. The hydro-dynamical change in the conduit gives rise to the fluctuating self-potential which is detected efficiently by the ULEM. Here we do not present its calculation, referring to another paper.

(3) Spatio-temporal Distribution of Electric Fields

Here we will investigate the characteristics of electric fields for the simplest geometry of uniform space using the derived equations. Although the uniform model seems too simple for the practical application, it will provide us with a useful clue to understand general features of the electromagnetic field induced by the electro-kinetic effect, such as the detectability distribution and the source mechanism of the observed electric field anomalies.

In the case of isolated source starting at time $t = 0$, the electric field is described by the Green's function (13). This formula for the diffusion phenomena indicates that the electric signal is very large near the source and diffuses gradually at remote points. Fig. 23 illustrates the spatial field distribution $G^{(3)}$ at several time points from which the source appears for the uniform 3-D medium with crustal conductivity $\sigma =$ 0.01 S/m.

The signal decreases to less than one hundred compared with the initial strength after several ten seconds at the source point. Assuming that the relative signal detection limit corresponds to $G^{(3)} = 10^{-8}$, the signal at point $r = 50$ km can not be detected till the time $t = 1$ s, then increases over the threshold limit at about $t = 5$ s, and diminishing below the threshold at about $t = 50$ s. This means the signal can be detected in the time interval:

$$t_s(r, \sigma) \leqq t \leqq t_e(r, \sigma) \tag{17}$$

where t_s and t_e are the start times of the signal detec-

tion at the distance r nearer than the detection limit r_0, and the ending time, respectively. No signal can be detected at the remote point $r > r_0$. The maximum detection distance r_0 depends on the conductivity σ, and :

$$\begin{aligned} \sigma = 0.1; \quad & r_0 \fallingdotseq 40\text{km} \\ 0.01; \quad & 90\text{km} \\ 0.001; \quad & 200\text{km} \end{aligned} \tag{18}$$

for typical conductivity for assumed detection limit. The critical distance depends on conductivity. Eq. (17) indicates that the signal detection time is different at each observation point. The values of t_e and t_s, however, are less than several ten seconds for the conductivity ranges $\sigma = 0.1 \sim 0.001$ S/m, and never attain several ten minutes under a realistic crustal conductivity value. The larger retardation of the signal detection such as that observed at the time of the Noto Peninsula Earthquake of magnitude 6.6 in 1996 would seem to indicate different sources to induce signals at different sites.

There are several anomalous signal waveforms of electric fields in the ULF band i. e. dc-like changes and pulse-like changes (Fujinawa *et al.*, 1991, 1992, 2000a). The waveforms of the pulse-like signals of the dominant parts of the fluctuating higher frequency component are largely similar to those shown in Fig. 22. They are generally characterized by a sharp increase to a peak value A_P and decrease to several ten percent of the peak value, gradually decreasing at a duration almost identical to the pulse width T (several seconds ~ several hundreds seconds) as described in more detail below.

Phase 1 : Initial sharp rise attaining a peak A_P (time constant T_1 < several seconds)
Phase 2 : First decrease to several ten percent of Ap with time constant T_2 (several seconds ~ $0.5T$)
Phase 3 : Gradual decrease with time constant T_3 (several seconds ~ $O(T)$)
Phase 4 : Sharp decrease to about $0.1\,Ap$ with time constant T_4 ($\sim T_1$)
Phase 5 : Later gradual decrease to the background level with time constant T_5 ($\sim 0.1T$)

The peak value Ap is nearly uniform during a sufficient time interval of order several hours to several days probably corresponding to a globally stationary regime of the interaction field between confined water and induced electic filed (Fujinawa *et al.*, 1992, 2000a, b).

The evolution of the electric field changes of a typical waveform is very similar to the water pillar height change of a geyser (observation at one of the geysers in southern Hokkaido) supporting the hypothesis that the generation mechanism is related to coupling with the underground flow. We will infer the confined pressure changes in time giving rise to the observed electric signals. If the confined fluid pressure $P(\boldsymbol{r}, t)$ is assumed as,

$$P = P_1(\boldsymbol{r})g(t) \tag{19}$$

The electric field intensity E is ;

$$\psi_E = \frac{\chi^2}{(4\pi\chi^2)^{3/2}}(-\mu C \nabla P_1)\tilde{g} \cdot \int_0^t dt_0 \frac{dg^*(t_0)}{dt} \frac{e^{-r^2/(4\pi\kappa^2(t-t_0))}}{(t-t_0)^{3/2}} H(t-t_0) \tag{20}$$

where,

$$g(t) = \tilde{g} \cdot g^*(t) \tag{21}$$

As an example the electric field intensity ψ_E for $\sigma = 0.01$ S/m is calculated by taking $g^*(t)$ as

$$\begin{aligned} g^*(t) = & \quad 0, & & t < 0 \\ = & \quad 100, & & 0 \leqq t < 0.25\text{s} \\ = & \quad 0.6 \sim 0.5, & & 0.25 \leqq t < 10.25\text{s} \\ = & \quad 0.5 \sim 0, & & 10.25 < t \leqq 10.75\text{s} \end{aligned} \tag{22}$$

(see Fig. 24).

The time evolution of the electric field E is highly similar at the zone near the source because of the diffusion property i. e. the phase 1 and phase 2 of a sharp change are conserved in the near field (Fig. 25). But the signal is sufficiently diffused at several kilometers distance from the source to lose the sharpness of the driving force. It is seen that degree of signal deformation increases with distance from the source, and amplitude decreases very rapidly. In other words, signal waveform tells us about the source distance. We can infer that the typical anomalies containing sharp rise detected by the borehole antenna at the time of crustal activities (Fig. 15 and Fig. 21) were generated near the source. The amplitude ratio of the main phase 3 to the peak value is also conserved in the near field, but decrease rapidly in the far distance. The property could be also used to infer the source distance.

We need to compare the observed signals with those at the reference site to infer the distance of the source. Or, we can infer the source parameter using signal wareform at multiple sites based on the inversion techniqee. But more piadically, we could rely on the plausible assumption of the sharp rise causing failure

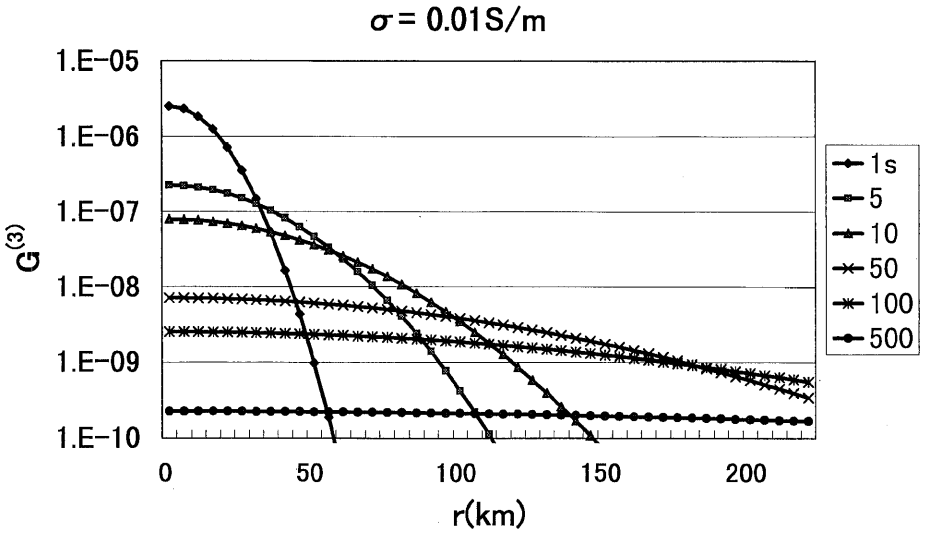

Fig. 23 Electric field strength distribution in space at several times from the onset of the localized source at origin, assuming an homogeneous medium of conductivity $\sigma=0.01$ S/m.

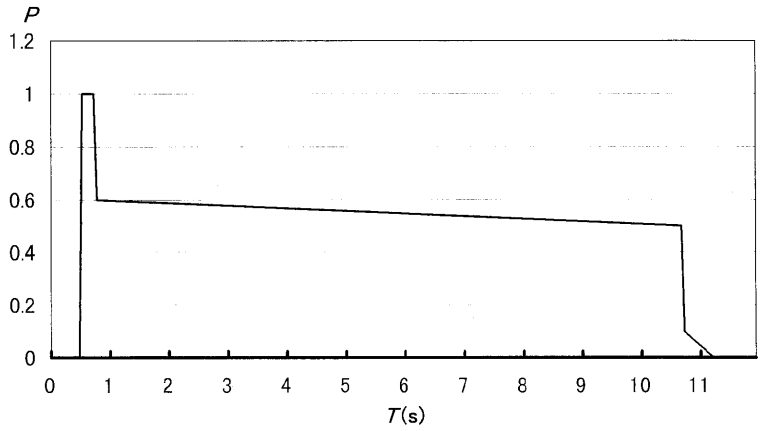

Fig. 24 Assumed time change of the rate of pressure change.

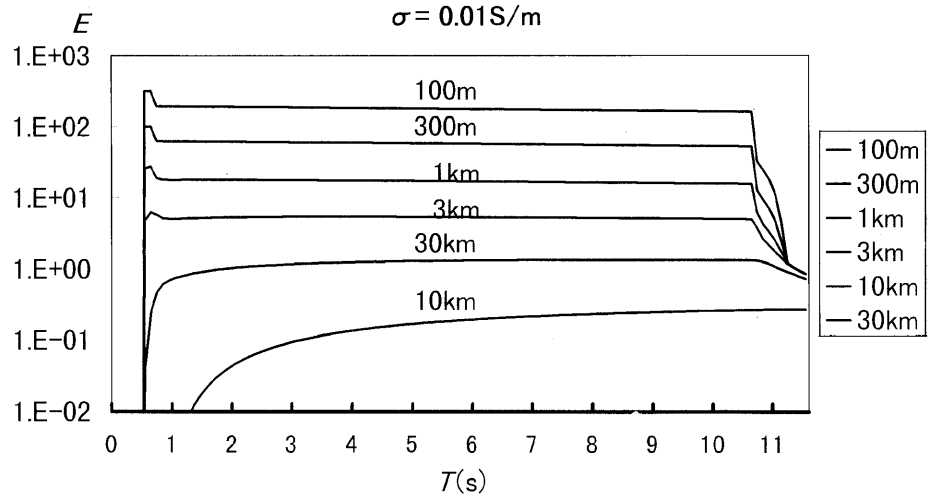

Fig. 25 Electric field strength evolution in time at several distances from the source in the homogeneous medium of $\sigma=0.01$ S/m when the forcing term is that shown in Fig. 24.

of sealed compartments (Byerlee, 1993 : Fenoglio *et al.*, 1995). The gradual increase means remote position from the source. The dominant phase 3 of signal evolution indicates the almost constant rate of the pressure change.

Attempts are made to match the electric field shown in Fig. 26 (sou.) with the time rate of the pressure change $\partial P/\partial t$ shown in the same Figure (ob.) by a method of trial and error. The calculated field is for the site $r = 300$ m, using the conductivity $\sigma = 0.01$ S/m. The obtained synthetic waveform corresponding to the assumed forcing term shown in Fig. 26 (sou.) is illustrated in Fig. 26 (cal.) with a typical signal (ob. in the Fig. 26) for the sake of comparison. In the near field there is a large degree of similarity between the waveform of the source function and the synthetic curve. The minor discrepancy in the synthetic waveform compared with the observed one (Fig. 26) could be reduced by choosing a more appropriate source function g^*. In principle we can calculate the source time function from the observed signals if we have sufficient knowledge of the streaming potential coefficient distribution, in the same way as for the seismic fault mechanism analysis. Estimations treating a more realistic situation are to be the subjects of future work.

The typical signals indicate that the rate of the

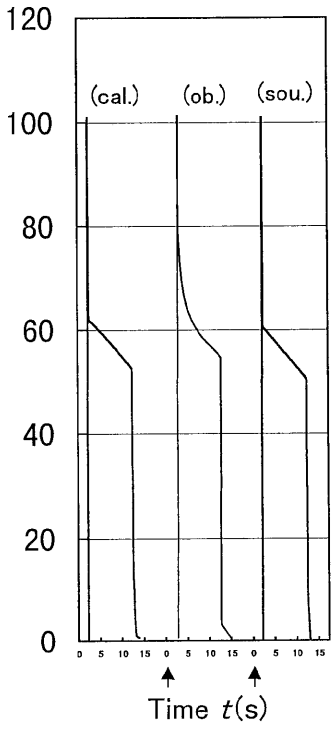

Fig. 26 A comparison of the synthetic waveform (cal.) for the source function (sou.) and the observed waveform (ob.)

confined pressure changes are dominantly positive, although polarity of the signals is negative during a small part of whole time period (Fujinawa *et al.*, 1992, 2000a, 2000b, 2000c). This implies that there must be a persistent increase or decrease in the confined pressure during these time periods. The longer period components of the pressure changes corresponding to the dc-like electric signals may compensate, more or less, the accumulated increase or decrease induced by a considerable number of the higher frequency components.

The electric field anomalies have been observed in Greece (Varotsos *et al.*, 1996) and in Japan (Nagao *et al.*, 1996) for the case of the main-shock-aftershock sequence. Those signals have longer period and much shorter duration than those discussed here. We could interpret the long period feature on the basis of the extinction of the higher frequency components at remote points as suggested from the dependence of signal waveforms distance.

From observational results the ULEM is known to provide us with a great potential to detect even a small signal induced by a confined water pressure change (Fujinawa *et al.*, 2000b, 2000c). Moreover, the remarkable long distance detectability amounting to several ten times the rupture area, as claimed in Greece (Varotsos *et al.*, 1996), if it is not artificial noise, could be understood due to the installment of the sensor near the ground surface zone in good contact to the local source which is well connected with the earthquake ruptur zone. The zone is assumed to connect well to the seismic zone through ground water conduit. We need, however, to show the existence of the conduit on the basis of the crustal structure of a high resolution survey for the purpose of further development.

Conclusion

The analysis of electromagnetic field variation data obtained by means of the ultra long vertical electric potential measurement (ULEM) around the time of a seismic swarm occurrence in central Japan in 1998 indicated,

1) The electric field anomaly is well correlated with the crustal activity around the site.
2) The field changes appeared in the dc, ULF and ELF/VLF bands, although the ELF/VLF bands were not always accompanied by other bands.
3) Electric signals associated with the seismic swarm are detected within 100 km spacing distance of the network.

4) The anomalies were observed more clearly by using the borehole antenna (ULEM).
5) The electric field anomaly is suggested to be caused by the electric-kinetic effects induced by variations in the confined water circulation regime.
6) The selectivity of the signal detection can be attributed to the heterogeneous distribution of the degree of connectivity between the source generation zone and the observation site.
7) It is suggested that pore water pressure changes causing earthquakes can be effectively observed using special sensors in the borehole itself or an electric field sensor embedded in the borehole.

Our records show that clear electric anomalies precede seismic swarms and vapor ejections, and this lead us to conclude that clear anomalies could also be detected before shallow earthquakes if the sensors are carefully installed.

Acknowledgments

We would like to express our thanks to the many persons, institutes and organizations contributing to this research, especially to Dr. Hiroshi Takahashi, Dr. Ryuji Ikeda, Dr. Yukio Hagiwara, Dr. Shigetsugu Uyehara, NEC Corporation, Nippon Steel Welding Products & Engineering Co., Ltd., Tecs Inc., Sankousha Corporation, Franklin Japan Co., Ltd., and land owners, Mr. Tanaka. We thank Ms. Yumiko Yamauchi and Mr. Wu Yueshung for their helps to prepare this manuscript. Careful check by an anonymous reviewer is greatly appreciated.

Correspondence and requests for materials should be addressed to Yukio Fujinawa (e-mail: fujinawa @bosai.go.jp)

References

1) Allen, C. R. (1982): Earthquake prediction-1982 overview. Bull. Seis. Soc. Am. **72**, S331.
2) Bernard, P. (1992): Plausibility of long distance electrotelluric precursors to earthquakes. J. Geophys. Res. **97**, 17531-17546. Bernard P., Lemouel, J. L., 1996, On electrotelluric signals, In: J. Lighthill (Editor), A Critical Review of Van. World Scientific Pub. Co. Ltd., 118-154.
3) Bernard P., Lemouel, J.L., 1996, On electrotelluric signals, In: J. Lighthill (Editor), A Critical Review of Van. World Scientific Pub. Co. Ltd., 118-154.
4) Byerlee, J. (1993): Model for episodic flow of high pressure water in fault zone before earthquakes. Geology **21**, 303-306.
5) Dobrovolsky, I. P., Gershenzon, N. I. and Gokhberg, M. B. (1989): Theory of electrokinetic effects occurring at the final stage in the preparation of a tectonic earthquake. Phys. Earth Planet. Inter. **57**, 144-156.
6) Fenoglio, M. A., Johnston, M. J. S. and Byerlee, J. D. (1995): Magnetic and electric fields associated with changes in high pore pressure in fault zones: Application to the Loma Prieta ULF emissions. J. Geophys. Res. **100**, 12951-12958.
7) Fujinawa, Y. and Takahashi, K. (1990): Emission of electromagnetic radiation preceding the Ito seismic swarm of 1989. Nature **347**, 376-378.
8) Fujinawa, Y. and Takahashi, K. (1996): in A Critical Review of VAN (ed. Lighthill, J.) 314-323 (World Scientific, 1996).
9) Fujinawa, Y. and Takahashi, K. (1998): Electromagnetic radiations associated with major earthquakes. Phys. Earth Planetary Inter. **105**, 249-259.
10) Fujinawa, Y., Takahashi, K. and Kumagai, T. (1992): A study of anomalous underground electric field variations associated with a volcanic eruption. Geophys. Res. Lett. **19**, 9-12.
11) Fujinawa, Y., Takahashi, K., Matsumoto, T. and Kawakami, N. (1997): Proc. Japan Acad. 33-38.
12) Fujinawa, Y., Shimada, S., Ohmi, S., Sekiguchi, S., Eguchi, T., Okada, Y. (1991): Fixed-Point GPS Observation of Crustal Movement Associated with the 1989 Seismic Swarm and Submarine Volcanic Activities off Ito, Central Japan. J. Phys. Earth **39**, 141-153.
13) Fujinawa, Y., Takahashi, K., Matsumoto, T., Iitaka, H., Yamane, S., Nakayama, T., Sawada, T., Sakai, H. (2000a): Electromagnetic Field Anomaly Associated with the 1998 Seismic Swarm in Central Japan. Physics and Chemistry of the Earth. **25**, 247-253.
14) Fujinawa, Y., Takahashi, K., Matsumoto, T., Iitaka, H., Yamane, S., Nakayama, T., Sawada, T., Sakai, H. (2000b): Characteristics of Electromagnetic Field Changes Related with Earthquakes Swarms. Journal of Applied Geophysics
15) Fujinawa, Y., Matsumoto, T. and Takahashi, K. (2000c): Some Features of ULF Band electromagnetic Field Changes Related with Earthquakes. J. of Applied Geophysics
16) Fitterman, D. V. (1978): Electrokinetic and magnetic anomalies associated with dilatant regions in a layered Earth. J. Geophys. Res. **83**, 5923-5928.
17) Fitterman, D. (1979): Calculations of self-potential anomalies near vertical contacts. Geophysics **44**, 195-205.
18) Geller, R. J. (1991): Shake-up for earthquakes predic-

tion. Nature **352**, 275-276.

19) Geller, R. J. (1996) (ed.): Debate on evaluation of the VAN Method. Geophys. Res. Lett. **23**, 1291-1452.

20) Gokhberg, M. B., Gufeld, I. L., Marenko, V. F., Rozhnoy, A. A., Ponomarev, E. A., Yampolsky, V. S. (1987): Investigation of disturbances of natural and artificial electromagnetic fields by a source of seismic origin. Izv. Acad. Sci. USSR, Phys. Solid Earth (U.S.A.) **2**, 17-24.

21) Hamada, K. (1991): Unpredictable earthquakes. Nature **353**, 611-612.

22) Hayakawa, M. (1999) (ed.): Atmospheric and Ionospheric Electromagnetic Phenomena Associated with Earthquakes (Terra Scienctific Pub. Co., Tokyo, 1999).

23) Hayakawa, M. and Fujinawa, Y. (1994) (eds.): Electromagnetic phenomena related to earthquake prediction (Terra Scientific Pub., Tokyo,).

24) Ida, Y. and Mizoue, M. (1991): Seismic and volcanic activity in around the Izu Peninsula and its tectonic implications. J. Physics. Earth **39**, 1-460.

25) Ishido, T. and Pritchett, J. W. (1999): Numerical Simulation of electrotelluric potentials associated with subsurface florid flow. Geophys. Res. Lett.

26) Ishido, T. and Mizutani, H. (1981): Experimental and theoretical basis of electrokinetic phenomena in rock-water systems and its applications to geophysics. J. Geophys. Res. **86**, 1763-1775.

27) Main, I. (1996): Statistical Physics, seismogeneisis and seismic hazards, Rev. Geophysics **34**, 433-462.

28) Main, I. (1997): Long odds or predicion. Nature **385**, 19-20.

29) Majaeva, O., Fujinawa, Y. and Zhitomirsky, M. E. (1997): Modeling of non-stationary electrokinetic effect in a conductive crust. J. Geomag. Geoelectr. **49**, 1317-1326.

30) Matsumoto, T., Fujinawa, Y. and Takahashi, K. (1996): ULF-bands electric field changes related to seismic swarms. J. Atmospher. Electri. **16**, 175-191.

31) Mizutani, H., Ishido, T., Yokokura, T. and Ohnishi, S. (1976): Electrokinetic phenomena associated with earthquakes. Geophys. Res. Lett. **3**, 365-368.

32) Morse, P. M. and Feshbach, H. (1953): Methods of Theoretical Physics (Mcgraw-Hill Book Compnay, Inc., Tokyo,).

33) Murakami, H. (1989): Geomagnetic Fields Produced by Electrokinetic Sources. J. Geomag. Geoelectri. **41**, 221-247.

34) Nagao, T., Uyeda, S., Asai, Y. and Kono, Y. (1996): Anomalous changes in geoelectric potential preceding four earthquakes in Japan in A Critical Review of Van (ed. Lighthill, J.) 292-300 (World Scientific Pub. Co. Ltd., 1996)

35) Nakayama, T., Sawada, T., Takahashi, K. and Fujinawa, Y. (1997): Electric field increase preceding the vapor eruption of 1996 at the foot of mount Yakedake. Proc. 1997 Conductivity Anomaly Research, 195-201.

36) Nourbehecht, B. (1963): Irreversible thermodynamic effects in inhomogeneous media and their applications in certain geoelectric problems, Mass. Inst. of Technol., Cambridge, Mass.

37) Oike, K. and Yamada, T. (1994): Relationship between shallow earthquakes and electromagnetic noises, in the LF and VLF ranges, in Electromagnetic Phenomena Related to Earthquake Prediction (eds. Hayakawa, M. & Fujinawa, Y.), 115-130, Terra Scientific Pub., Tokyo, 1994.

38) Overbeek, J. T. (1953): Thermodynamics of electrokinetic phenomena. J. Colloid Sci. 8, 420.

39) Park, S. K., Johnston, M. J. S., Madden, T. R., Morgan, F. D. and Morrison, F. (1993): Electromagnetic precursors to earthquake in the ULF band: A review of observations and mechanisms. Rev. Geophys. **31**, 117-132.

40) Parrot, M., Achache, J., Berthelier, J. J., Blanc, E., Deschamps, A., Lefeuvre, F., Menvielle, M., Plantet, J. L., Tarits, P., Villain, J. P. (1993): High-frequency seismo-electromagnetic effects. Phys. Earth Planet. Inter. **77**, 65-83.

41) Popov, L. N., Krakovetzkiy, Y. K., Gokhberg, M. B. & Pilipenko, V. A. (1989): Terrogenic effects in the ionosphere: a review. Phys. Earth Planet. Inter. **57**, 115-128.

42) Raiche, A. P. (1974): An integral equation approach to three-dimensional modelling. Geophys. J. R. astr. Soc. **36**, 363-376.

43) Rokityansky, I. I. (1982): Geoelectromagnetic Investigatin of the Earth's Crust and Mantle (Springer-Verlag, Berlin,).

44) Rikitake, T. (1976): Earthquake Prediction (Elsevier, New York,).

45) Rhoades, D. A. and Evison, F. F. (1989): Time variable foactors in earthquake hazard. Tectonopysics **167**, 201-210.

46) Takahashi, H. and Takahashi, K. (1989): Tomography of seismo-radio wave source regions for predicting imminent earthquakes. Phys. Earth and Planetary Inter. **51**, 40-44.

47) Varotsos, P. and Lazaridou, M. (1991): Latest aspects on earthquake prediction in Greece based on seismicelectric signals. Tectonophysics **188**, 321-347.

48) Varotsos, P., Lazaridou, M., Eftaxias, K., Antonopoulos, G., Makris, J., Kopanas, Varotsos, P. (1996): Short term earthquake prediction in Greece by seismic electric signals, in A critical review of VAN

(ed. Lighthill, J.) 29-76 (World Science Publishing Co., Pte Ltd., Singapore, 1996).

49) Weidelt, P. (1975): Electromagnetic inductin in three -dimensional structures. J. Geophys. **41**, 85-109.

50) White, G. F. and Haas, J. E. (1975): Assessment of research on natural 1299. hazards. MIT press, 487.

51) Wood, H. O. and Gutenburg, B. (1935): Earthquake prediction. Science **82**, 219-220.

52) Wyss, M. (1991): Evaluation of Proposed2Earthquake Precursors (AGU, Washington, D. C.,).

53) Wyss, M. and Booth, D. C. (1997): The IASPEI procedure for the evaluation of earthquake precursors. Geophys. J. Internat. **131**, 423-424.

54) Yamada, T. and Oike, K. (1996): Electric radiation phenomena before and after the 1995 Hyogo-ken Nanbu Earthquake. J. Phys. Earth **44**, 405-412.

55) Yoshida, S., Clint, O. C. and Sammonds, P. R. (1998): Electric potentail changes prior to chear fracure in dry and saturated rocks. Geophycs. Res. Lett. **25**, 1577 -1580.

56) Zlotnicki, J. and Le Mouel, J. L. (1990): Possible electrokinetic origin of large magnetic variations at La Fournaise Volcano. Nature **343**, 633-636.

Technical Note of the National Research Institute for Earth Science and Disaster Prevention, No. 204 ; March, 2000

穂高における電界変動観測（19935—1999）

高橋耕三*・藤縄幸雄**・松本拓巳**・中山　武***・
澤田豊明***・酒井英男****・飯高　弘*****

要　旨

地震発生に伴って生起する現象と地震との関係を定量的に調べ，地震前兆現象としての評価に資するため，関東東海地域で，主としてボアホールアンテナを用い電磁界計測を行っている．1993年から穂高において，長さ400mの蒸気井のためのケーシングパイプを用いた電場観測をほぼ連続して行っている．観測点の近くで1998年8月より群発地震が発生し，それに伴って顕著な異常電界変動が記録された．その異常信号について，その特徴，発生機構について述べる．粟野，伊豆大島をはじめ10観測点の長期にわたるデータを含めた解析の結果，火山活動，群発型の地震の場合には，地下間隙水の変動に伴うと思われる電磁界変動が発生し，ボアホールなどを使った超長電極による計測（Ultra Long Electrode Measurement： ULEM）によって，異常信号を十分大きなS/Nで検出できることを明らかにした．なお，検出された異常電磁界変動の特異性を示すため，デジタル記録開始以降の全モニター記録も合わせて公刊する．

キーワード：地震予知，前兆現象，評価，電磁界変動

*通信総合研究所
**防災科学技術研究所
***京都大学防災研究所
****富山大学
*****電子技術総合研究所

Appended Table

Amplitude gain data from the start of the observation for dc, ULF, and ELF/VLF bands. The scales shown in Fig. 5～7, 8～12, Fig. 15 are real ones corrected for these values. But the results shown in Appended Figures are not corrected for the calibration constant. Reader can infer the absolute value by considering these constants and whole monitoring records (as Fig. 5～7) are shown in the appended Figure without any deletion.

Hodaka AMP-GAIN

	1995				1996				1997			
	1/13	3/16	5/18	9/12	4/23	6/25	8/26	10/28	3/17	7/14		
DC Offset (mV)	975	950	1000	1050	1060	1100	1050	1090	-			
0 – 0.7 Hz	50	100	-	-	-	-	-	-	200			
0.01 – 0.7 Hz	500	5000	-	-	-	-	2000	-	-			
1 – 9 kHz	250	1000	-	500	1000	-	-	-	-			

	1997		1998			1999					
	7/14	12/9	3/29	5/31	7/12	6/8	8/12	10/12	10/14	12/26・27	
DC Offset (mV)	1100	-	-	-	1000	-	-	1050	-	1000	
0 – 0.7 Hz	200	Gain Down	100	200	-	100	-	-	-	10	
0.01 – 0.7 Hz	2000	-	-	-	-	-	1000	-	500	125	
1 – 9 kHz	1000	2000	-	-	-	-	-	4000	-	Rest	

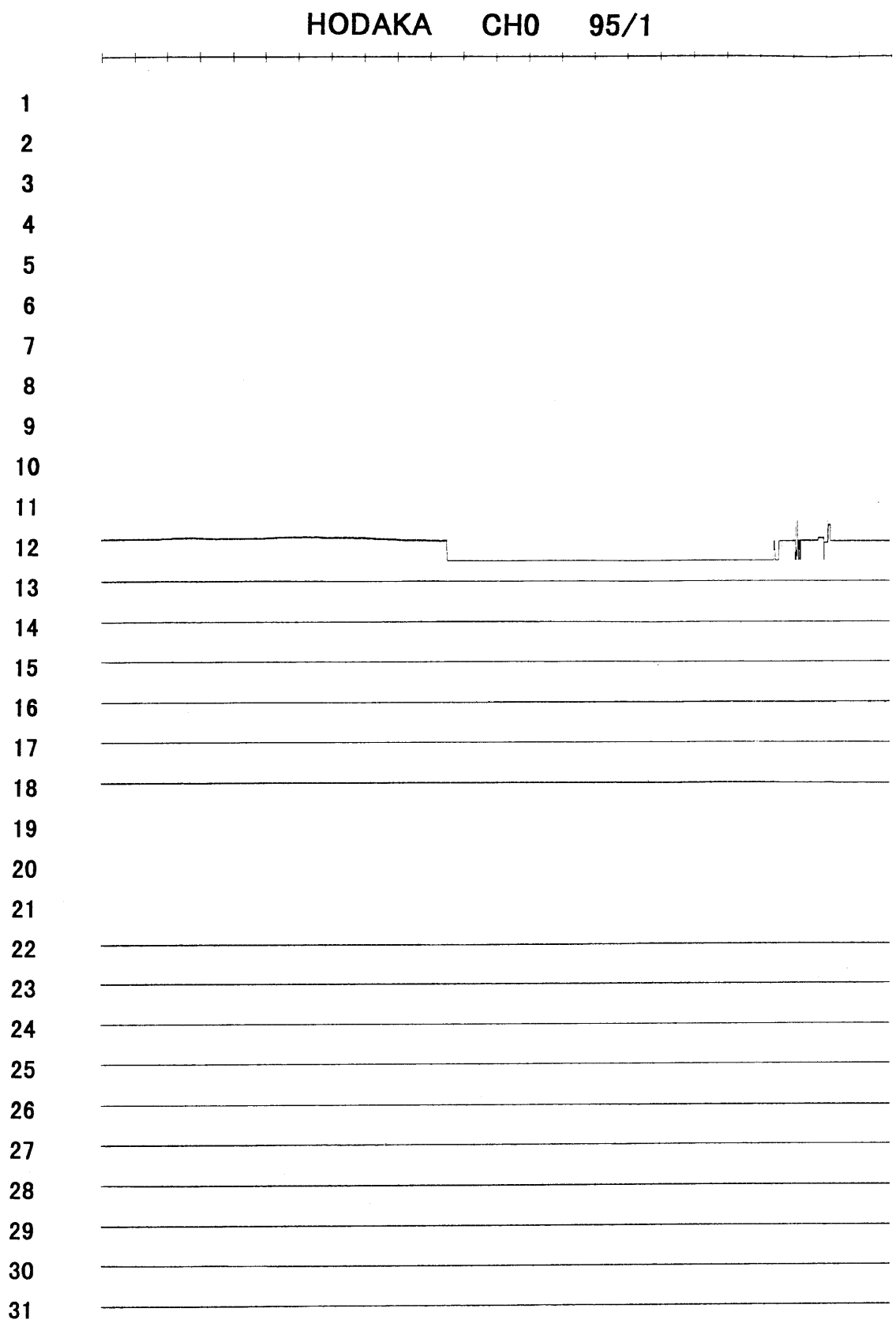

Fig. A-95-1-0 Monitoring records of electric field measurement suing a long borehole (VLEM) at Hodaka site from January 1995 through December 1999. Each sheet is recorded for one frequency band (CH0 : dc, CH1 : ULF, CH2 : ELF/VLF) during the one month indicated. The Saturation level is the same as shown in fig. 15. A particular Figure is to be referred to as Fig. A-a-b-c, where a : year, b : month, d : channel number. Note that amplification factors are not constant. They are shown in the appended Table.

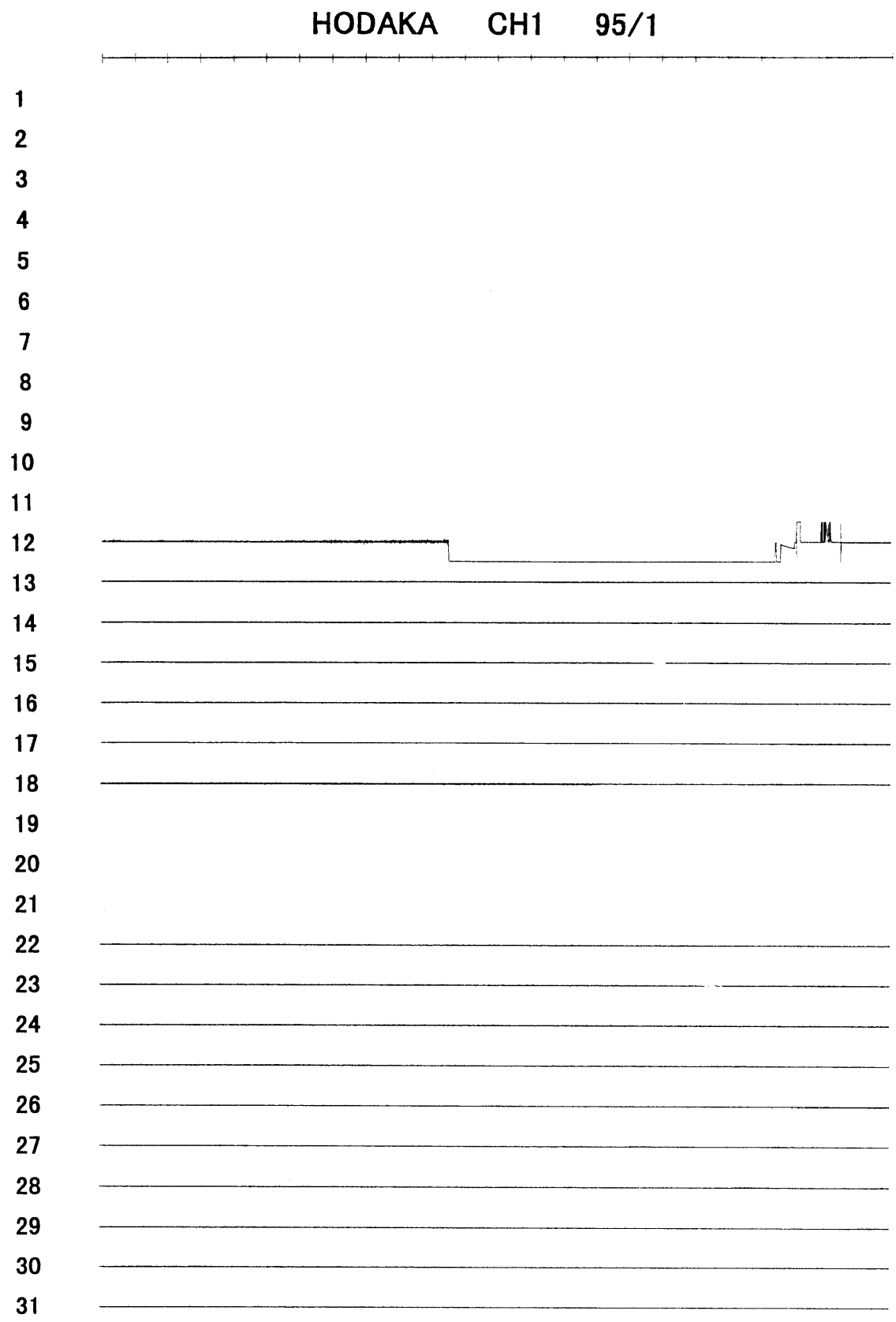
HODAKA CH1 95/1
1
2
3
4
5
6
7
8
9
10
11
12
13
14
15
16
17
18
19
20
21
22
23
24
25
26
27
28
29
30
31

Fig. A-95-1-1

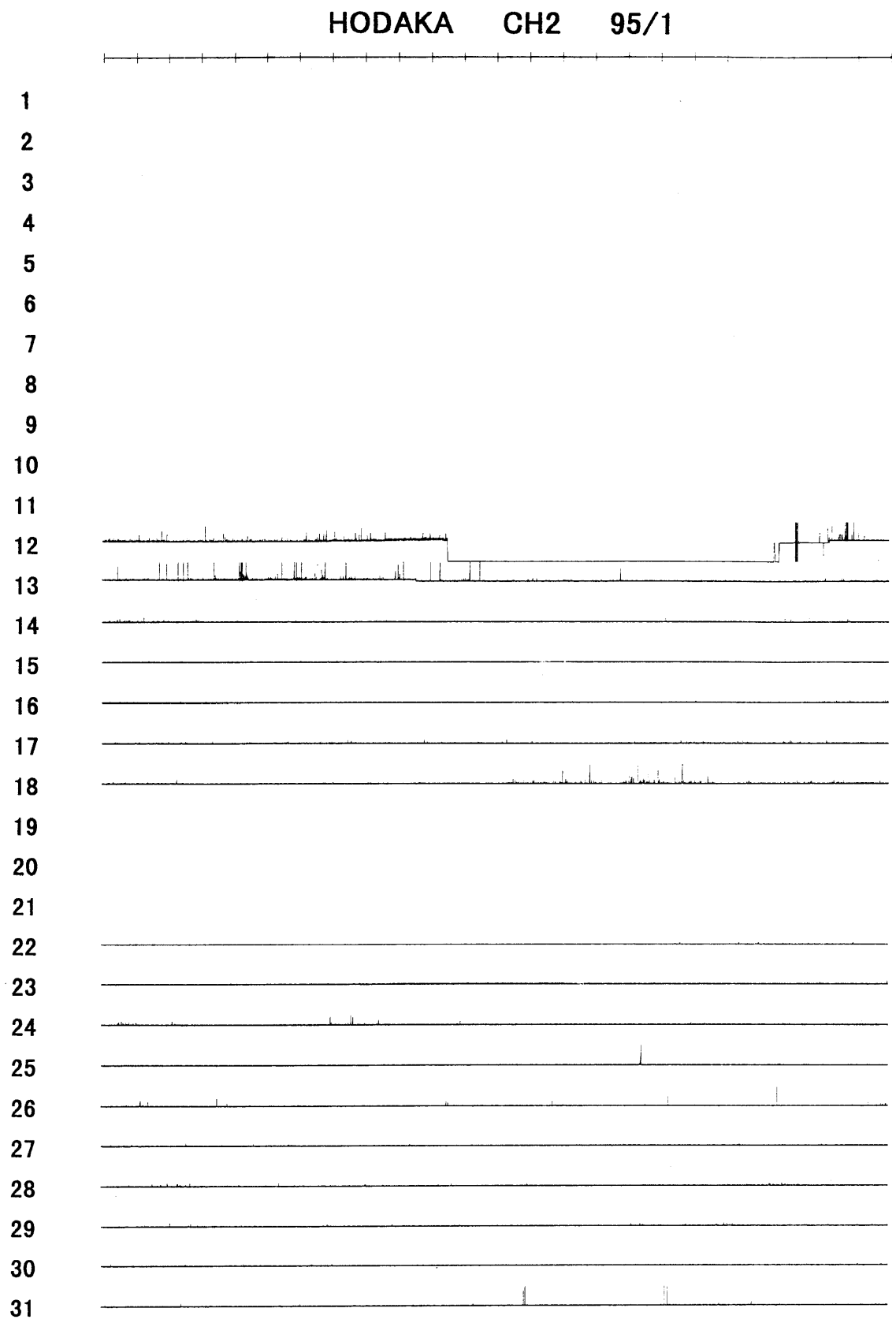
HODAKA CH2 95/1
1
2
3
4
5
6
7
8
9
10
11
12
13
14
15
16
17
18
19
20
21
22
23
24
25
26
27
28
29
30
31

Fig. A-95-1-2

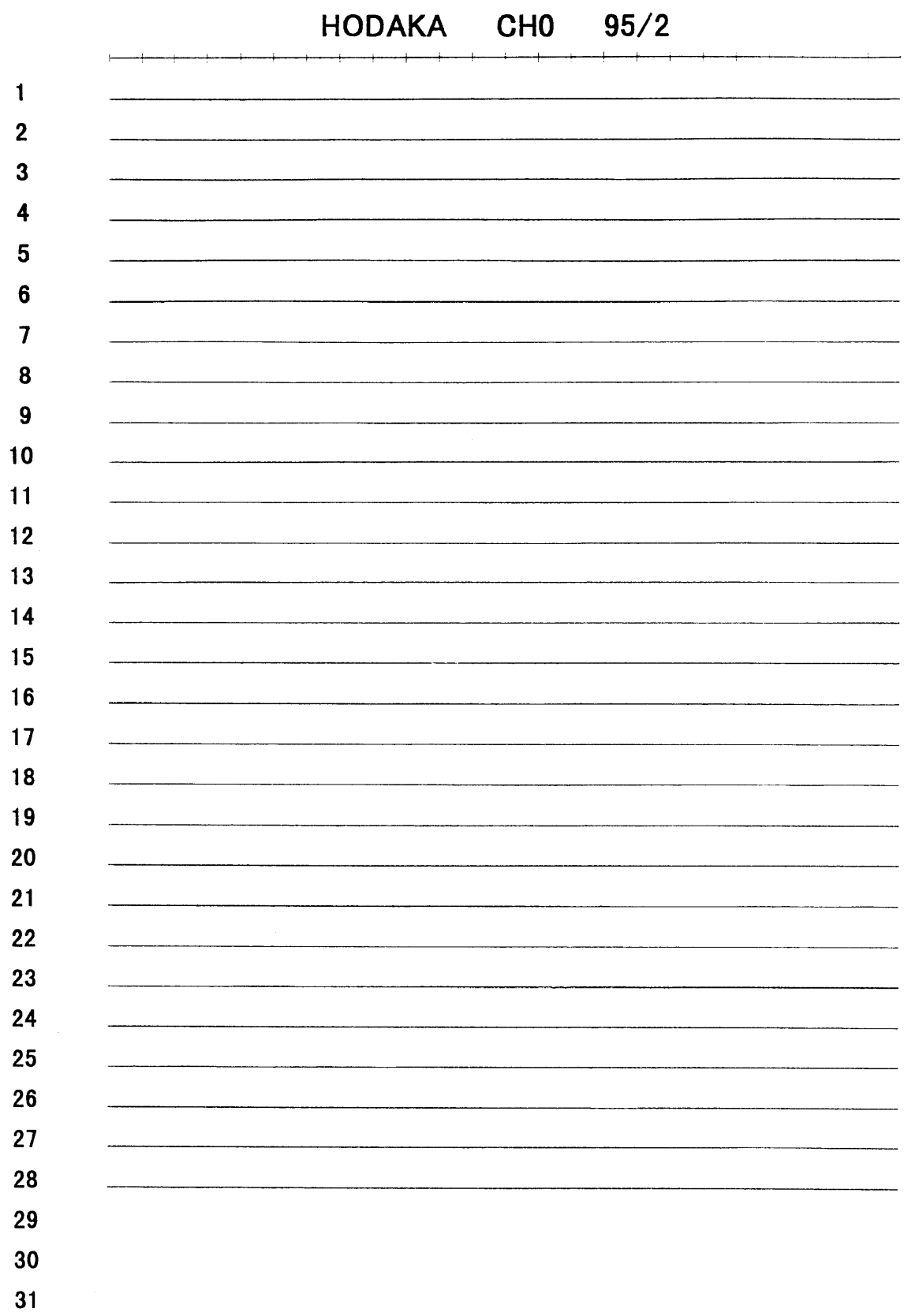
HODAKA CH0 95/2
1
2
3
4
5
6
7
8
9
10
11
12
13
14
15
16
17
18
19
20
21
22
23
24
25
26
27
28
29
30
31

Fig. A-95-2-0

HODAKA CH1 95/2

1
2
3
4
5
6
7
8
9
10
11
12
13
14
15
16
17
18
19
20
21
22
23
24
25
26
27
28
29
30
31

Fig. A-95-2-1

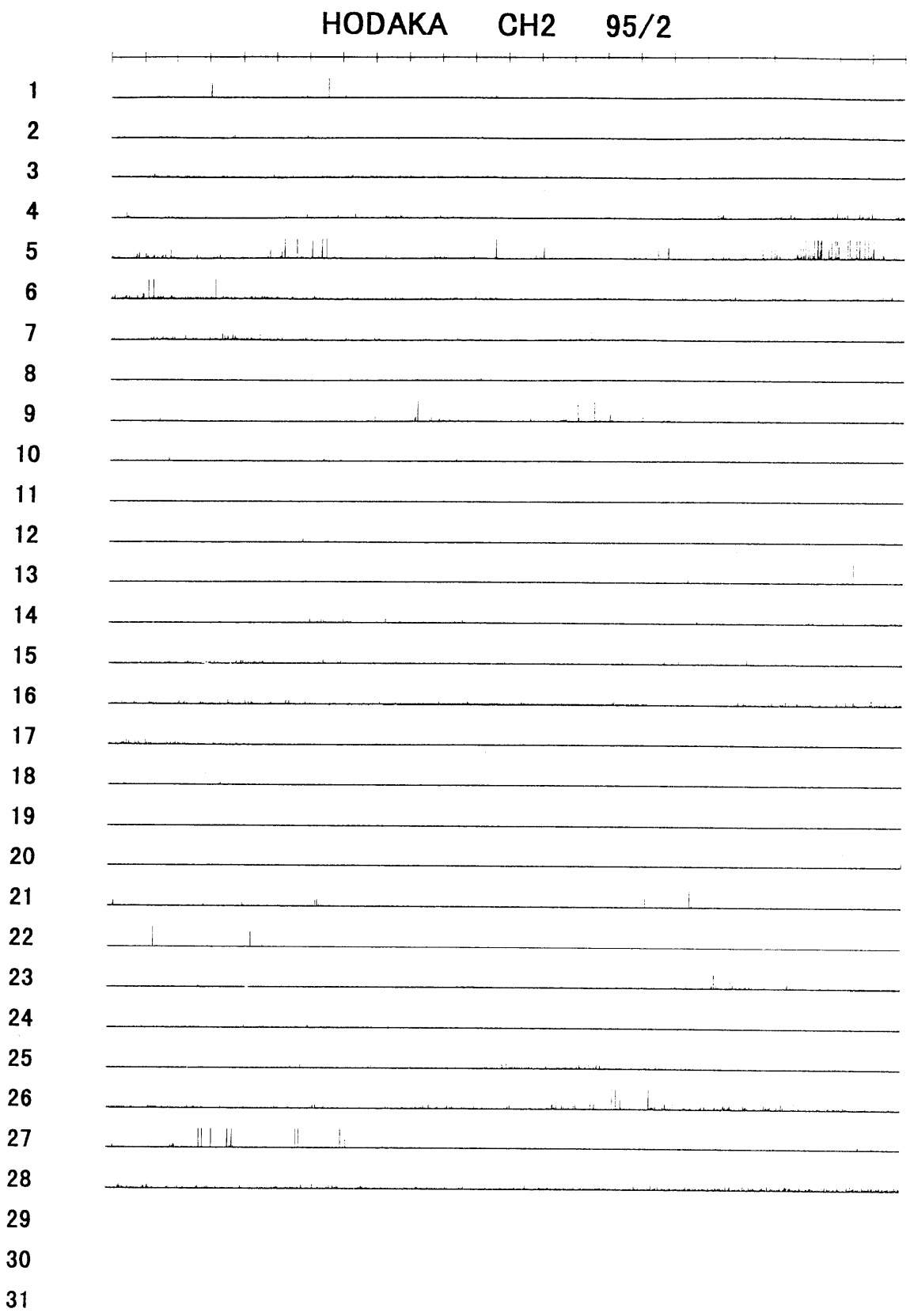
HODAKA CH2 95/2
1
2
3
4
5
6
7
8
9
10
11
12
13
14
15
16
17
18
19
20
21
22
23
24
25
26
27
28
29
30
31

Fig. A-95-2-2

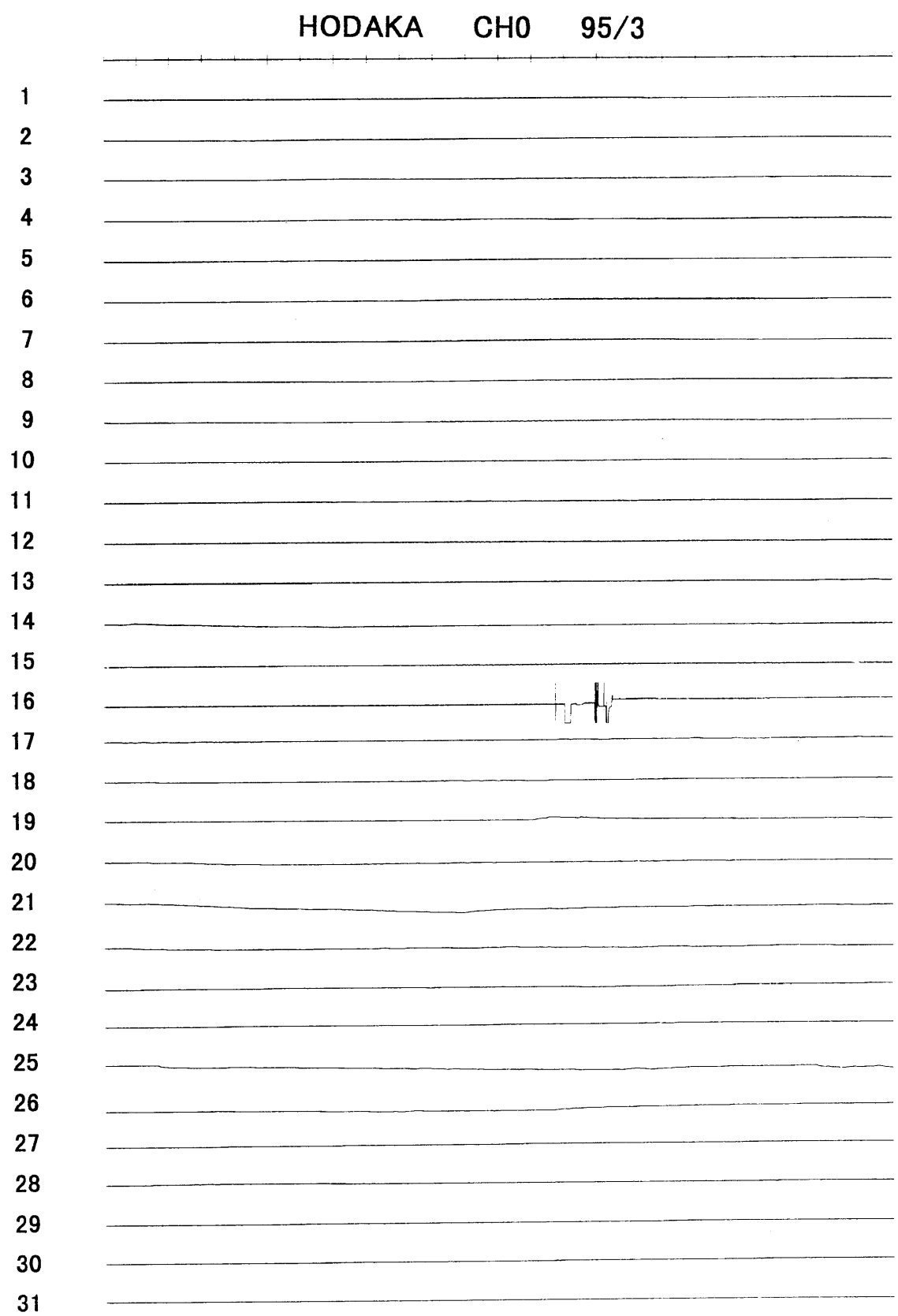
HODAKA CH0 95/3
1
2
3
4
5
6
7
8
9
10
11
12
13
14
15
16
17
18
19
20
21
22
23
24
25
26
27
28
29
30
31

Fig. A-95-3-0

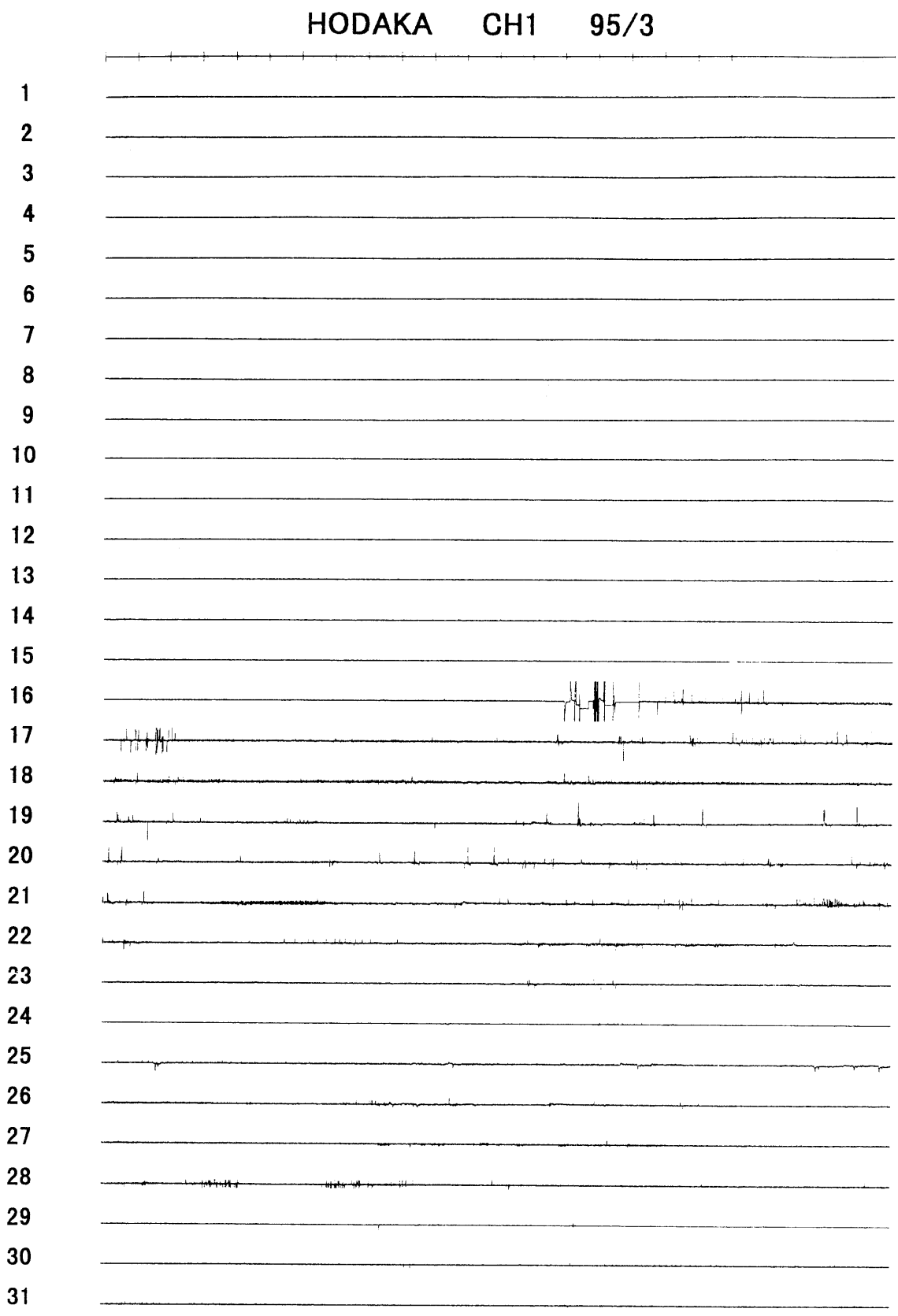
HODAKA CH1 95/3
1
2
3
4
5
6
7
8
9
10
11
12
13
14
15
16
17
18
19
20
21
22
23
24
25
26
27
28
29
30
31

Fig. A-95-3-1

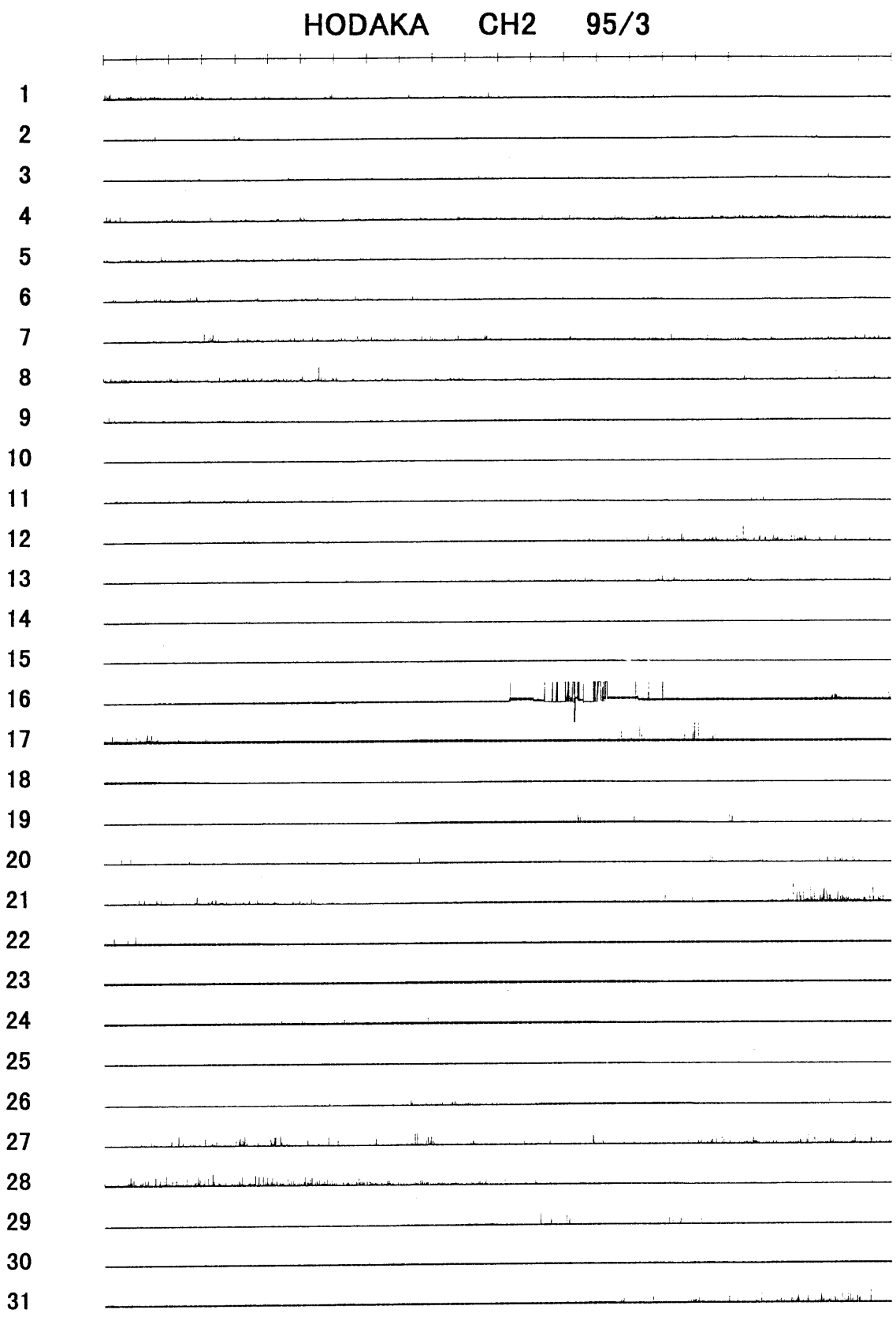
HODAKA CH2 95/3
1
2
3
4
5
6
7
8
9
10
11
12
13
14
15
16
17
18
19
20
21
22
23
24
25
26
27
28
29
30
31

Fig. A-95-3-2

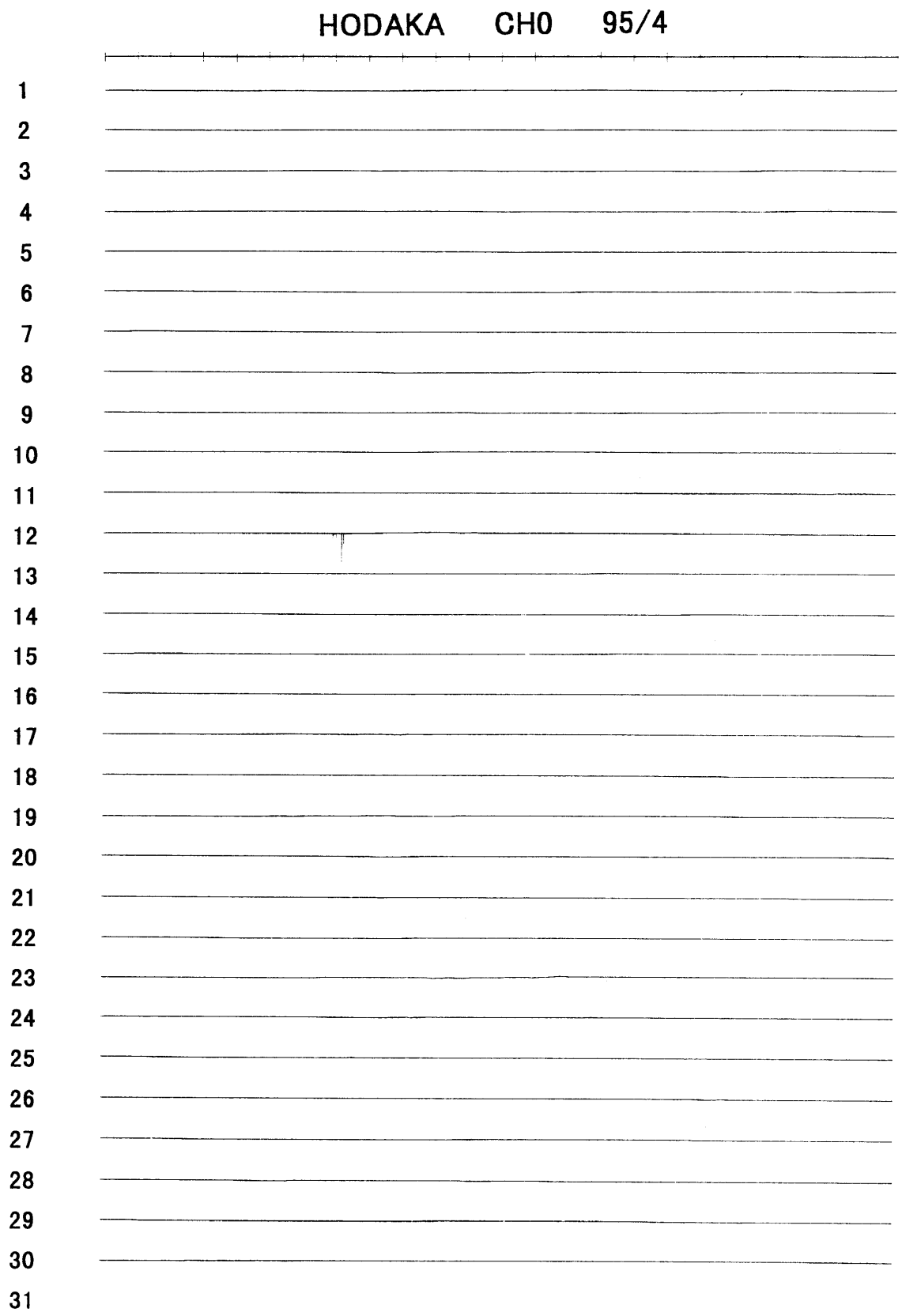
HODAKA CH0 95/4
1
2
3
4
5
6
7
8
9
10
11
12
13
14
15
16
17
18
19
20
21
22
23
24
25
26
27
28
29
30
31

Fig. A-95-4-0

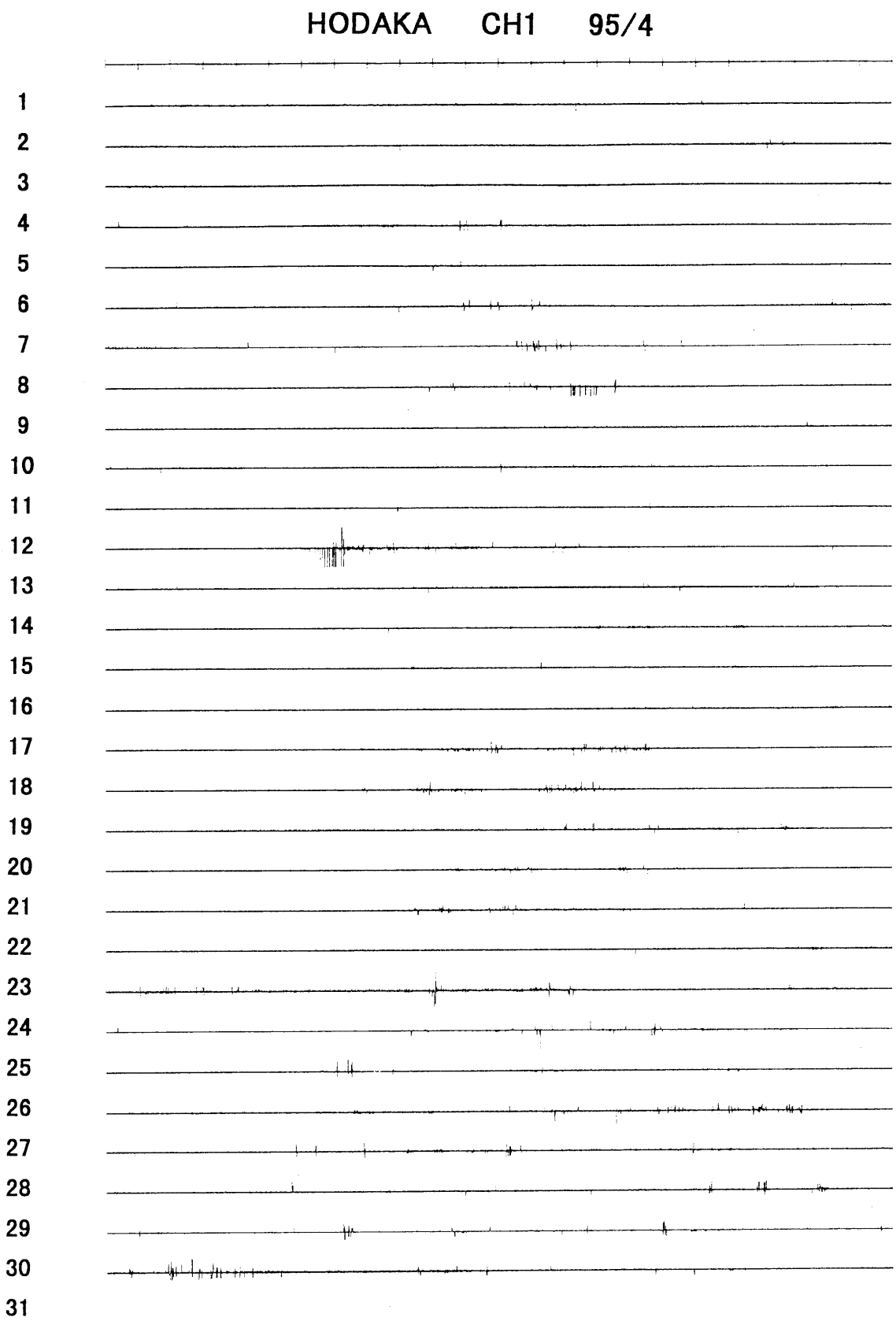
HODAKA CH1 95/4
1
2
3
4
5
6
7
8
9
10
11
12
13
14
15
16
17
18
19
20
21
22
23
24
25
26
27
28
29
30
31

Fig. A-95-4-1

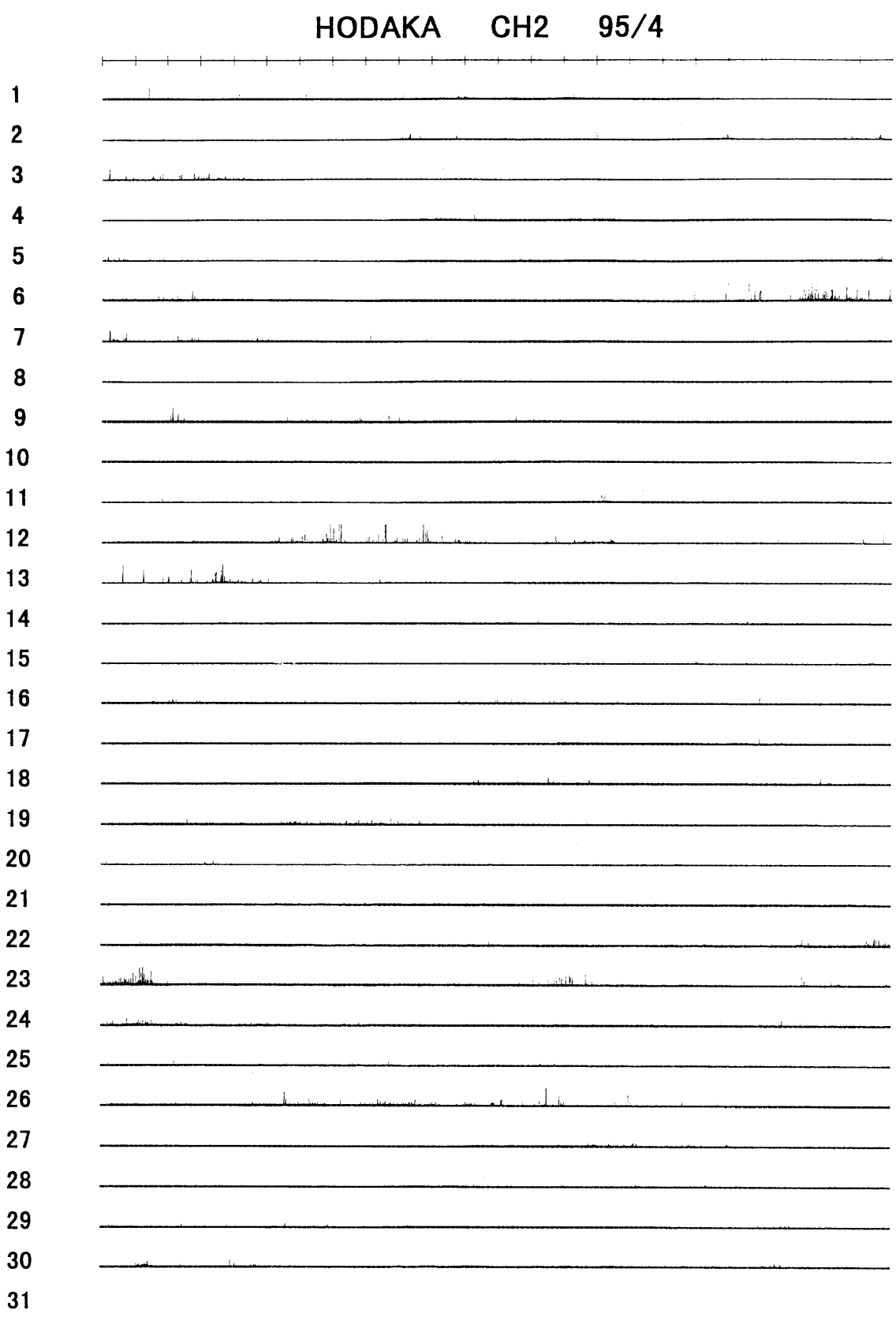
HODAKA CH2 95/4
1
2
3
4
5
6
7
8
9
10
11
12
13
14
15
16
17
18
19
20
21
22
23
24
25
26
27
28
29
30
31

Fig. A-95-4-2

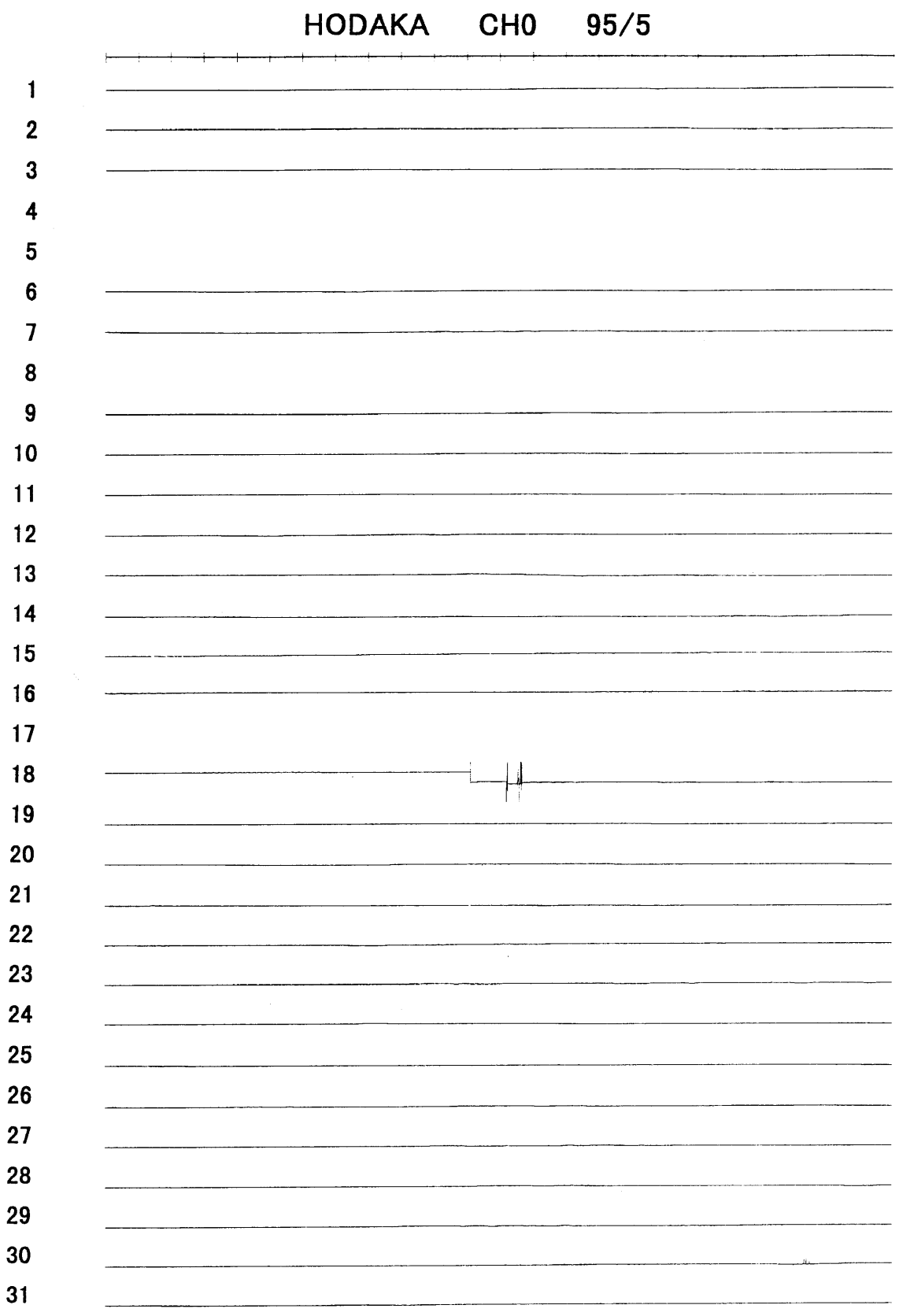
HODAKA CH0 95/5
1
2
3
4
5
6
7
8
9
10
11
12
13
14
15
16
17
18
19
20
21
22
23
24
25
26
27
28
29
30
31

Fig. A-95-5-0

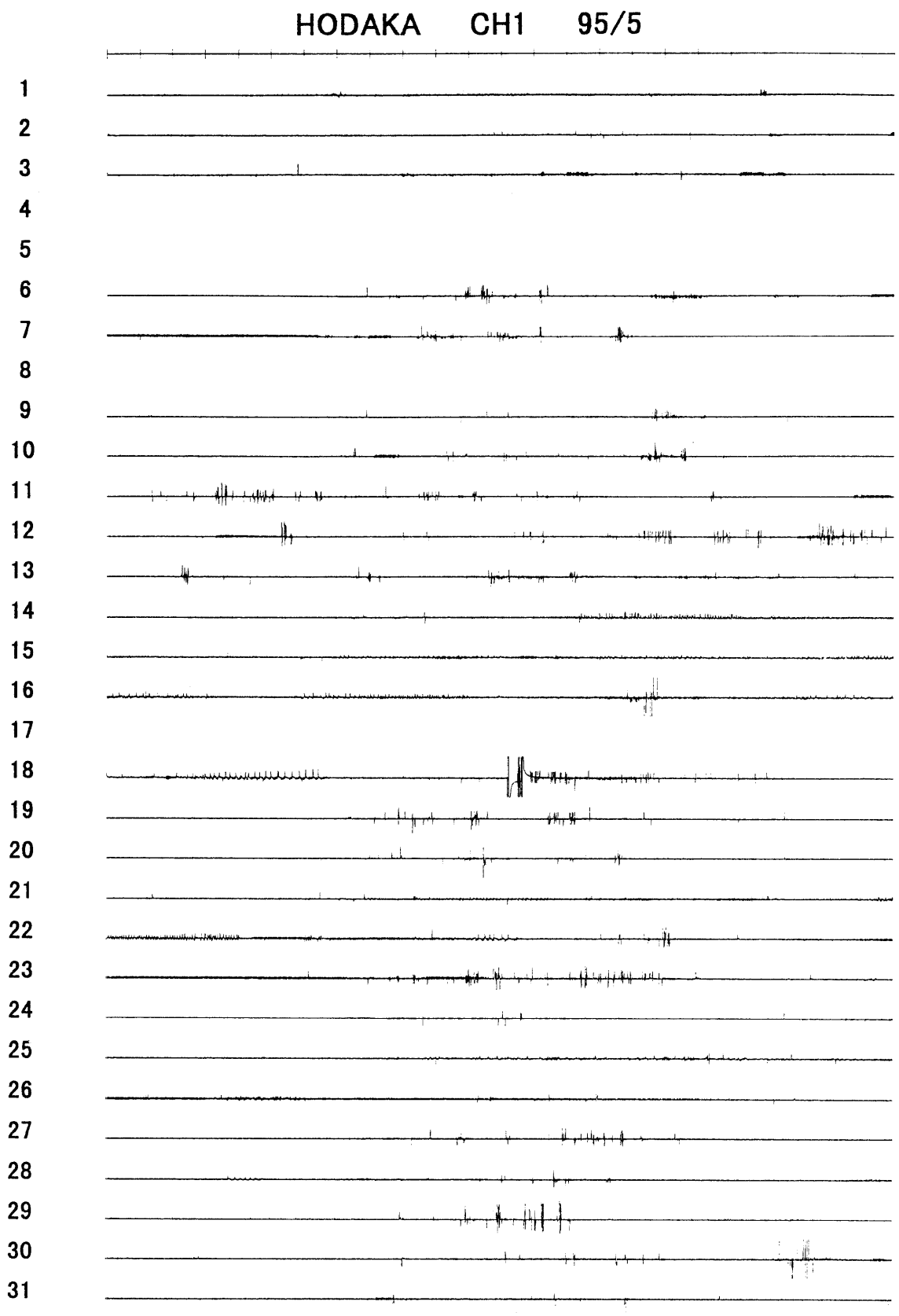
HODAKA CH1 95/5
1
2
3
4
5
6
7
8
9
10
11
12
13
14
15
16
17
18
19
20
21
22
23
24
25
26
27
28
29
30
31

Fig. A-95-5-1

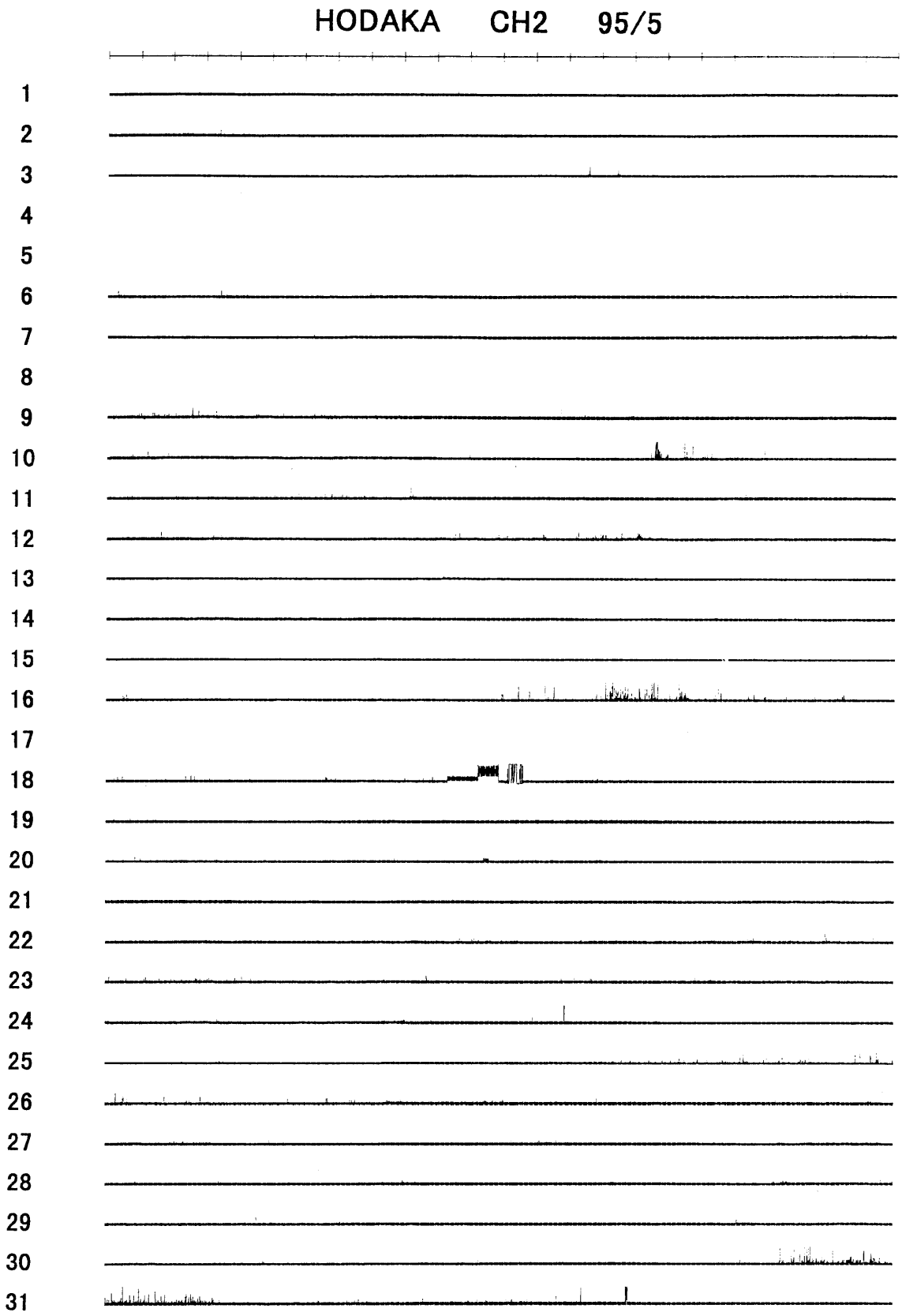
HODAKA CH2 95/5
1
2
3
4
5
6
7
8
9
10
11
12
13
14
15
16
17
18
19
20
21
22
23
24
25
26
27
28
29
30
31

Fig. A-95-5-2

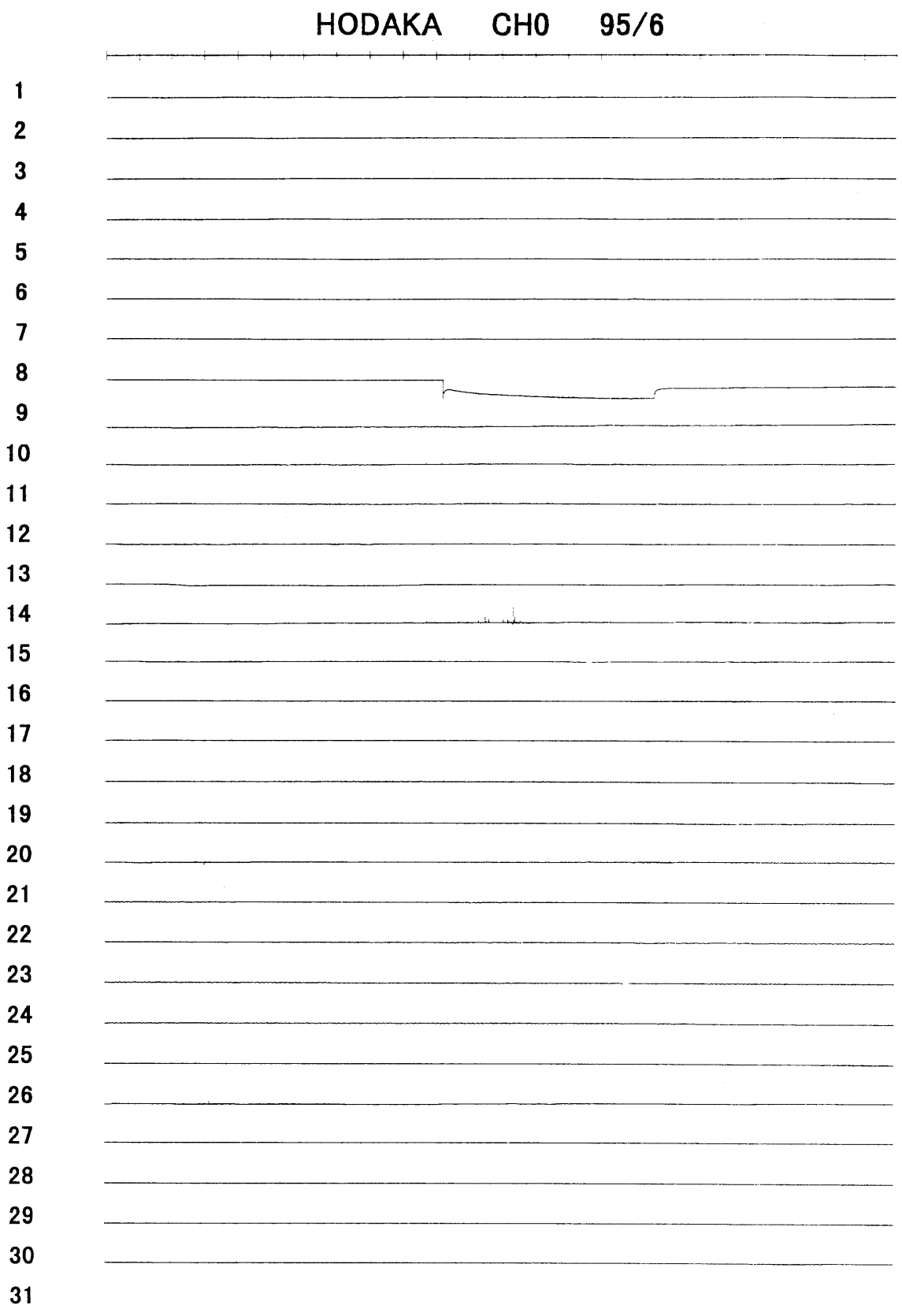
HODAKA CH0 95/6
1
2
3
4
5
6
7
8
9
10
11
12
13
14
15
16
17
18
19
20
21
22
23
24
25
26
27
28
29
30
31

Fig. A-95-6-0

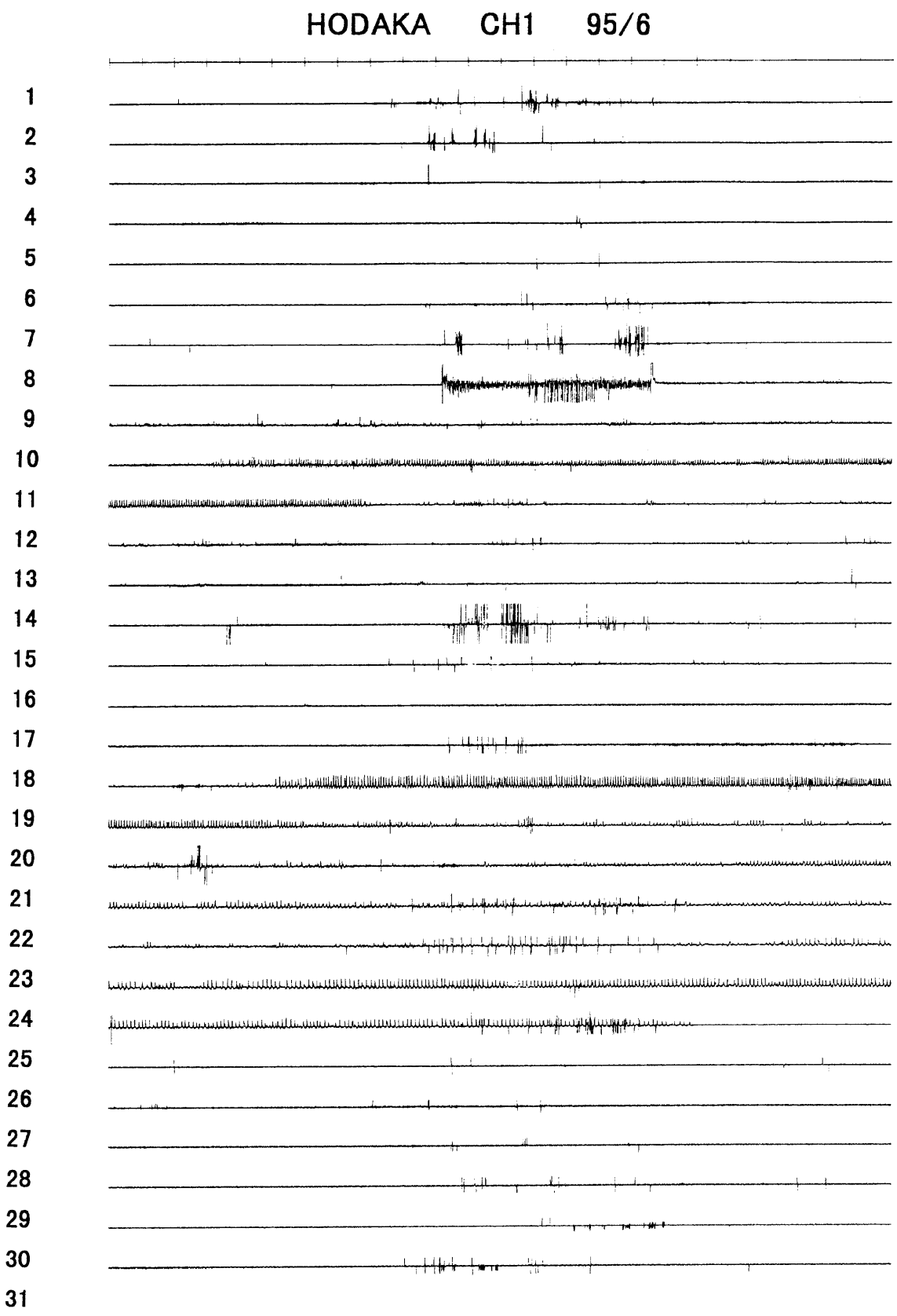
HODAKA CH1 95/6
1
2
3
4
5
6
7
8
9
10
11
12
13
14
15
16
17
18
19
20
21
22
23
24
25
26
27
28
29
30
31

Fig. A-95-6-1

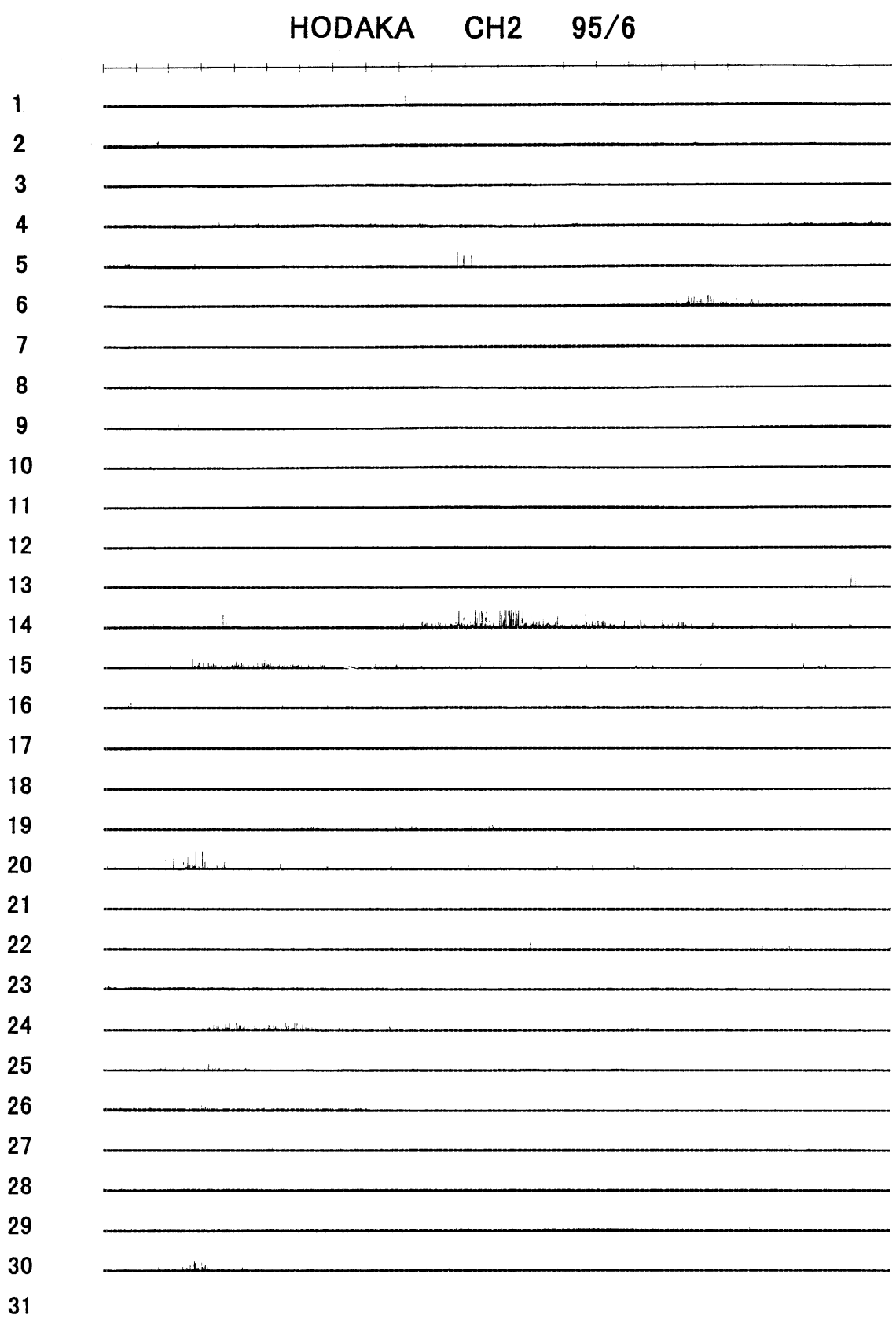
HODAKA CH2 95/6
1
2
3
4
5
6
7
8
9
10
11
12
13
14
15
16
17
18
19
20
21
22
23
24
25
26
27
28
29
30
31

Fig. A-95-6-2

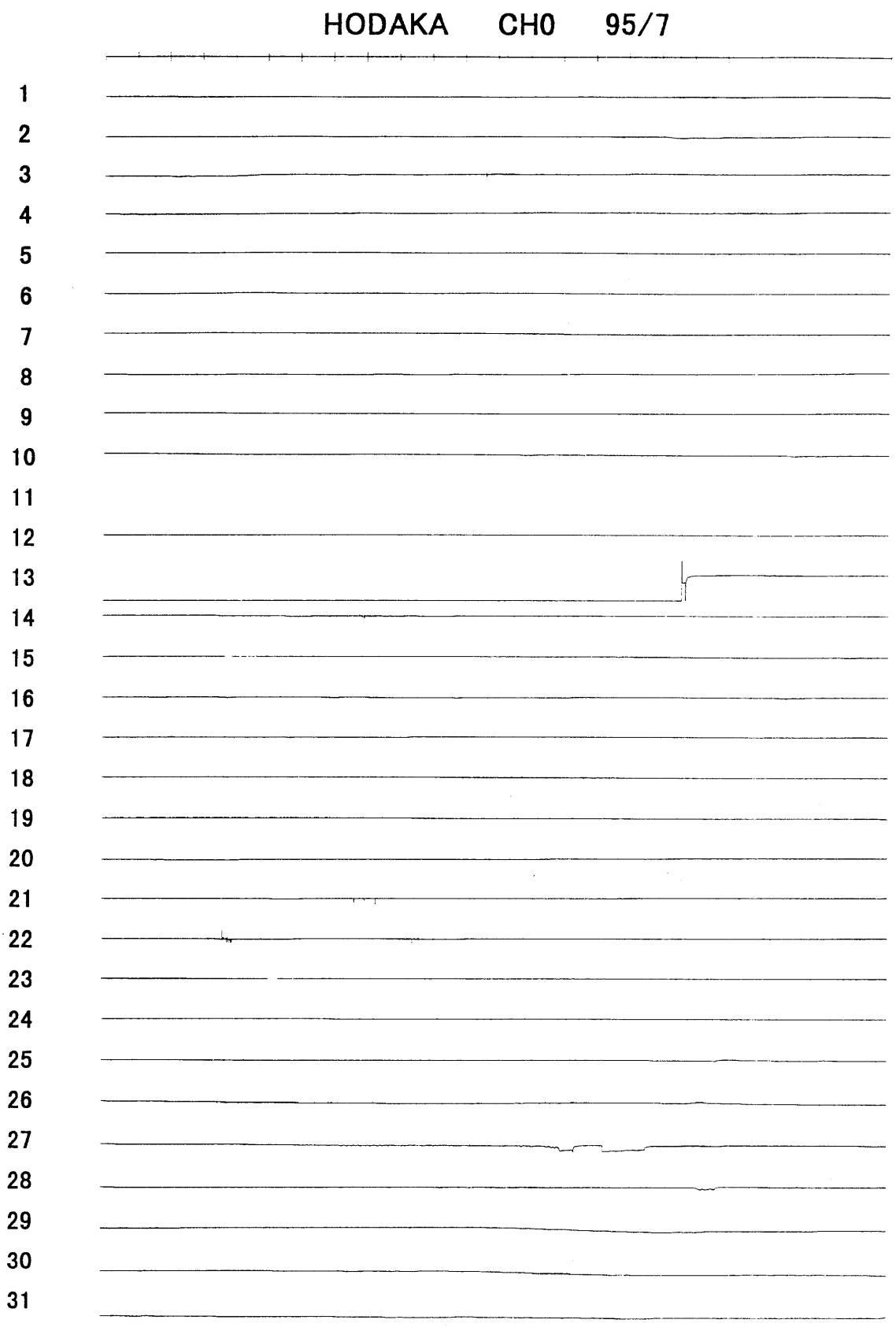
HODAKA CH0 95/7
1
2
3
4
5
6
7
8
9
10
11
12
13
14
15
16
17
18
19
20
21
22
23
24
25
26
27
28
29
30
31

Fig. A-95-7-0

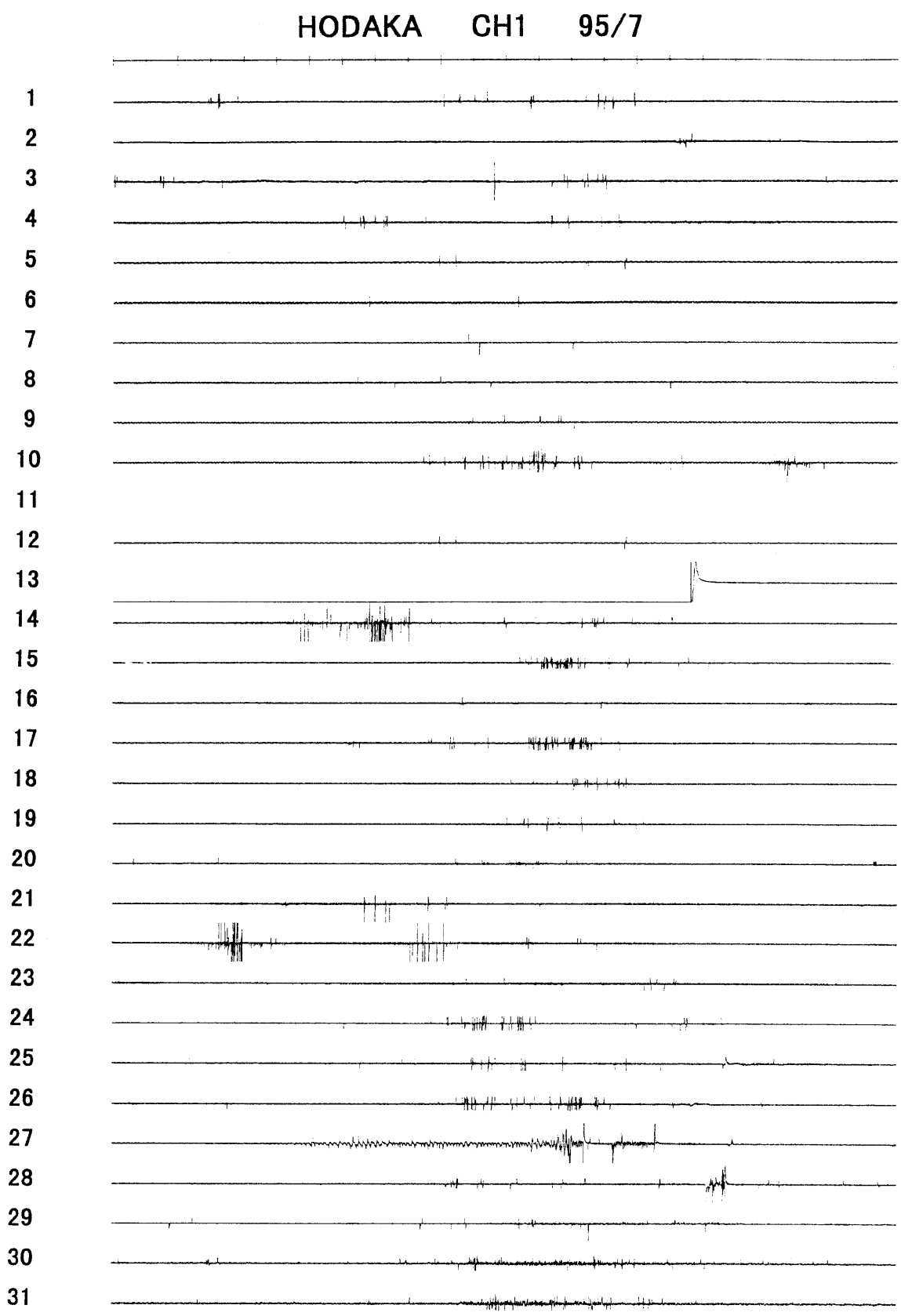
HODAKA CH1 95/7
1
2
3
4
5
6
7
8
9
10
11
12
13
14
15
16
17
18
19
20
21
22
23
24
25
26
27
28
29
30
31

Fig. A-95-7-1

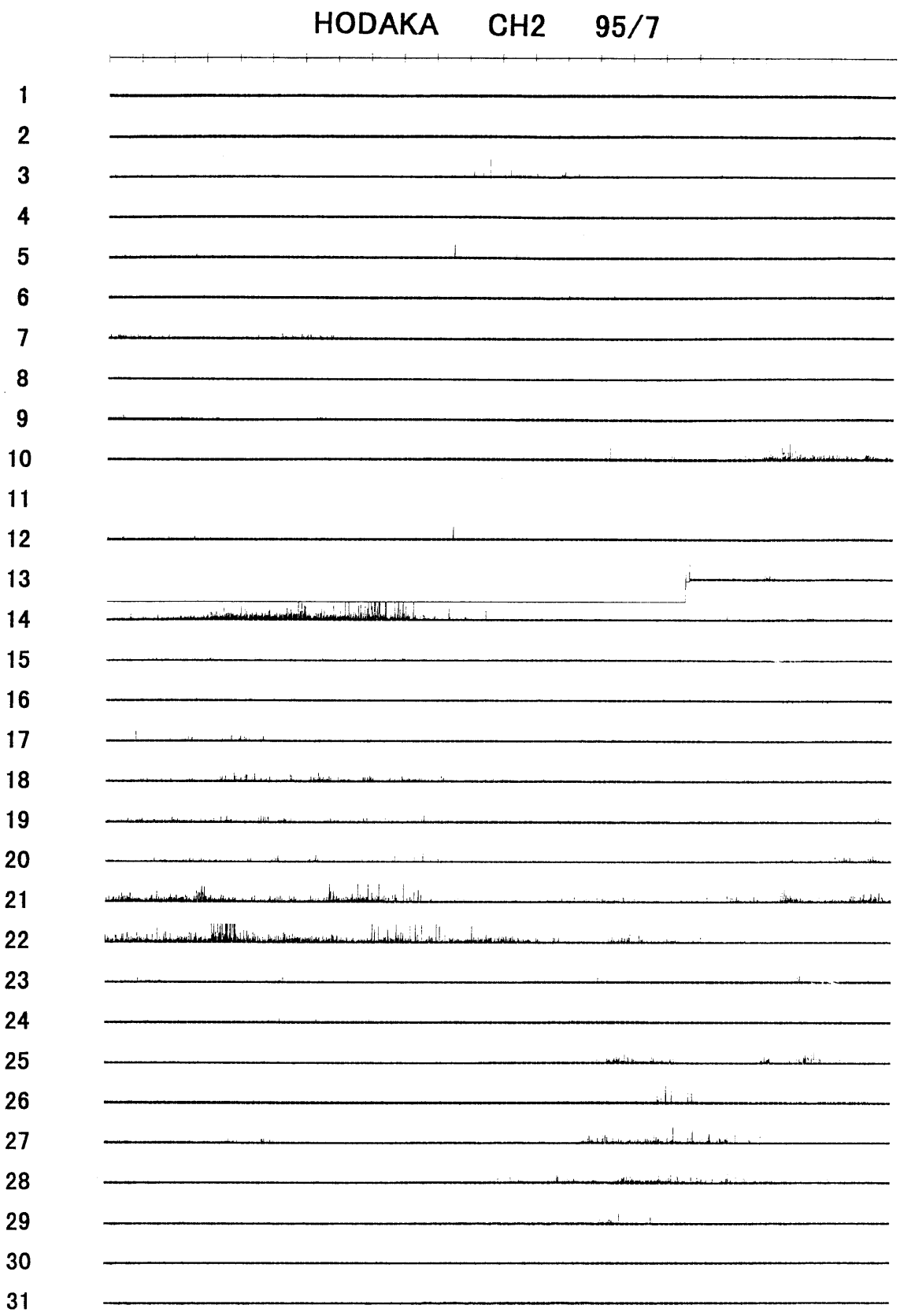
HODAKA CH2 95/7
1
2
3
4
5
6
7
8
9
10
11
12
13
14
15
16
17
18
19
20
21
22
23
24
25
26
27
28
29
30
31

Fig. A-95-7-2

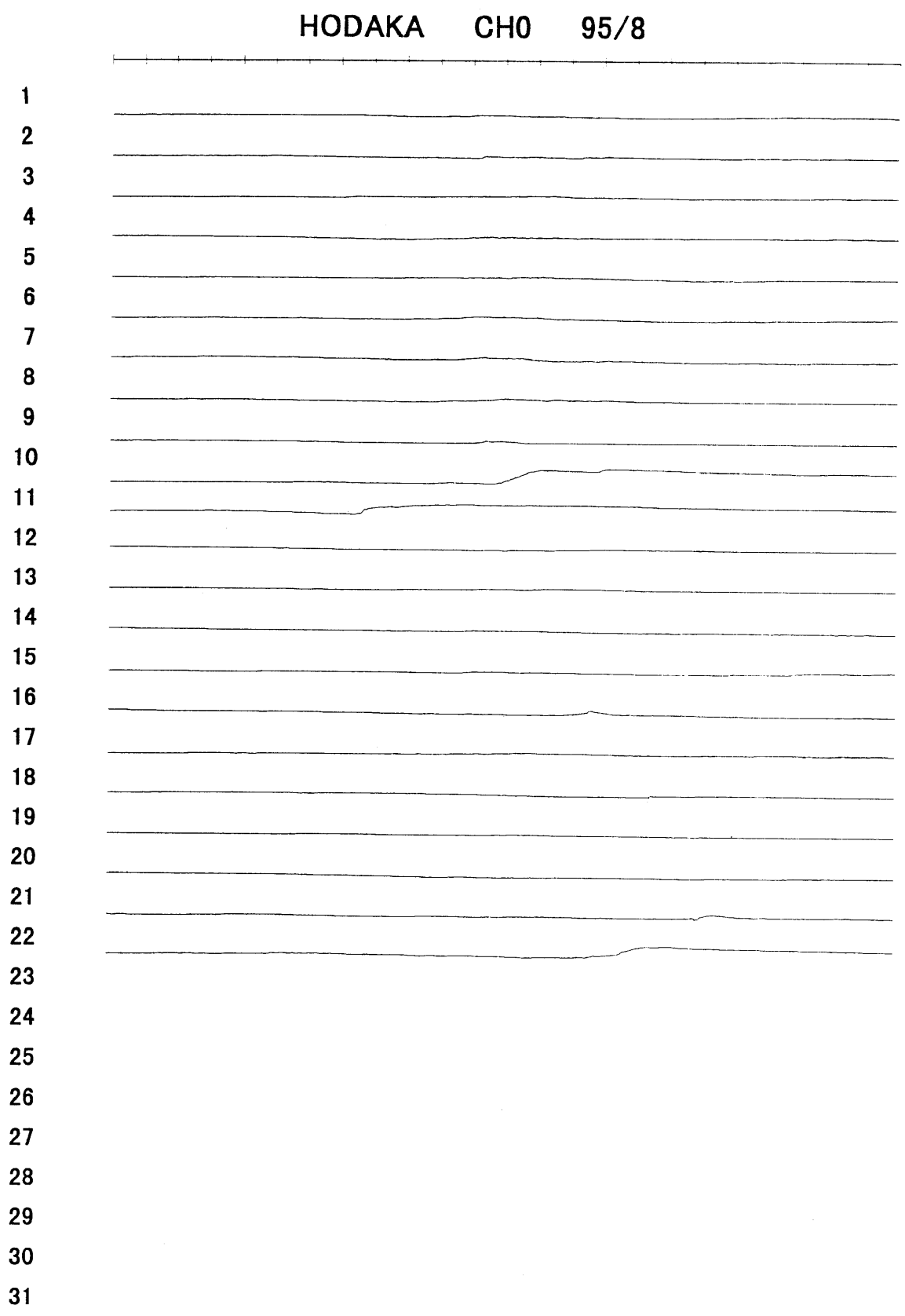
HODAKA CH0 95/8
1
2
3
4
5
6
7
8
9
10
11
12
13
14
15
16
17
18
19
20
21
22
23
24
25
26
27
28
29
30
31

Fig. A-95-8-0

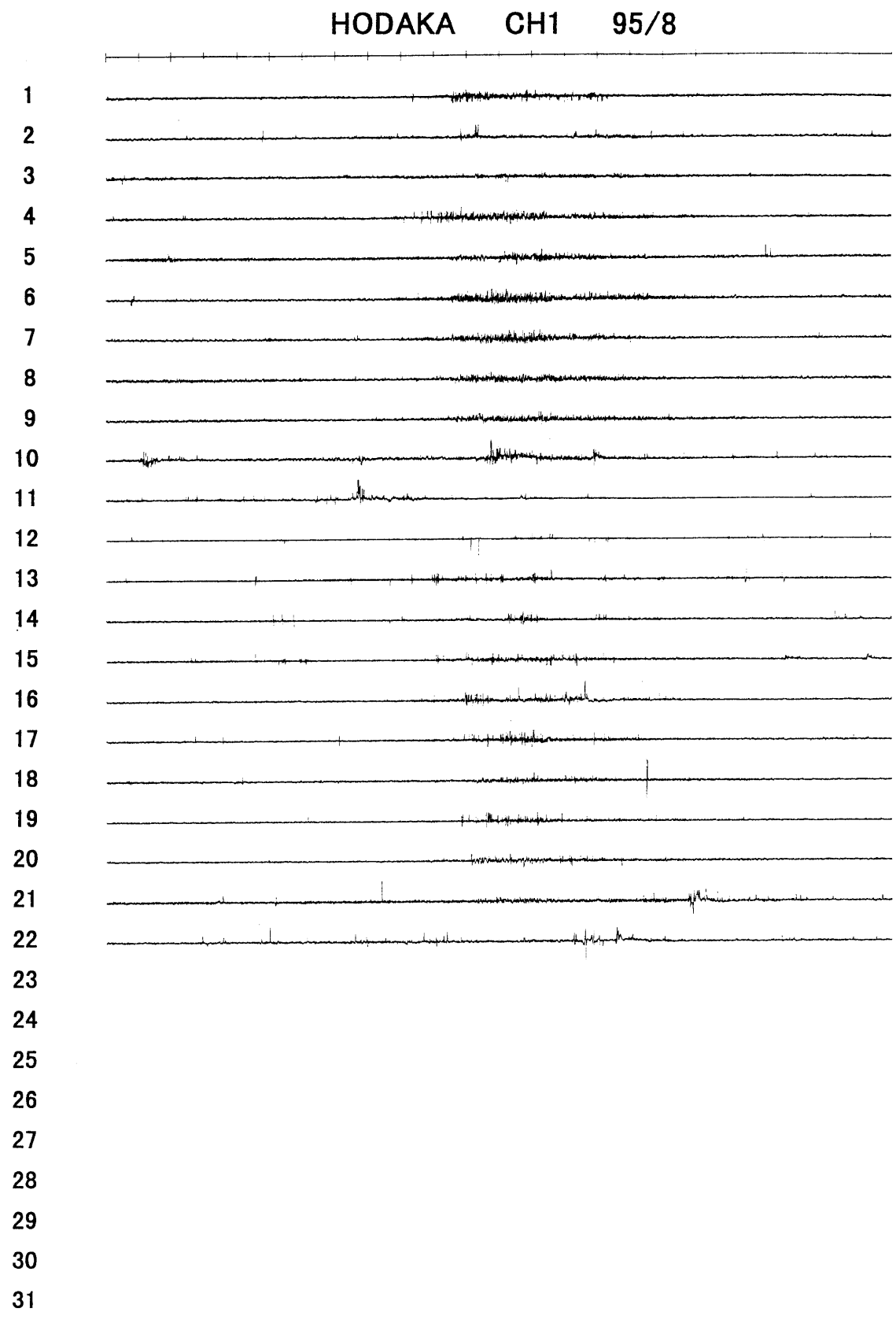
HODAKA CH1 95/8
1
2
3
4
5
6
7
8
9
10
11
12
13
14
15
16
17
18
19
20
21
22
23
24
25
26
27
28
29
30
31

Fig. A-95-8-1

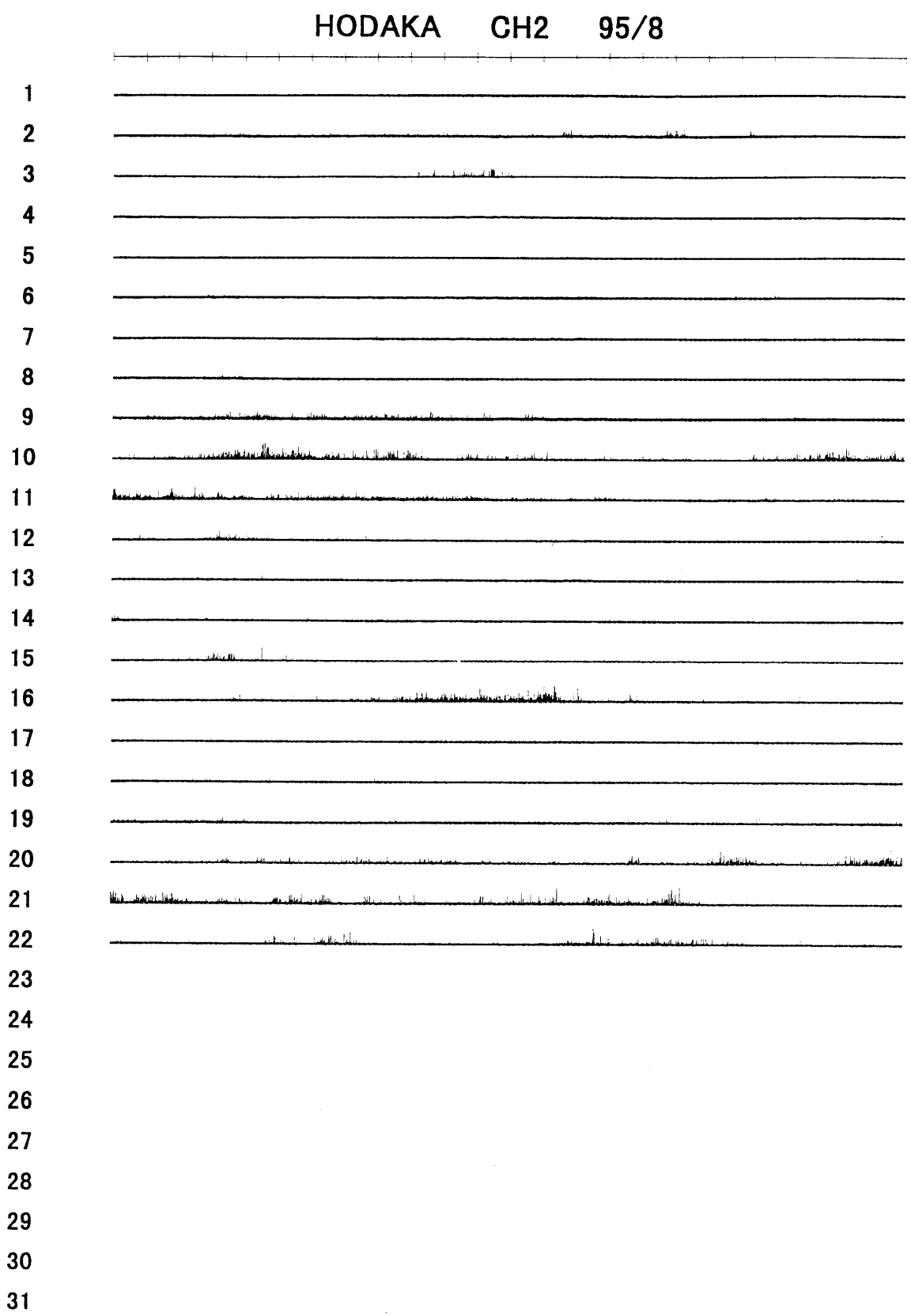
HODAKA CH2 95/8
1
2
3
4
5
6
7
8
9
10
11
12
13
14
15
16
17
18
19
20
21
22
23
24
25
26
27
28
29
30
31

Fig. A-95-8-2

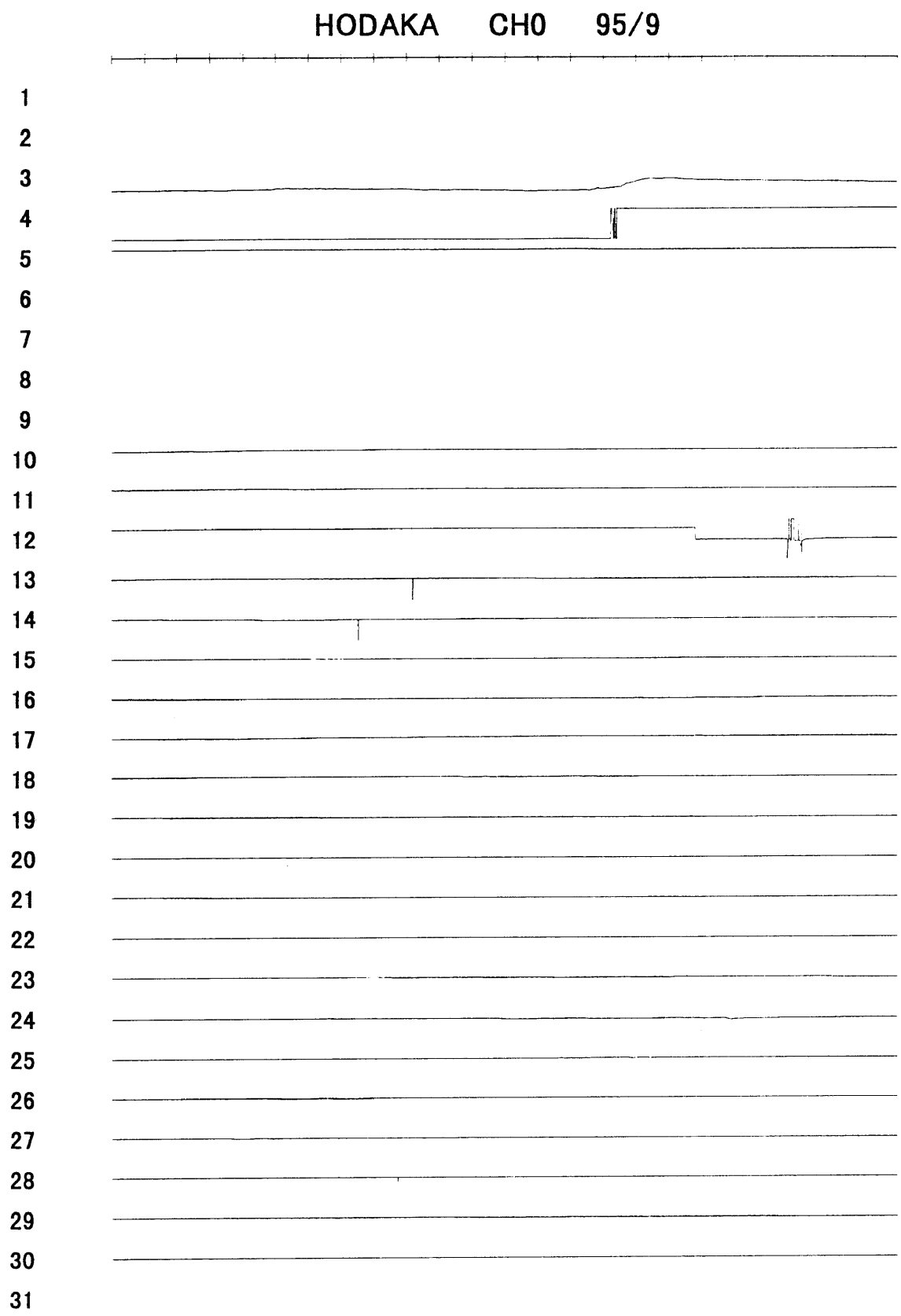
HODAKA CH0 95/9
1
2
3
4
5
6
7
8
9
10
11
12
13
14
15
16
17
18
19
20
21
22
23
24
25
26
27
28
29
30
31

Fig. A-95-9-0

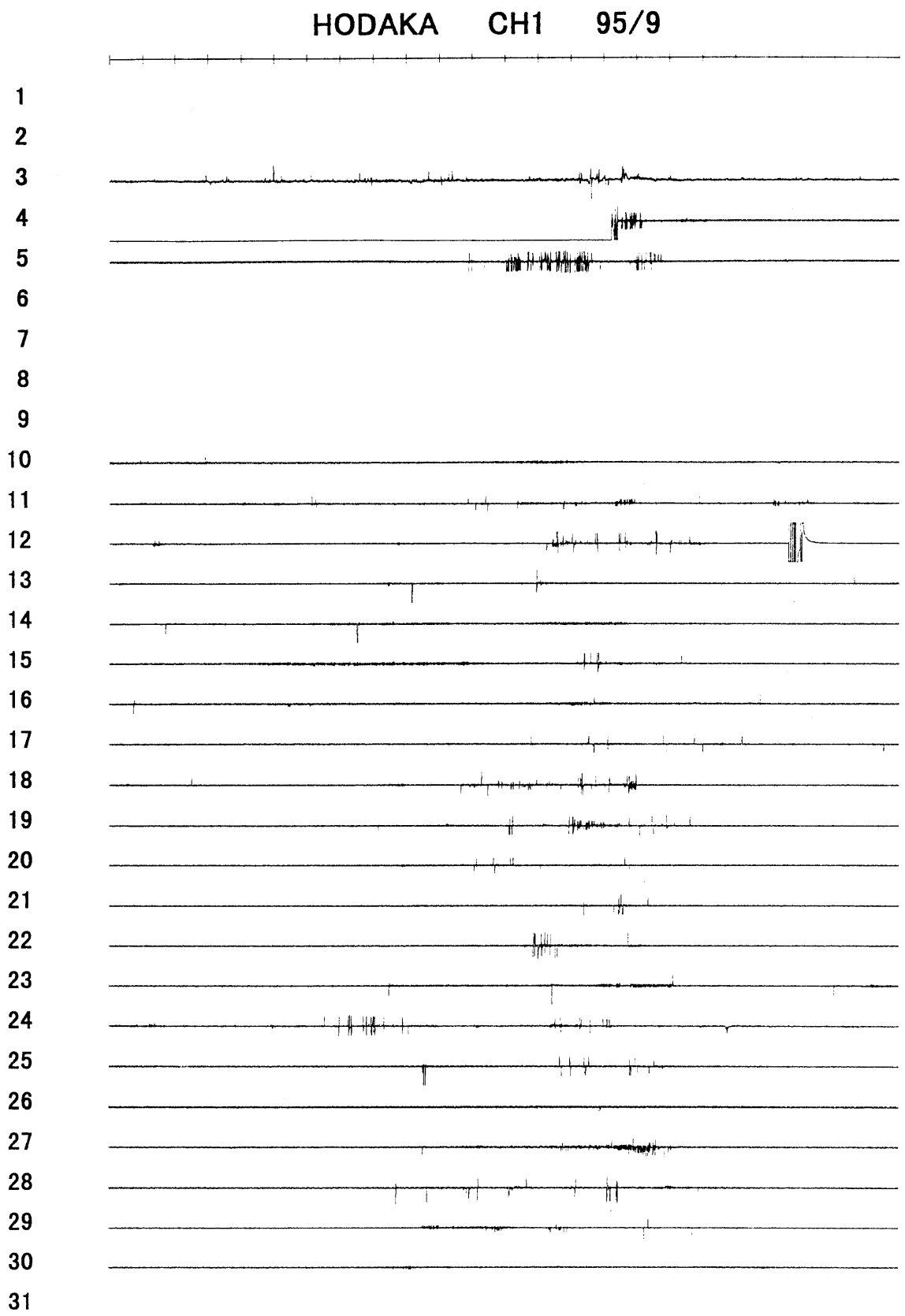
HODAKA CH1 95/9
1
2
3
4
5
6
7
8
9
10
11
12
13
14
15
16
17
18
19
20
21
22
23
24
25
26
27
28
29
30
31

Fig. A-95-9-1

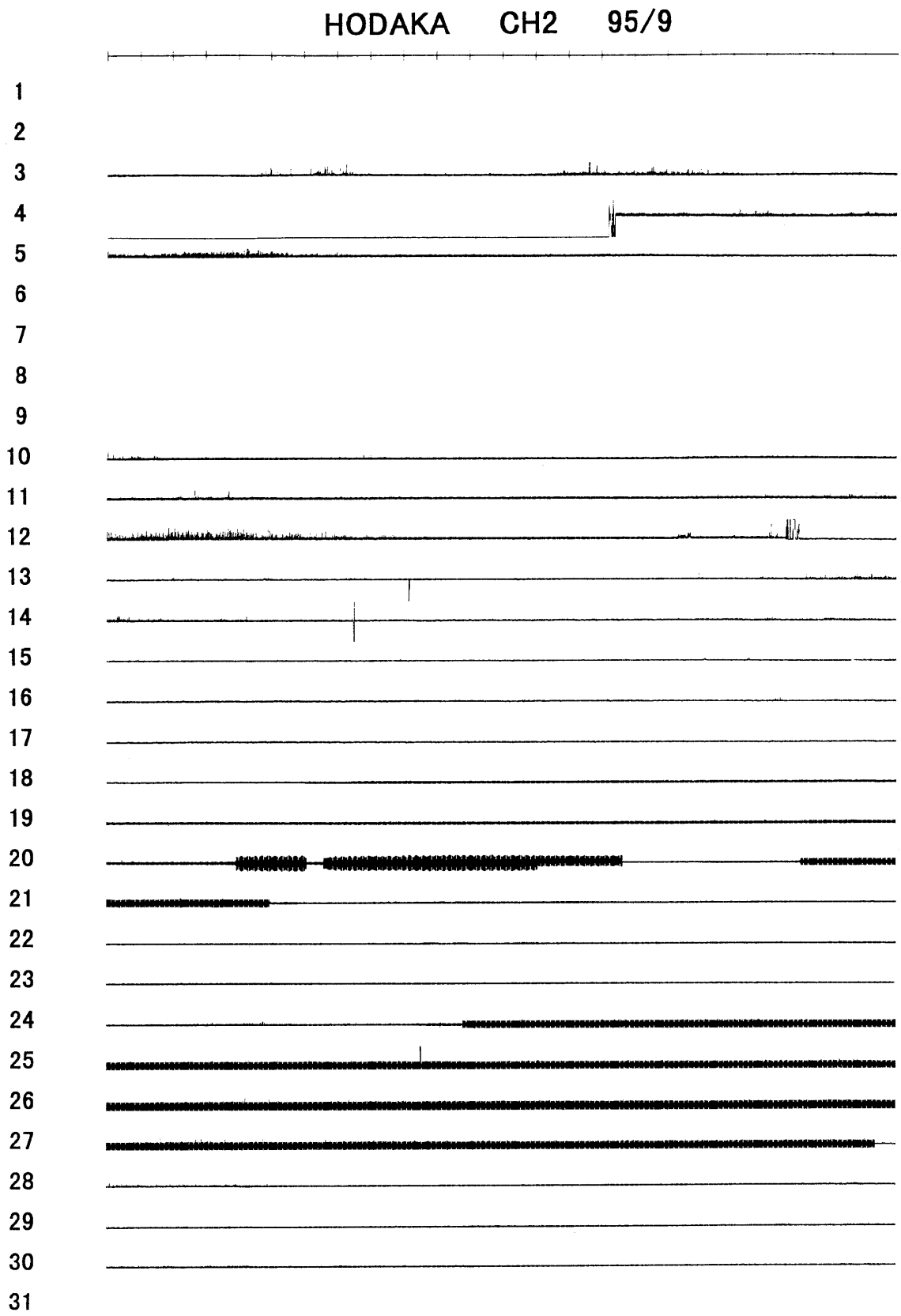
HODAKA CH2 95/9
1
2
3
4
5
6
7
8
9
10
11
12
13
14
15
16
17
18
19
20
21
22
23
24
25
26
27
28
29
30
31

Fig. A-95-9-2

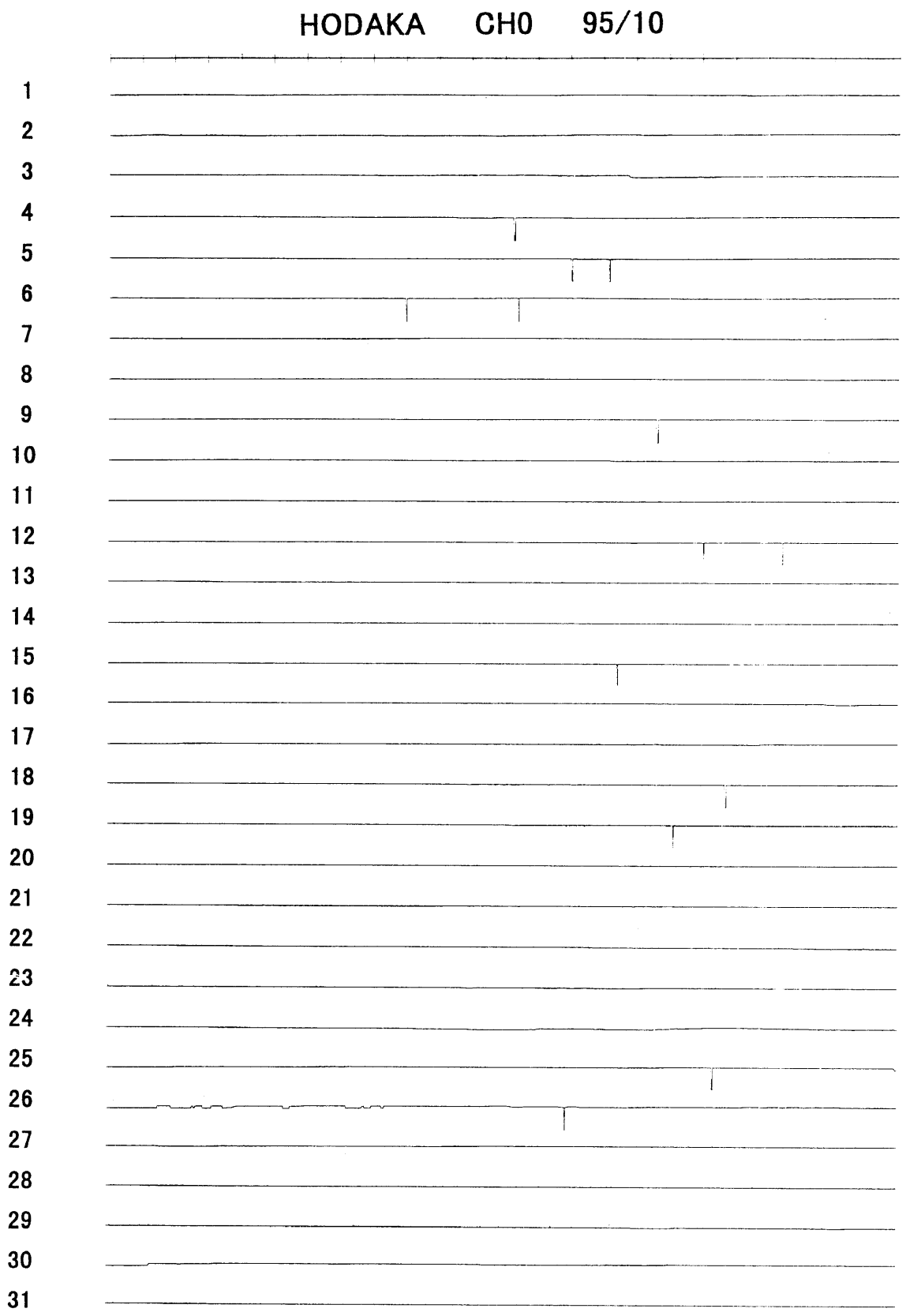
HODAKA CH0 95/10
1
2
3
4
5
6
7
8
9
10
11
12
13
14
15
16
17
18
19
20
21
22
23
24
25
26
27
28
29
30
31

Fig. A-95-10-0

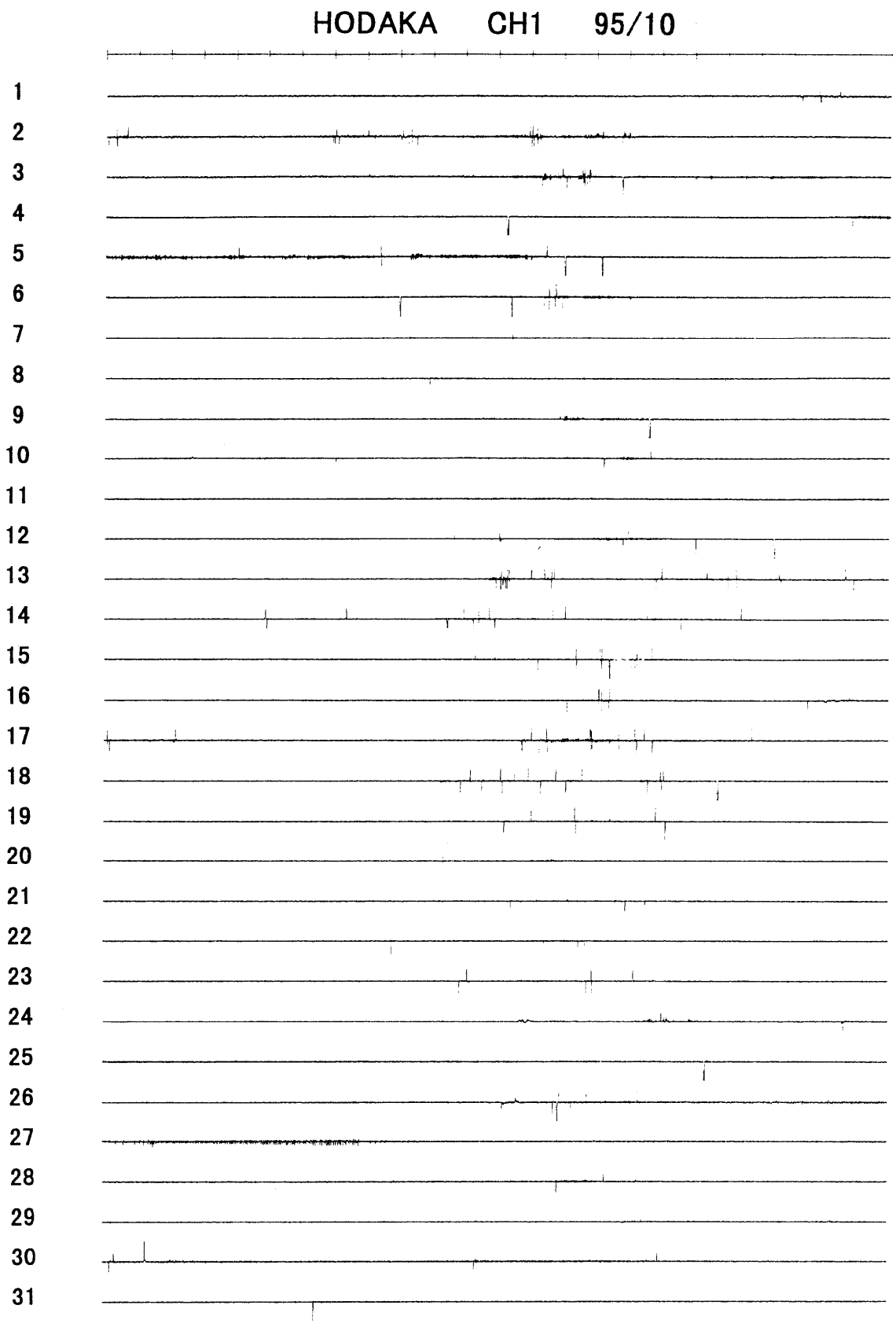
HODAKA CH1 95/10
1
2
3
4
5
6
7
8
9
10
11
12
13
14
15
16
17
18
19
20
21
22
23
24
25
26
27
28
29
30
31

Fig. A-95-10-1

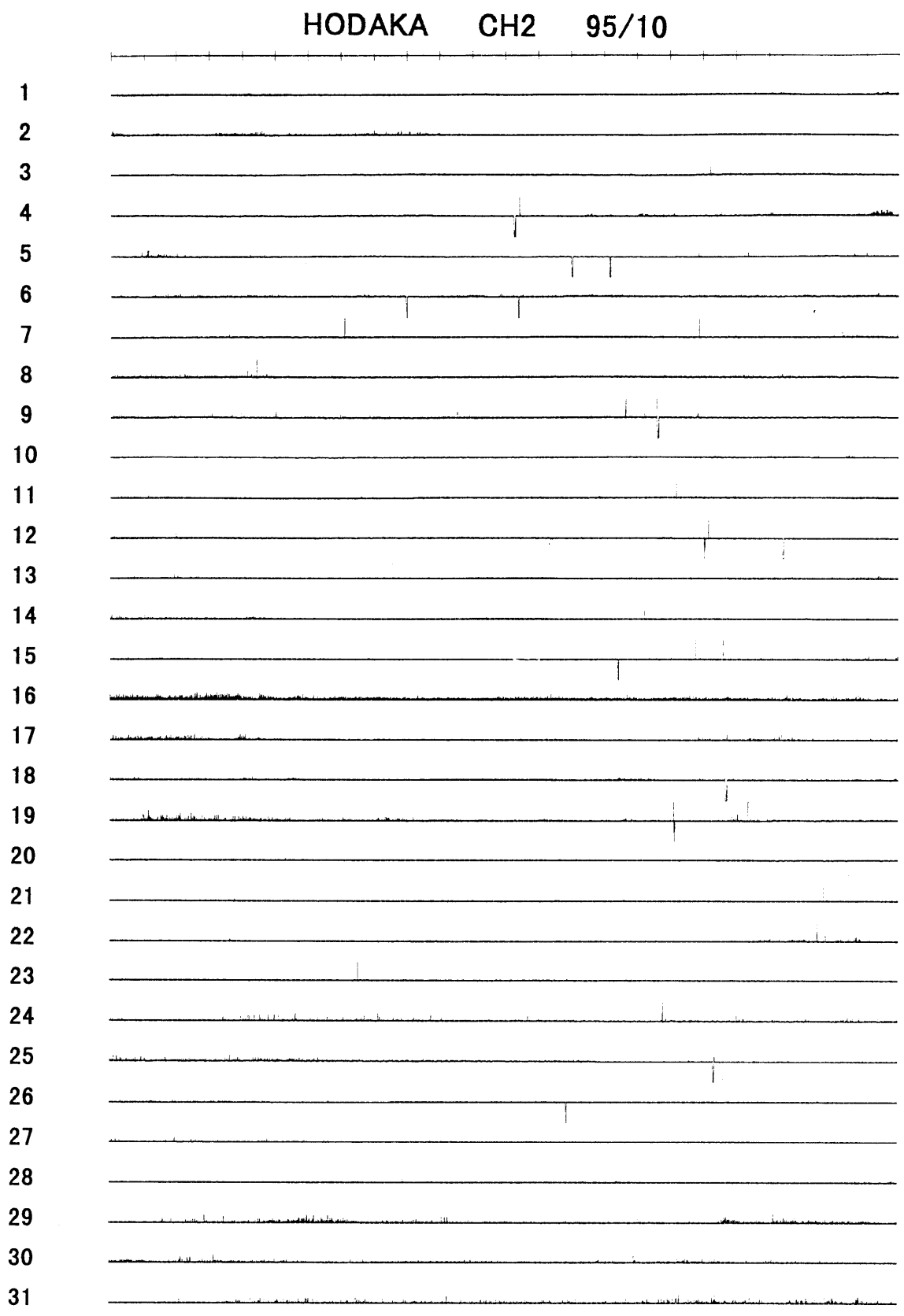
HODAKA CH2 95/10
1
2
3
4
5
6
7
8
9
10
11
12
13
14
15
16
17
18
19
20
21
22
23
24
25
26
27
28
29
30
31

Fig. A-95-10-2

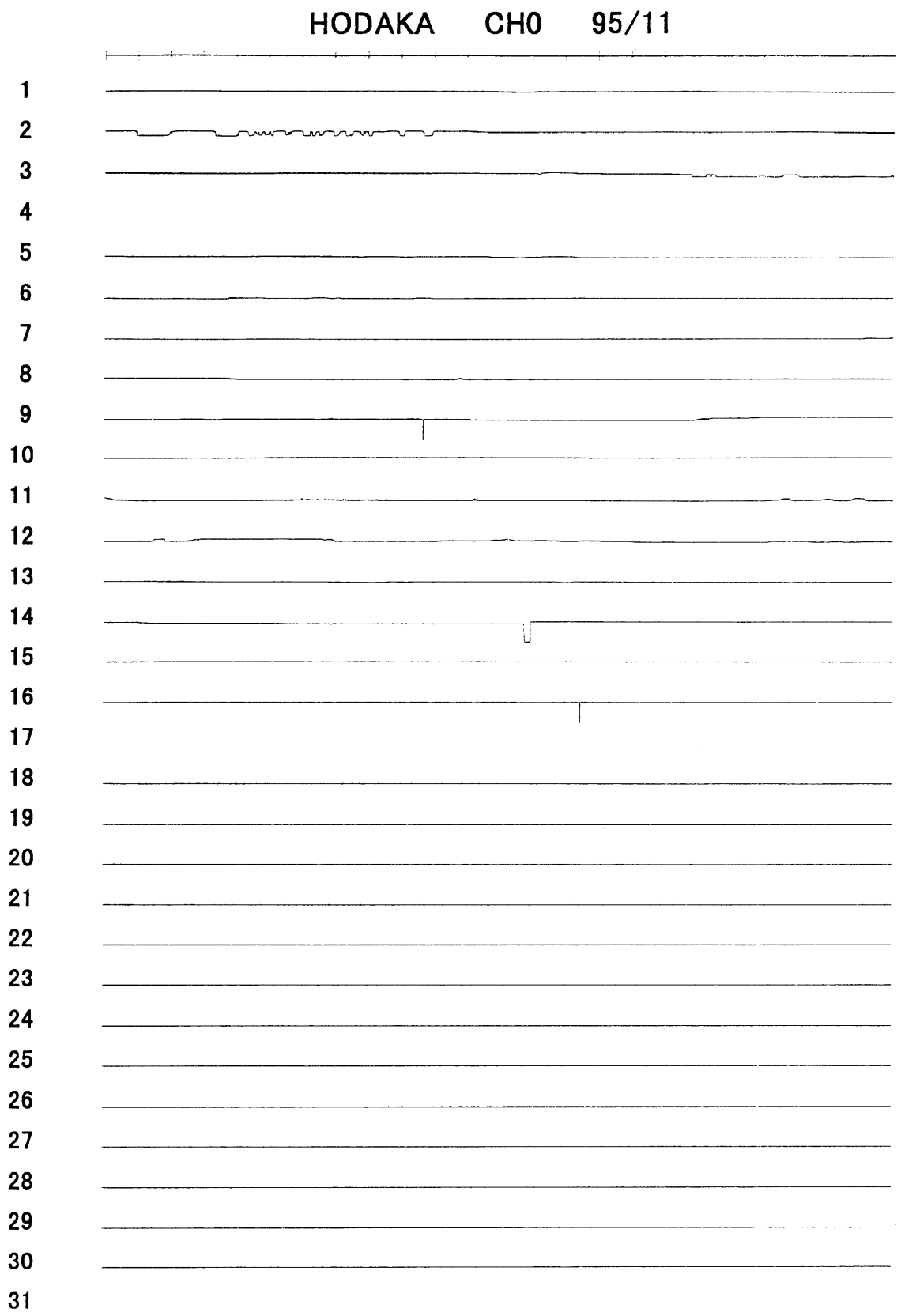
HODAKA CH0 95/11
1
2
3
4
5
6
7
8
9
10
11
12
13
14
15
16
17
18
19
20
21
22
23
24
25
26
27
28
29
30
31

Fig. A-95-11-0

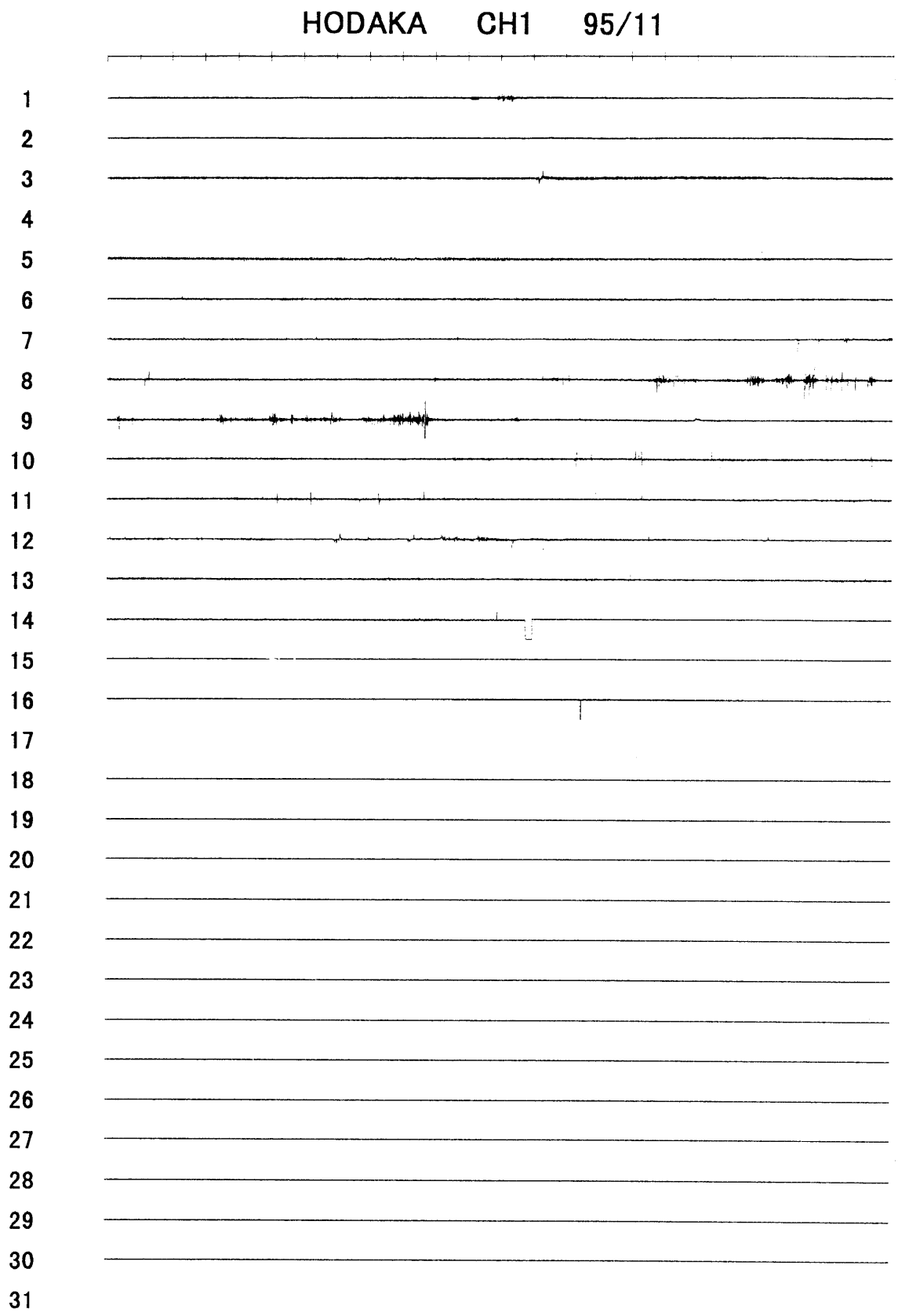
HODAKA CH1 95/11
1
2
3
4
5
6
7
8
9
10
11
12
13
14
15
16
17
18
19
20
21
22
23
24
25
26
27
28
29
30
31

Fig. A-95-11-1

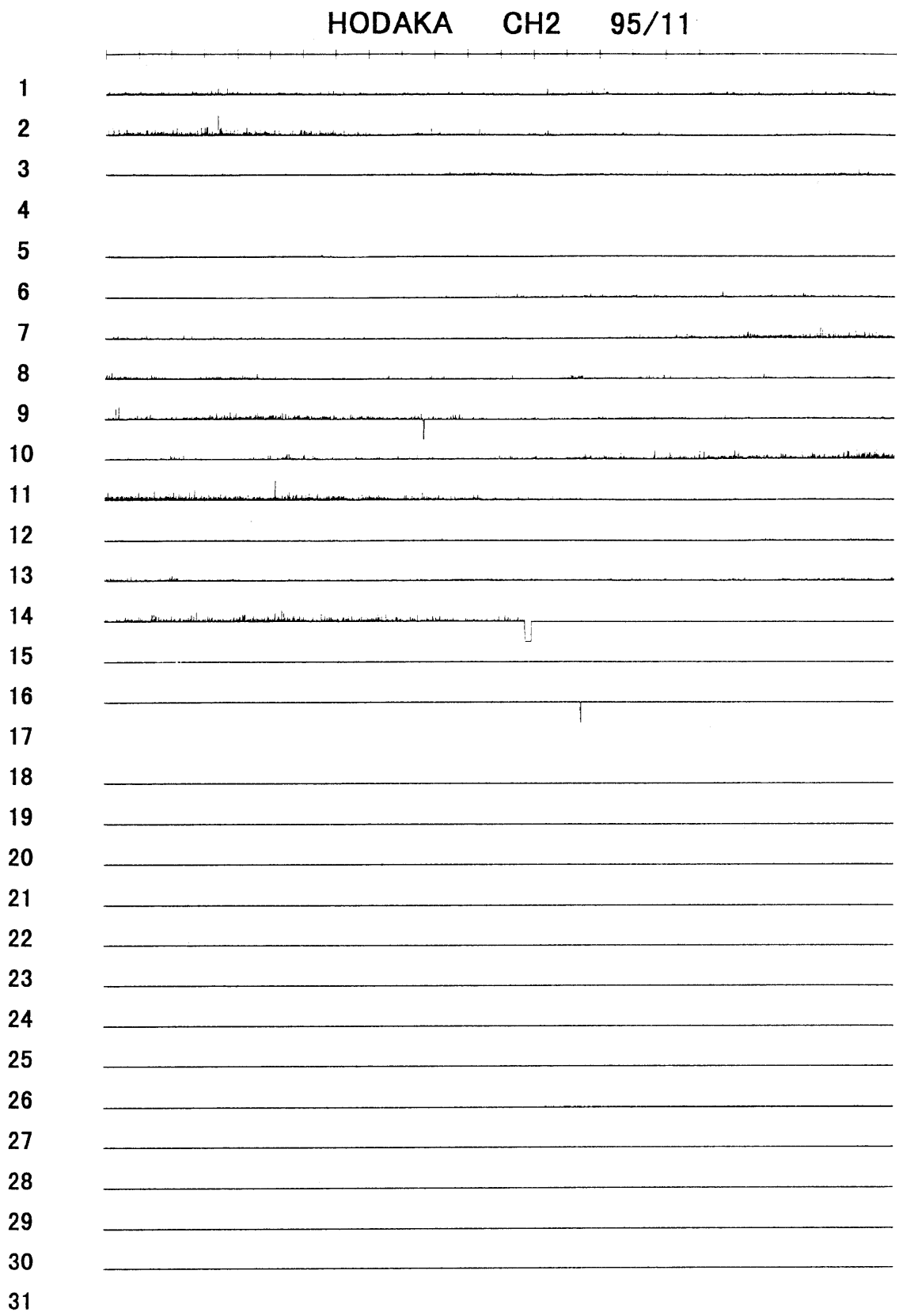
HODAKA CH2 95/11
1
2
3
4
5
6
7
8
9
10
11
12
13
14
15
16
17
18
19
20
21
22
23
24
25
26
27
28
29
30
31

Fig. A-95-11-2

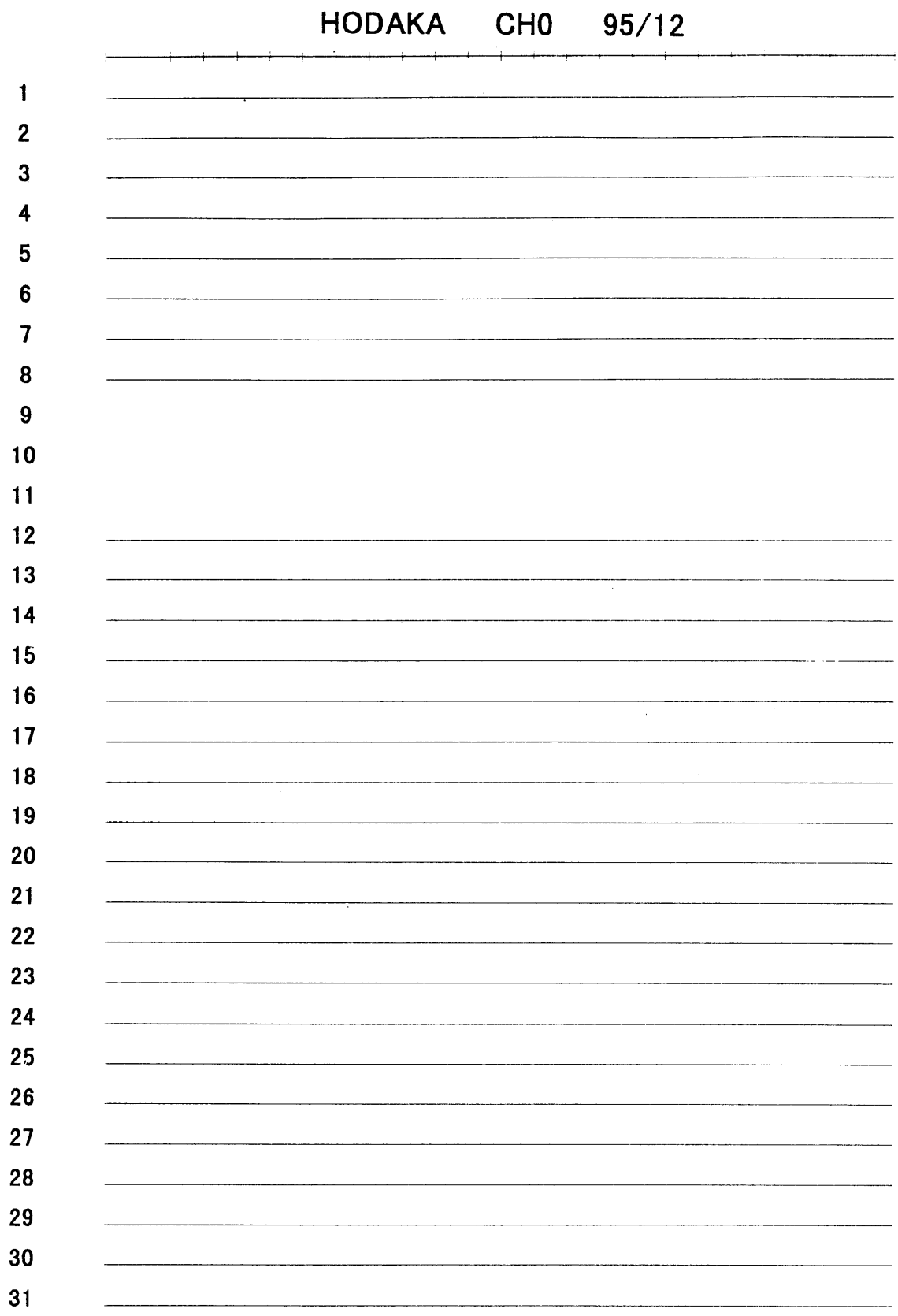
HODAKA CH0 95/12
1
2
3
4
5
6
7
8
9
10
11
12
13
14
15
16
17
18
19
20
21
22
23
24
25
26
27
28
29
30
31

Fig. A-95-12-0

HODAKA CH1 95/12

1
2
3
4
5
6
7
8
9
10
11
12
13
14
15
16
17
18
19
20
21
22
23
24
25
26
27
28
29
30
31

Fig. A-95-12-1

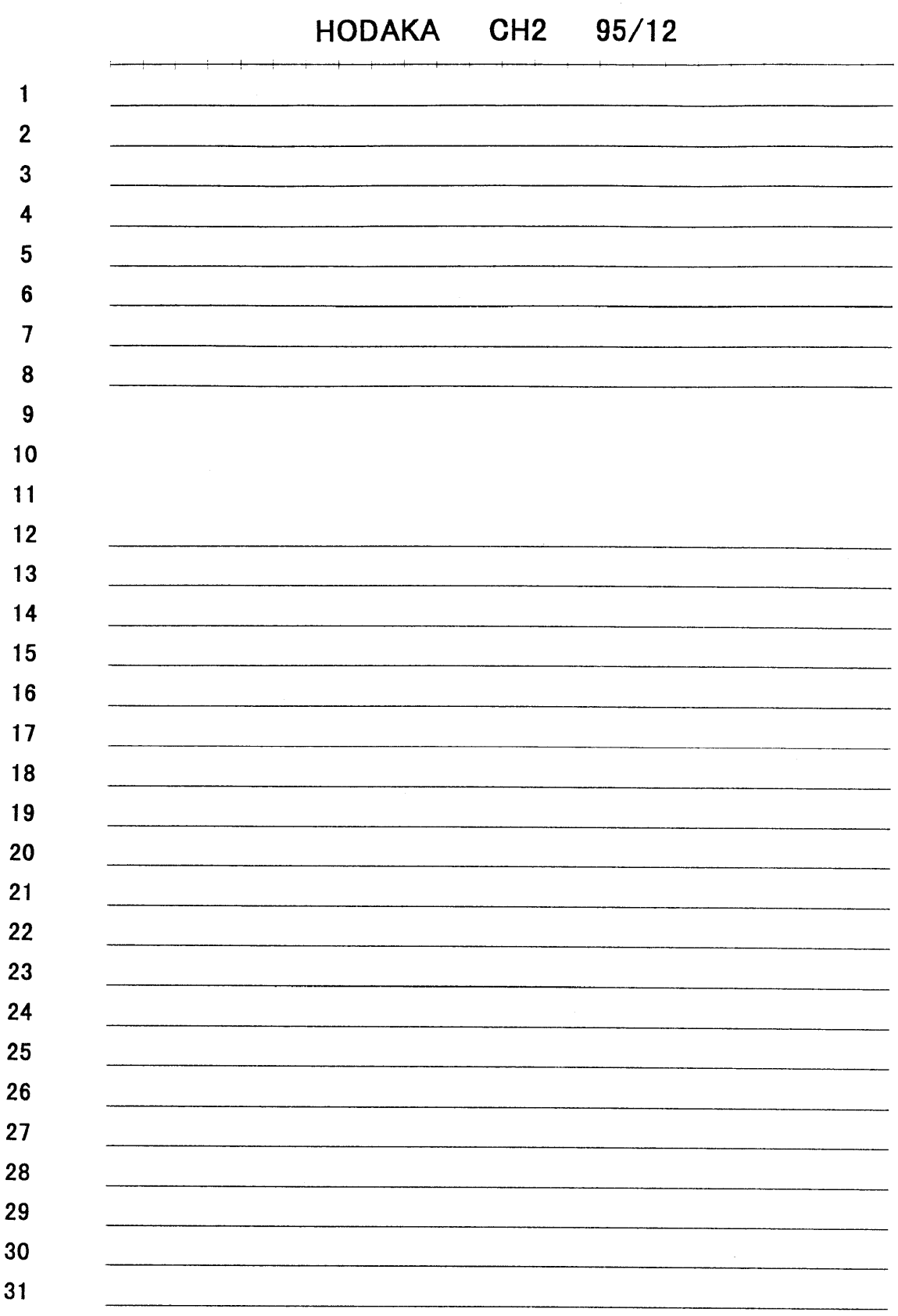
HODAKA CH2 95/12
1
2
3
4
5
6
7
8
9
10
11
12
13
14
15
16
17
18
19
20
21
22
23
24
25
26
27
28
29
30
31

Fig. A-95-12-2

HODAKA CH0 96/1

1
2
3
4
5
6
7
8
9
10
11
12
13
14
15
16
17
18
19
20
21
22
23
24
25
26
27
28
29
30
31

Fig. A-96-1-0

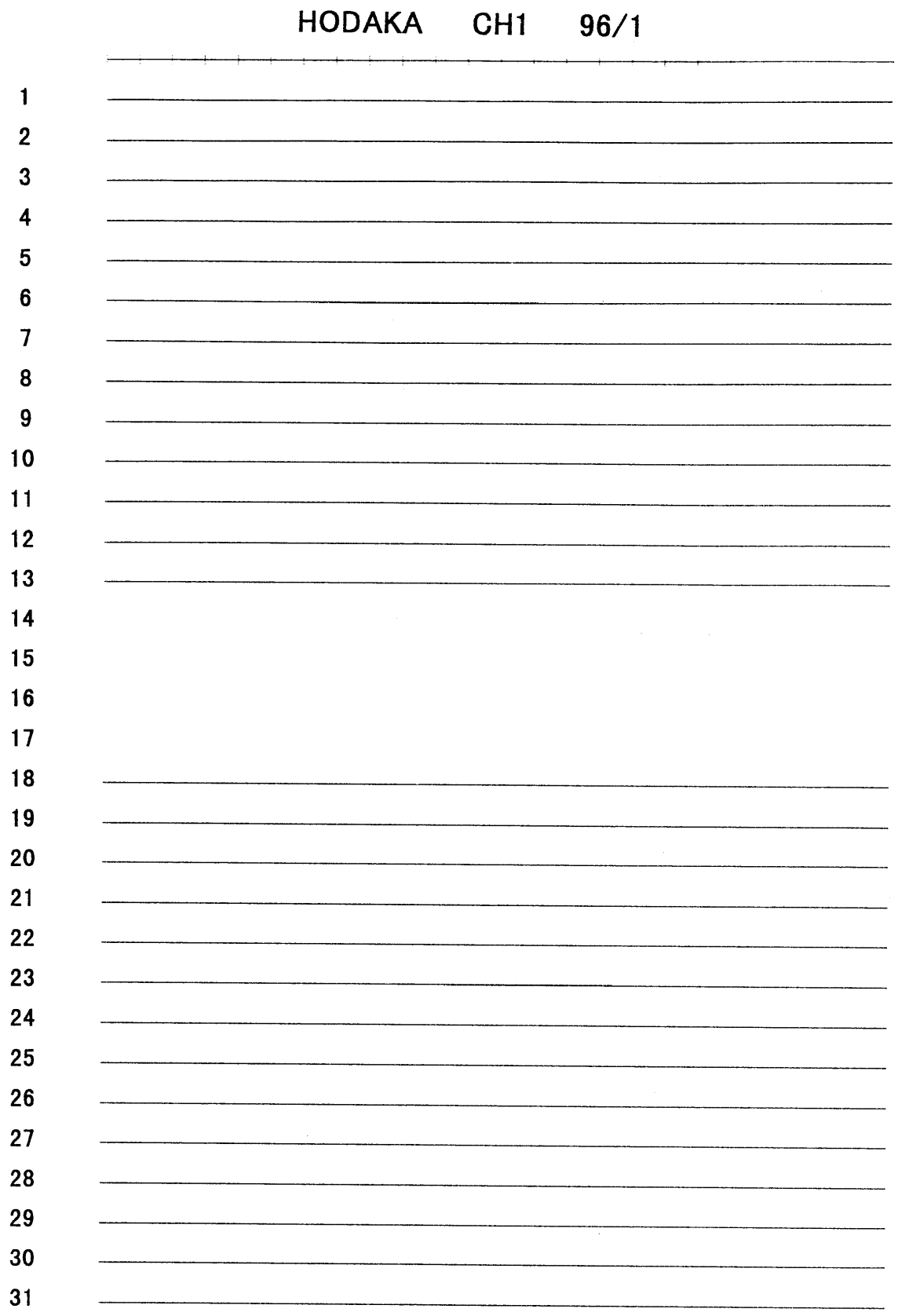
HODAKA CH1 96/1
1
2
3
4
5
6
7
8
9
10
11
12
13
14
15
16
17
18
19
20
21
22
23
24
25
26
27
28
29
30
31

Fig. A-96-1-1

HODAKA CH2 96/1

1
2
3
4
5
6
7
8
9
10
11
12
13
14
15
16
17
18
19
20
21
22
23
24
25
26
27
28
29
30
31

Fig. A-96-1-2

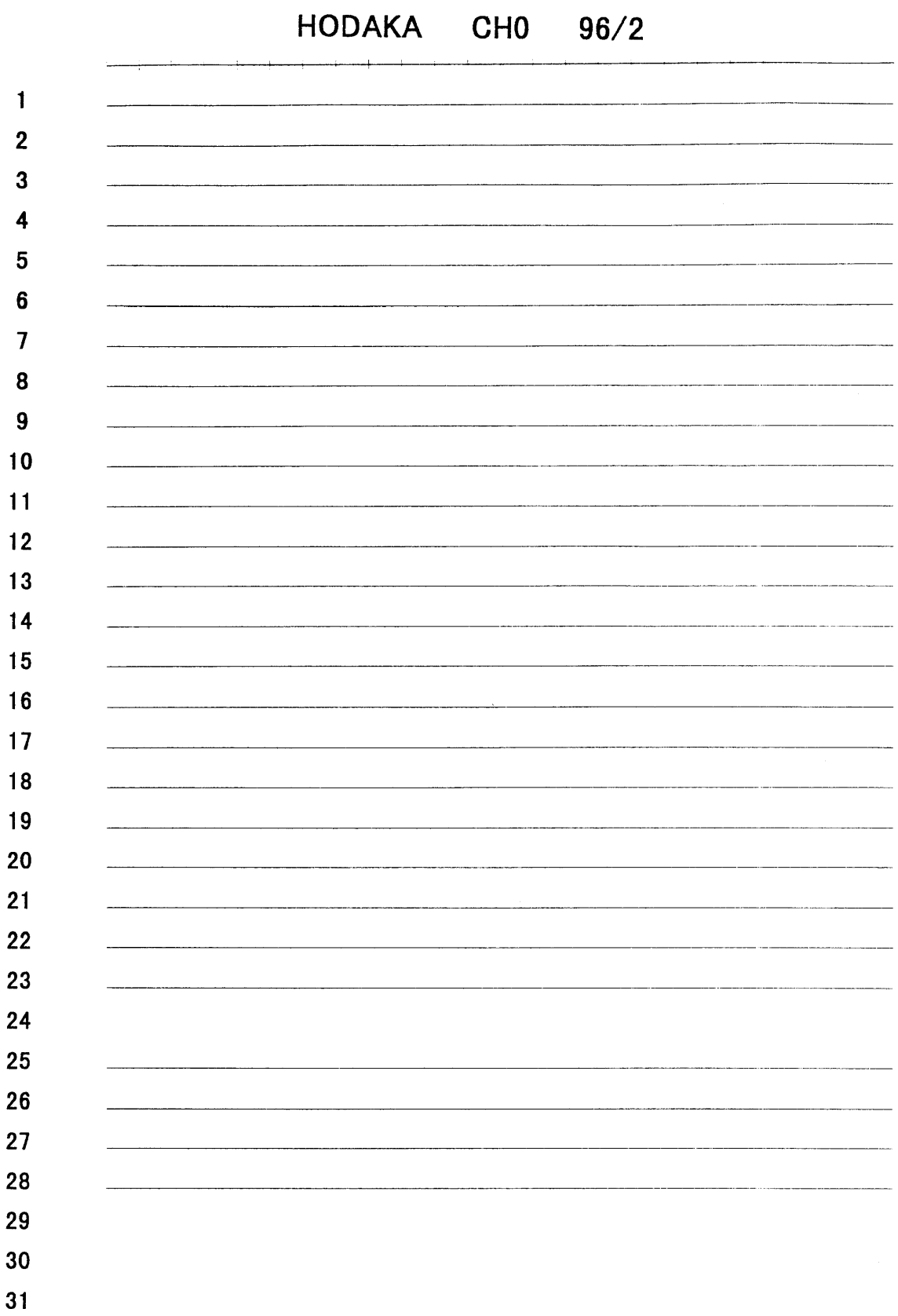
HODAKA CH0 96/2
1
2
3
4
5
6
7
8
9
10
11
12
13
14
15
16
17
18
19
20
21
22
23
24
25
26
27
28
29
30
31

Fig. A-96-2-0

HODAKA CH1 96/2

1
2
3
4
5
6
7
8
9
10
11
12
13
14
15
16
17
18
19
20
21
22
23
24
25
26
27
28
29
30
31

Fig. A-96-2-1

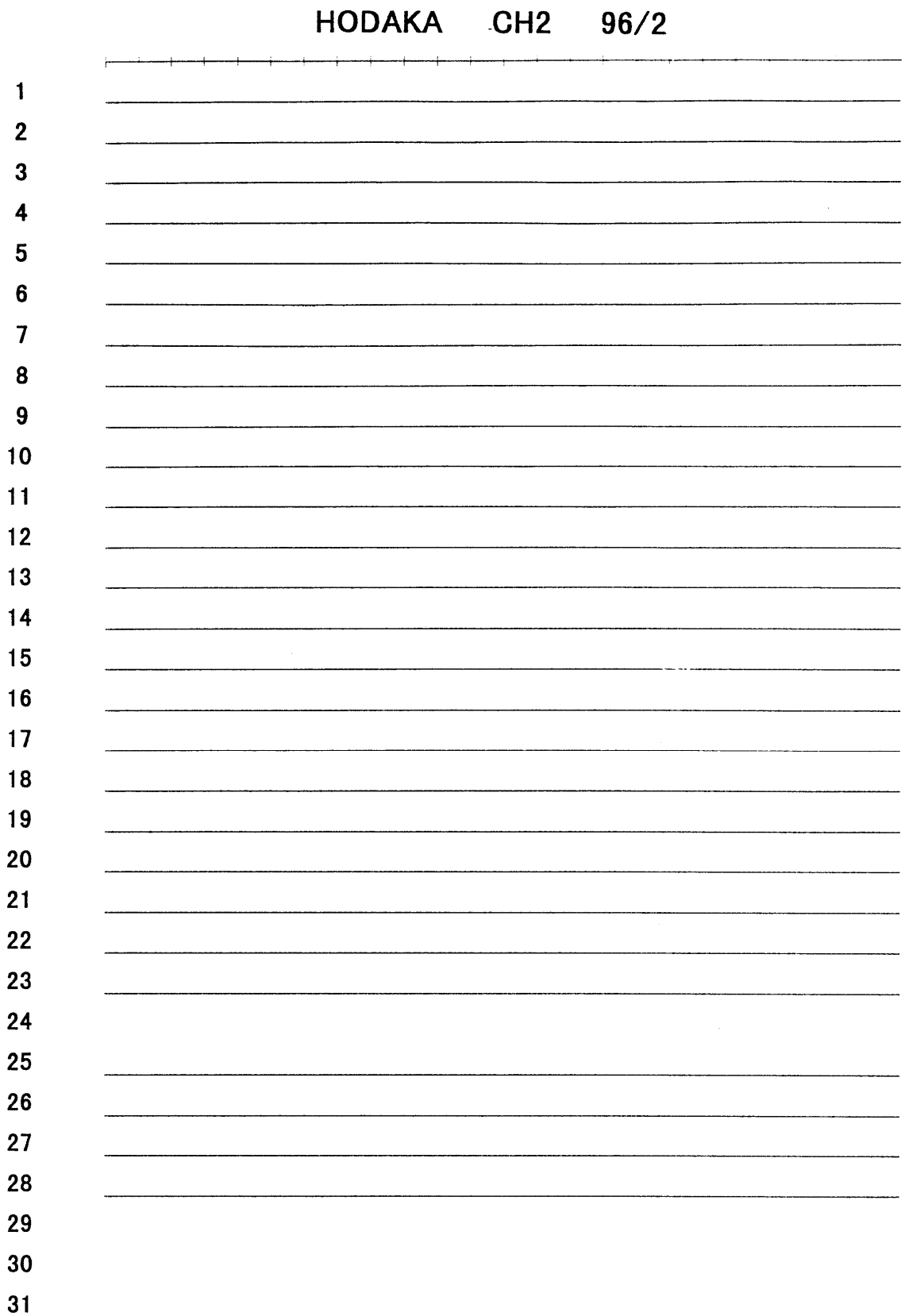
HODAKA CH2 96/2
1
2
3
4
5
6
7
8
9
10
11
12
13
14
15
16
17
18
19
20
21
22
23
24
25
26
27
28
29
30
31

Fig. A-96-2-2

HODAKA CH0 96/3

1
2
3
4
5
6
7
8
9
10
11
12
13
14
15
16
17
18
19
20
21
22
23
24
25
26
27
28
29
30
31

Fig. A-96-3-0

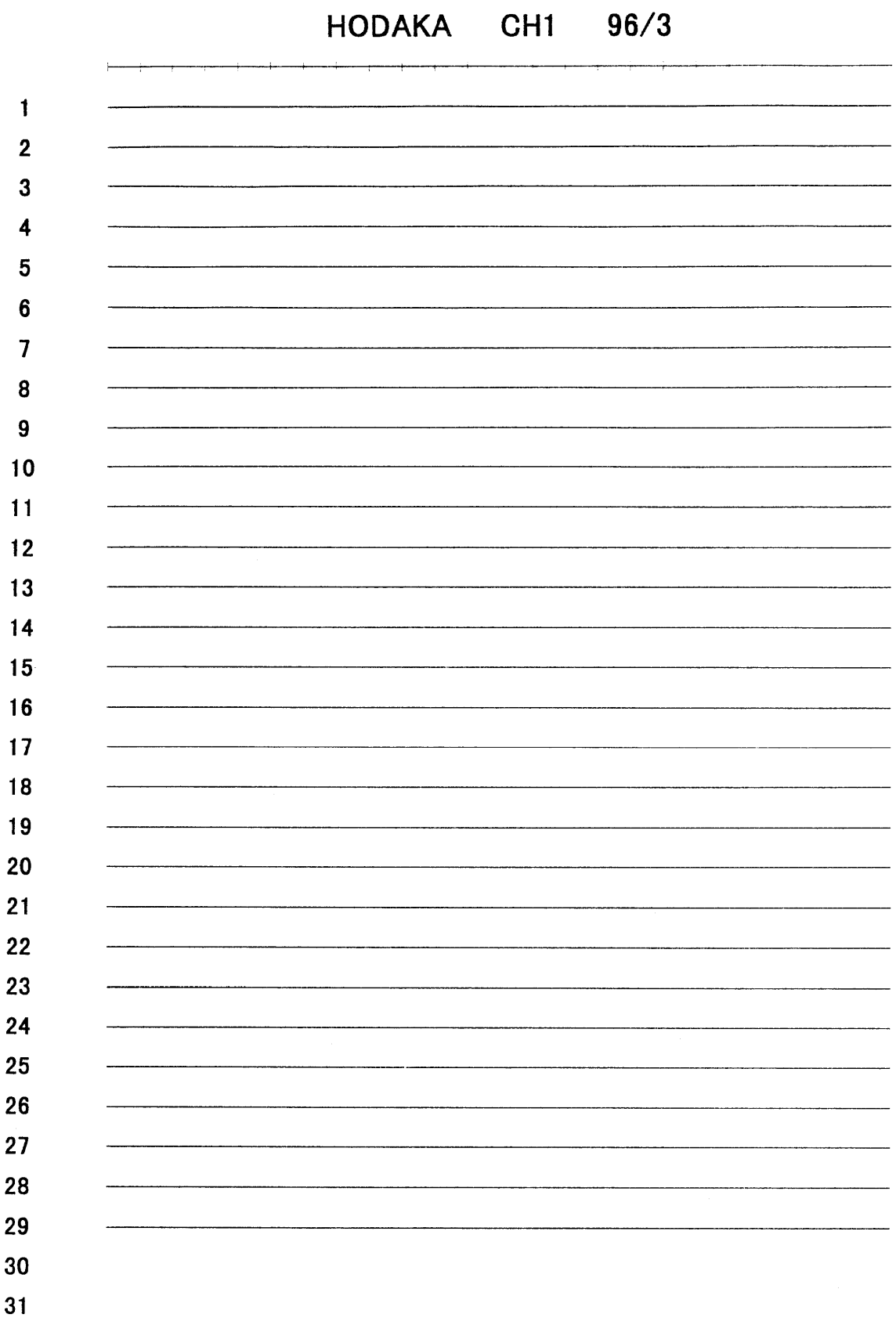
HODAKA CH1 96/3
1
2
3
4
5
6
7
8
9
10
11
12
13
14
15
16
17
18
19
20
21
22
23
24
25
26
27
28
29
30
31

Fig. A-96-3-1

HODAKA CH2 96/3

1
2
3
4
5
6
7
8
9
10
11
12
13
14
15
16
17
18
19
20
21
22
23
24
25
26
27
28
29
30
31

Fig. A-96-3-2

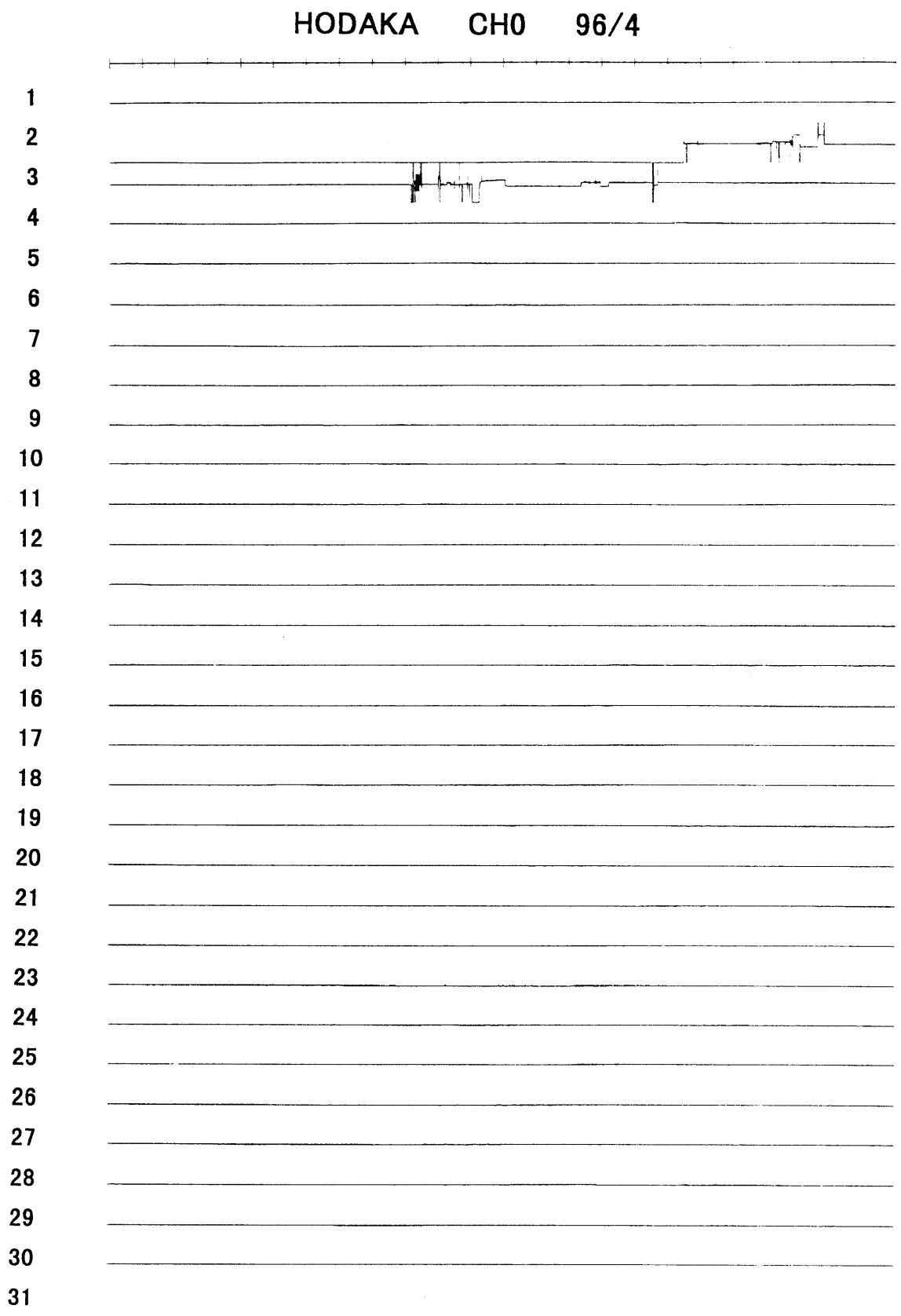
HODAKA CH0 96/4
1
2
3
4
5
6
7
8
9
10
11
12
13
14
15
16
17
18
19
20
21
22
23
24
25
26
27
28
29
30
31

Fig. A-96-4-0

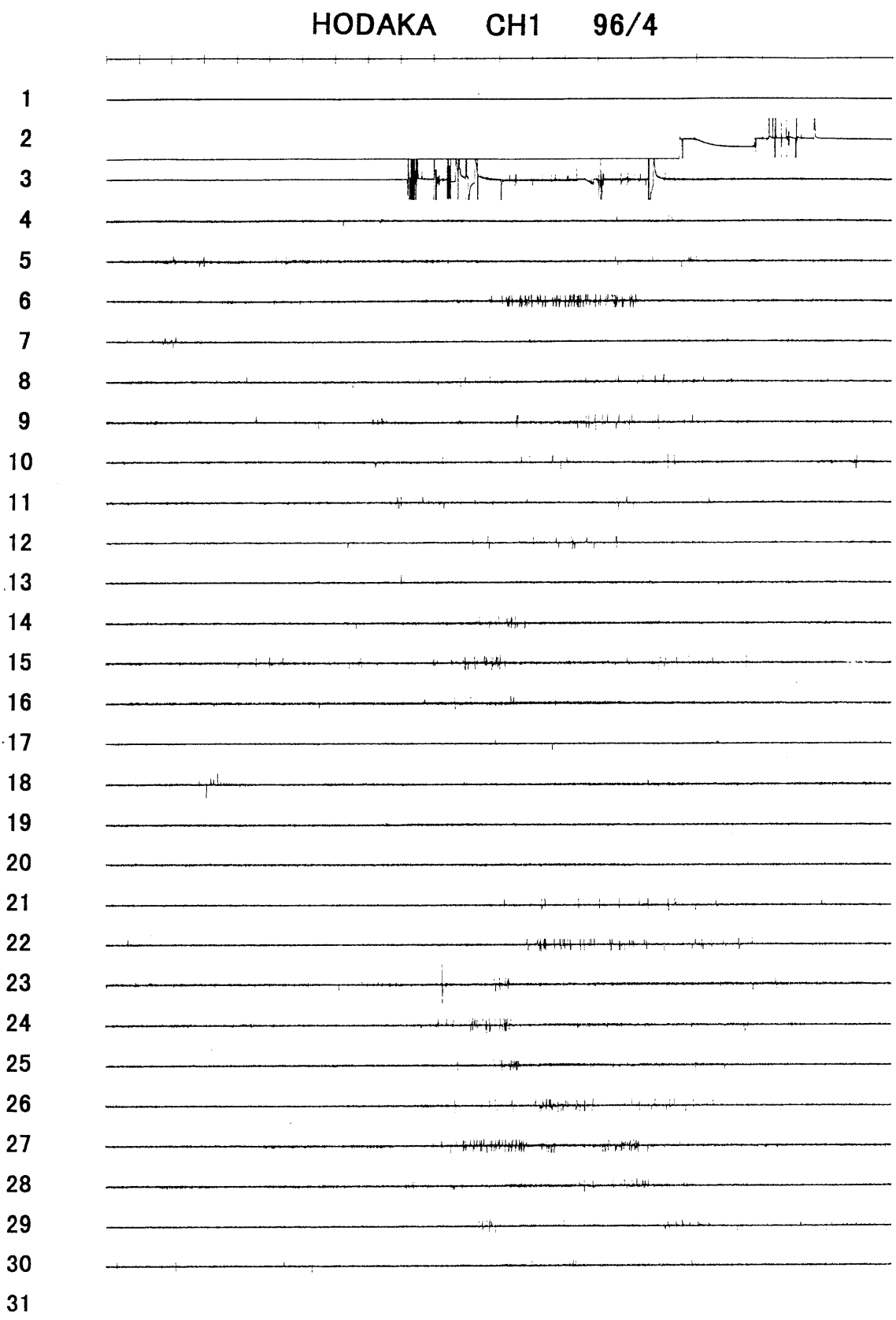
HODAKA CH1 96/4
1
2
3
4
5
6
7
8
9
10
11
12
13
14
15
16
17
18
19
20
21
22
23
24
25
26
27
28
29
30
31

Fig. A-96-4-1

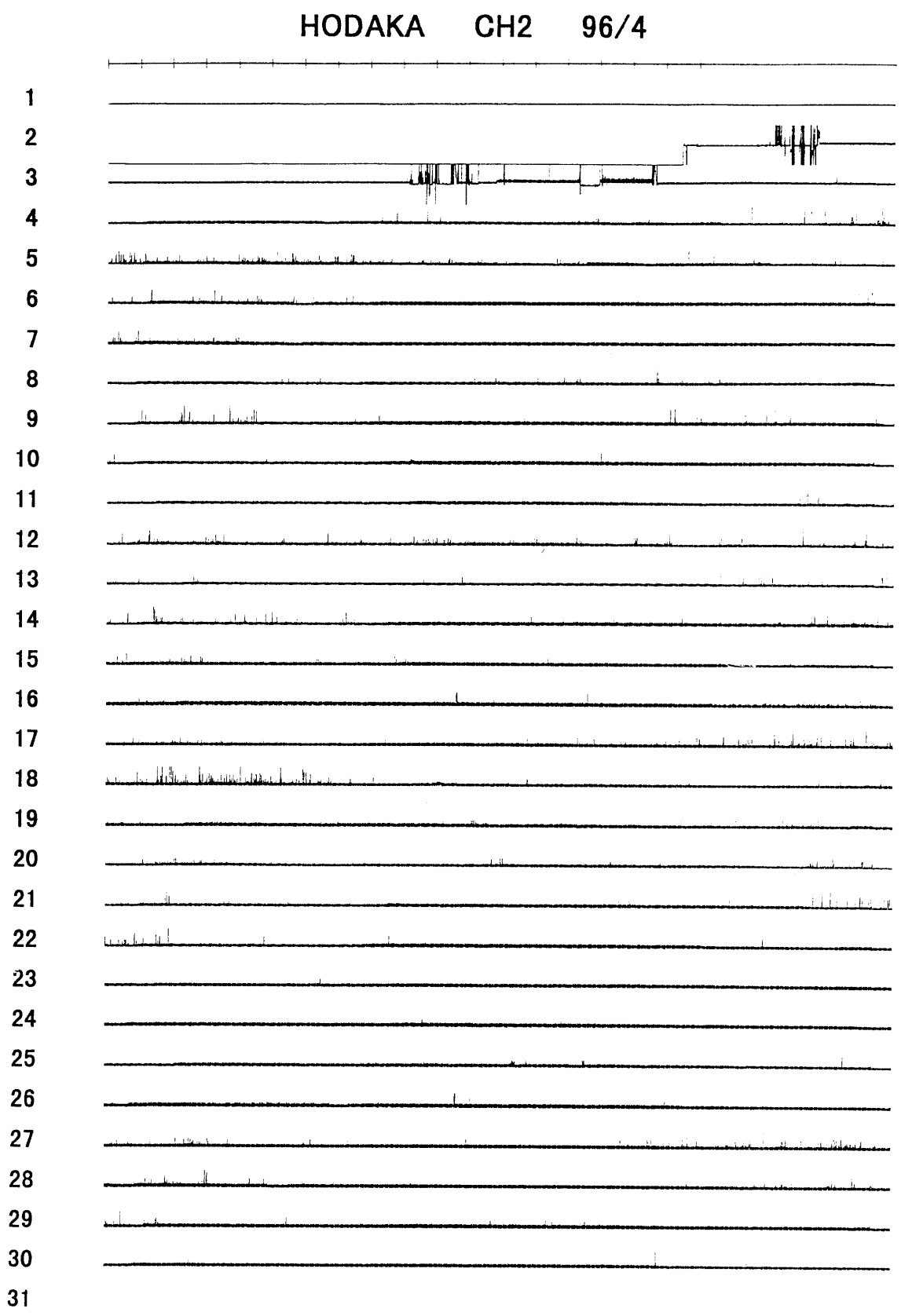
HODAKA CH2 96/4
1
2
3
4
5
6
7
8
9
10
11
12
13
14
15
16
17
18
19
20
21
22
23
24
25
26
27
28
29
30
31

Fig. A-96-4-2

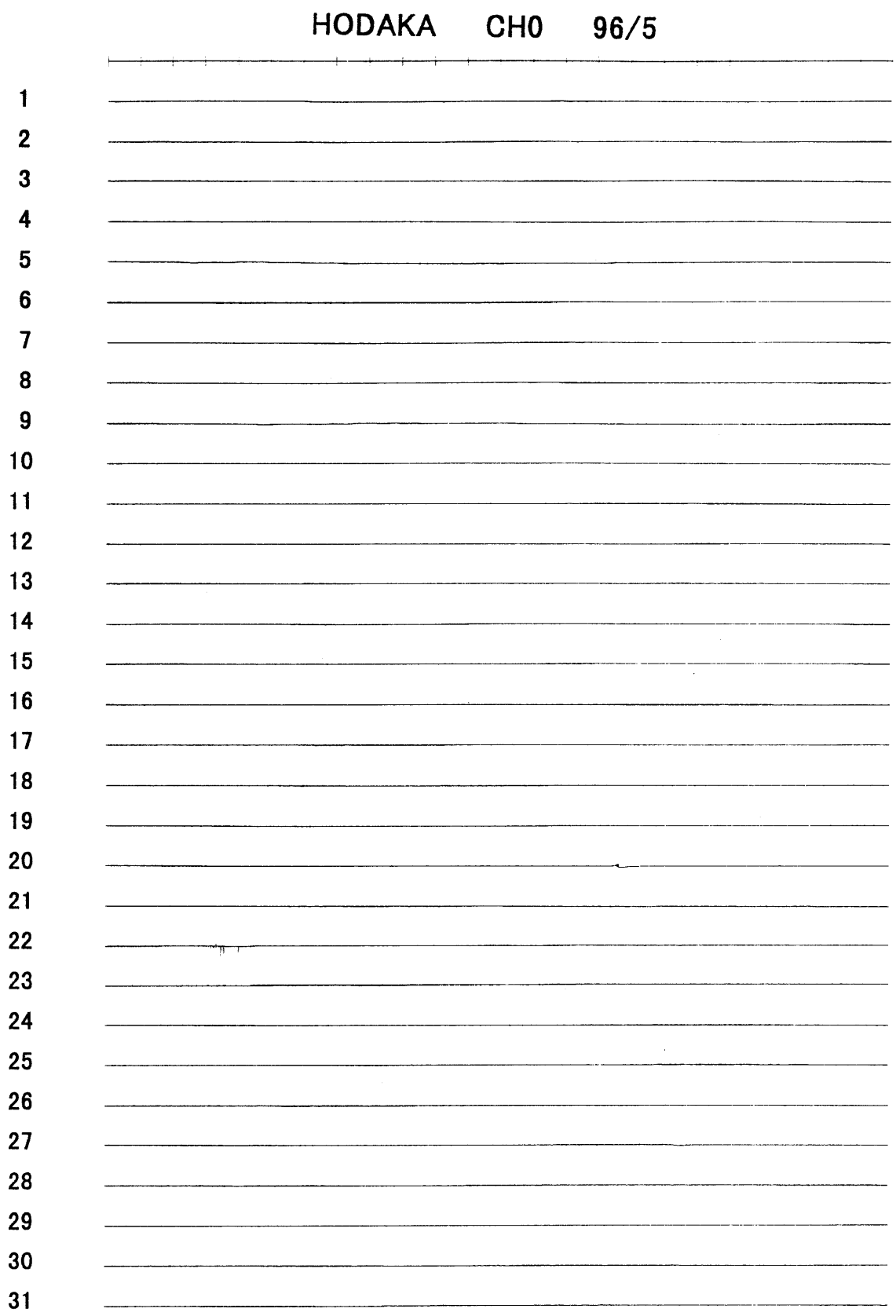
HODAKA CH0 96/5
1
2
3
4
5
6
7
8
9
10
11
12
13
14
15
16
17
18
19
20
21
22
23
24
25
26
27
28
29
30
31

Fig. A-96-5-0

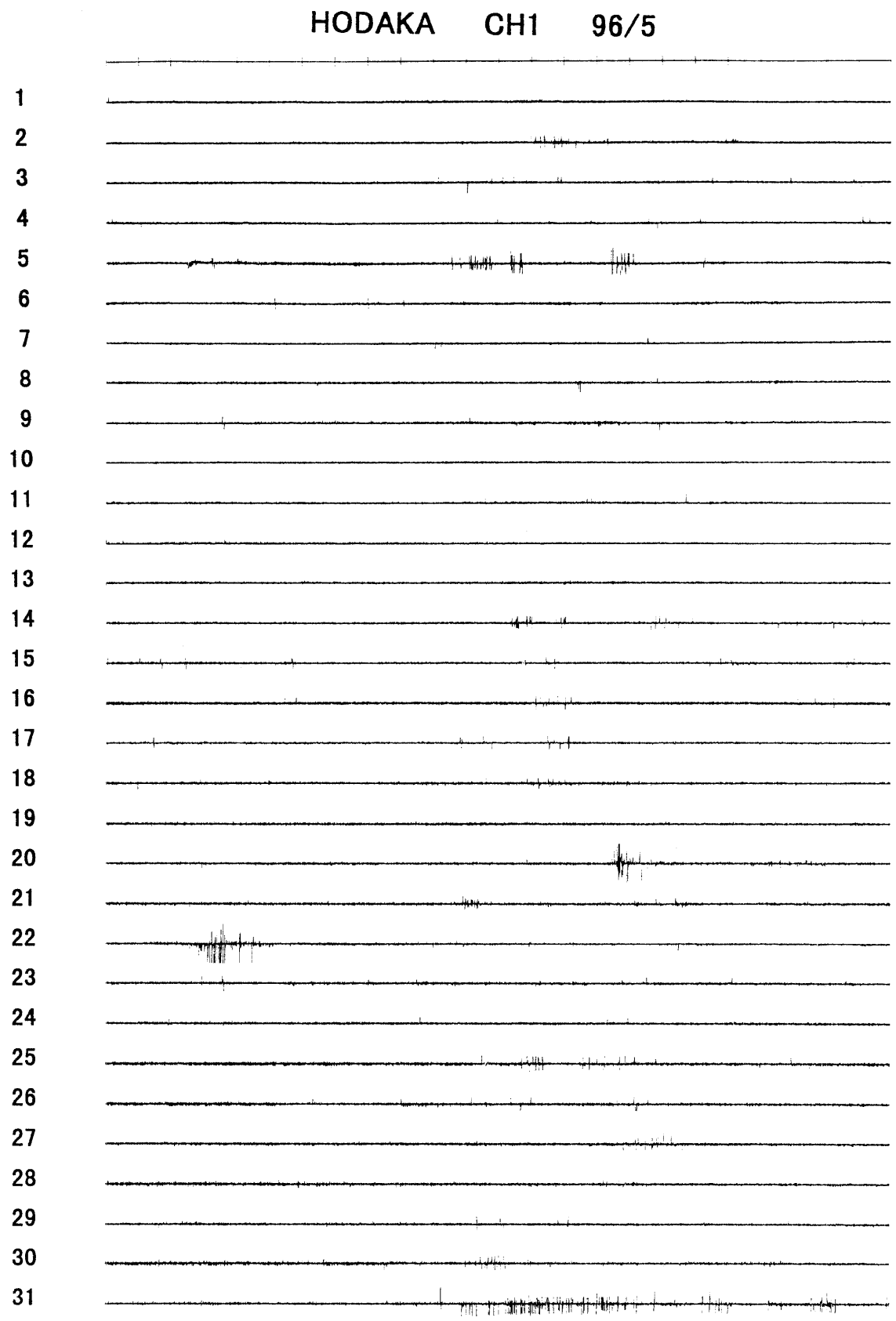
HODAKA CH1 96/5
1
2
3
4
5
6
7
8
9
10
11
12
13
14
15
16
17
18
19
20
21
22
23
24
25
26
27
28
29
30
31

Fig. A-96-5-1

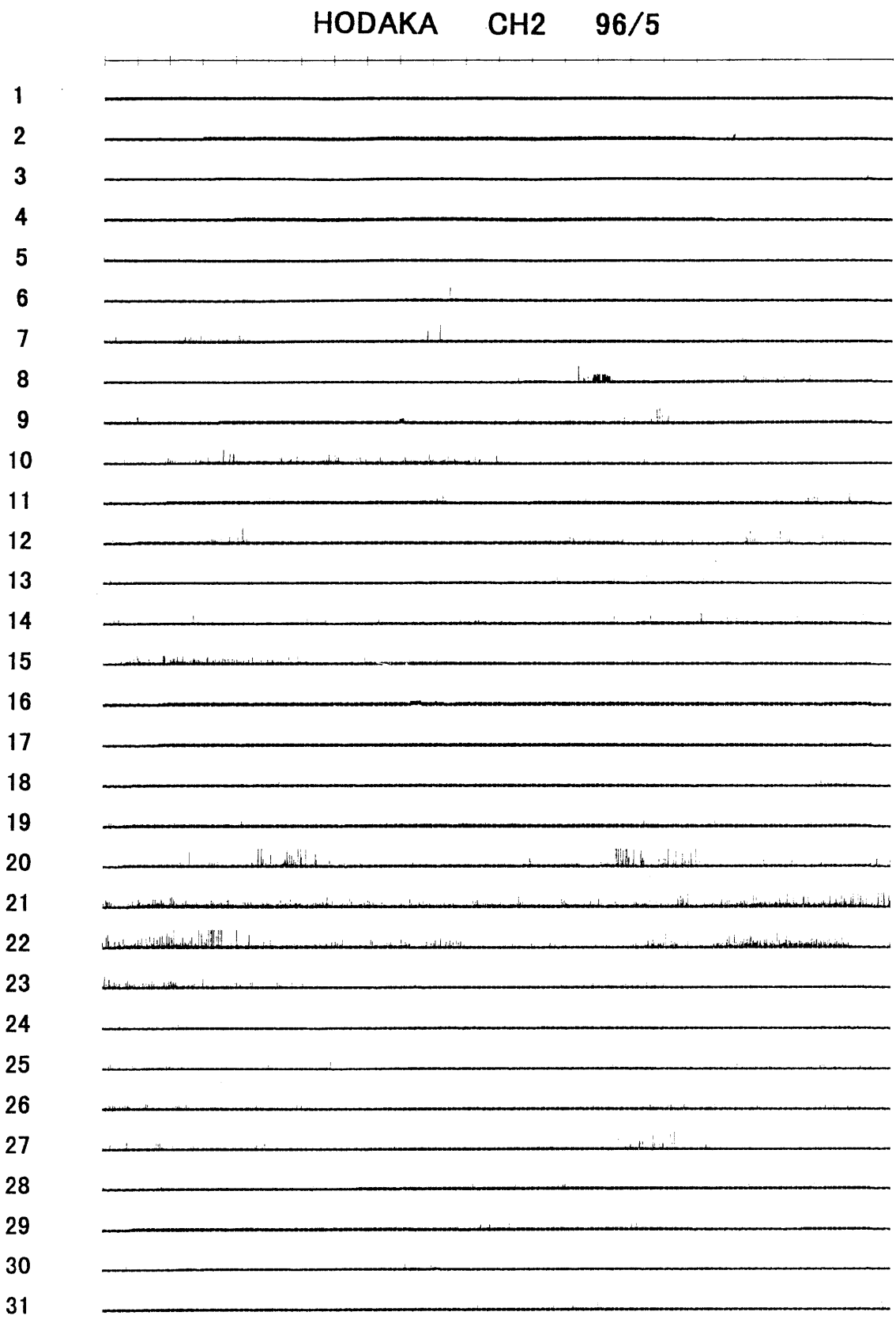
HODAKA CH2 96/5
1
2
3
4
5
6
7
8
9
10
11
12
13
14
15
16
17
18
19
20
21
22
23
24
25
26
27
28
29
30
31

Fig. A-96-5-2

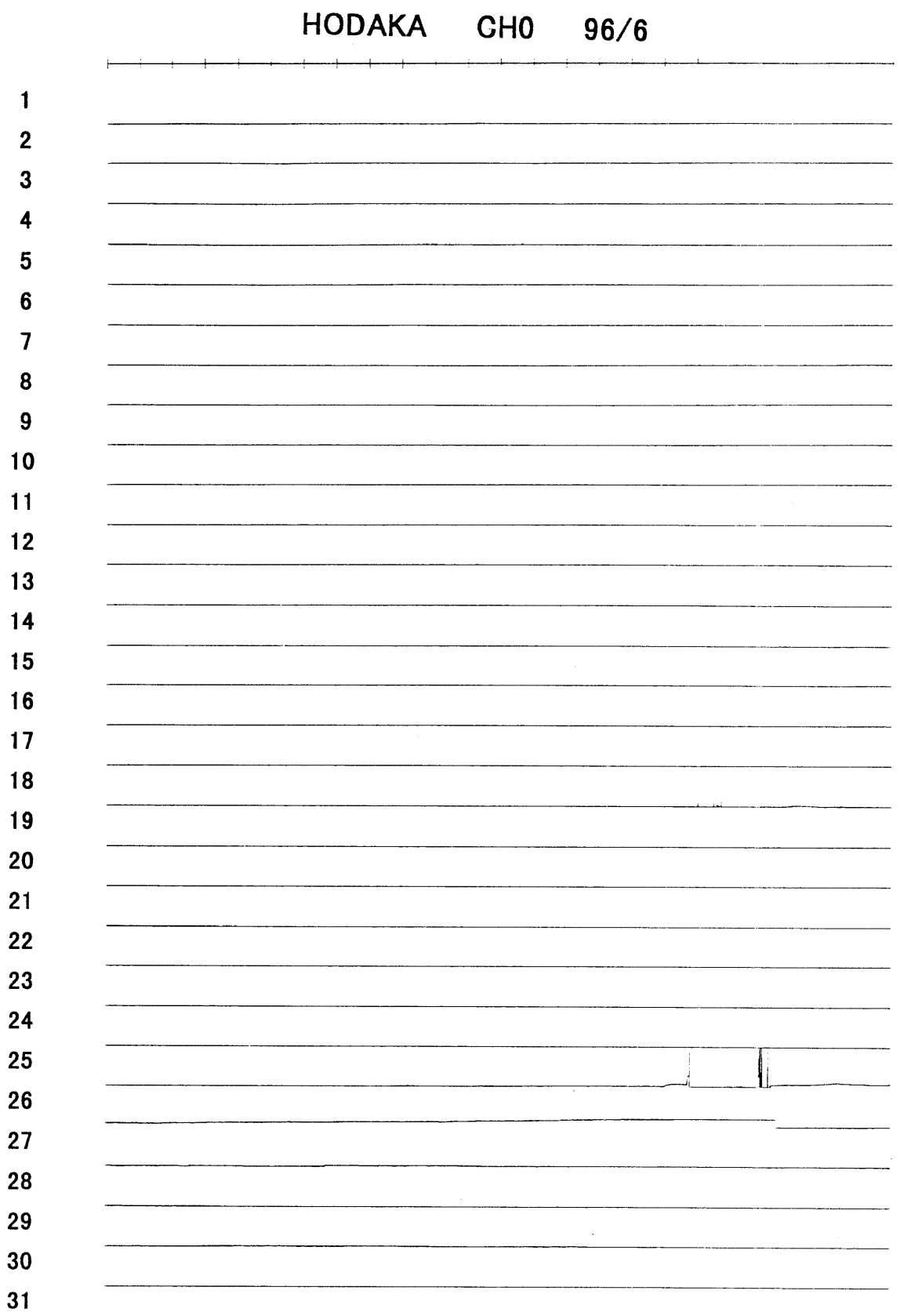
HODAKA CH0 96/6
1
2
3
4
5
6
7
8
9
10
11
12
13
14
15
16
17
18
19
20
21
22
23
24
25
26
27
28
29
30
31

Fig. A-96-6-0

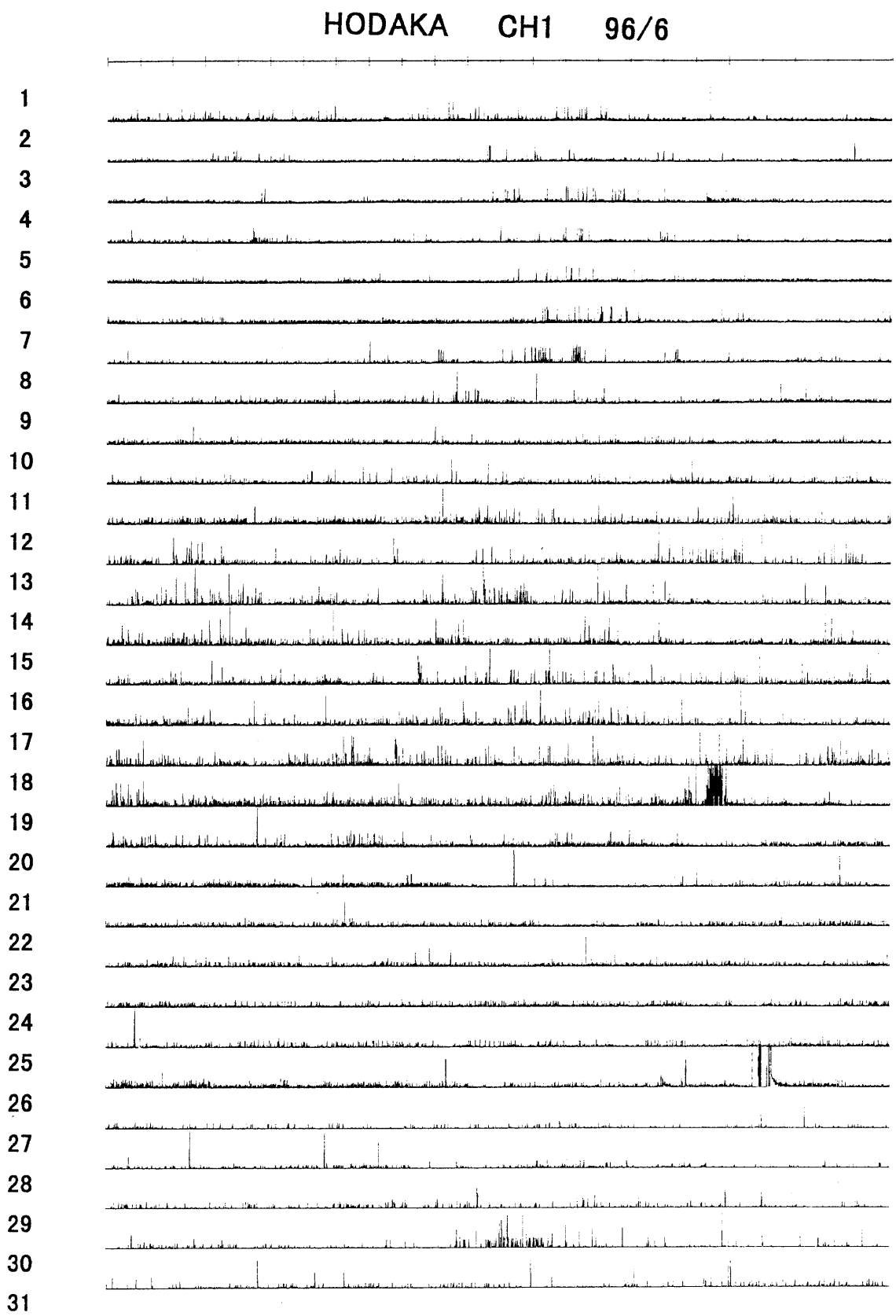
HODAKA CH1 96/6
1
2
3
4
5
6
7
8
9
10
11
12
13
14
15
16
17
18
19
20
21
22
23
24
25
26
27
28
29
30
31

Fig. A-96-6-1

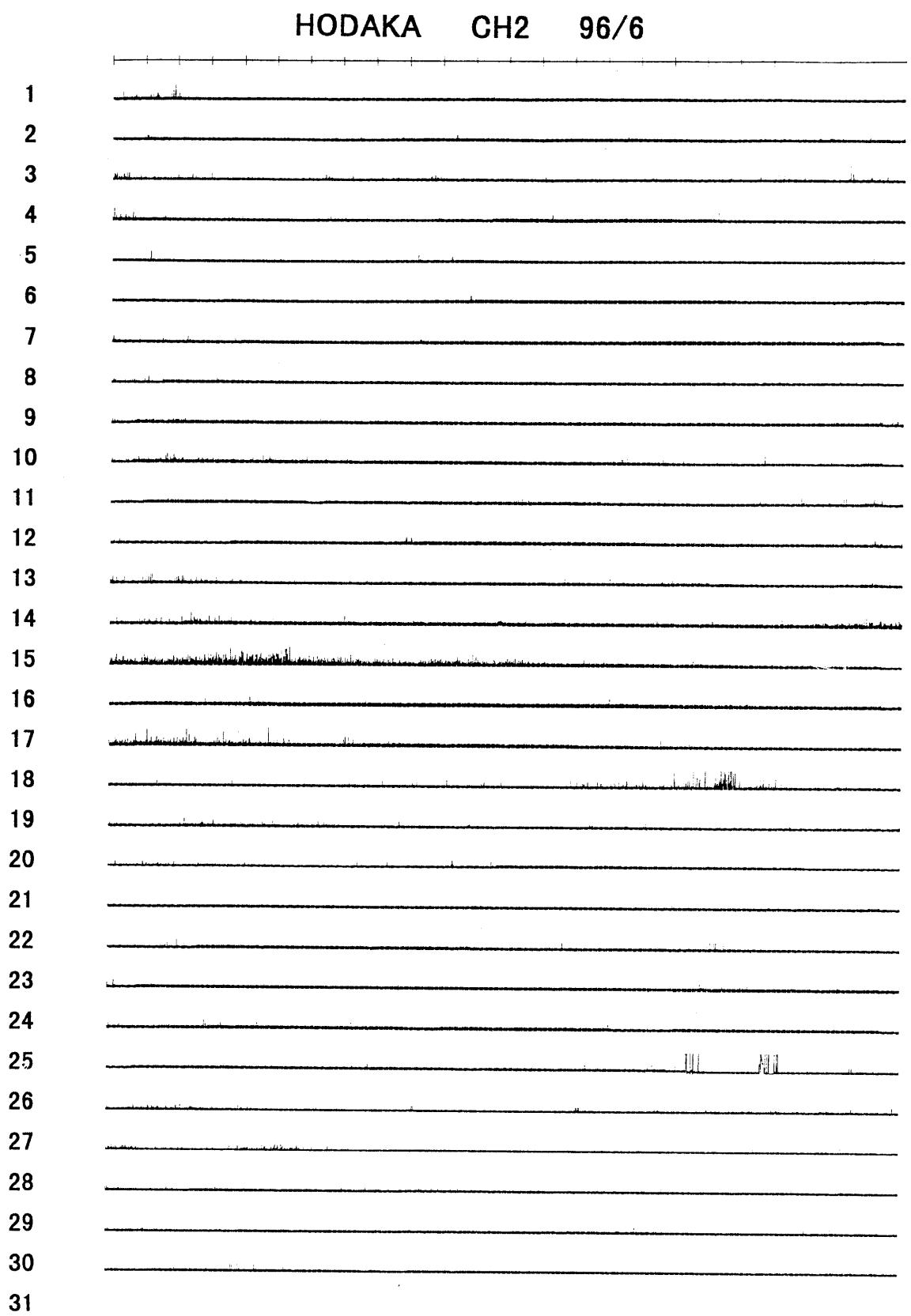
HODAKA CH2 96/6
1
2
3
4
5
6
7
8
9
10
11
12
13
14
15
16
17
18
19
20
21
22
23
24
25
26
27
28
29
30
31

Fig. A-96-6-2

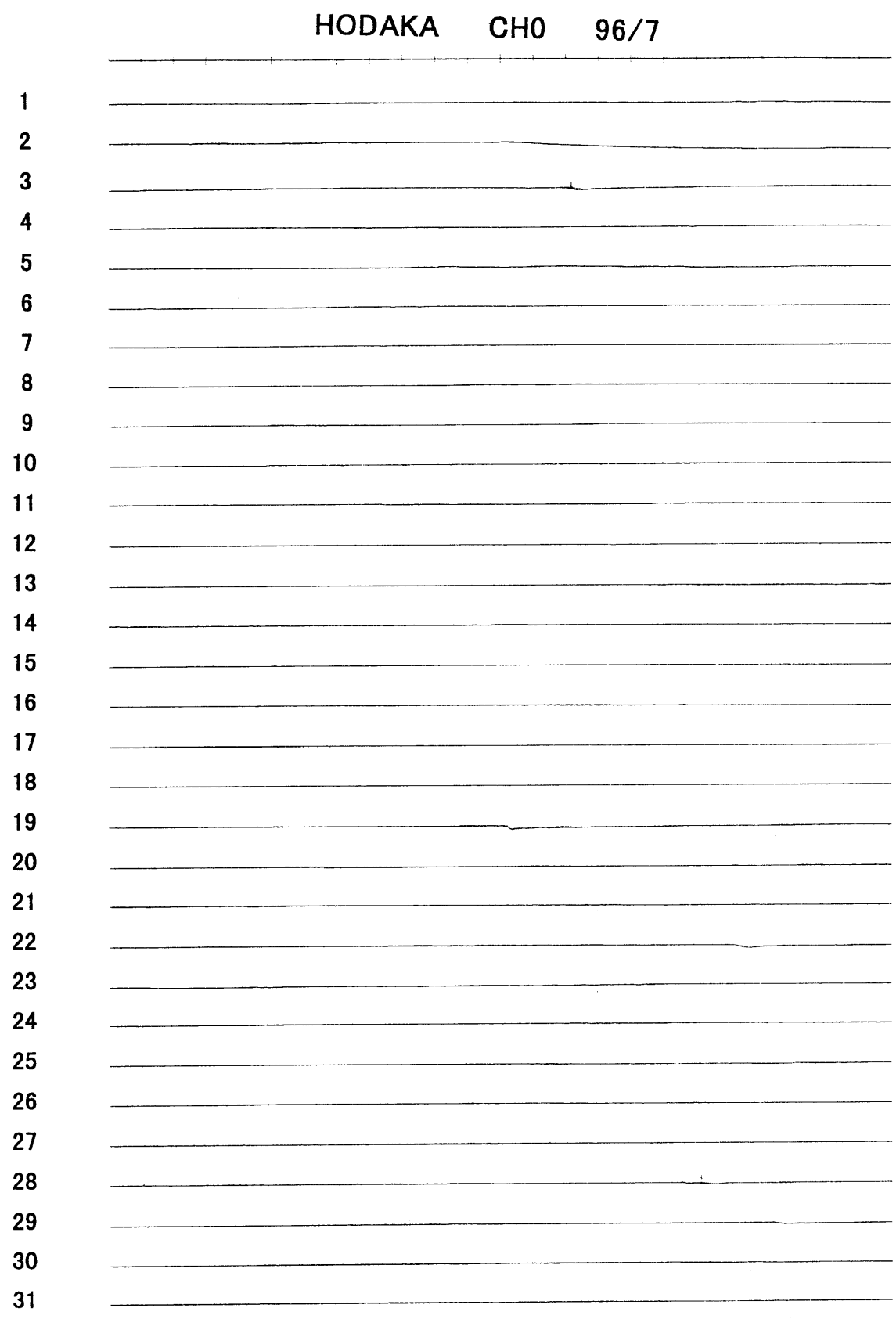
HODAKA CH0 96/7
1
2
3
4
5
6
7
8
9
10
11
12
13
14
15
16
17
18
19
20
21
22
23
24
25
26
27
28
29
30
31

Fig. A-96-7-0

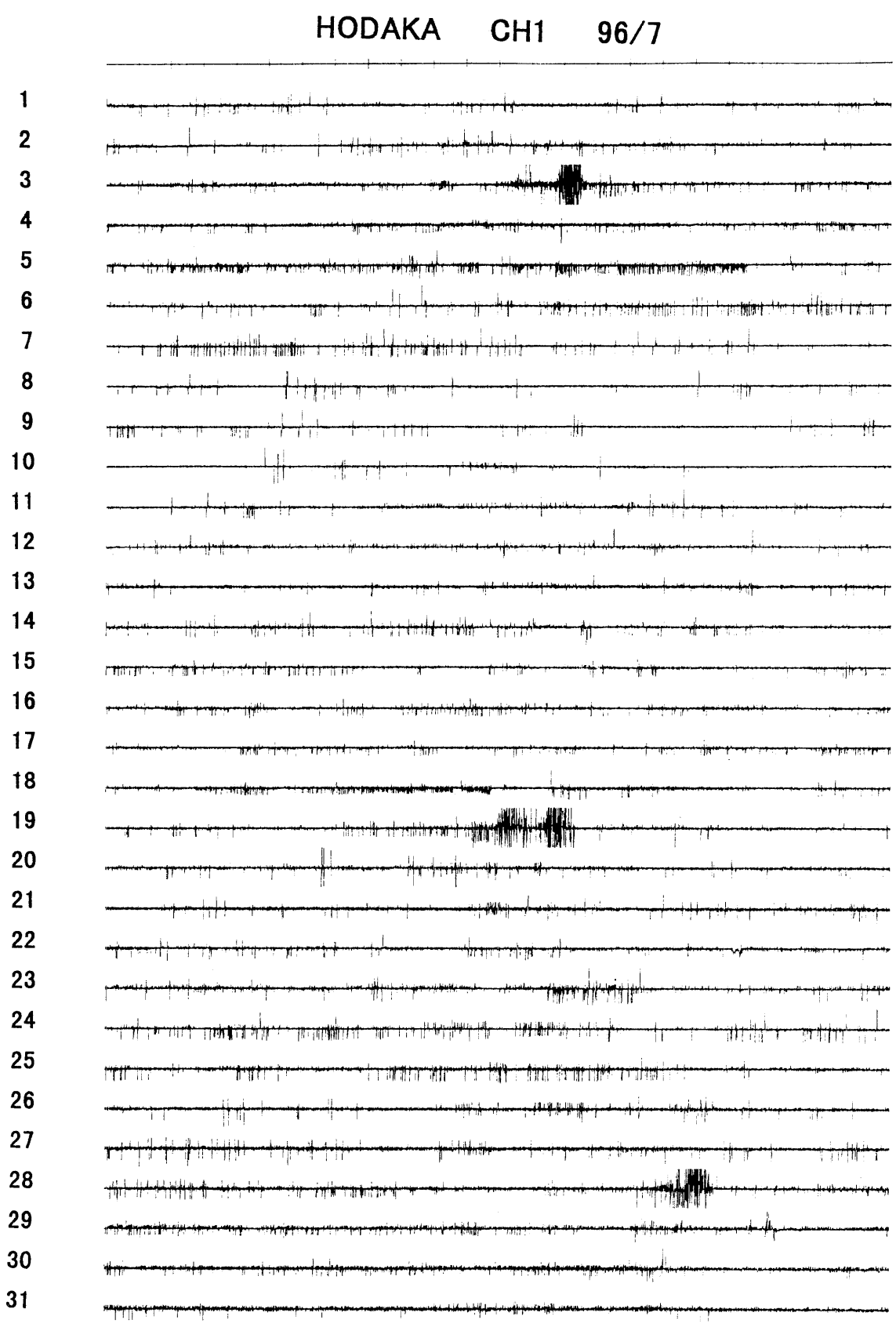
HODAKA CH1 96/7
1
2
3
4
5
6
7
8
9
10
11
12
13
14
15
16
17
18
19
20
21
22
23
24
25
26
27
28
29
30
31

Fig. A-96-7-1

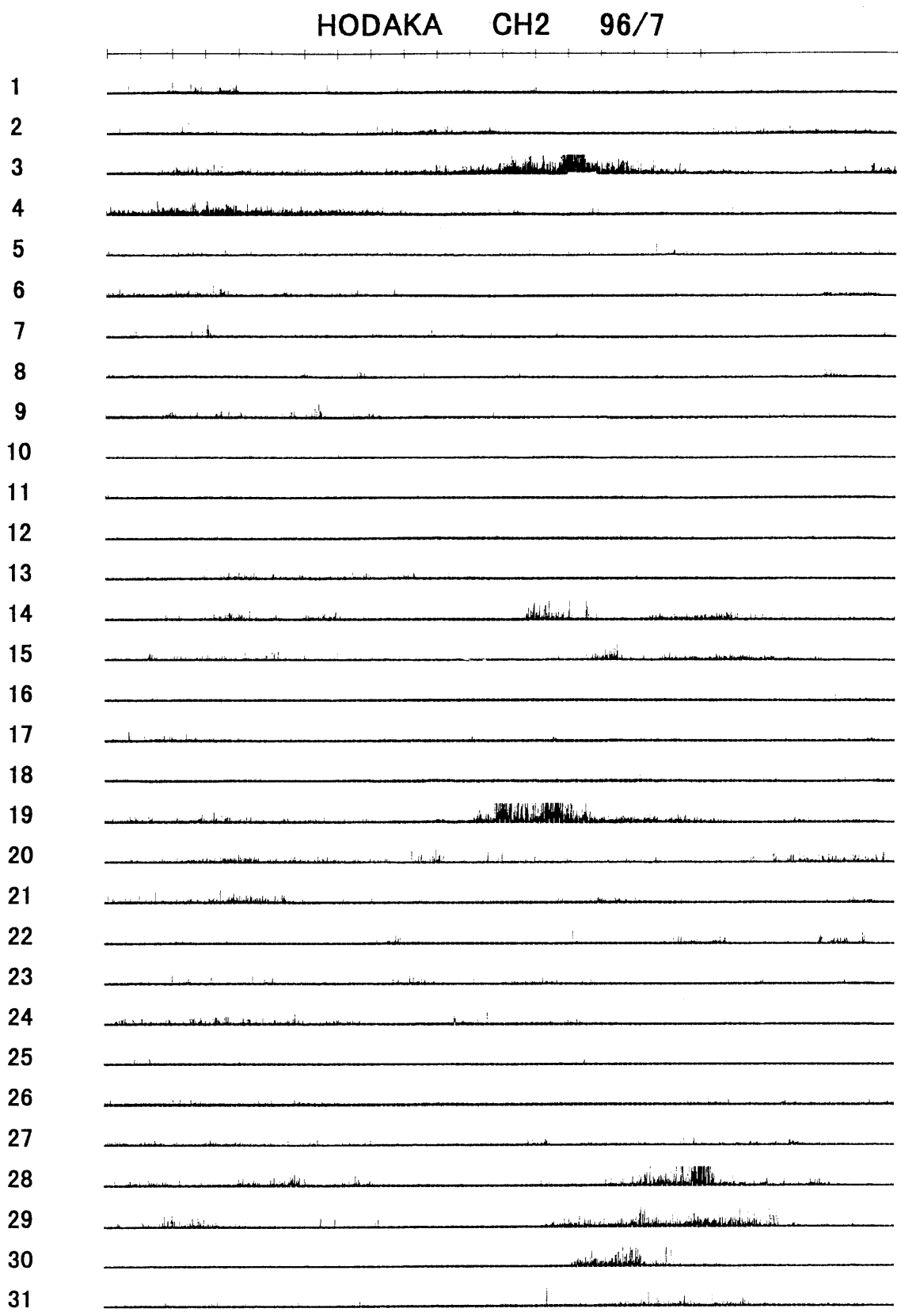
HODAKA CH2 96/7
1
2
3
4
5
6
7
8
9
10
11
12
13
14
15
16
17
18
19
20
21
22
23
24
25
26
27
28
29
30
31

Fig. A-96-7-2

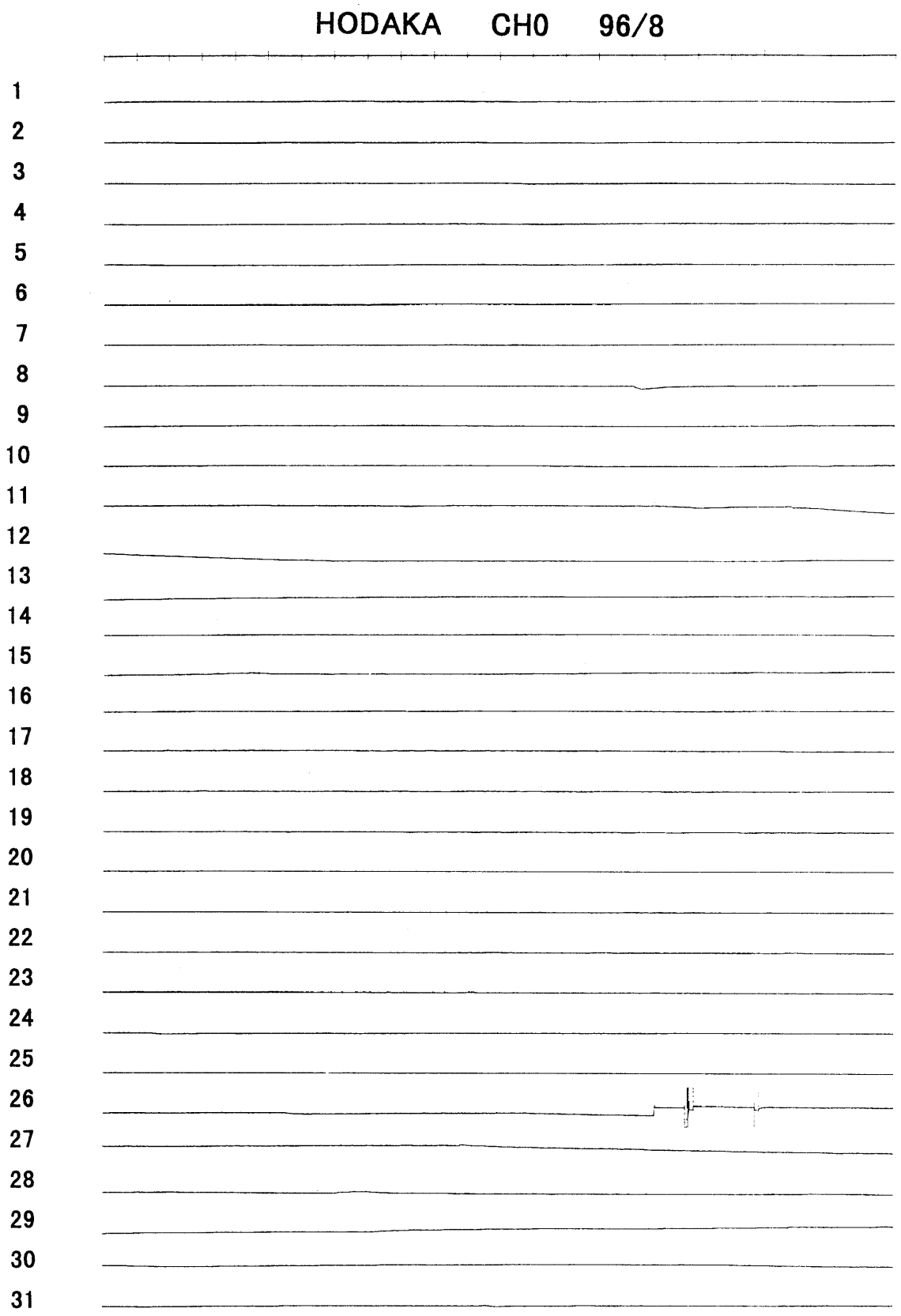
HODAKA CH0 96/8
1
2
3
4
5
6
7
8
9
10
11
12
13
14
15
16
17
18
19
20
21
22
23
24
25
26
27
28
29
30
31

Fig. A-96-8-0

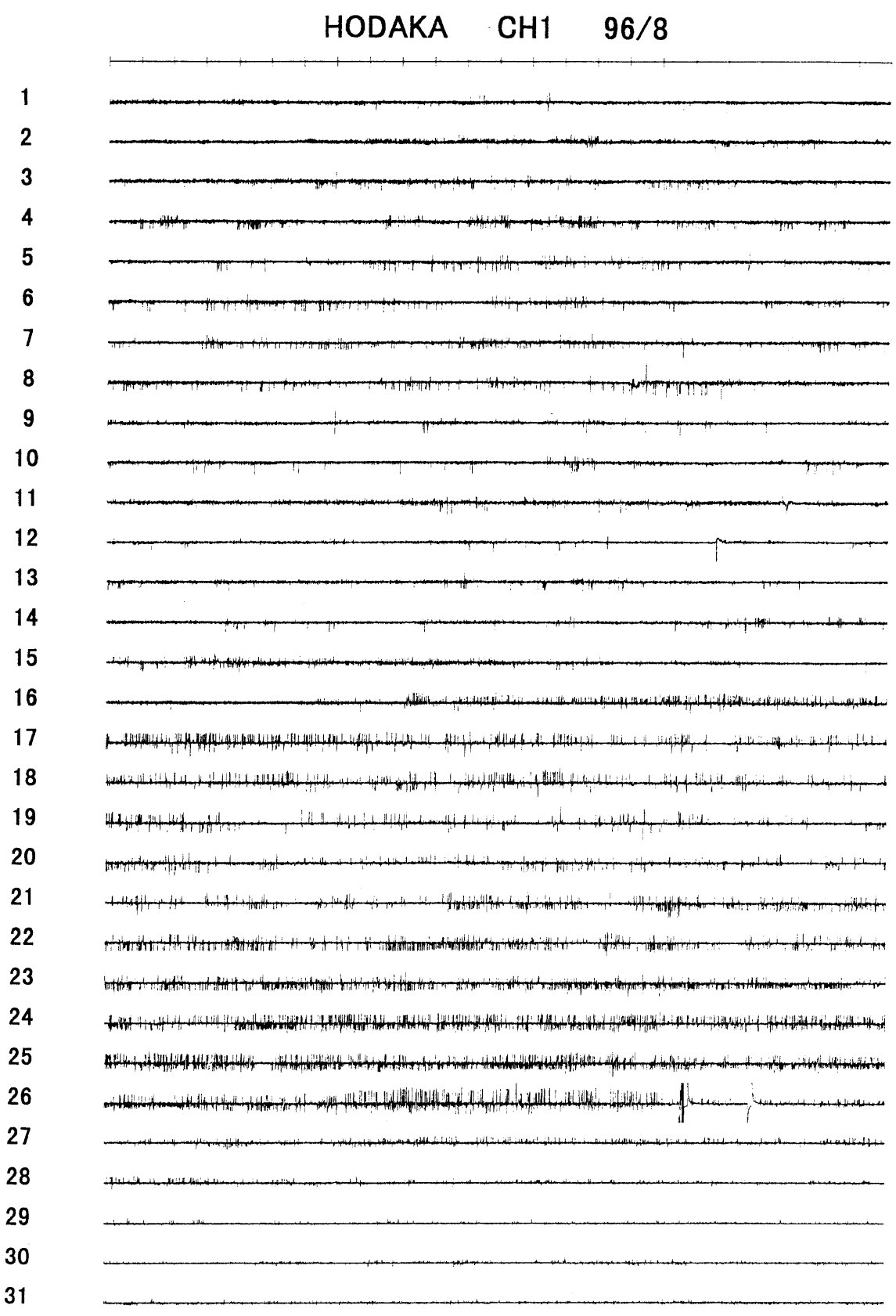
HODAKA CH1 96/8
1
2
3
4
5
6
7
8
9
10
11
12
13
14
15
16
17
18
19
20
21
22
23
24
25
26
27
28
29
30
31

Fig. A-96-8-1

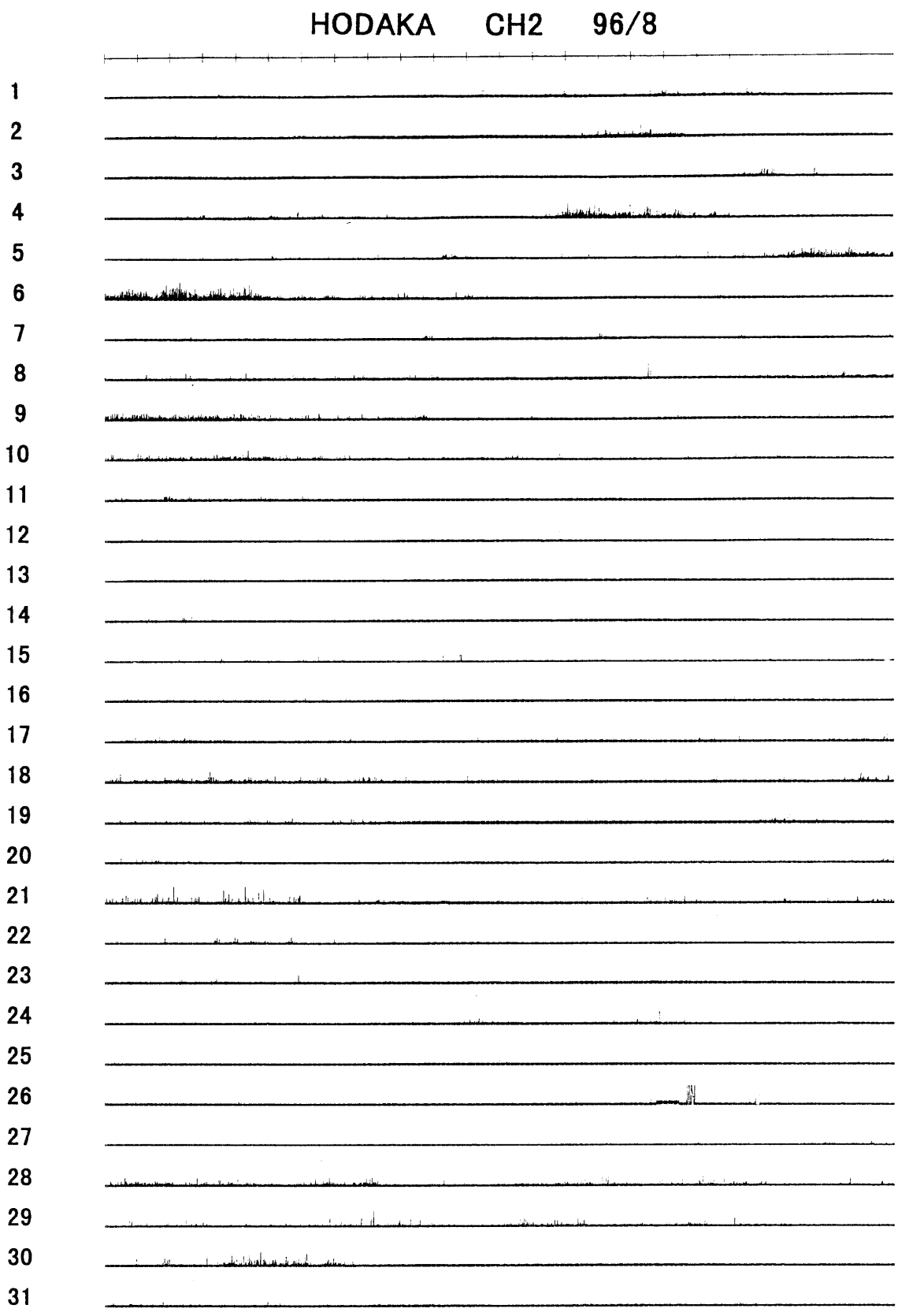
HODAKA CH2 96/8
1
2
3
4
5
6
7
8
9
10
11
12
13
14
15
16
17
18
19
20
21
22
23
24
25
26
27
28
29
30
31

Fig. A-96-8-2

HODAKA CH0 96/9

1
2
3
4
5
6
7
8
9
10
11
12
13
14
15
16
17
18
19
20
21
22
23
24
25
26
27
28
29
30
31

Fig. A-96-9-0

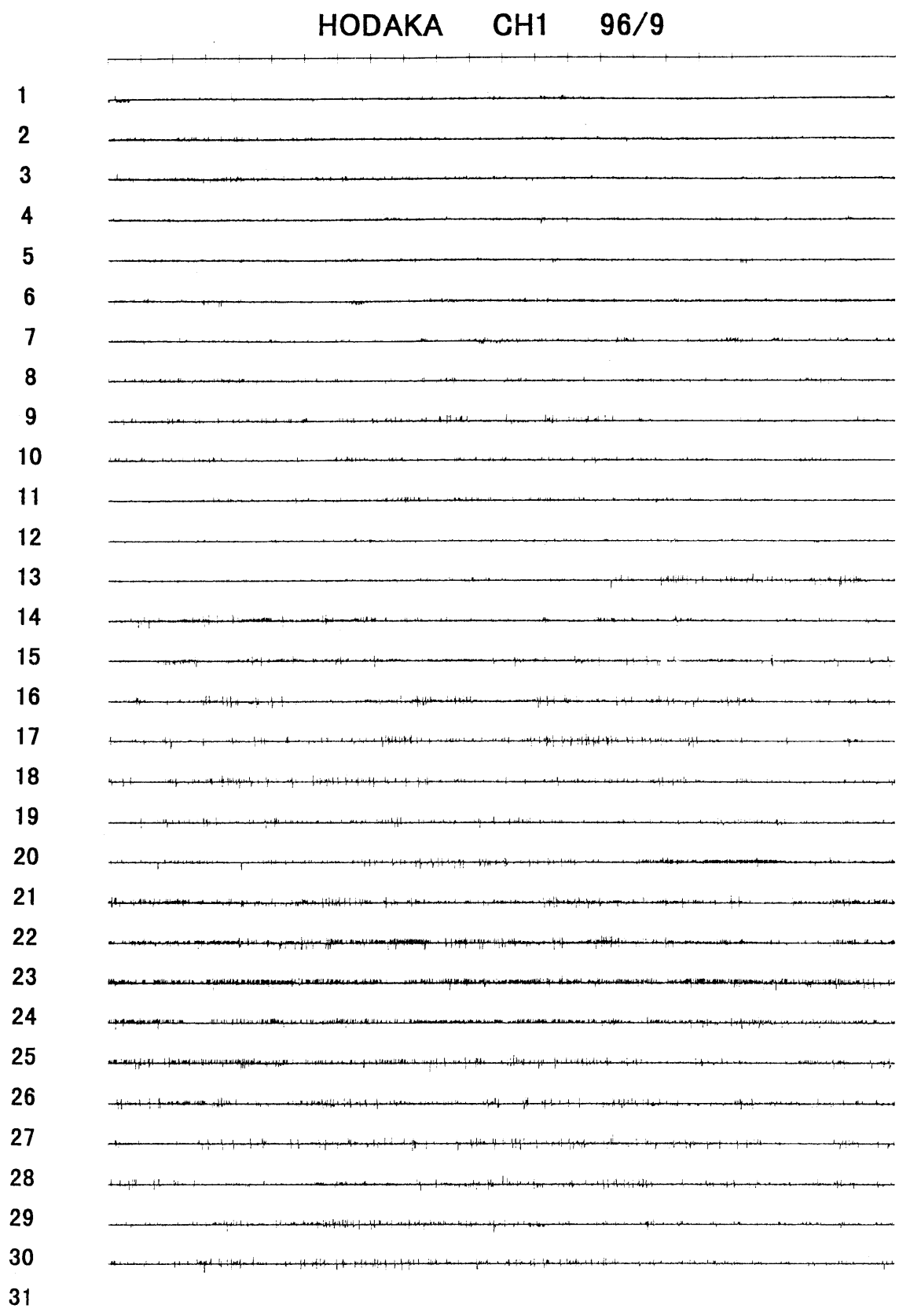
HODAKA CH1 96/9
1
2
3
4
5
6
7
8
9
10
11
12
13
14
15
16
17
18
19
20
21
22
23
24
25
26
27
28
29
30
31

Fig. A-96-9-1

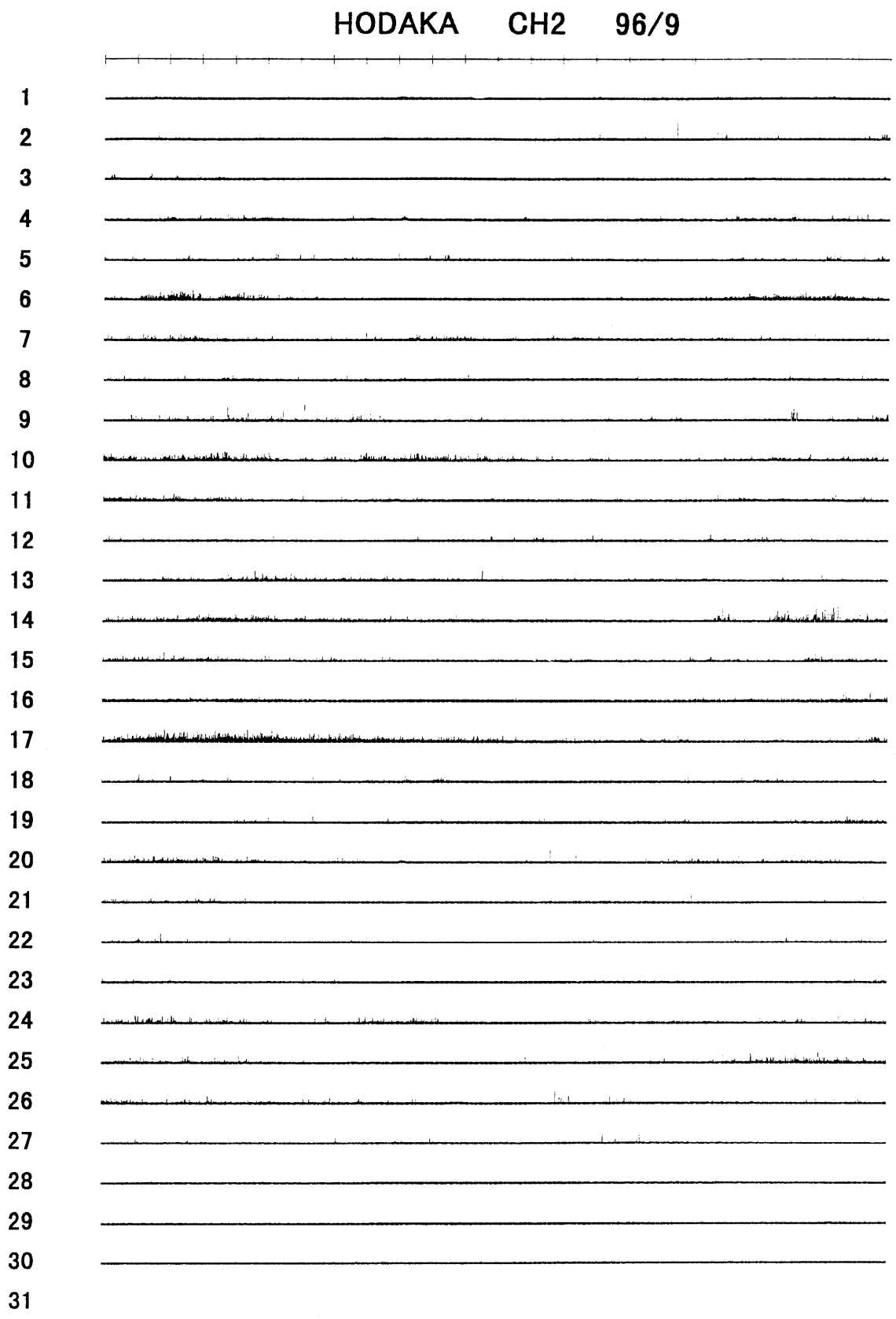
HODAKA CH2 96/9
1
2
3
4
5
6
7
8
9
10
11
12
13
14
15
16
17
18
19
20
21
22
23
24
25
26
27
28
29
30
31

Fig. A-96-9-2

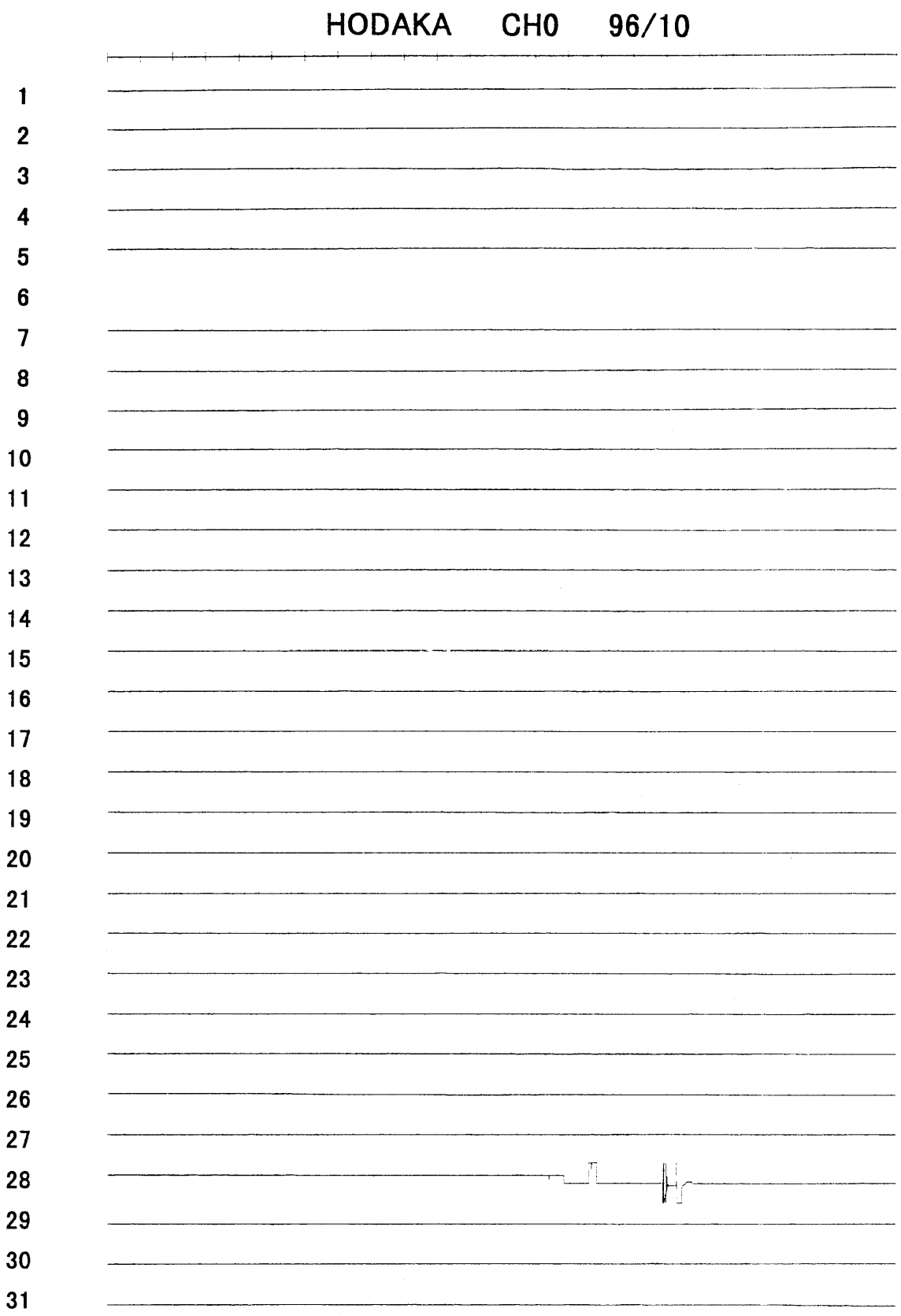
HODAKA CH0 96/10
1
2
3
4
5
6
7
8
9
10
11
12
13
14
15
16
17
18
19
20
21
22
23
24
25
26
27
28
29
30
31

Fig. A-96-10-0

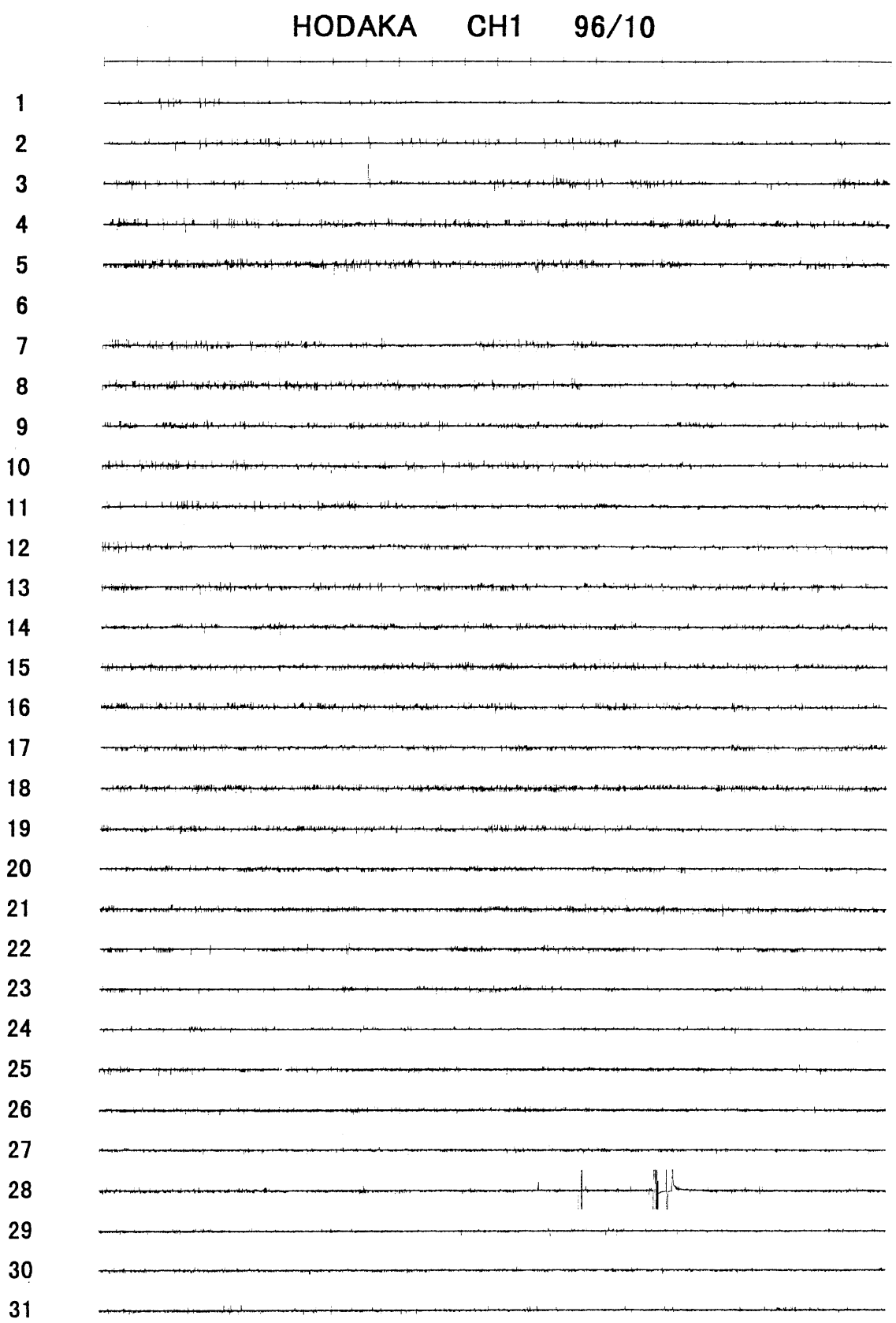
HODAKA CH1 96/10
1
2
3
4
5
6
7
8
9
10
11
12
13
14
15
16
17
18
19
20
21
22
23
24
25
26
27
28
29
30
31

Fig. A-96-10-1

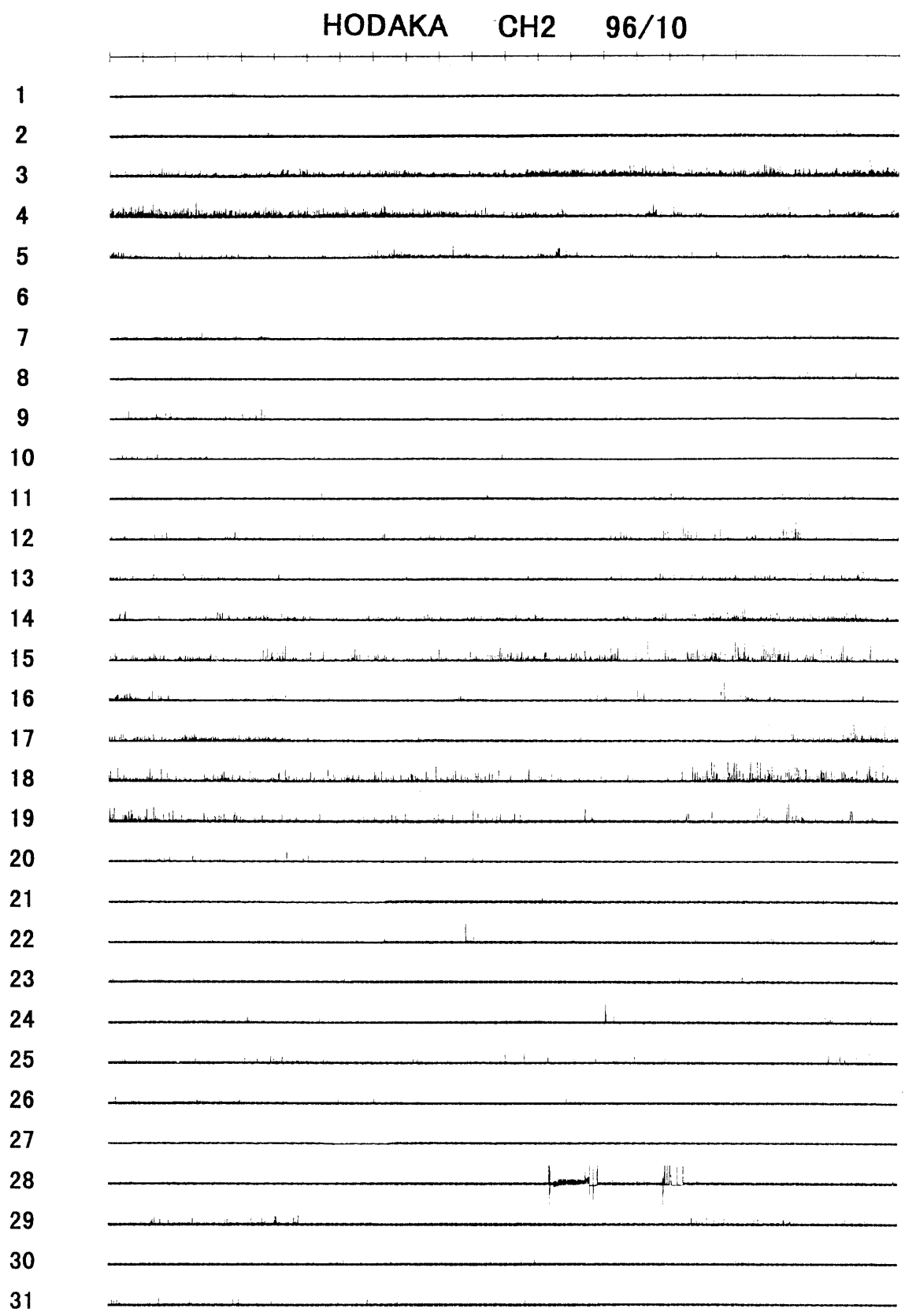
HODAKA CH2 96/10
1
2
3
4
5
6
7
8
9
10
11
12
13
14
15
16
17
18
19
20
21
22
23
24
25
26
27
28
29
30
31

Fig. A-96-10-2

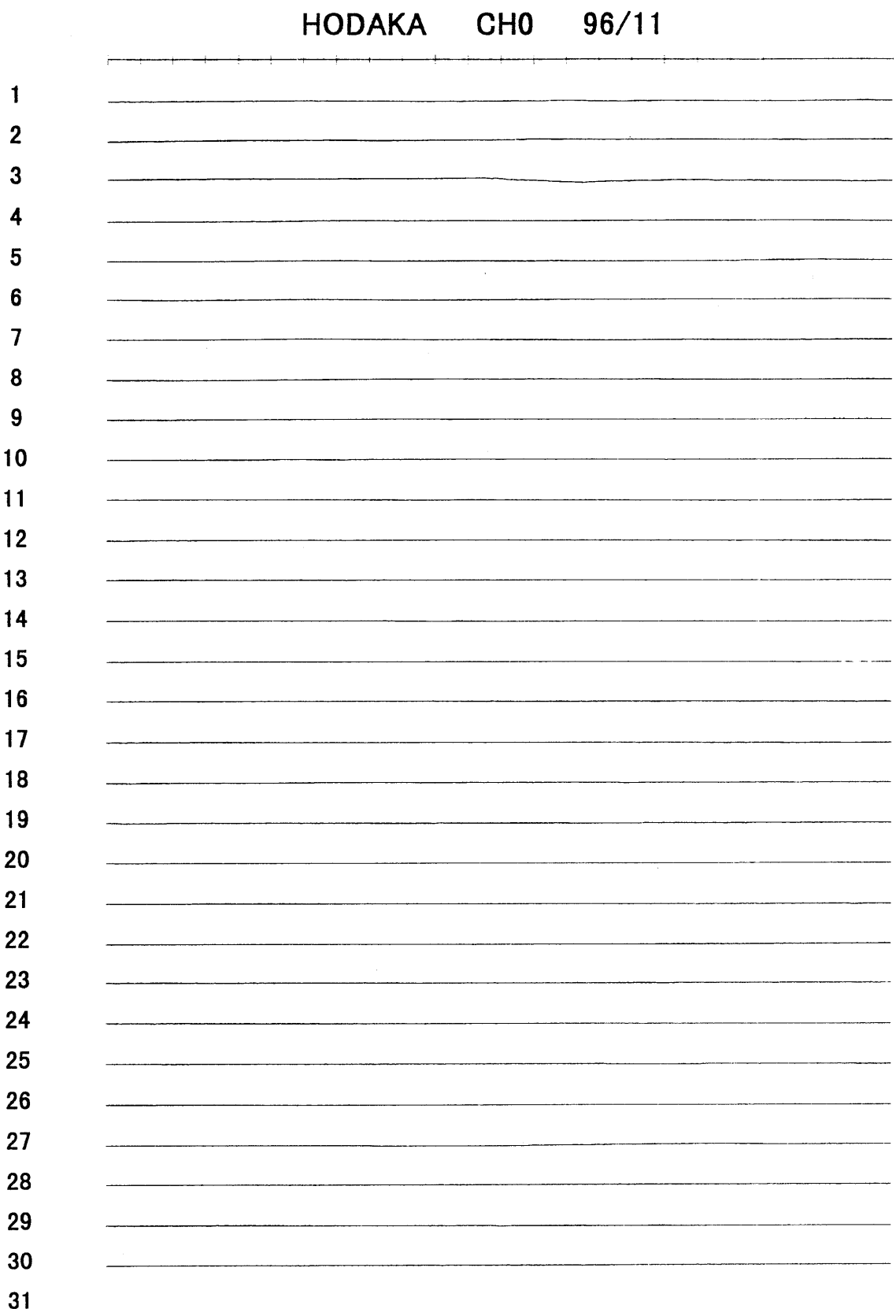
HODAKA CH0 96/11
1
2
3
4
5
6
7
8
9
10
11
12
13
14
15
16
17
18
19
20
21
22
23
24
25
26
27
28
29
30
31

Fig. A-96-11-0

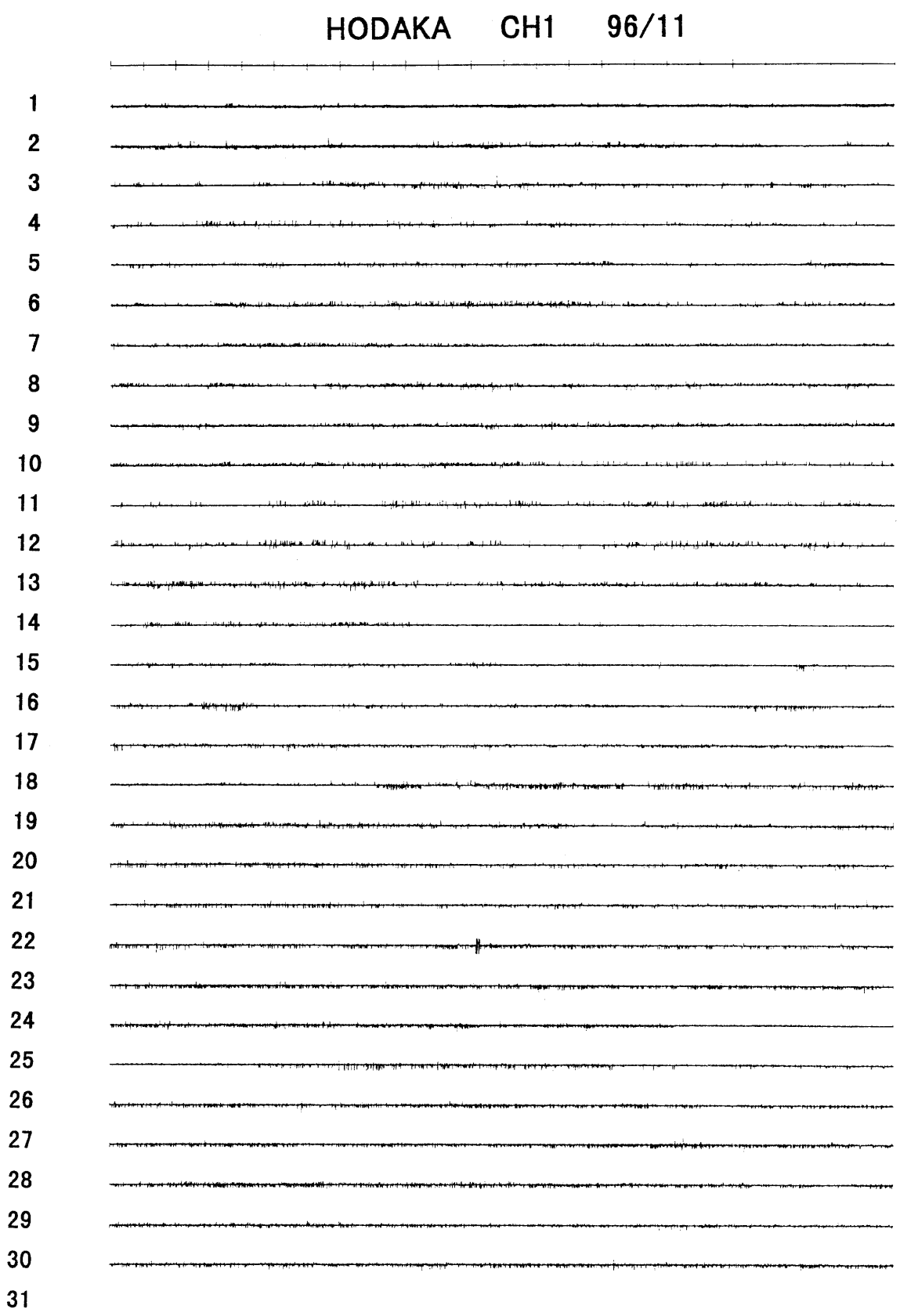
HODAKA CH1 96/11
1
2
3
4
5
6
7
8
9
10
11
12
13
14
15
16
17
18
19
20
21
22
23
24
25
26
27
28
29
30
31

Fig. A-96-11-1

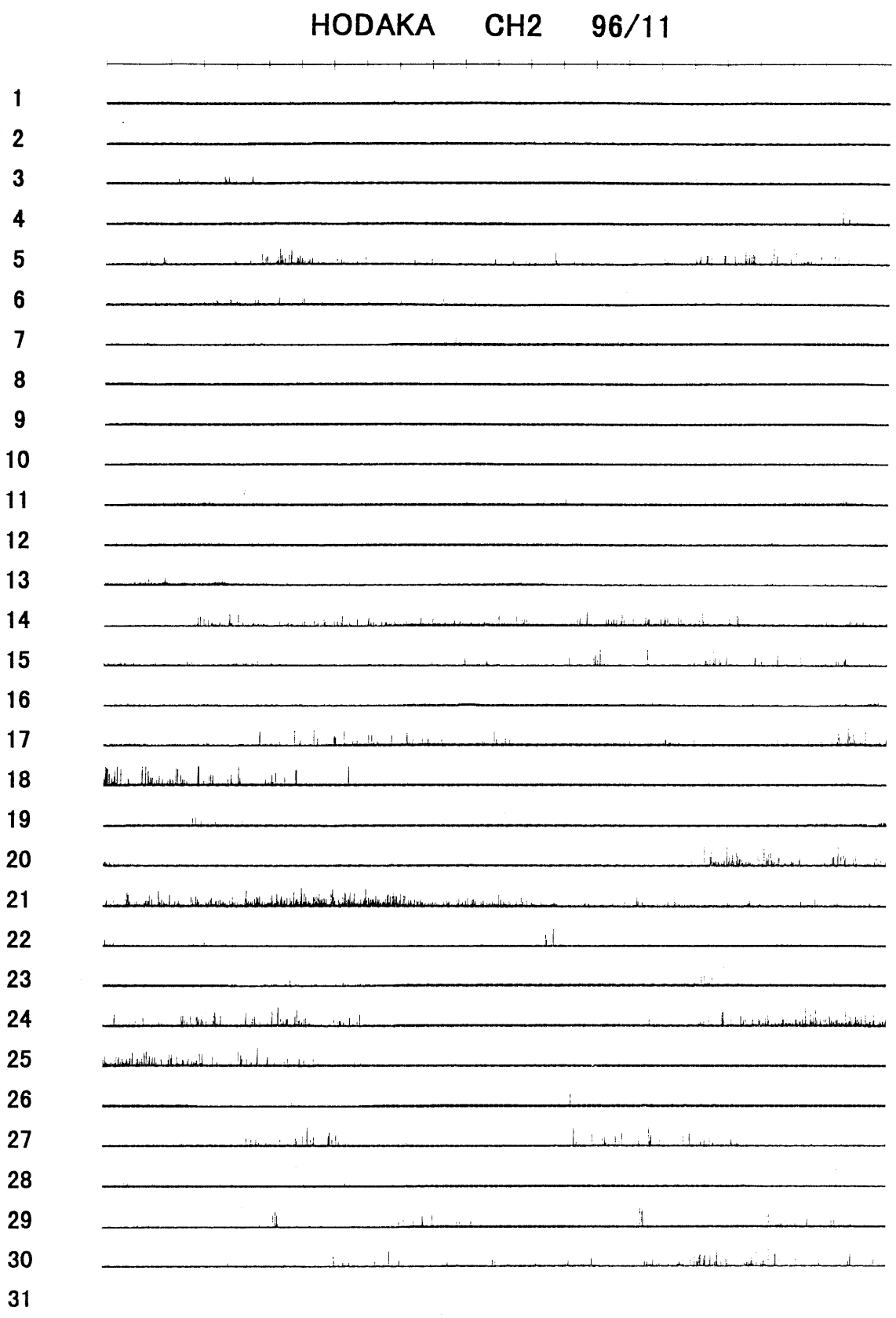
HODAKA CH2 96/11
1
2
3
4
5
6
7
8
9
10
11
12
13
14
15
16
17
18
19
20
21
22
23
24
25
26
27
28
29
30
31

Fig. A-96-11-2

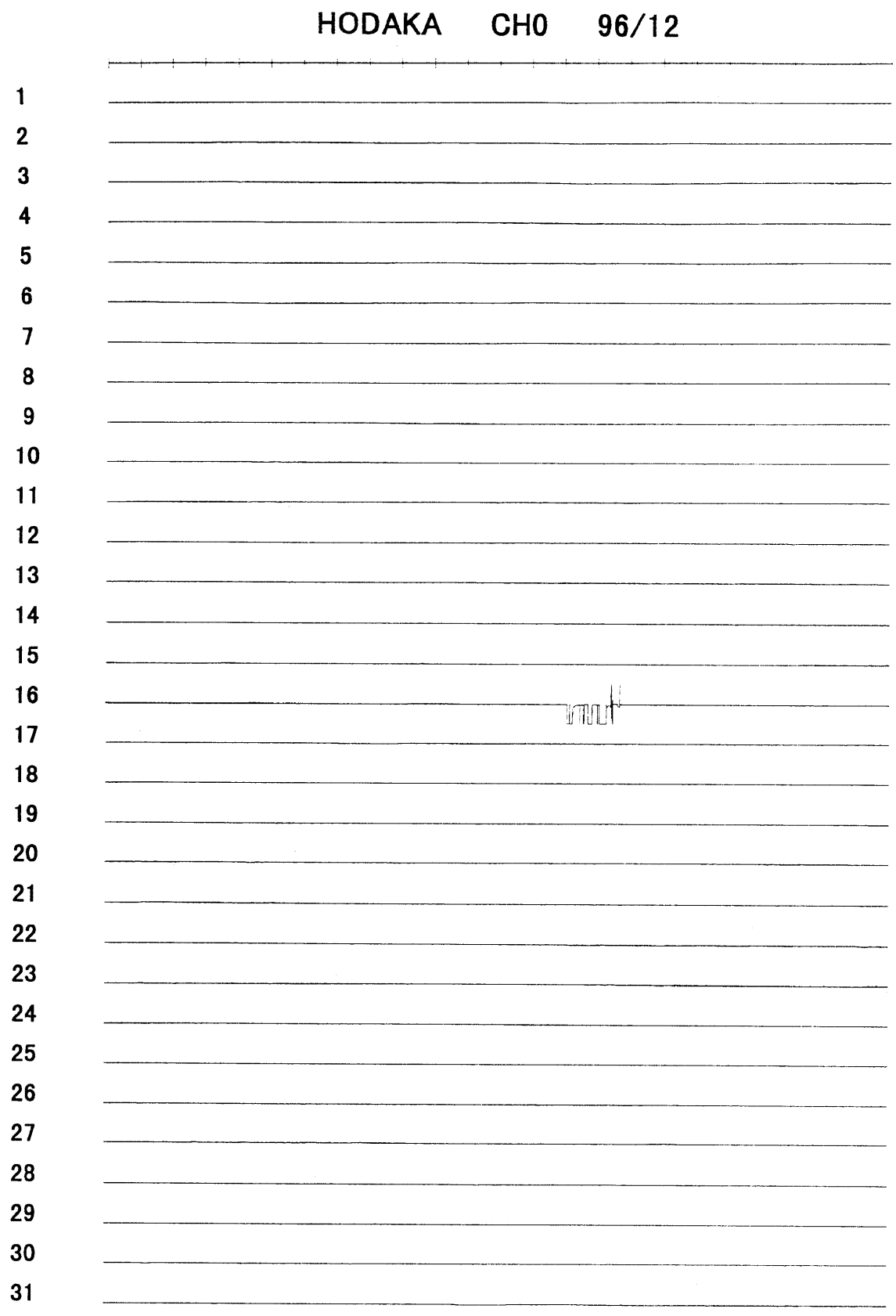
HODAKA CH0 96/12
1
2
3
4
5
6
7
8
9
10
11
12
13
14
15
16
17
18
19
20
21
22
23
24
25
26
27
28
29
30
31

Fig. A-96-12-0

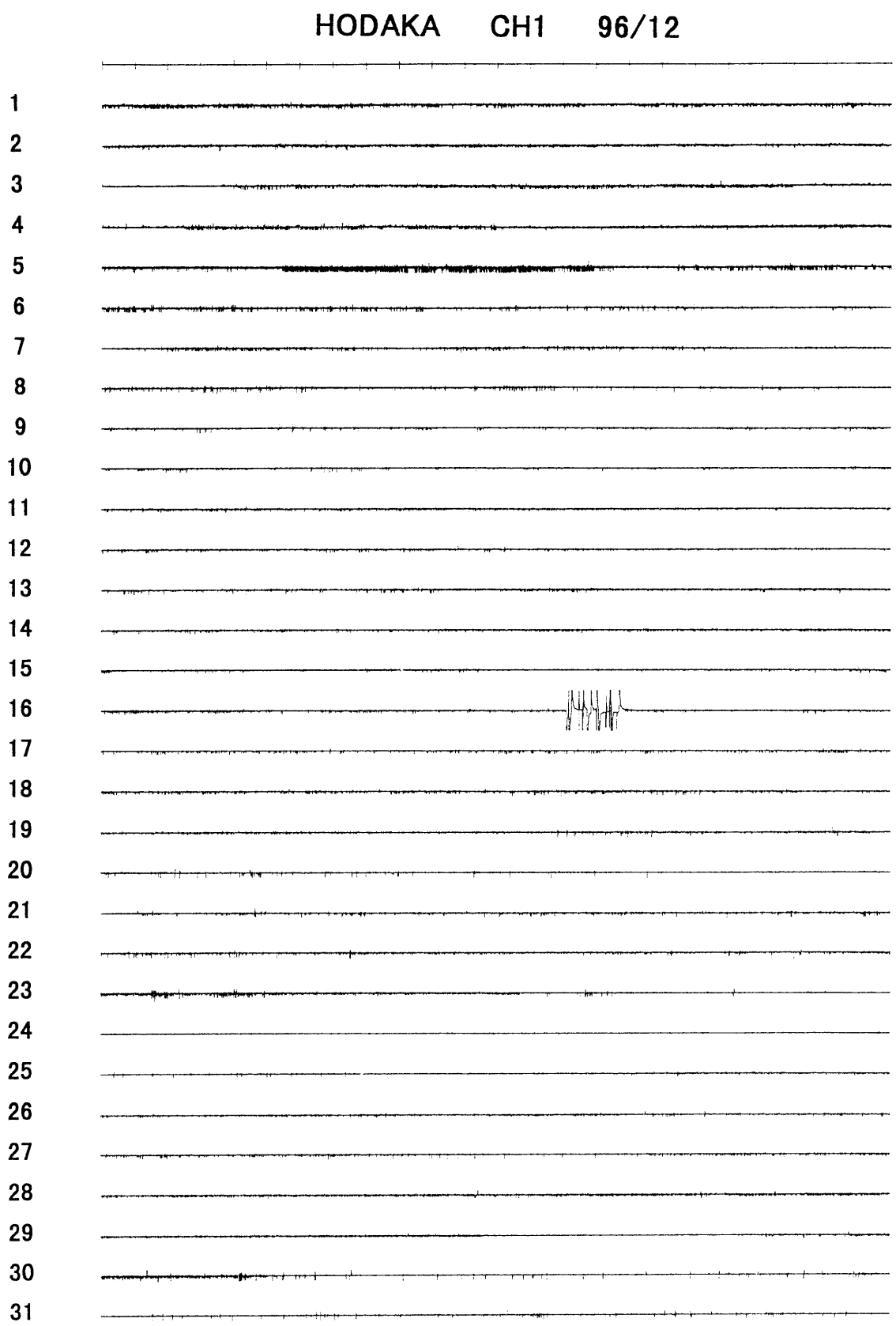
HODAKA CH1 96/12
1
2
3
4
5
6
7
8
9
10
11
12
13
14
15
16
17
18
19
20
21
22
23
24
25
26
27
28
29
30
31

Fig. A-96-12-1

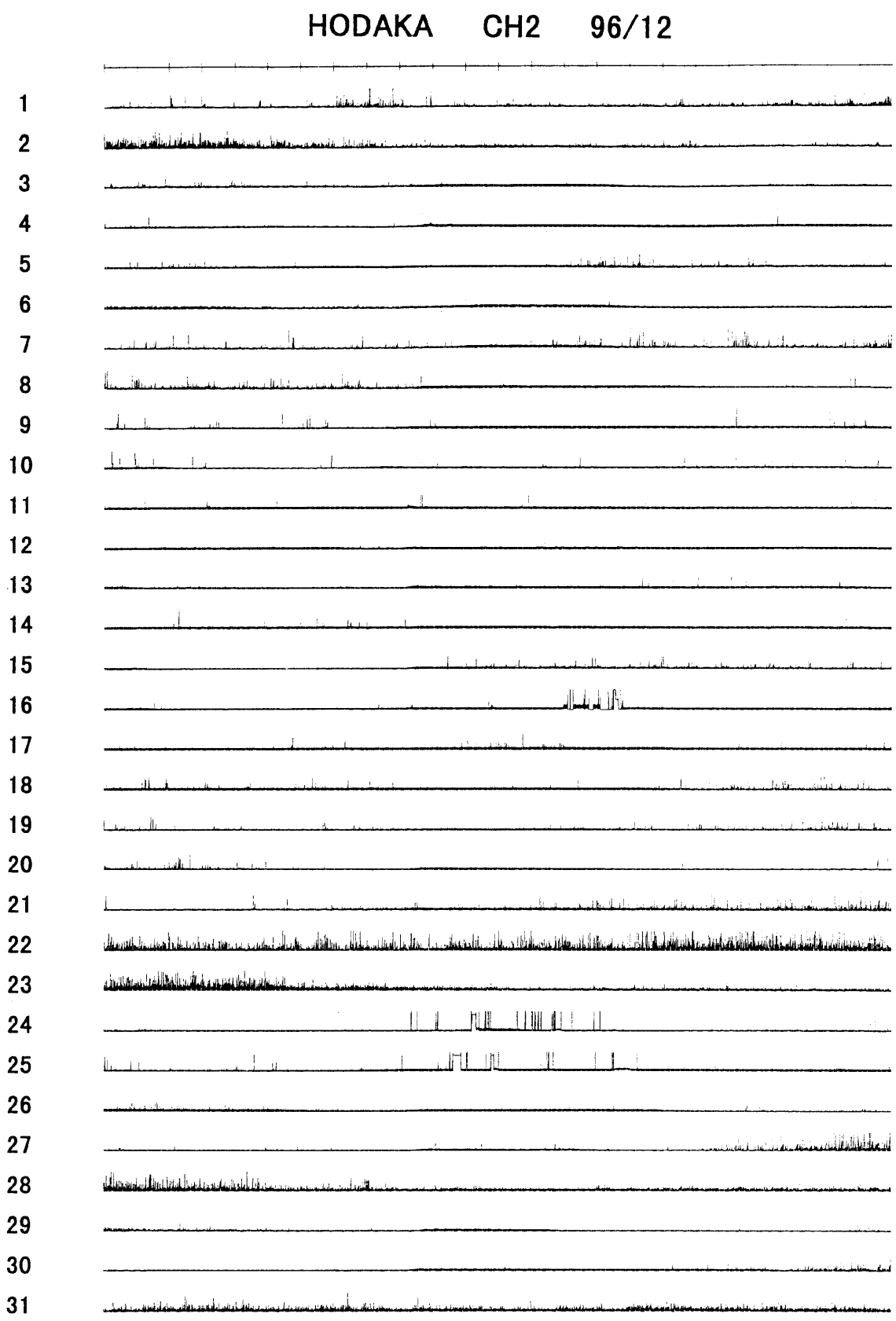
HODAKA CH2 96/12
1
2
3
4
5
6
7
8
9
10
11
12
13
14
15
16
17
18
19
20
21
22
23
24
25
26
27
28
29
30
31

Fig. A-96-12-2

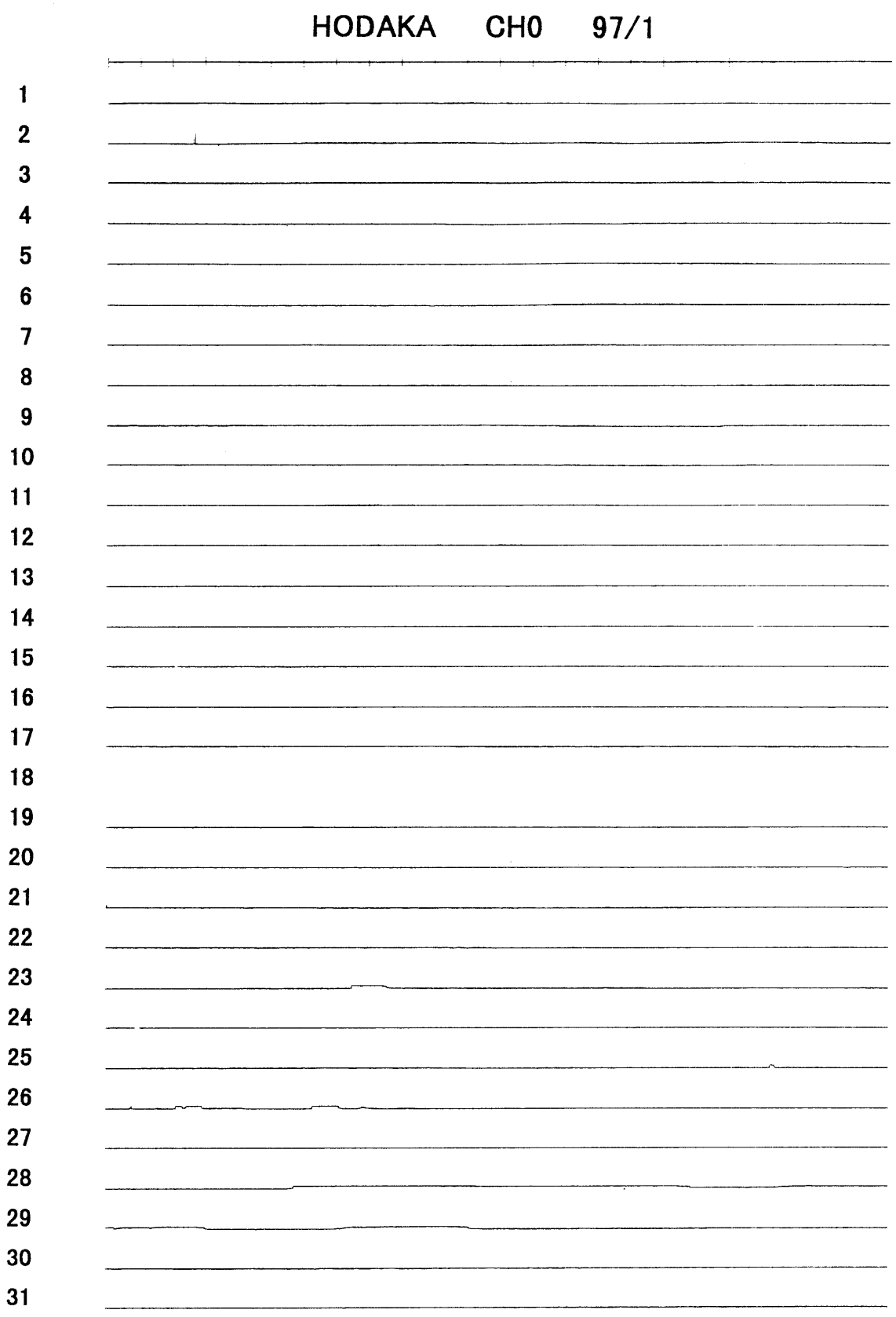
HODAKA CH0 97/1
1
2
3
4
5
6
7
8
9
10
11
12
13
14
15
16
17
18
19
20
21
22
23
24
25
26
27
28
29
30
31

Fig. A-97-1-0

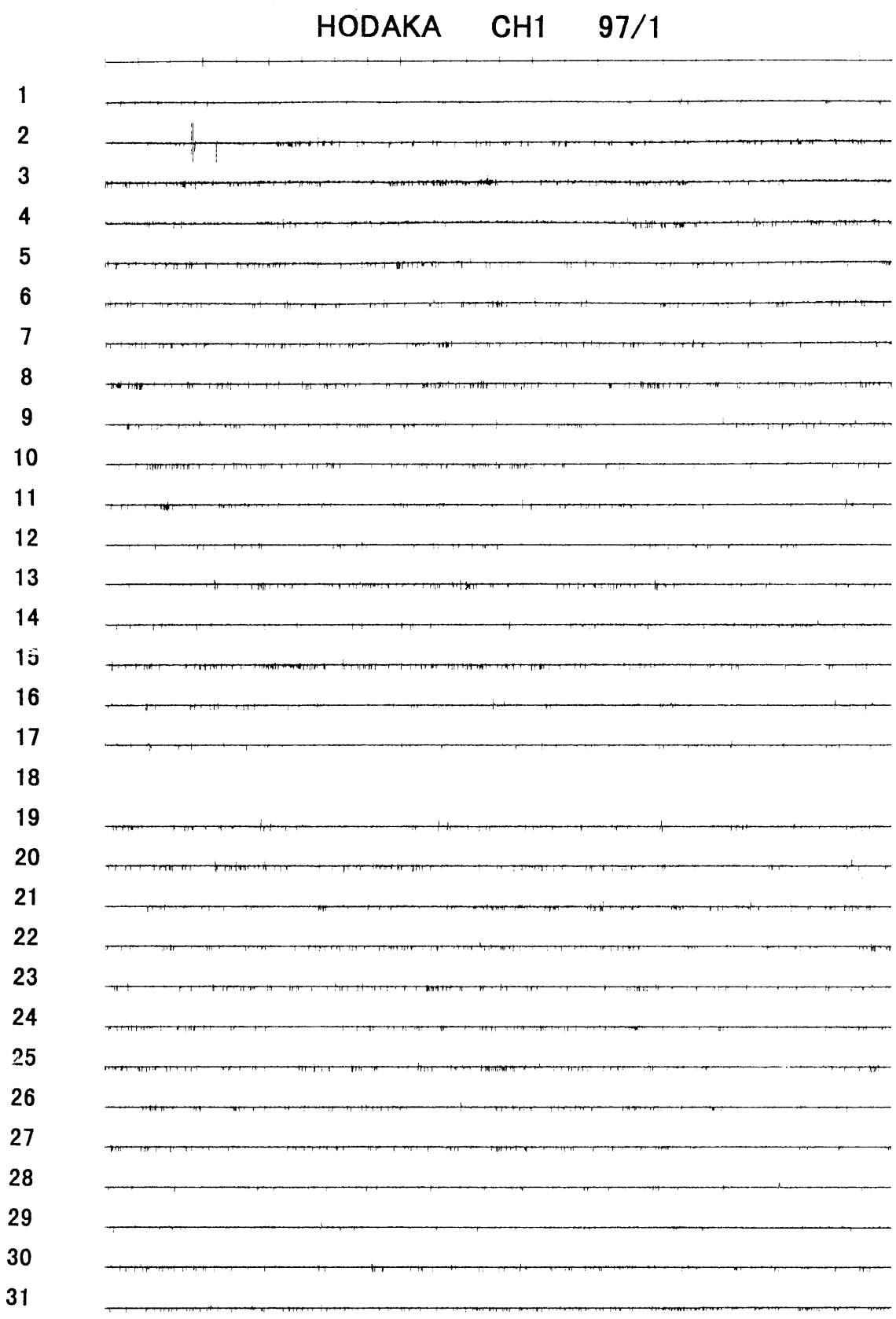
HODAKA CH1 97/1
1
2
3
4
5
6
7
8
9
10
11
12
13
14
15
16
17
18
19
20
21
22
23
24
25
26
27
28
29
30
31

Fig. A-97-1-1

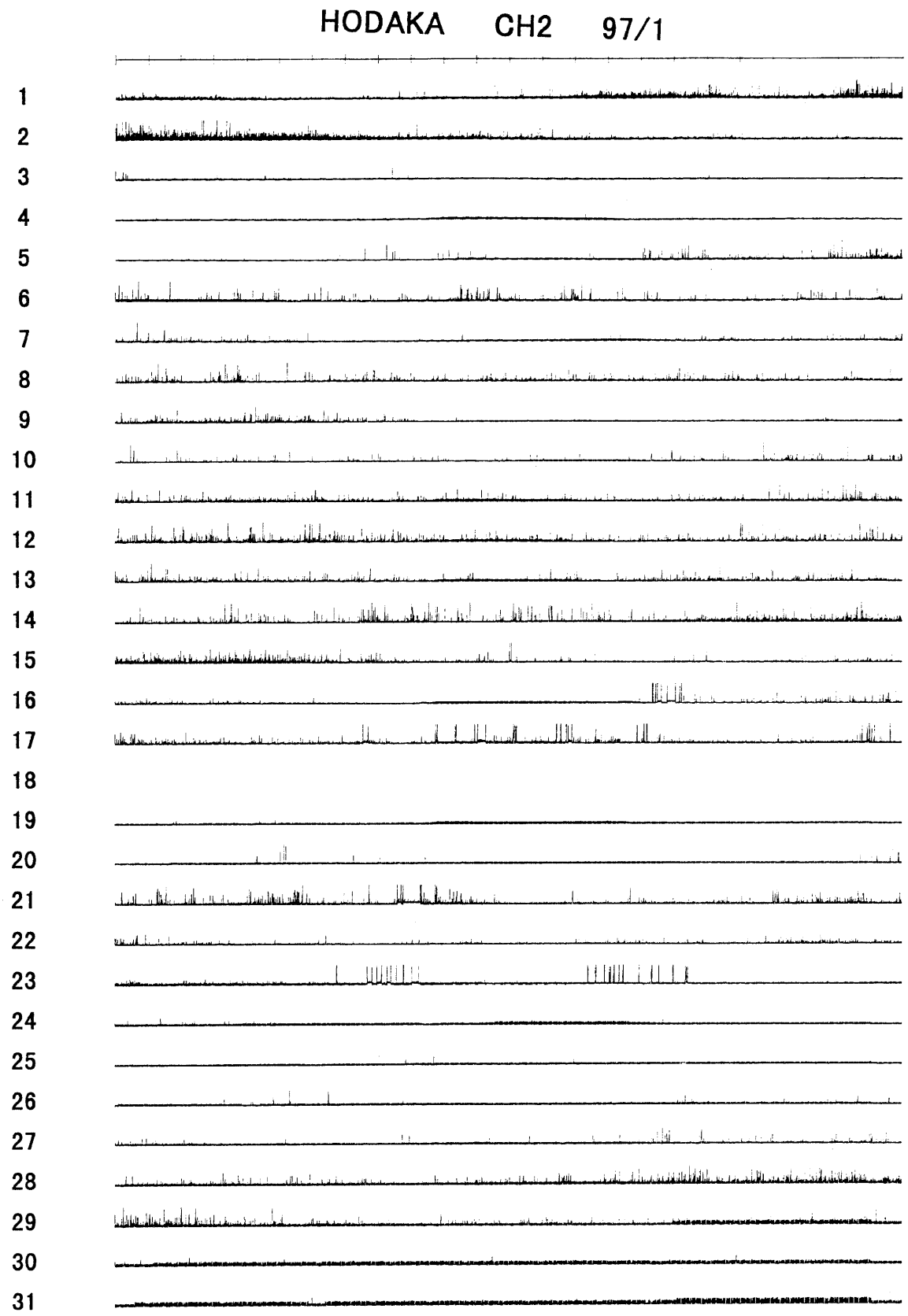
HODAKA CH2 97/1
1
2
3
4
5
6
7
8
9
10
11
12
13
14
15
16
17
18
19
20
21
22
23
24
25
26
27
28
29
30
31

Fig. A-97-1-2

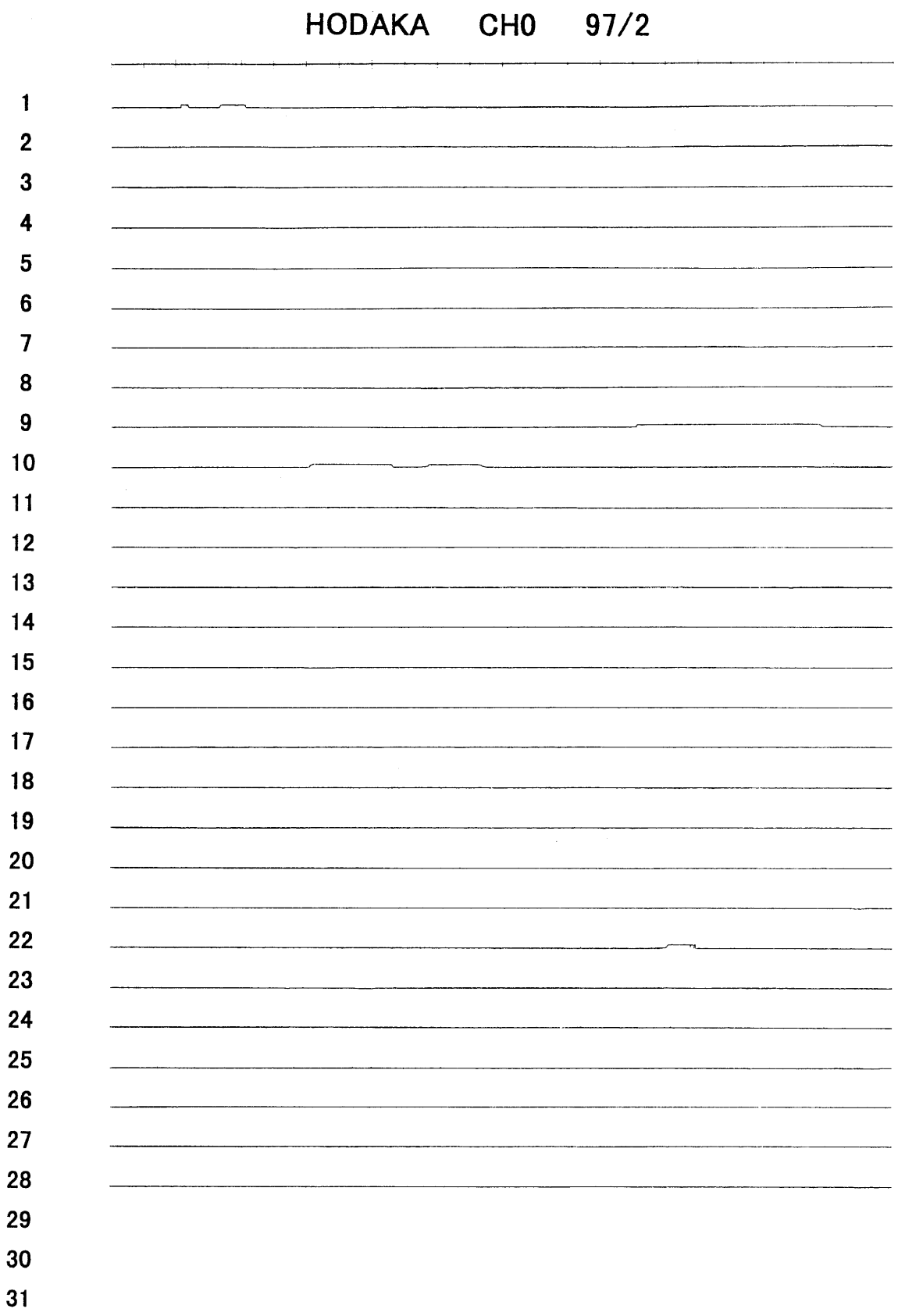
HODAKA CH0 97/2
1
2
3
4
5
6
7
8
9
10
11
12
13
14
15
16
17
18
19
20
21
22
23
24
25
26
27
28
29
30
31

Fig. A-97-2-0

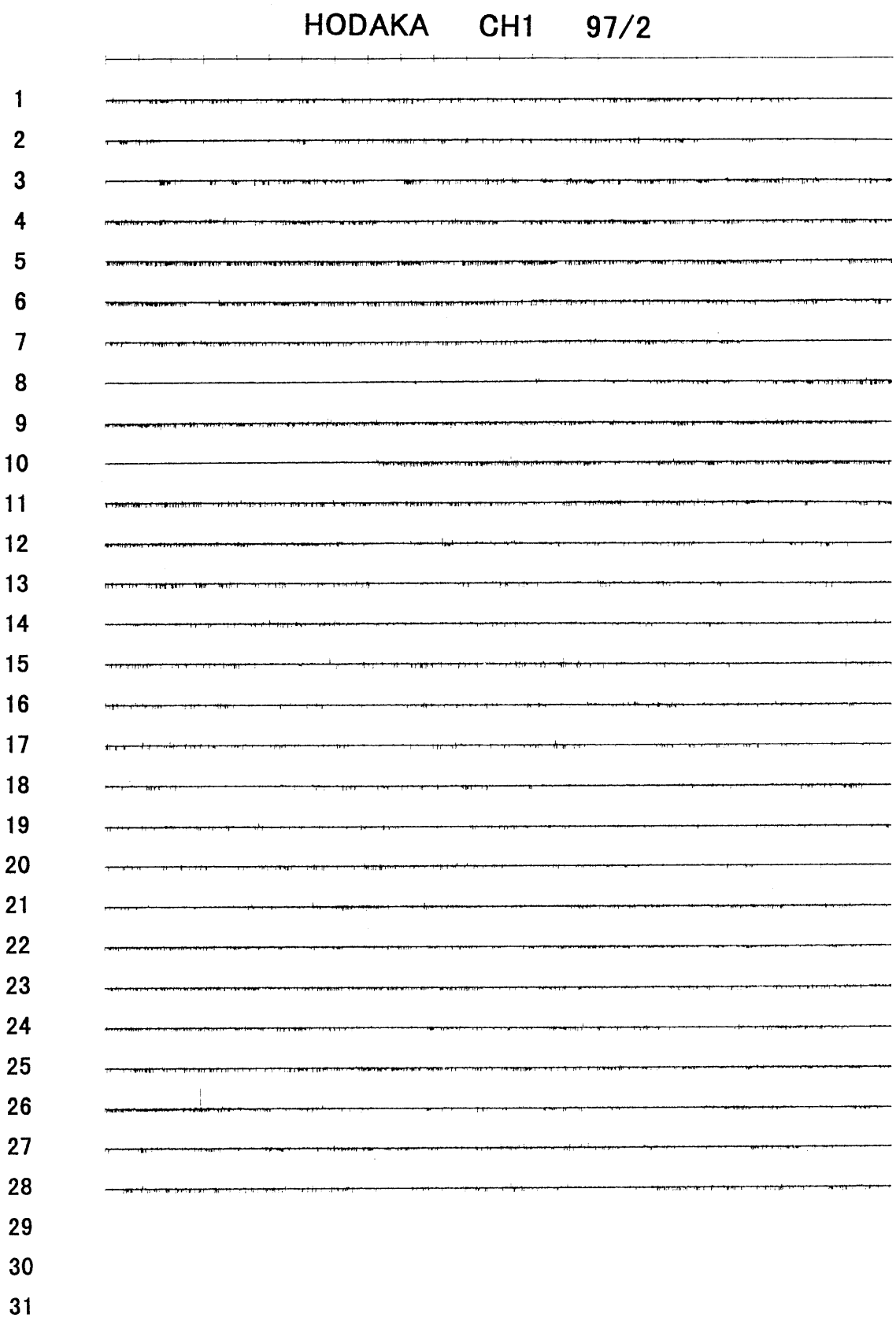
HODAKA CH1 97/2
1
2
3
4
5
6
7
8
9
10
11
12
13
14
15
16
17
18
19
20
21
22
23
24
25
26
27
28
29
30
31

Fig. A-97-2-1

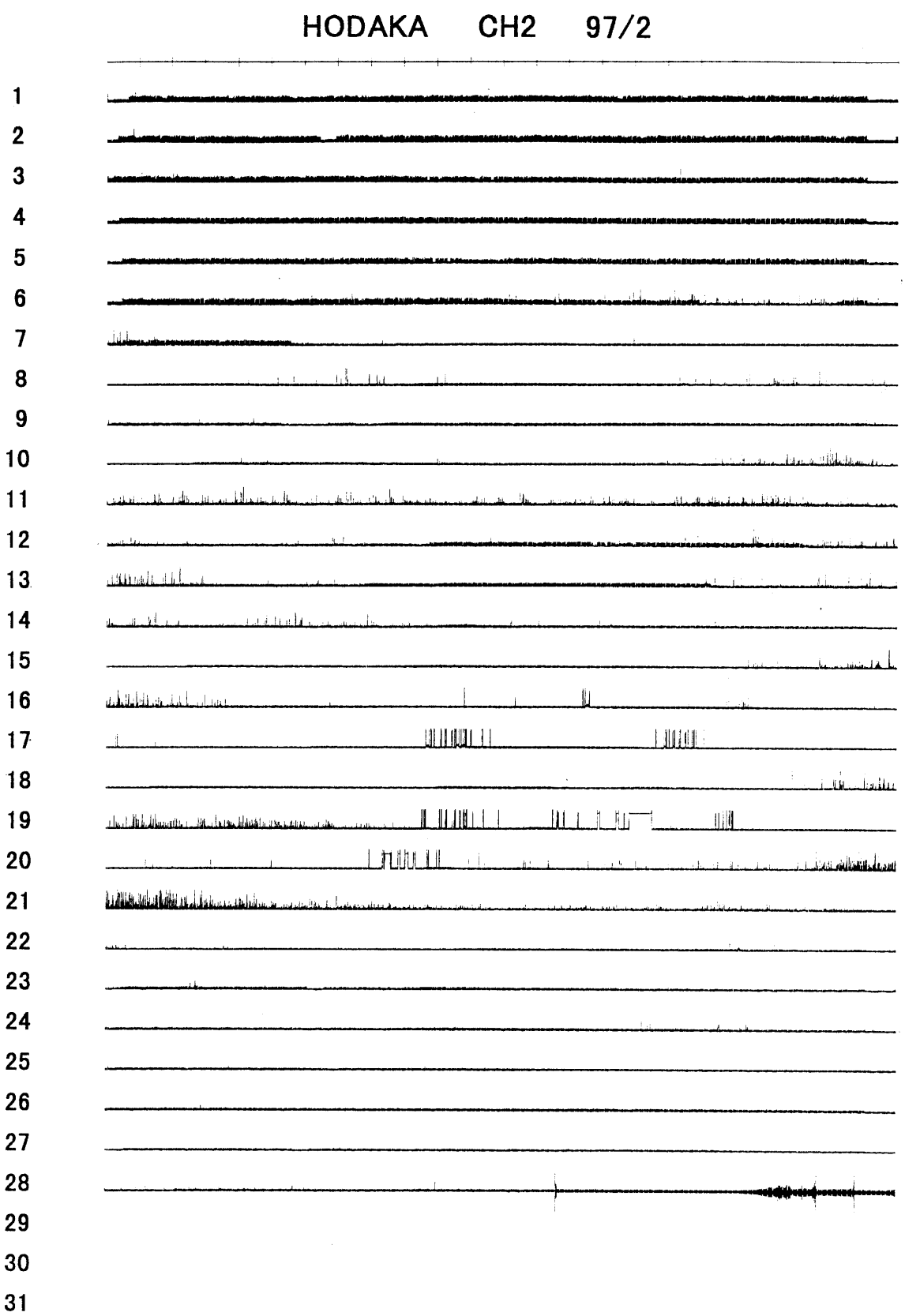
HODAKA CH2 97/2
1
2
3
4
5
6
7
8
9
10
11
12
13
14
15
16
17
18
19
20
21
22
23
24
25
26
27
28
29
30
31

Fig. A-97-2-2

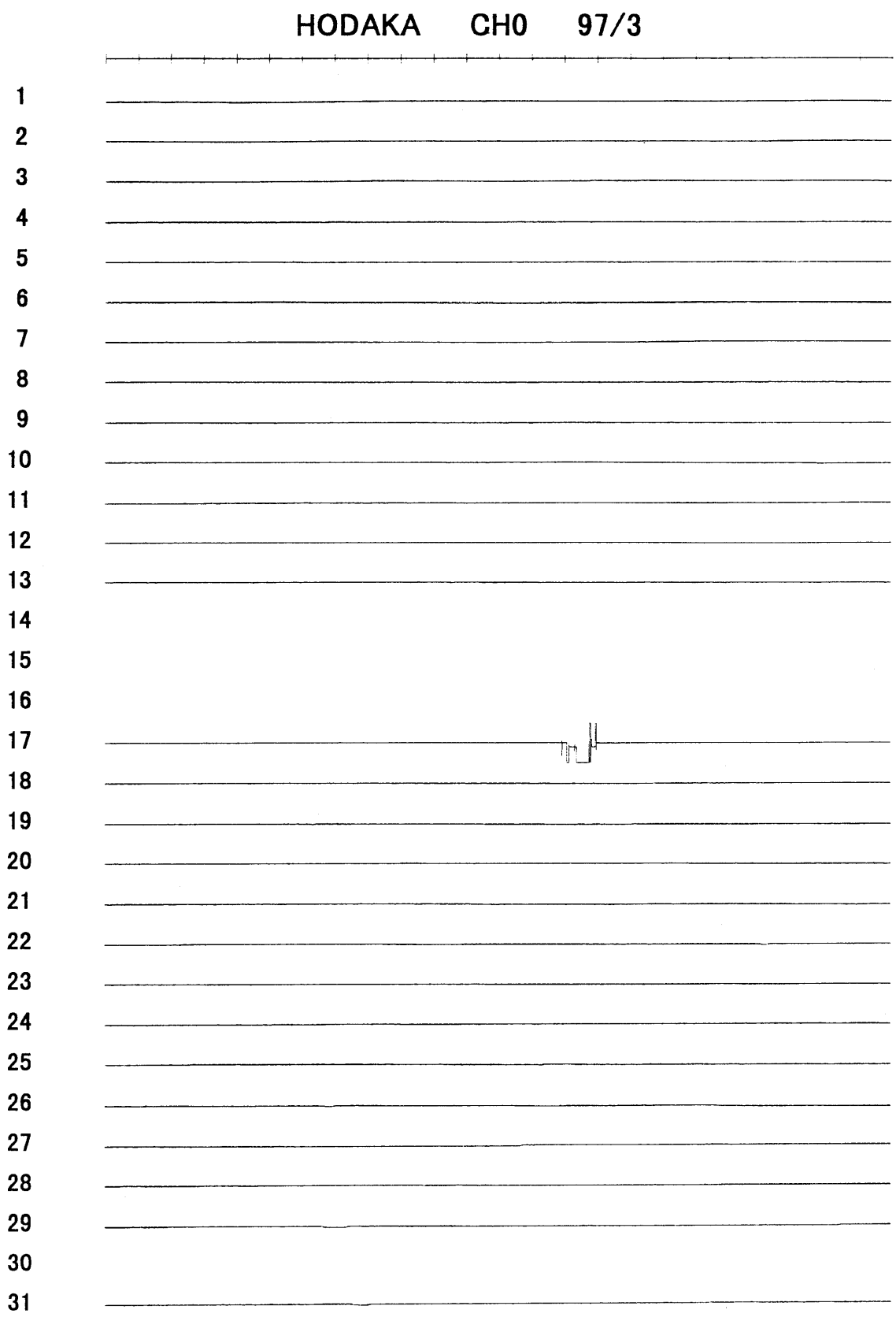
HODAKA CH0 97/3
1
2
3
4
5
6
7
8
9
10
11
12
13
14
15
16
17
18
19
20
21
22
23
24
25
26
27
28
29
30
31

Fig. A-97-3-0

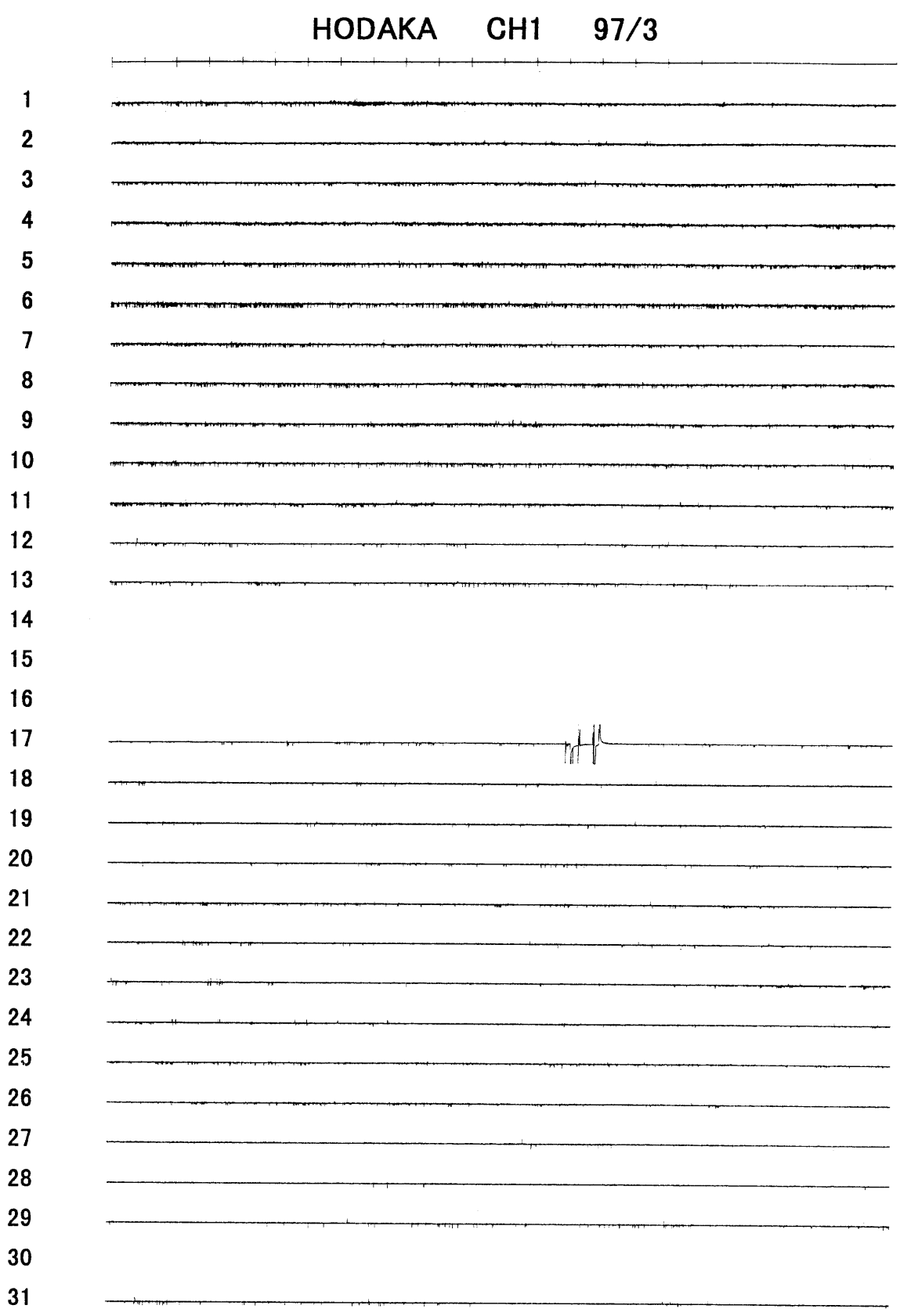
HODAKA CH1 97/3
1
2
3
4
5
6
7
8
9
10
11
12
13
14
15
16
17
18
19
20
21
22
23
24
25
26
27
28
29
30
31

Fig. A-97-3-1

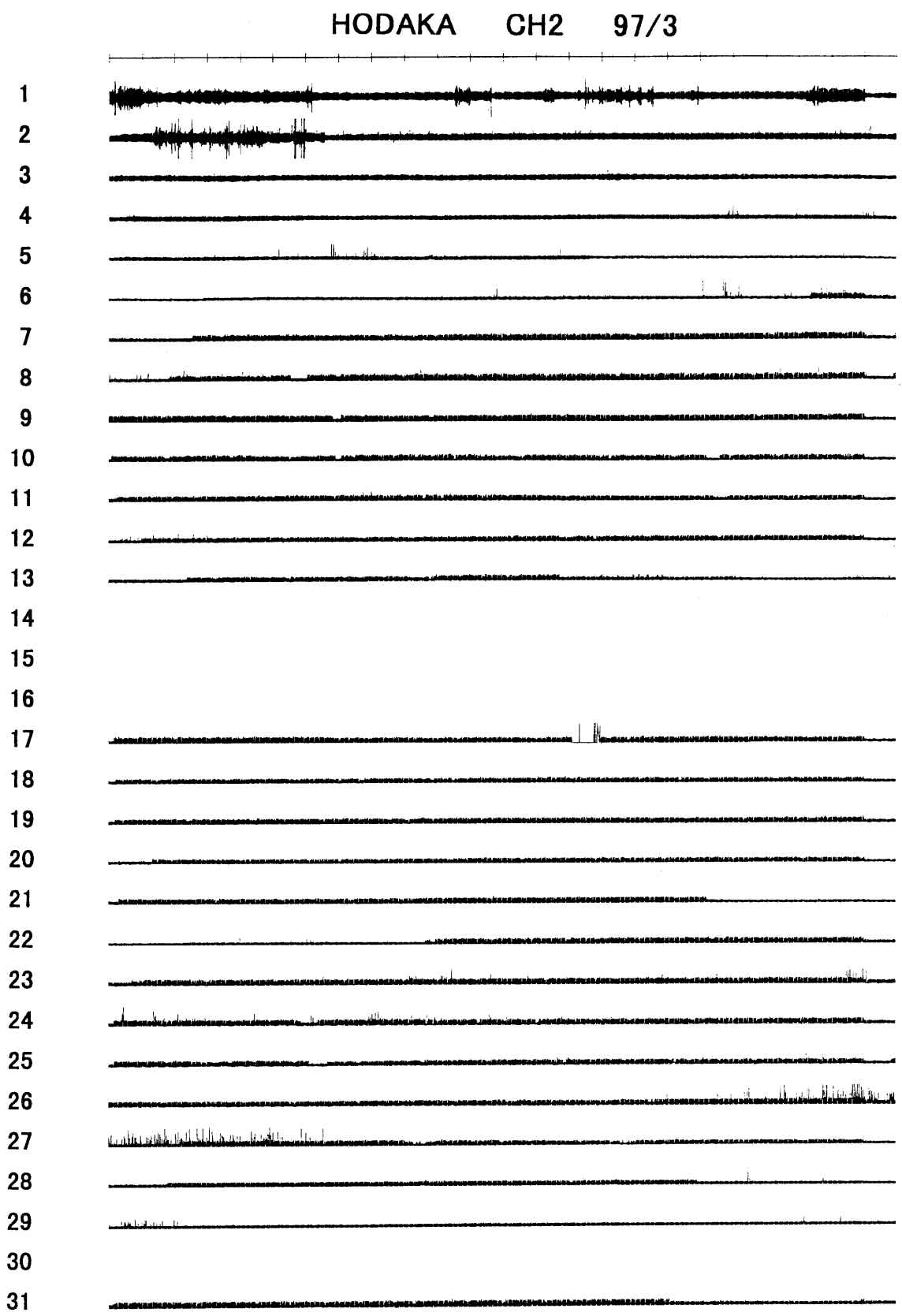
HODAKA CH2 97/3
1
2
3
4
5
6
7
8
9
10
11
12
13
14
15
16
17
18
19
20
21
22
23
24
25
26
27
28
29
30
31

Fig. A-97-3-2

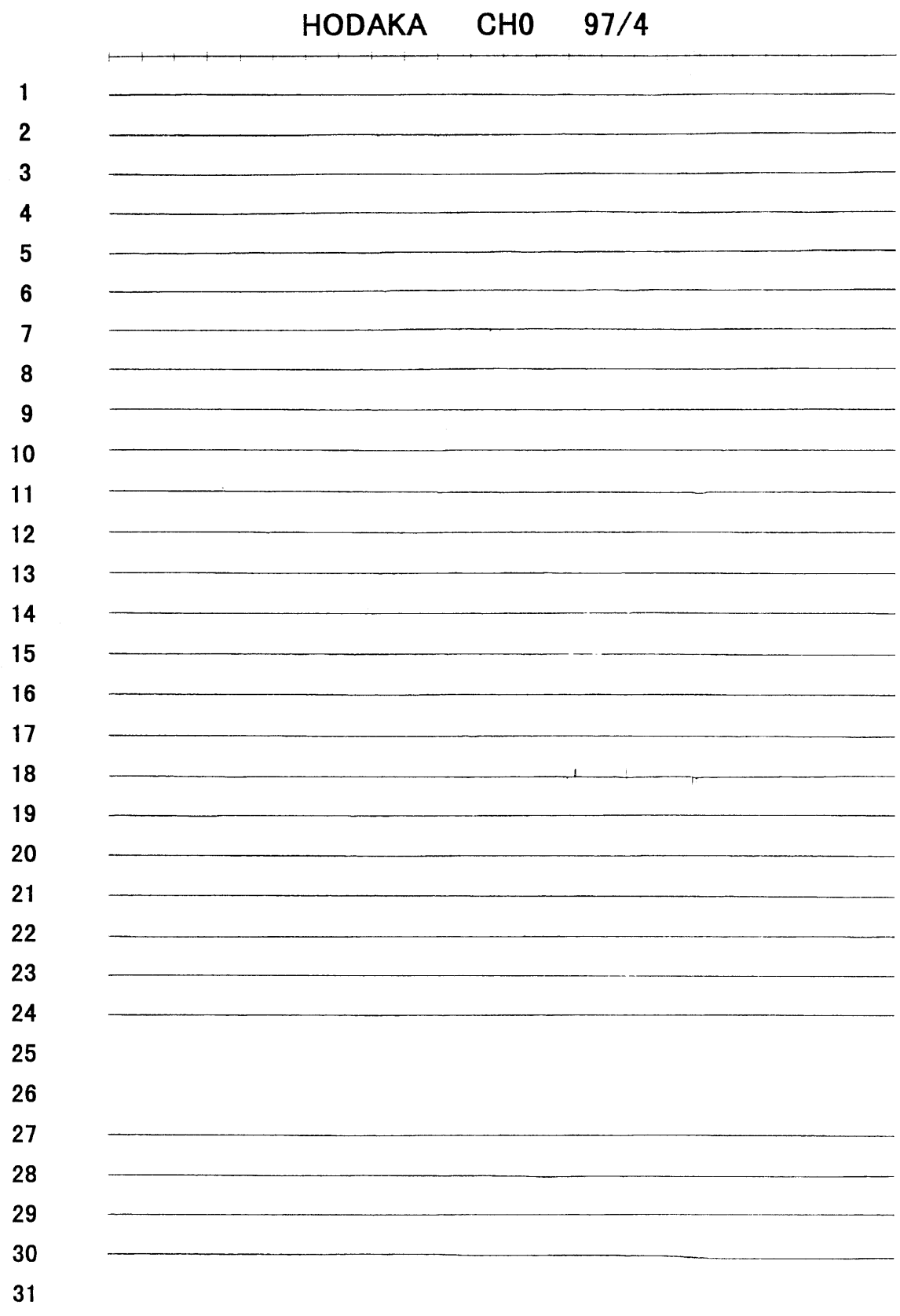
HODAKA CH0 97/4
1
2
3
4
5
6
7
8
9
10
11
12
13
14
15
16
17
18
19
20
21
22
23
24
25
26
27
28
29
30
31

Fig. A-97-4-0

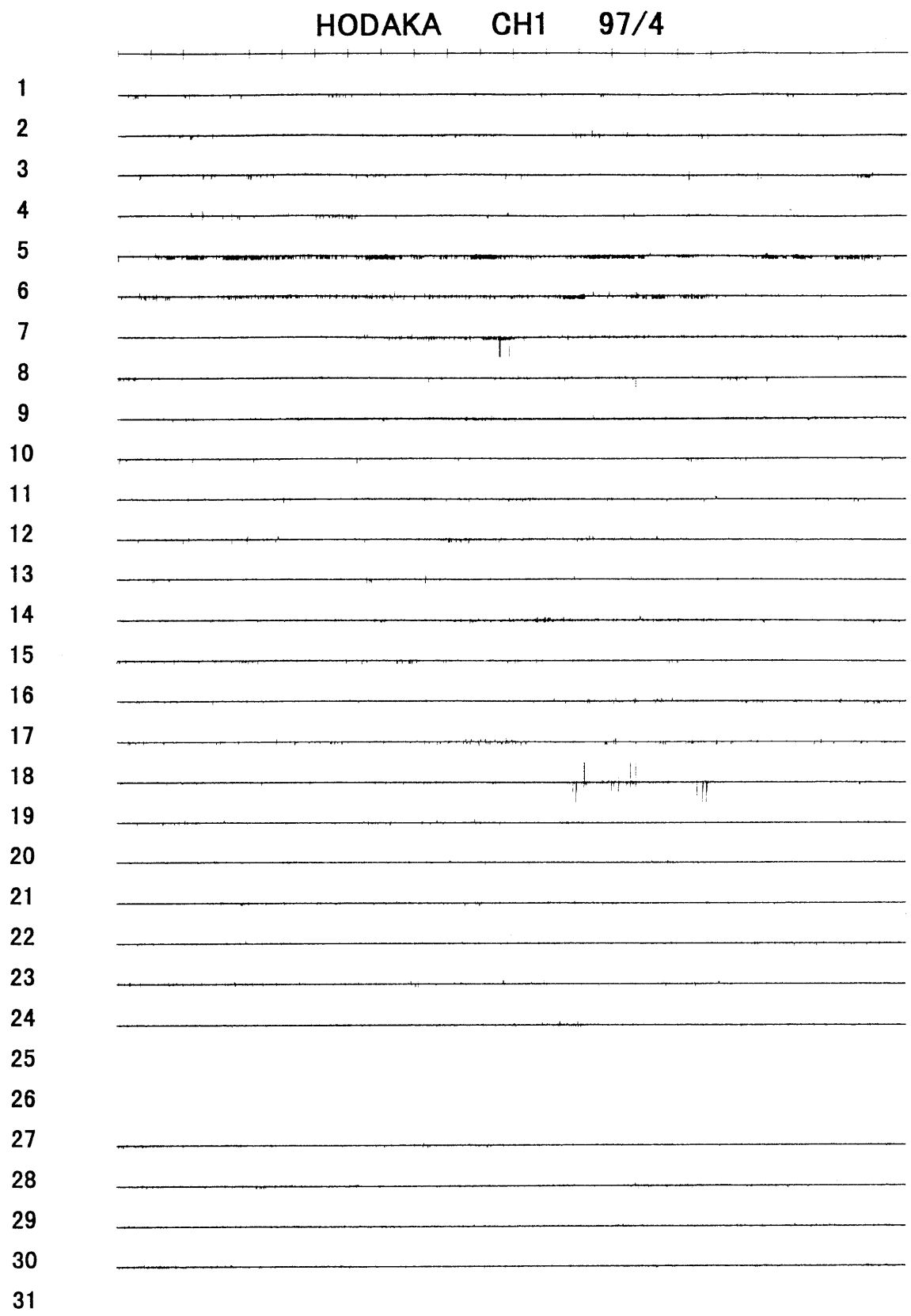
HODAKA CH1 97/4
1
2
3
4
5
6
7
8
9
10
11
12
13
14
15
16
17
18
19
20
21
22
23
24
25
26
27
28
29
30
31

Fig. A-97-4-1

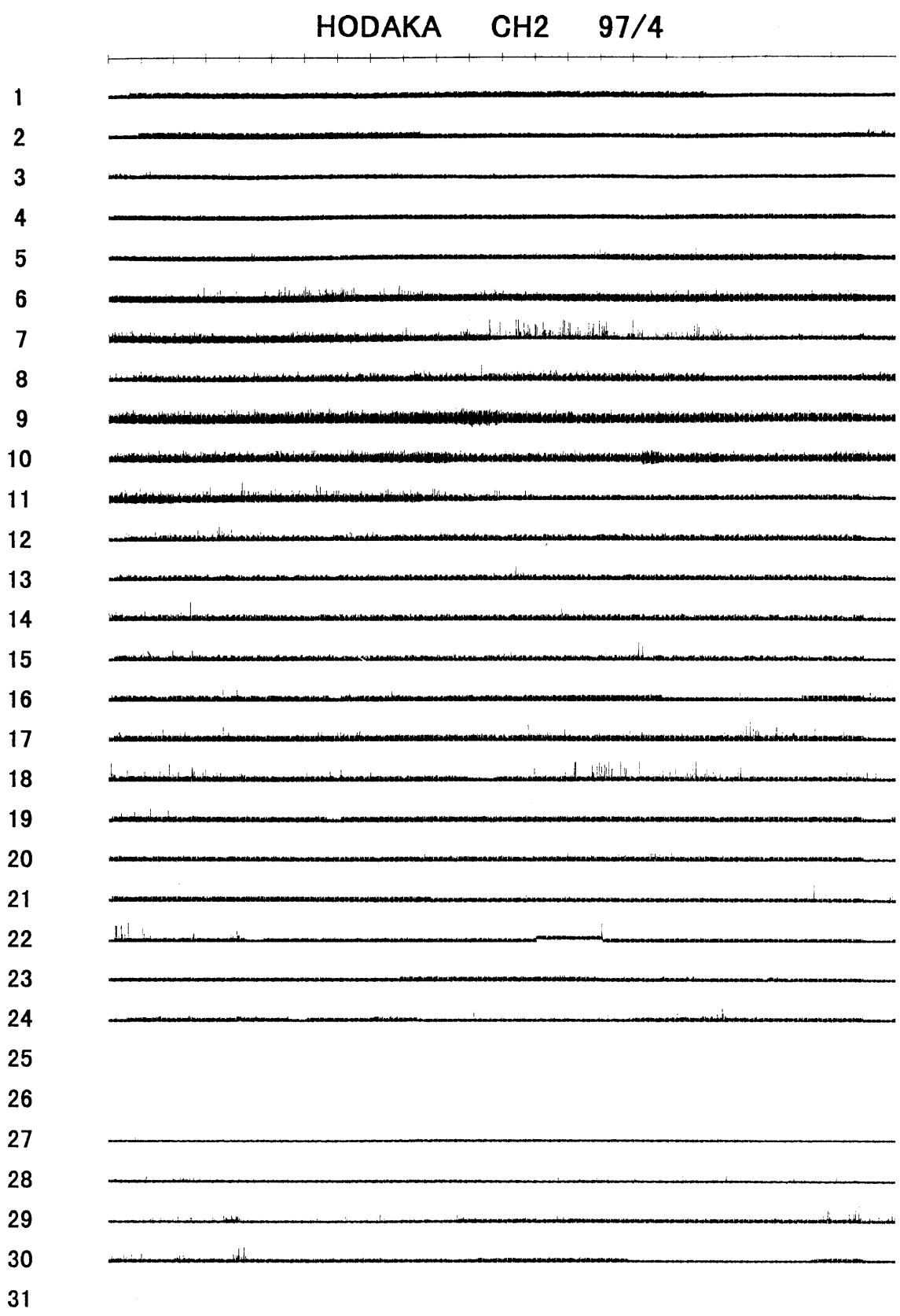
HODAKA CH2 97/4
1
2
3
4
5
6
7
8
9
10
11
12
13
14
15
16
17
18
19
20
21
22
23
24
25
26
27
28
29
30
31

Fig. A-97-4-2

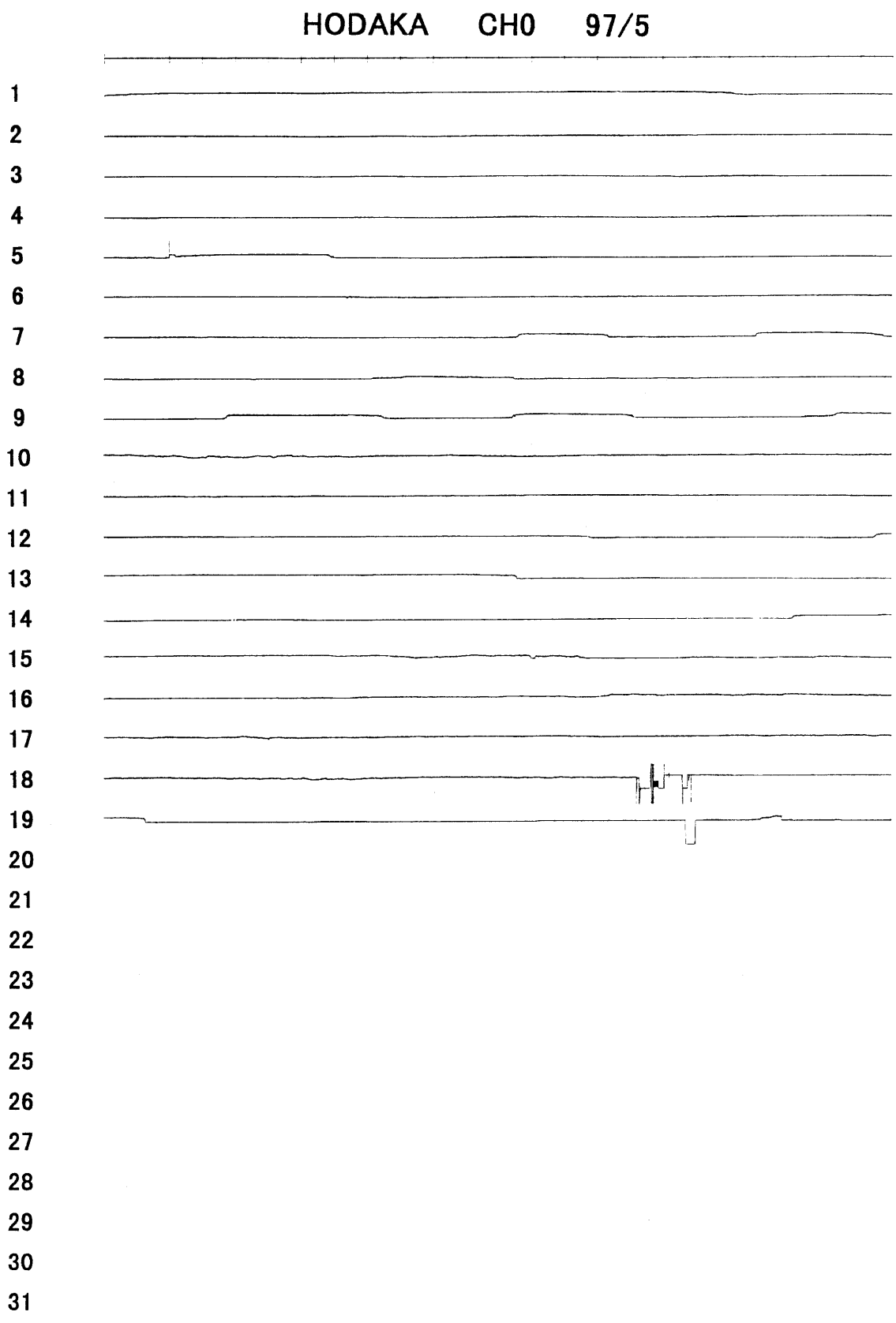
HODAKA CH0 97/5
1
2
3
4
5
6
7
8
9
10
11
12
13
14
15
16
17
18
19
20
21
22
23
24
25
26
27
28
29
30
31

Fig. A-97-5-0

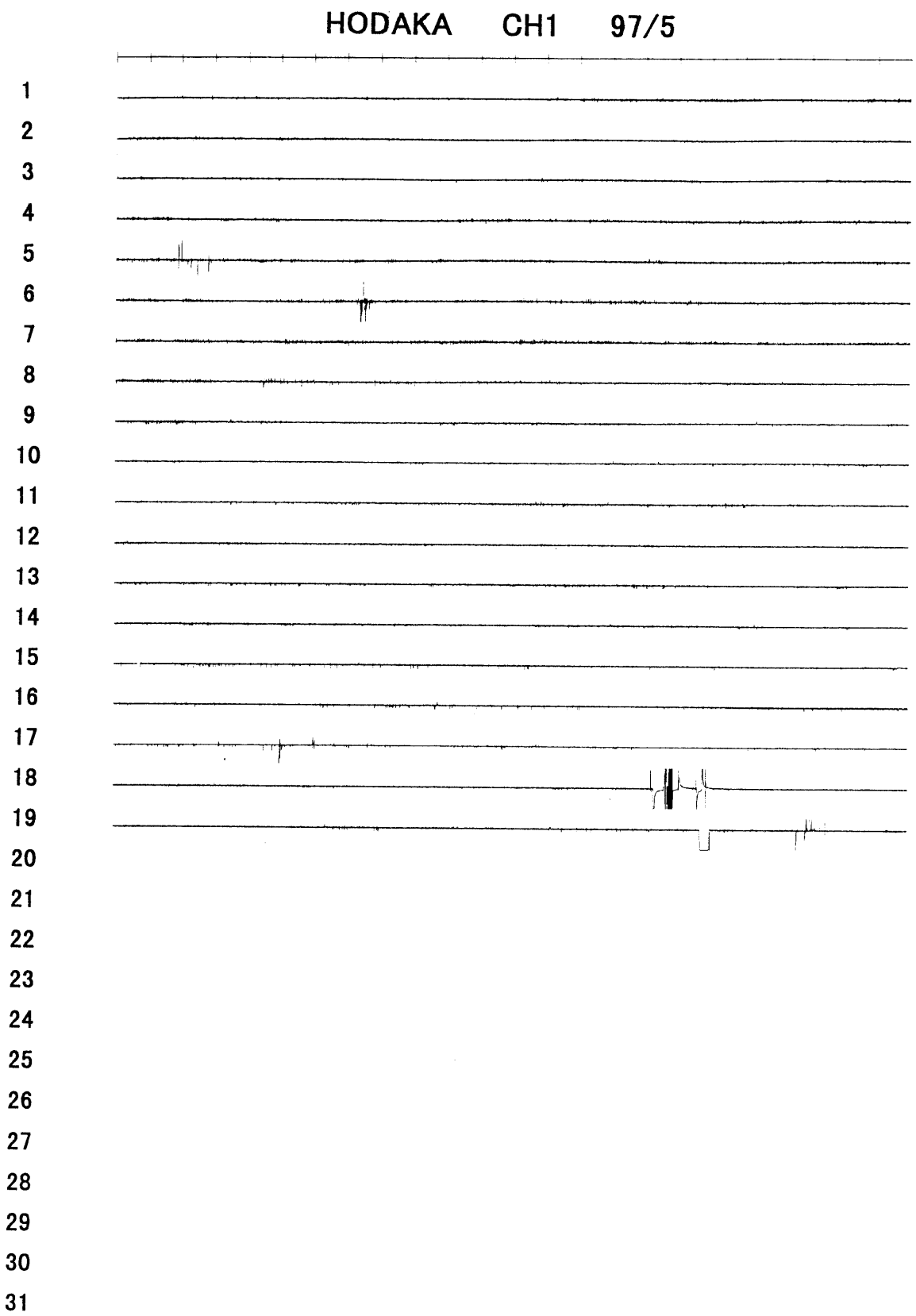
HODAKA CH1 97/5
1
2
3
4
5
6
7
8
9
10
11
12
13
14
15
16
17
18
19
20
21
22
23
24
25
26
27
28
29
30
31

Fig. A-97-5-1

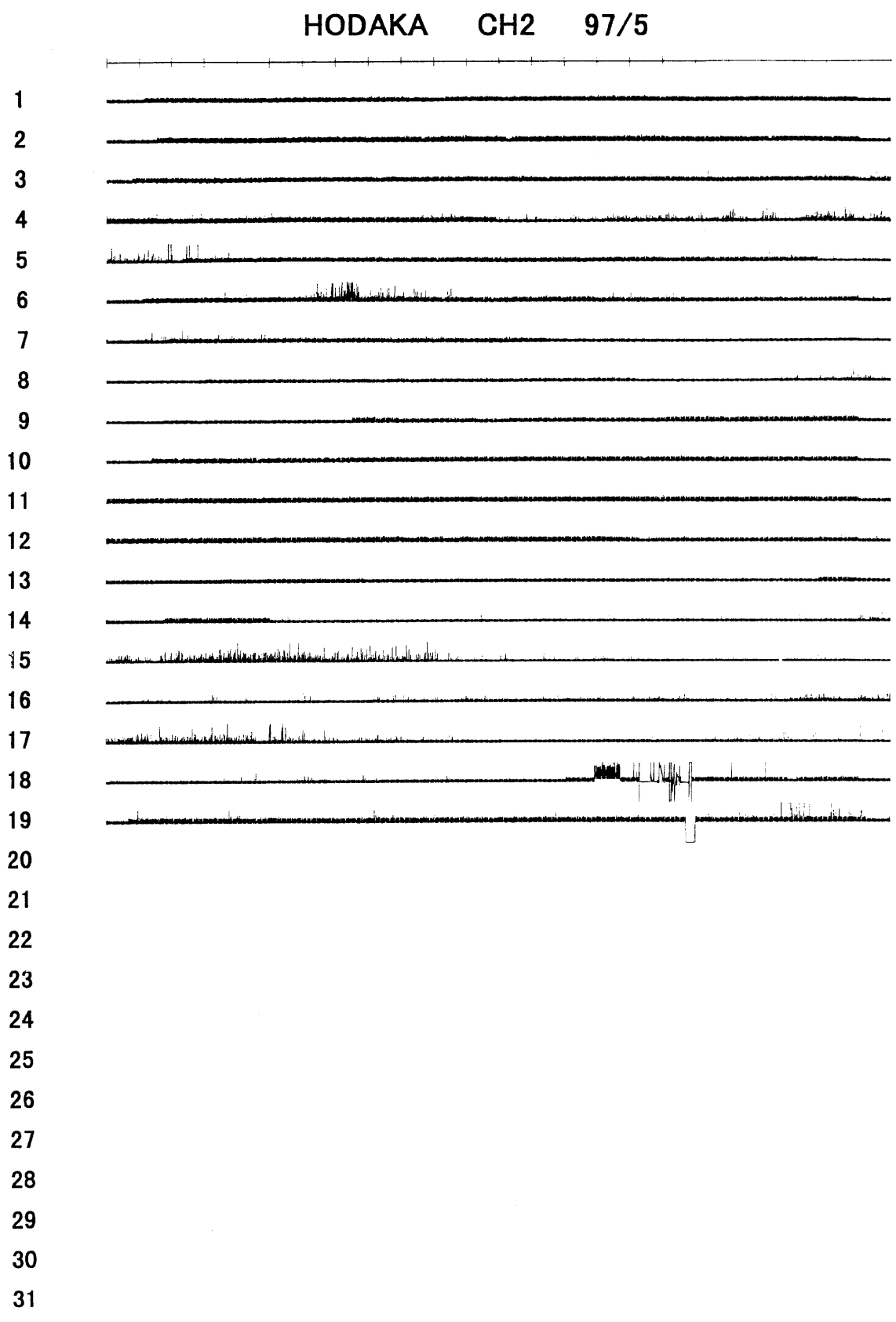
HODAKA CH2 97/5
1
2
3
4
5
6
7
8
9
10
11
12
13
14
15
16
17
18
19
20
21
22
23
24
25
26
27
28
29
30
31

Fig. A-97-5-2

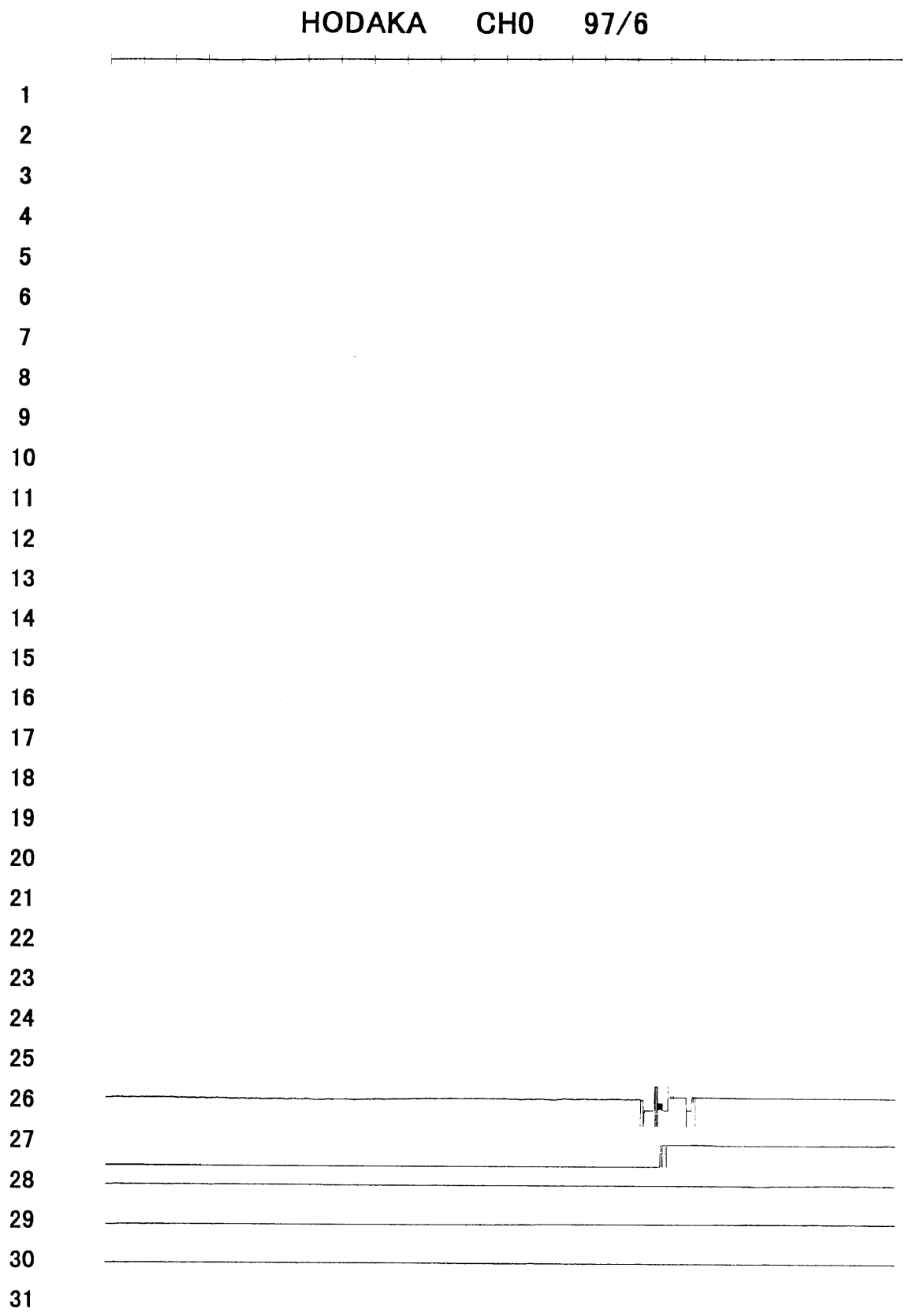
HODAKA CH0 97/6
1
2
3
4
5
6
7
8
9
10
11
12
13
14
15
16
17
18
19
20
21
22
23
24
25
26
27
28
29
30
31

Fig. A-97-6-0

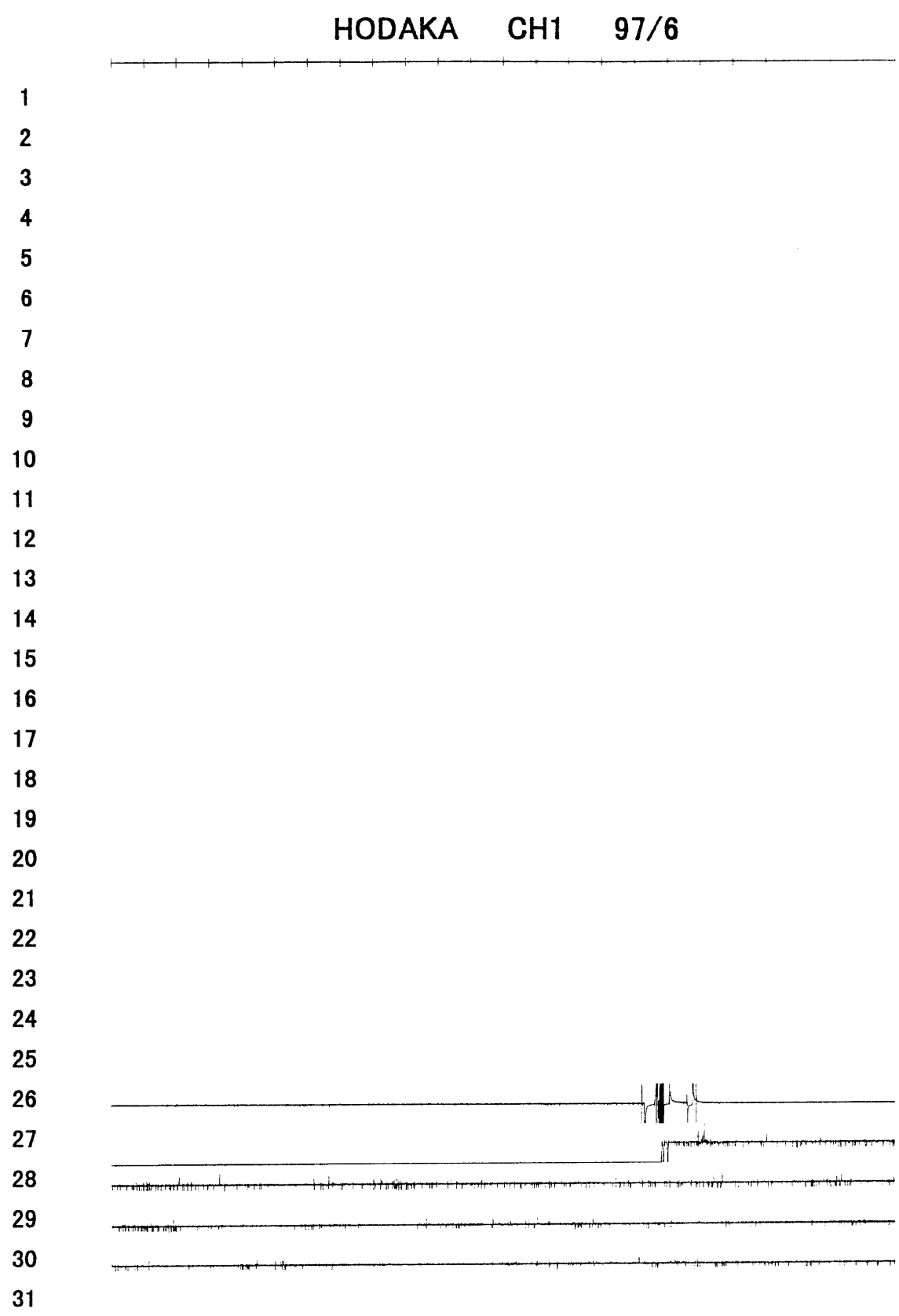
HODAKA CH1 97/6
1
2
3
4
5
6
7
8
9
10
11
12
13
14
15
16
17
18
19
20
21
22
23
24
25
26
27
28
29
30
31

Fig. A-97-6-1

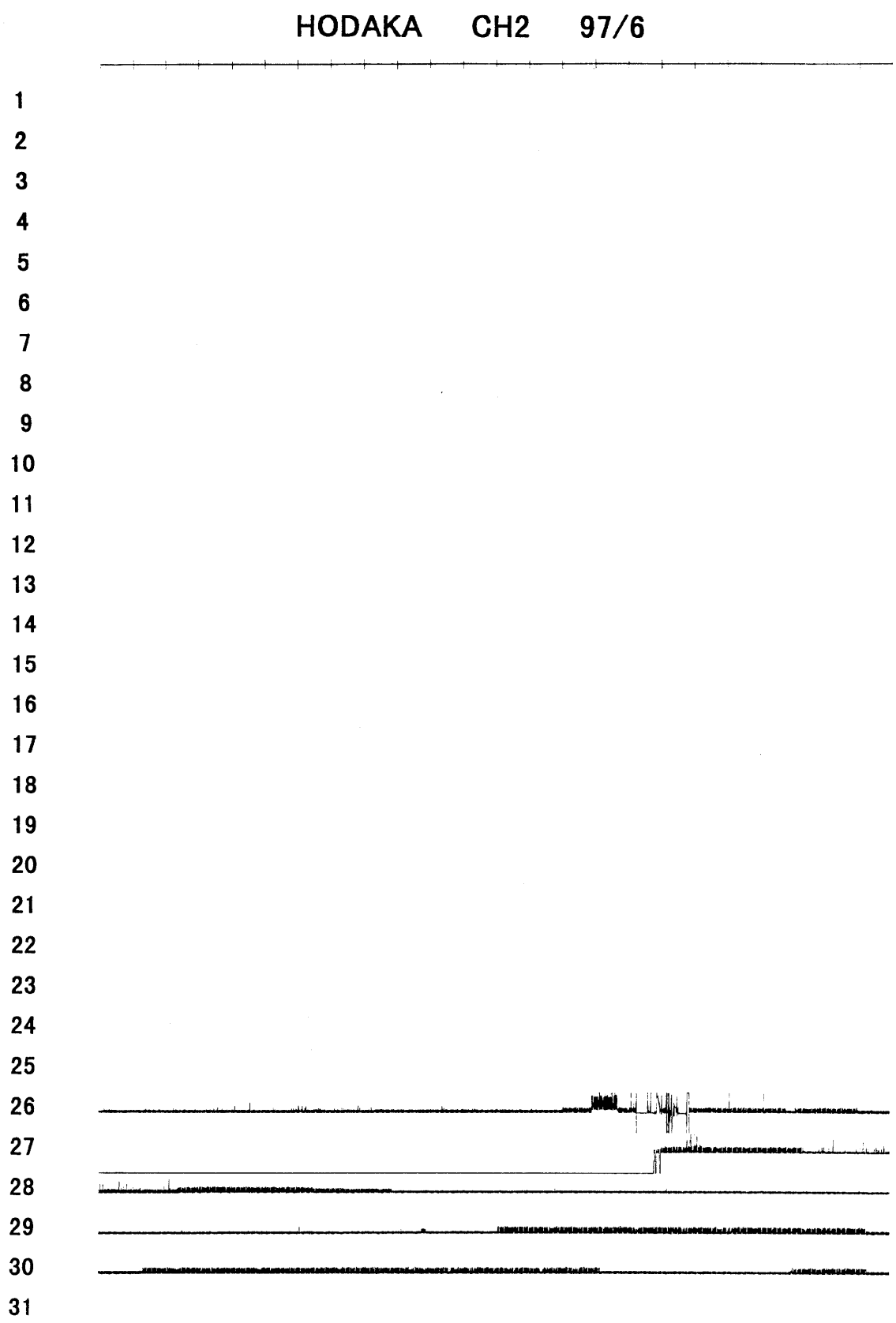
HODAKA CH2 97/6
1
2
3
4
5
6
7
8
9
10
11
12
13
14
15
16
17
18
19
20
21
22
23
24
25
26
27
28
29
30
31

Fig. A-97-6-2

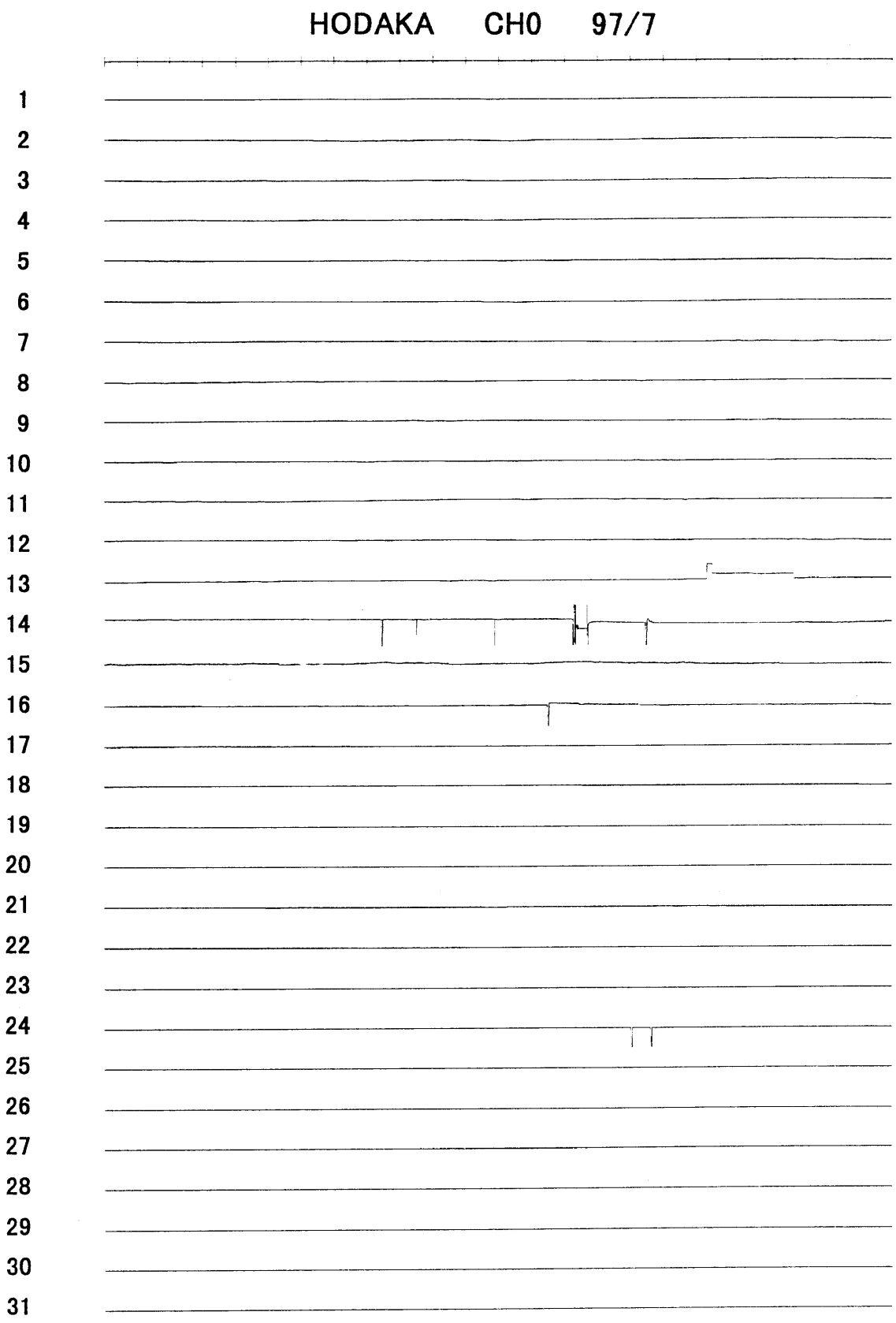
HODAKA CH0 97/7
1
2
3
4
5
6
7
8
9
10
11
12
13
14
15
16
17
18
19
20
21
22
23
24
25
26
27
28
29
30
31

Fig. A-97-7-0

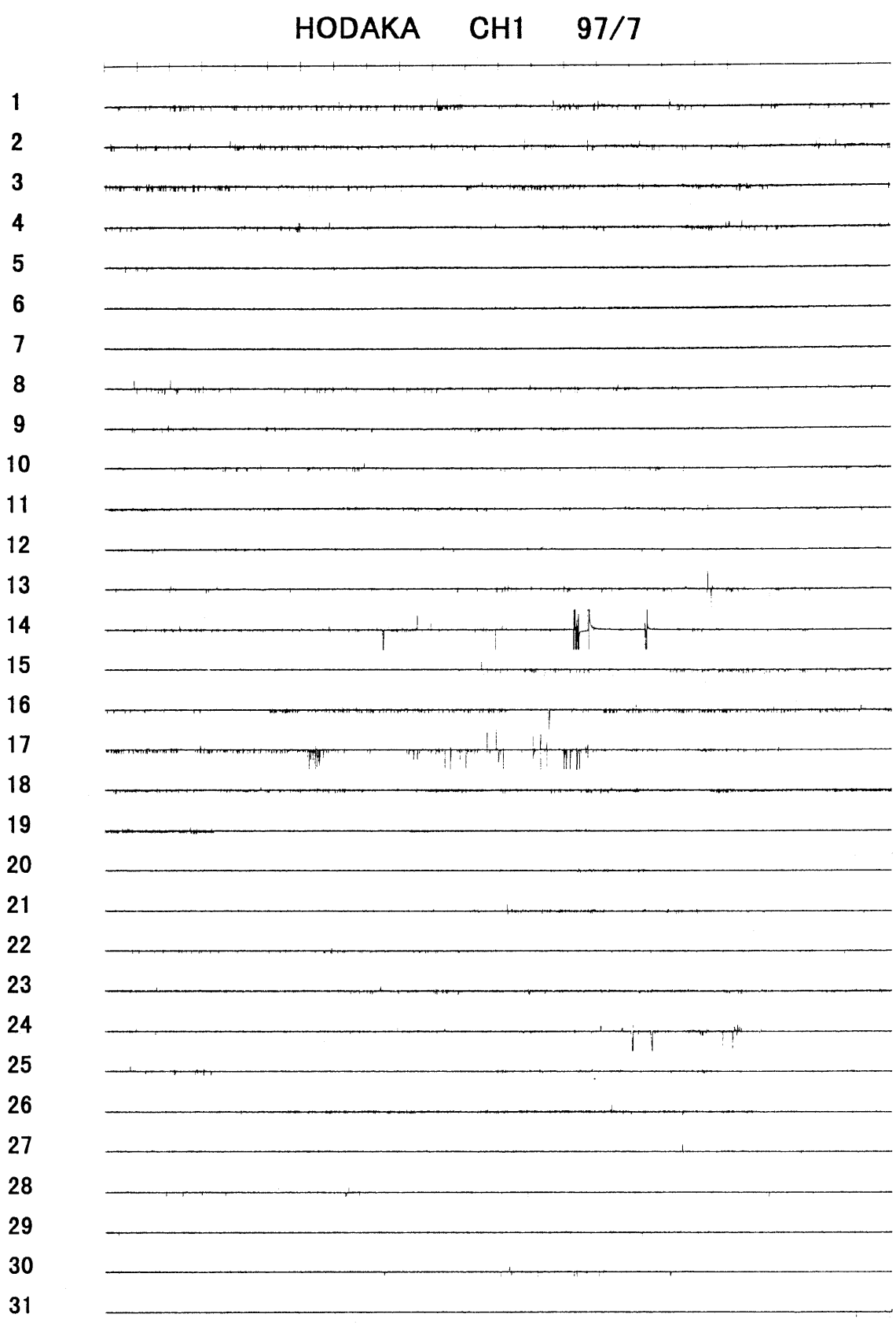
HODAKA CH1 97/7
1
2
3
4
5
6
7
8
9
10
11
12
13
14
15
16
17
18
19
20
21
22
23
24
25
26
27
28
29
30
31

Fig. A-97-7-1

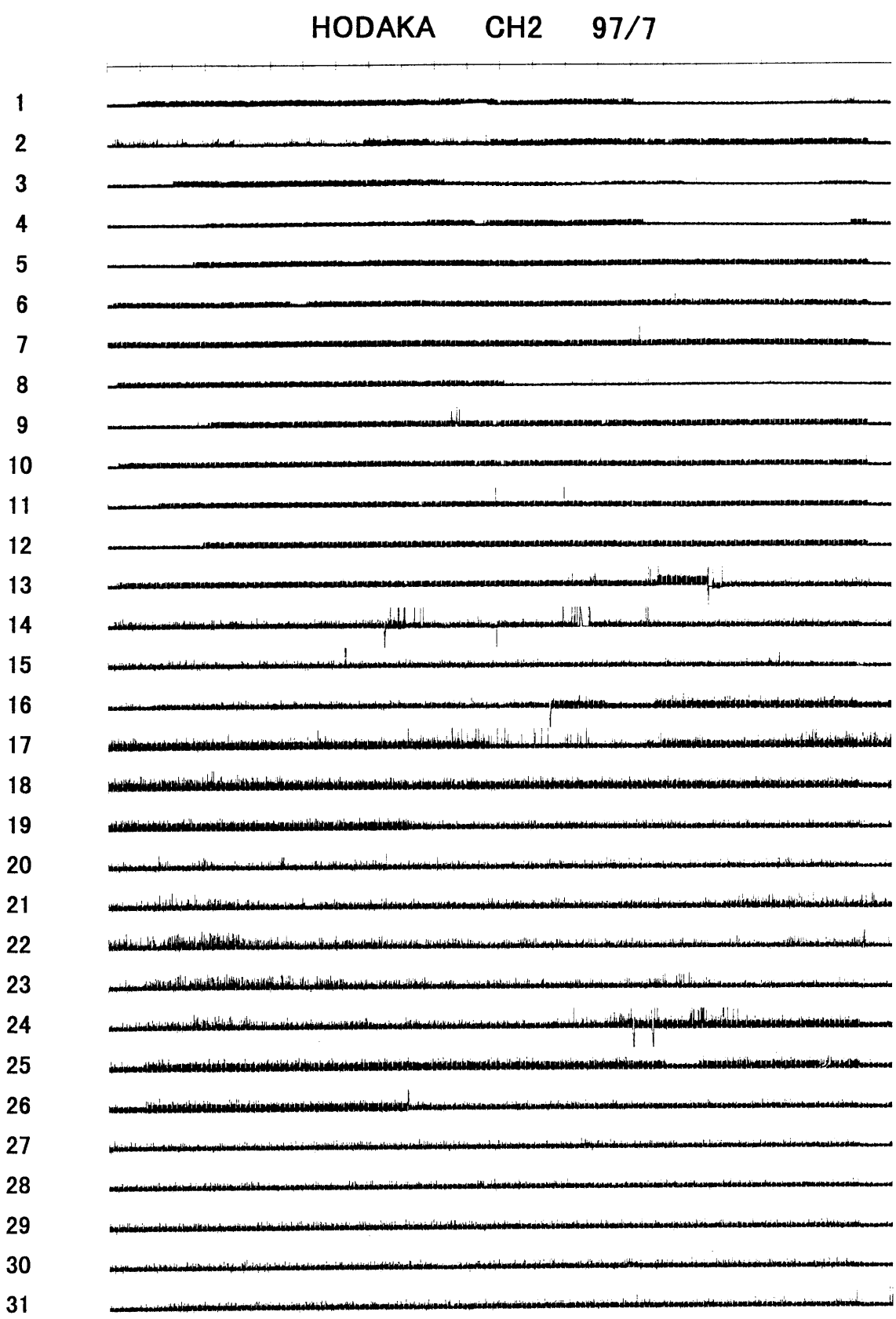
HODAKA CH2 97/7
1
2
3
4
5
6
7
8
9
10
11
12
13
14
15
16
17
18
19
20
21
22
23
24
25
26
27
28
29
30
31

Fig. A-97-7-2

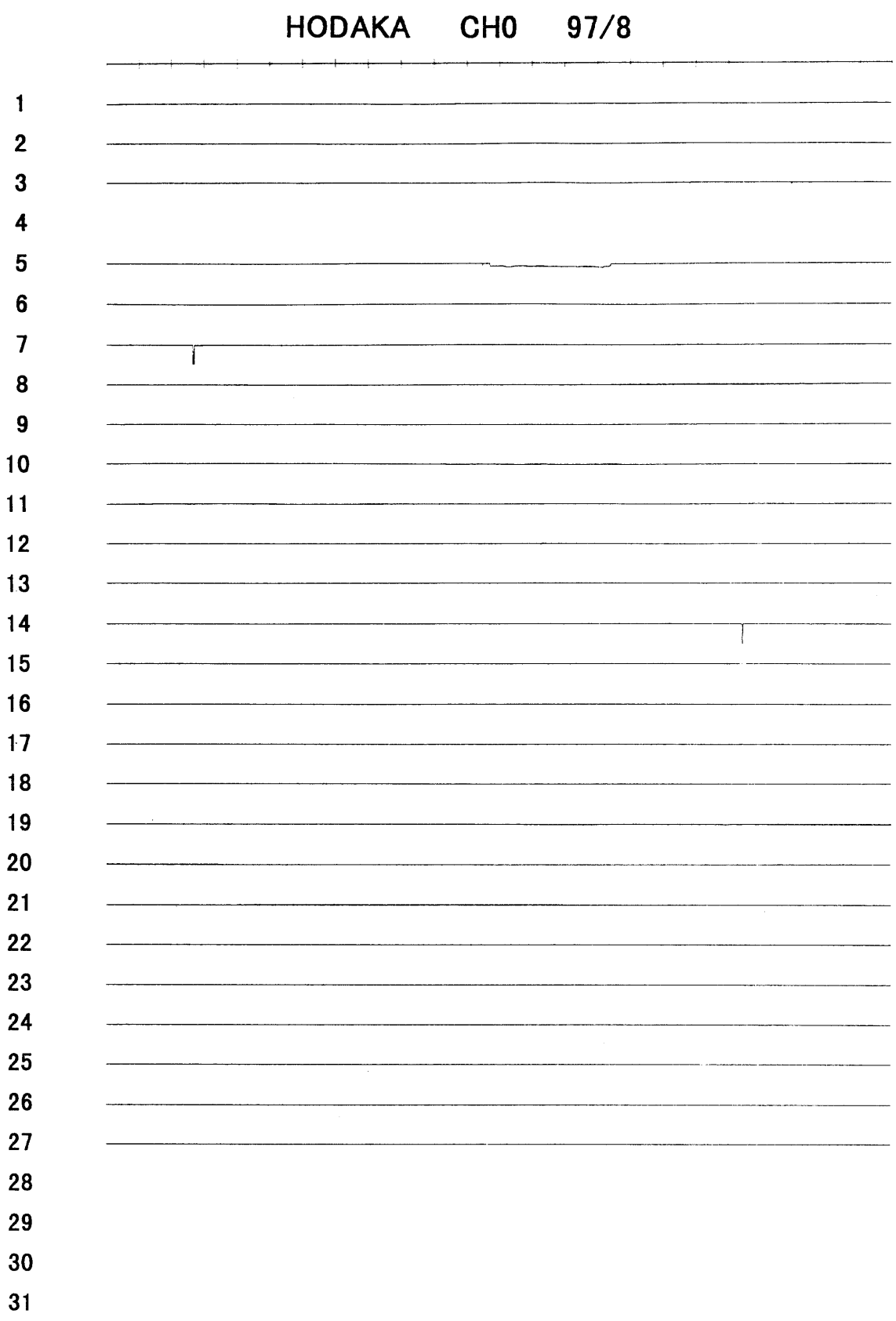
HODAKA CH0 97/8
1
2
3
4
5
6
7
8
9
10
11
12
13
14
15
16
17
18
19
20
21
22
23
24
25
26
27
28
29
30
31

Fig. A-97-8-0

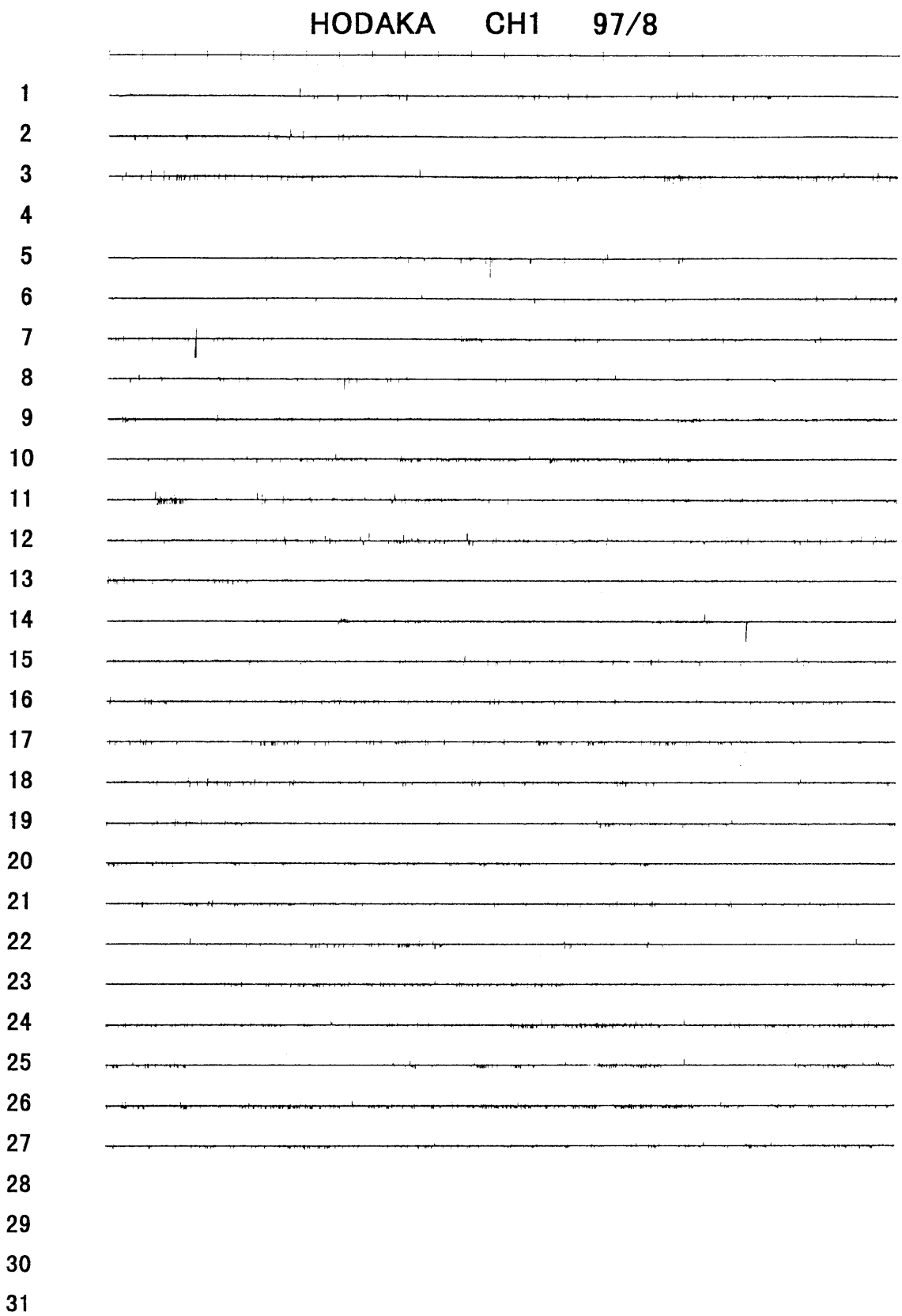
HODAKA CH1 97/8
1
2
3
4
5
6
7
8
9
10
11
12
13
14
15
16
17
18
19
20
21
22
23
24
25
26
27
28
29
30
31

Fig. A-97-8-1

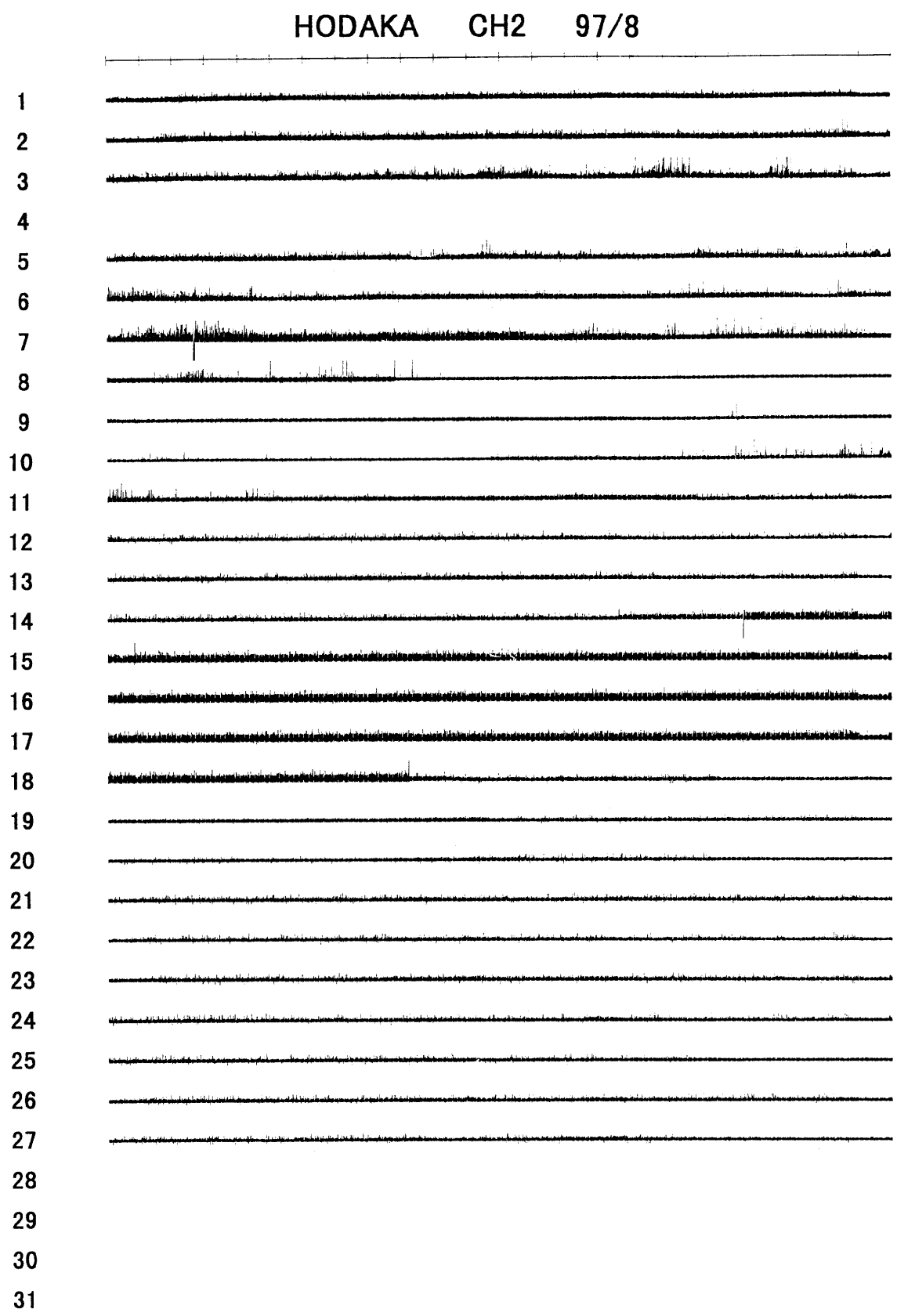
HODAKA CH2 97/8
1
2
3
4
5
6
7
8
9
10
11
12
13
14
15
16
17
18
19
20
21
22
23
24
25
26
27
28
29
30
31

Fig. A-97-8-2

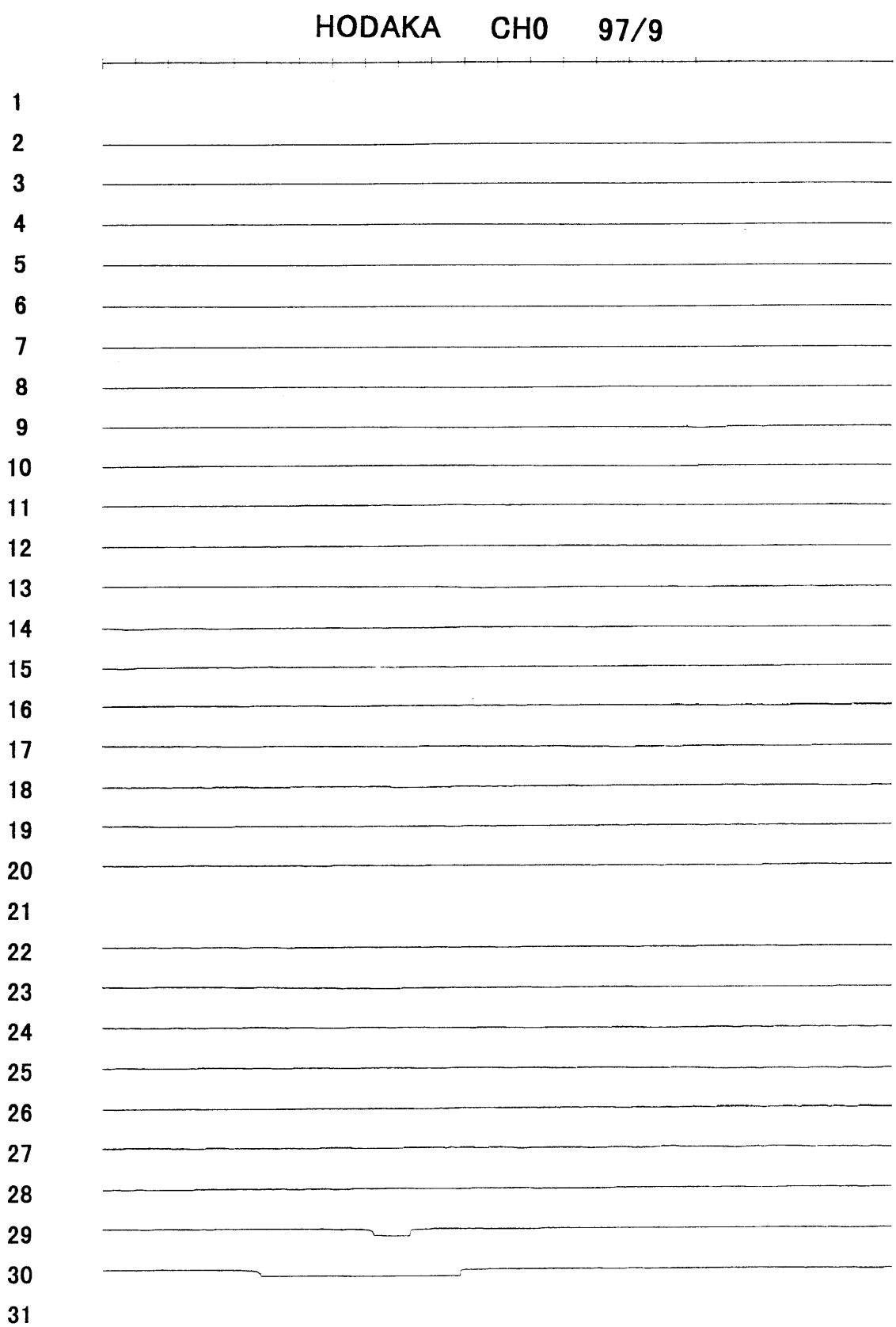
HODAKA CH0 97/9
1
2
3
4
5
6
7
8
9
10
11
12
13
14
15
16
17
18
19
20
21
22
23
24
25
26
27
28
29
30
31

Fig. A-97-9-0

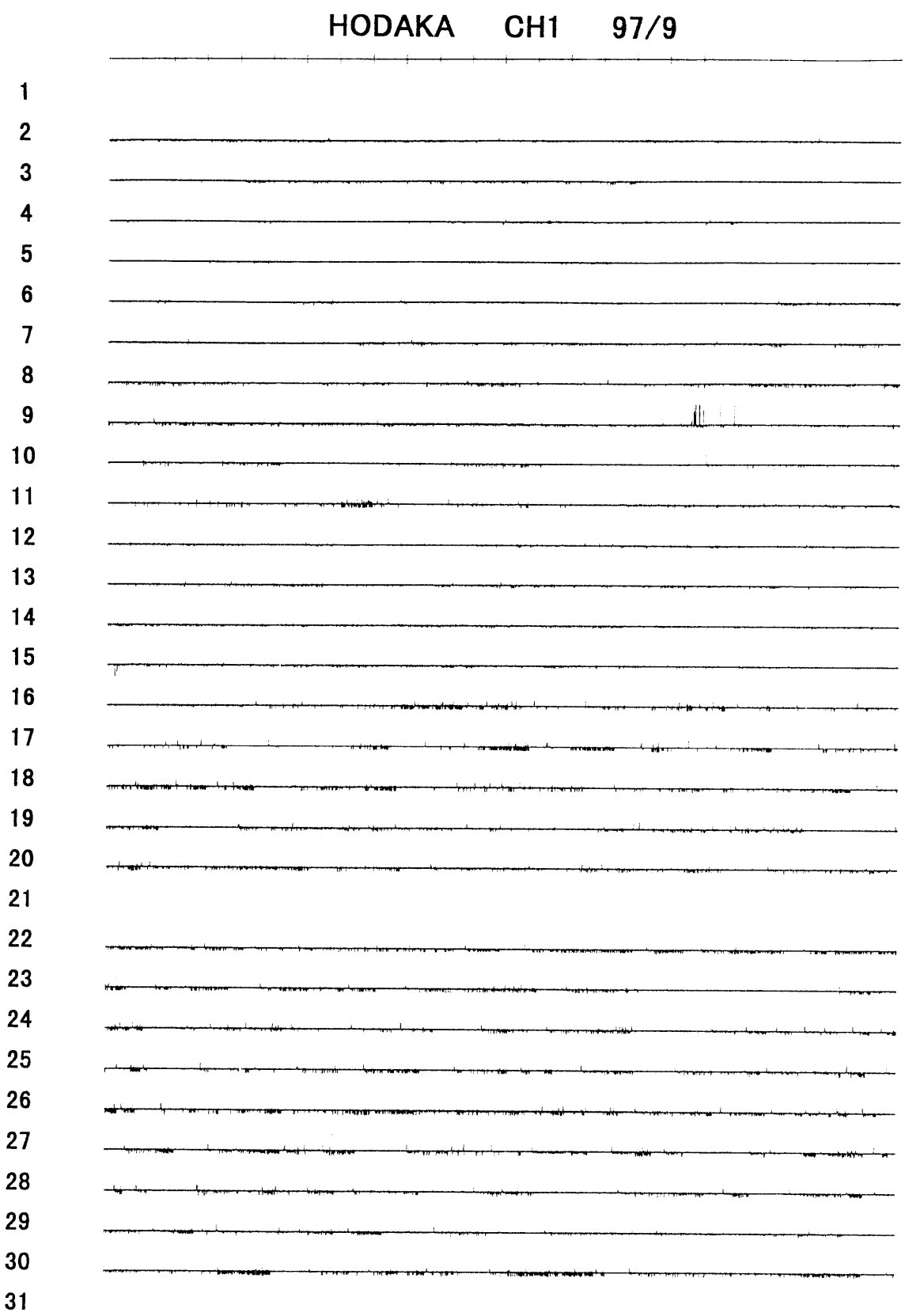
HODAKA CH1 97/9
1
2
3
4
5
6
7
8
9
10
11
12
13
14
15
16
17
18
19
20
21
22
23
24
25
26
27
28
29
30
31

Fig. A-97-9-1

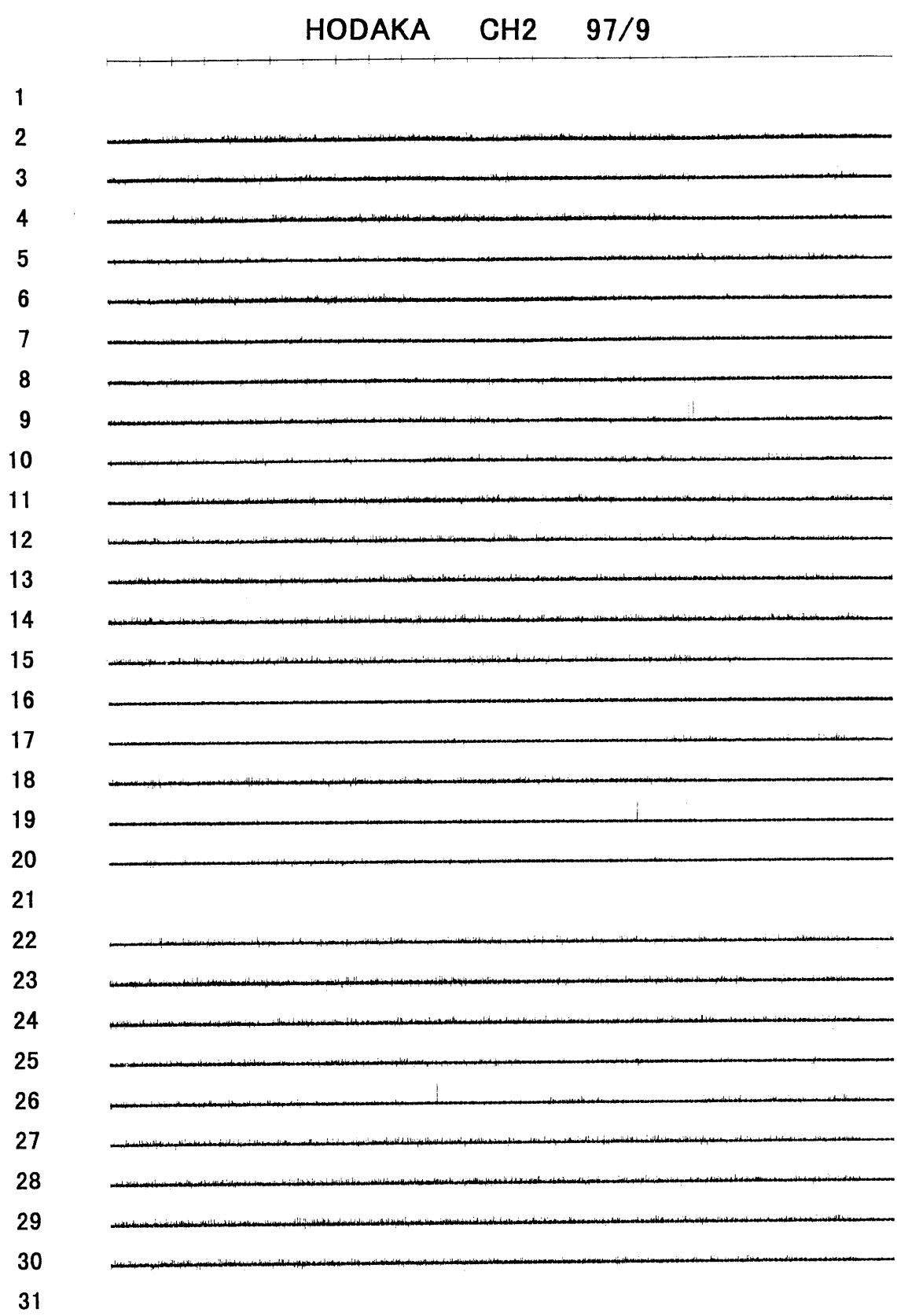
HODAKA CH2 97/9
1
2
3
4
5
6
7
8
9
10
11
12
13
14
15
16
17
18
19
20
21
22
23
24
25
26
27
28
29
30
31

Fig. A-97-9-2

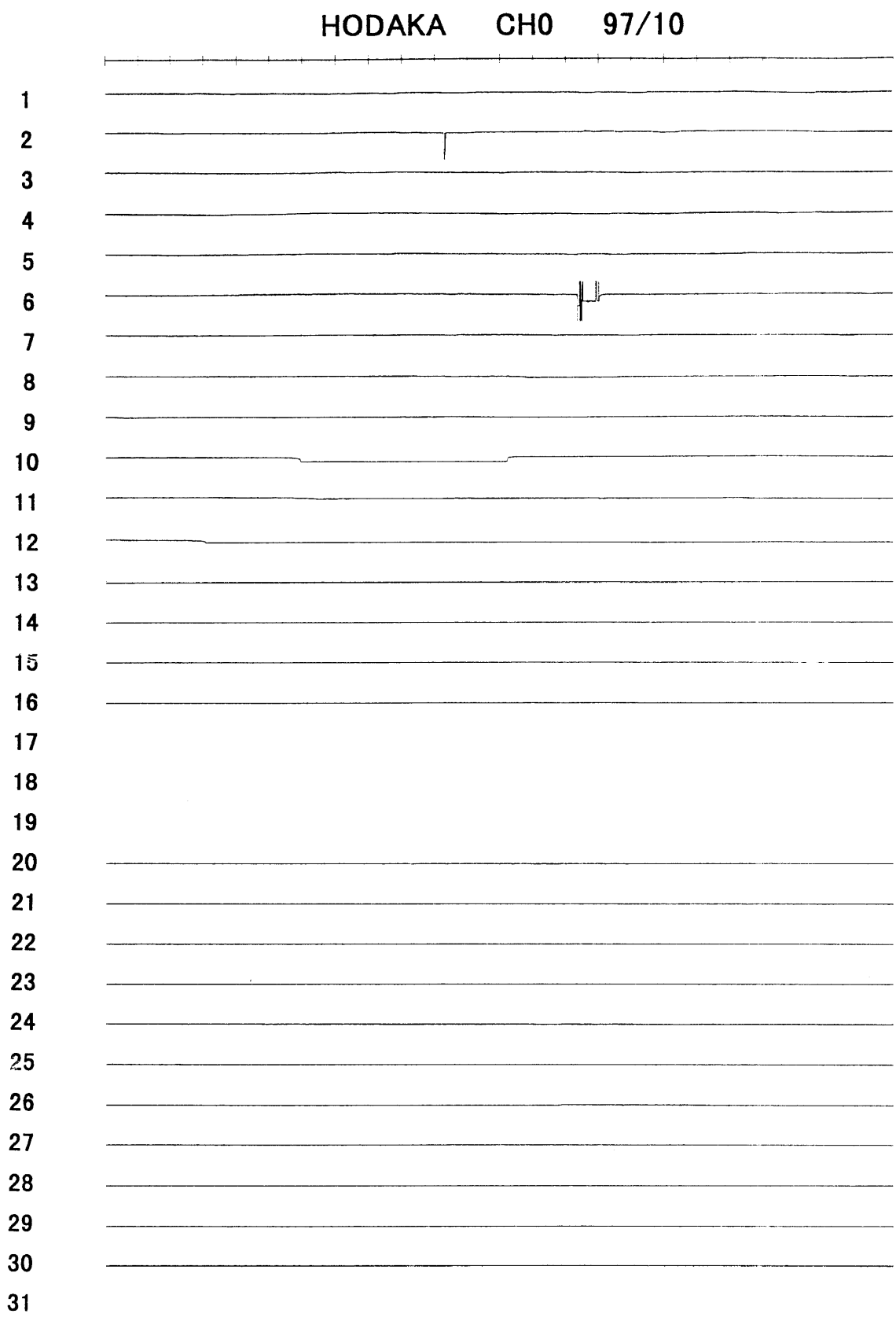
HODAKA CH0 97/10
1
2
3
4
5
6
7
8
9
10
11
12
13
14
15
16
17
18
19
20
21
22
23
24
25
26
27
28
29
30
31

Fig. A-97-10-0

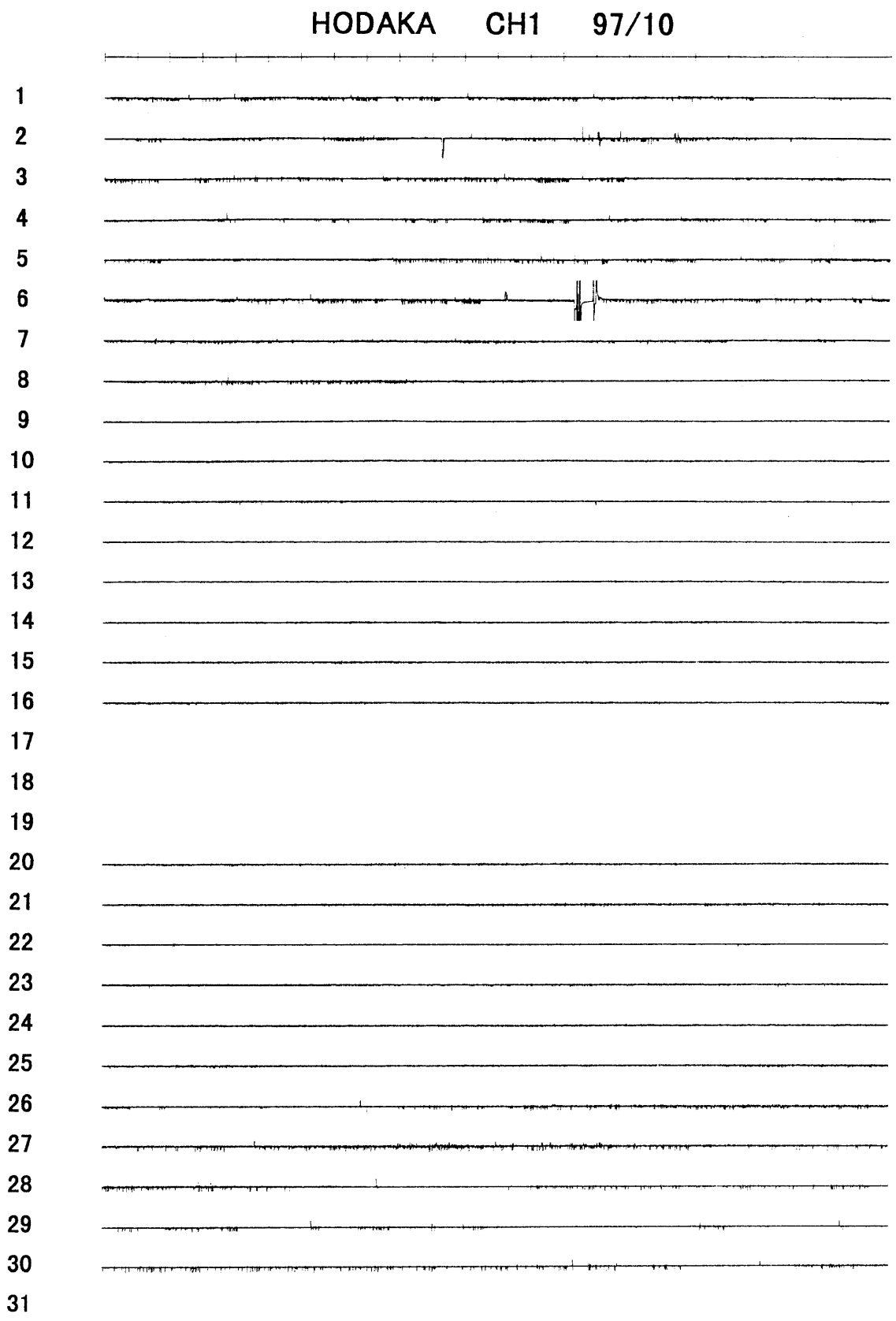
HODAKA CH1 97/10
1
2
3
4
5
6
7
8
9
10
11
12
13
14
15
16
17
18
19
20
21
22
23
24
25
26
27
28
29
30
31

Fig. A-97-10-1

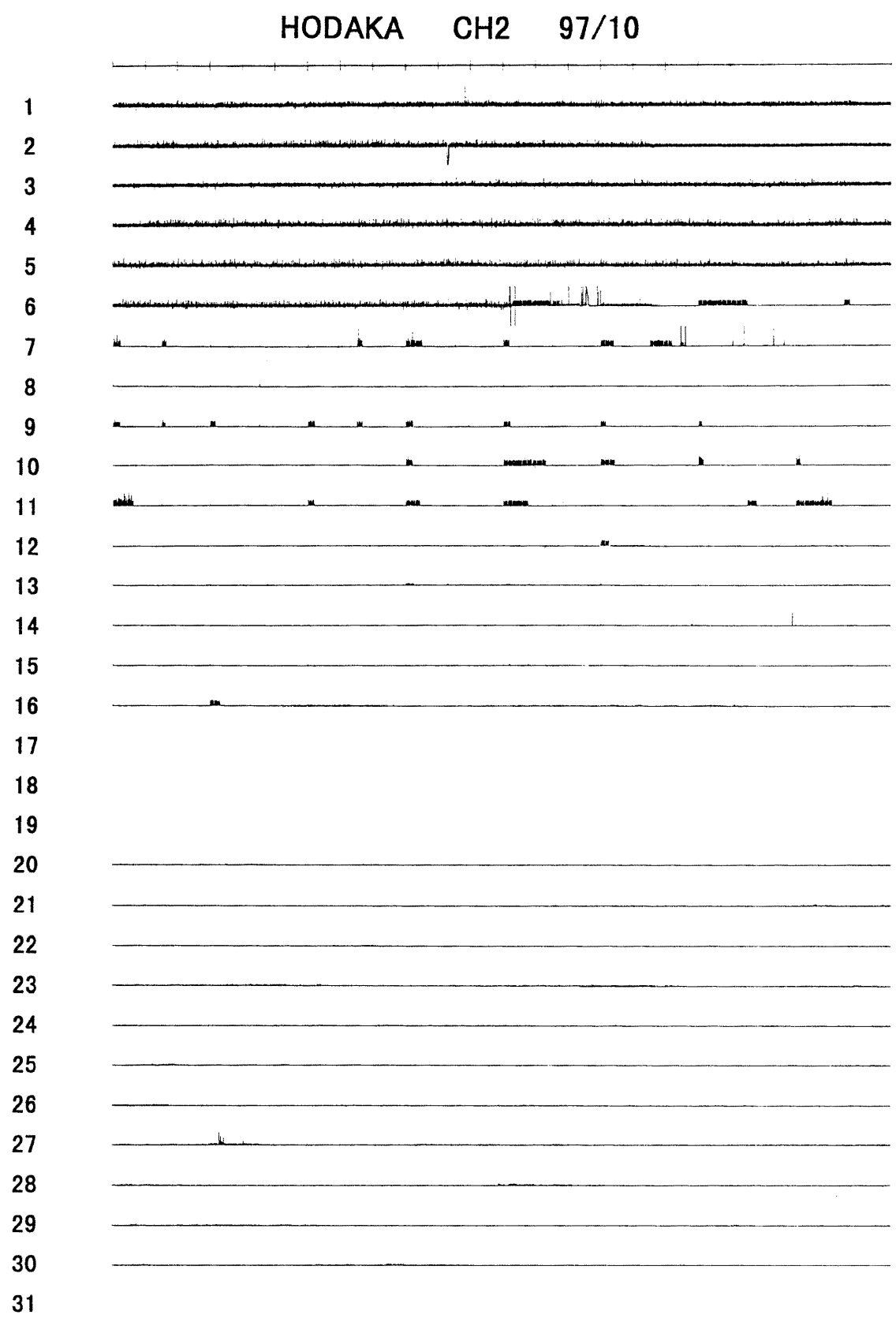
HODAKA CH2 97/10
1
2
3
4
5
6
7
8
9
10
11
12
13
14
15
16
17
18
19
20
21
22
23
24
25
26
27
28
29
30
31

Fig. A-97-10-2

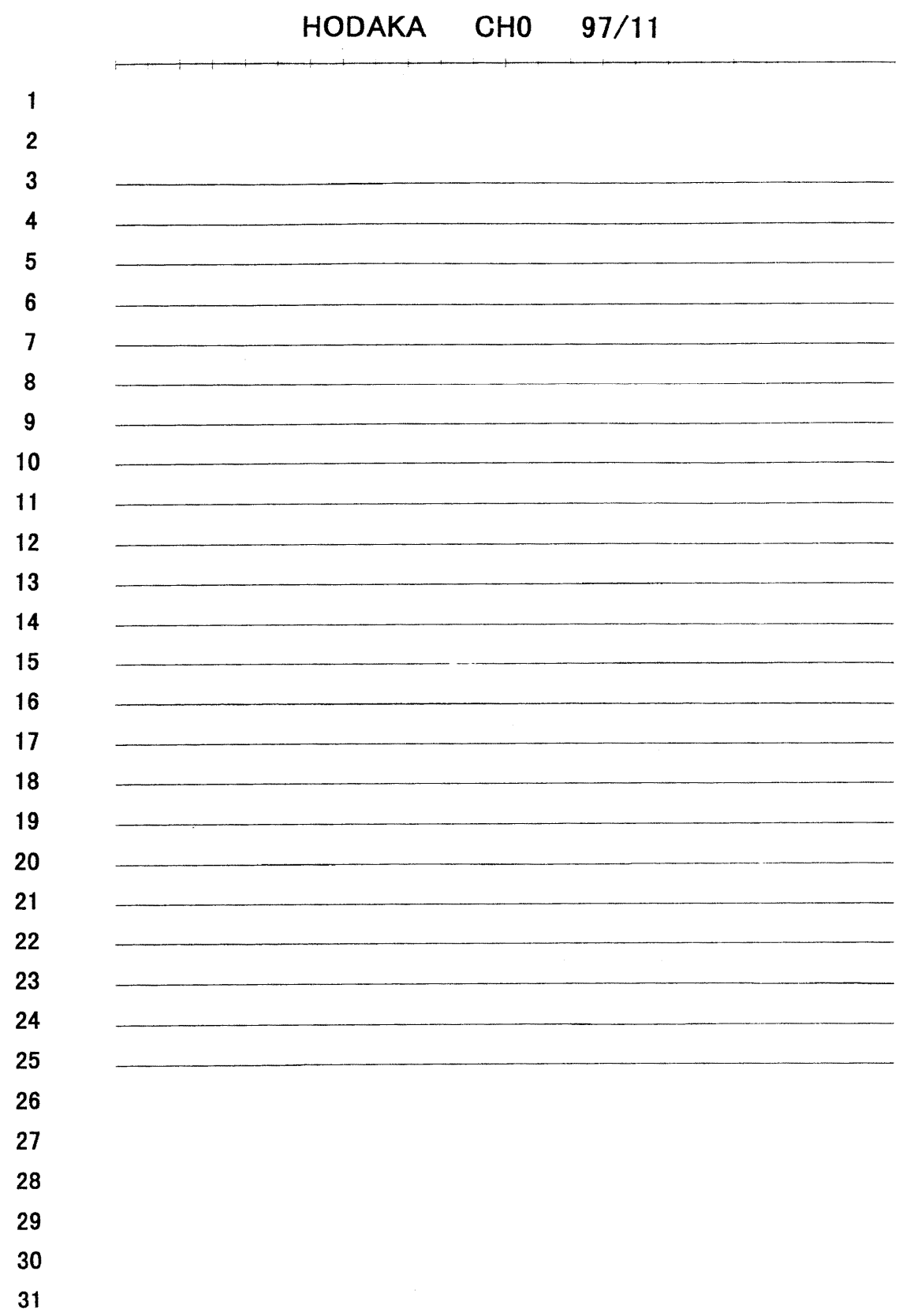
HODAKA CH0 97/11
1
2
3
4
5
6
7
8
9
10
11
12
13
14
15
16
17
18
19
20
21
22
23
24
25
26
27
28
29
30
31

Fig. A-97-11-0

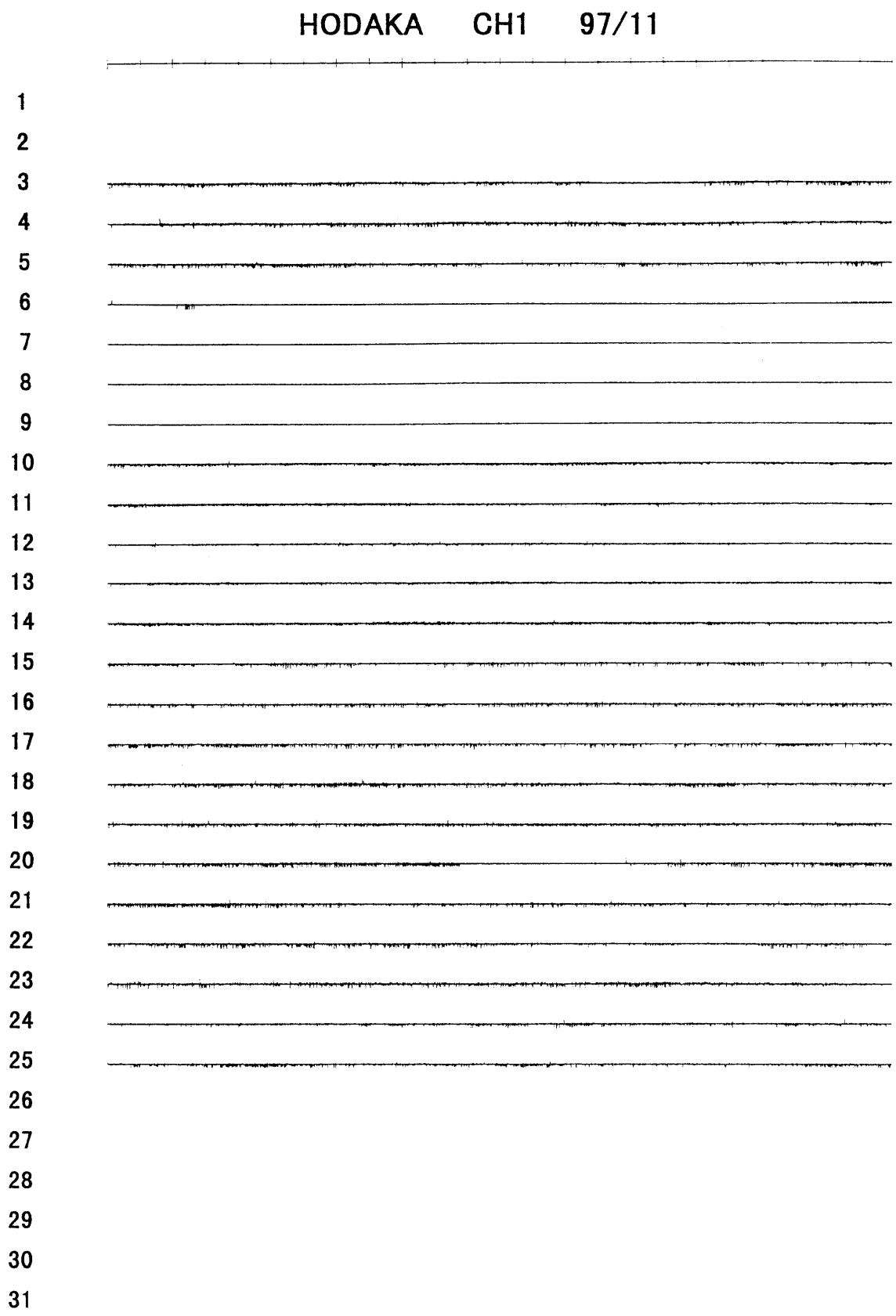
HODAKA CH1 97/11
1
2
3
4
5
6
7
8
9
10
11
12
13
14
15
16
17
18
19
20
21
22
23
24
25
26
27
28
29
30
31

Fig. A-97-11-1

HODAKA CH2 97/11

1
2
3
4
5
6
7
8
9
10
11
12
13
14
15
16
17
18
19
20
21
22
23
24
25
26
27
28
29
30
31

Fig. A-97-11-2

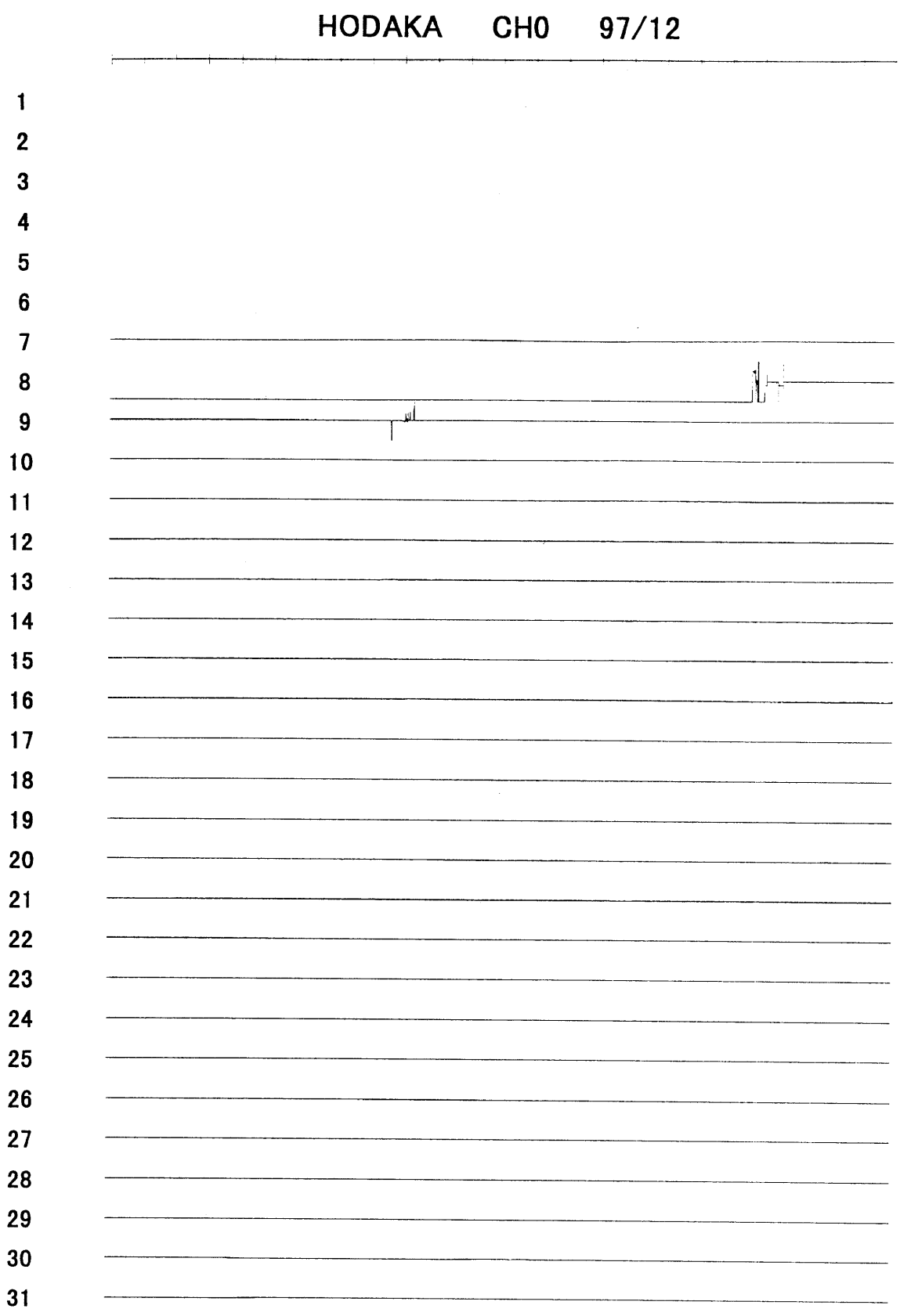
HODAKA CH0 97/12
1
2
3
4
5
6
7
8
9
10
11
12
13
14
15
16
17
18
19
20
21
22
23
24
25
26
27
28
29
30
31

Fig. A-97-12-0

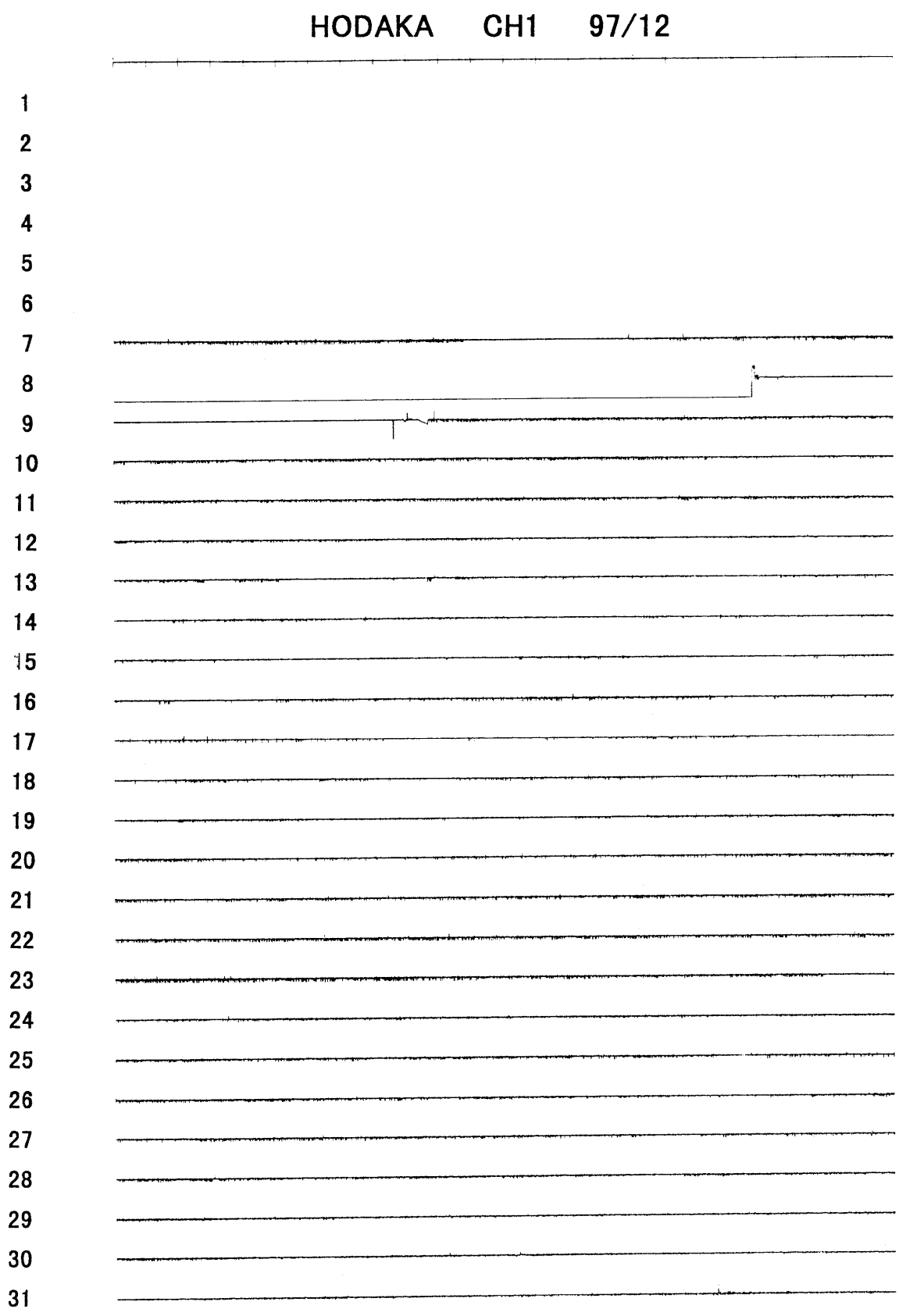
HODAKA CH1 97/12
1
2
3
4
5
6
7
8
9
10
11
12
13
14
15
16
17
18
19
20
21
22
23
24
25
26
27
28
29
30
31

Fig. A-97-12-1

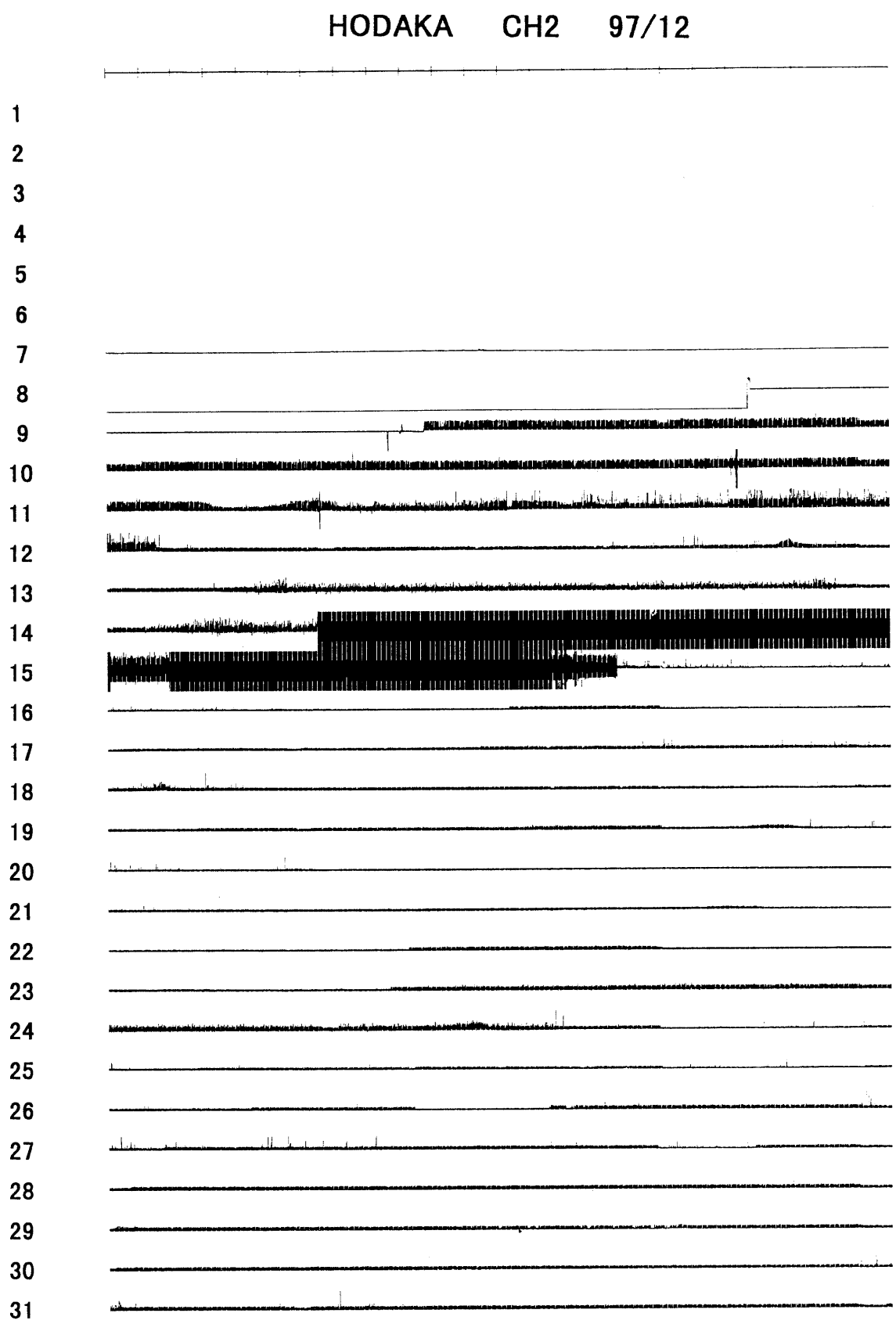
HODAKA CH2 97/12
1
2
3
4
5
6
7
8
9
10
11
12
13
14
15
16
17
18
19
20
21
22
23
24
25
26
27
28
29
30
31

Fig. A-97-12-2

HODAKA CH0 98/1

1
2
3
4
5
6
7
8
9
10
11
12
13
14
15
16
17
18
19
20
21
22
23
24
25
26
27
28
29
30
31

Fig. A-98-1-0

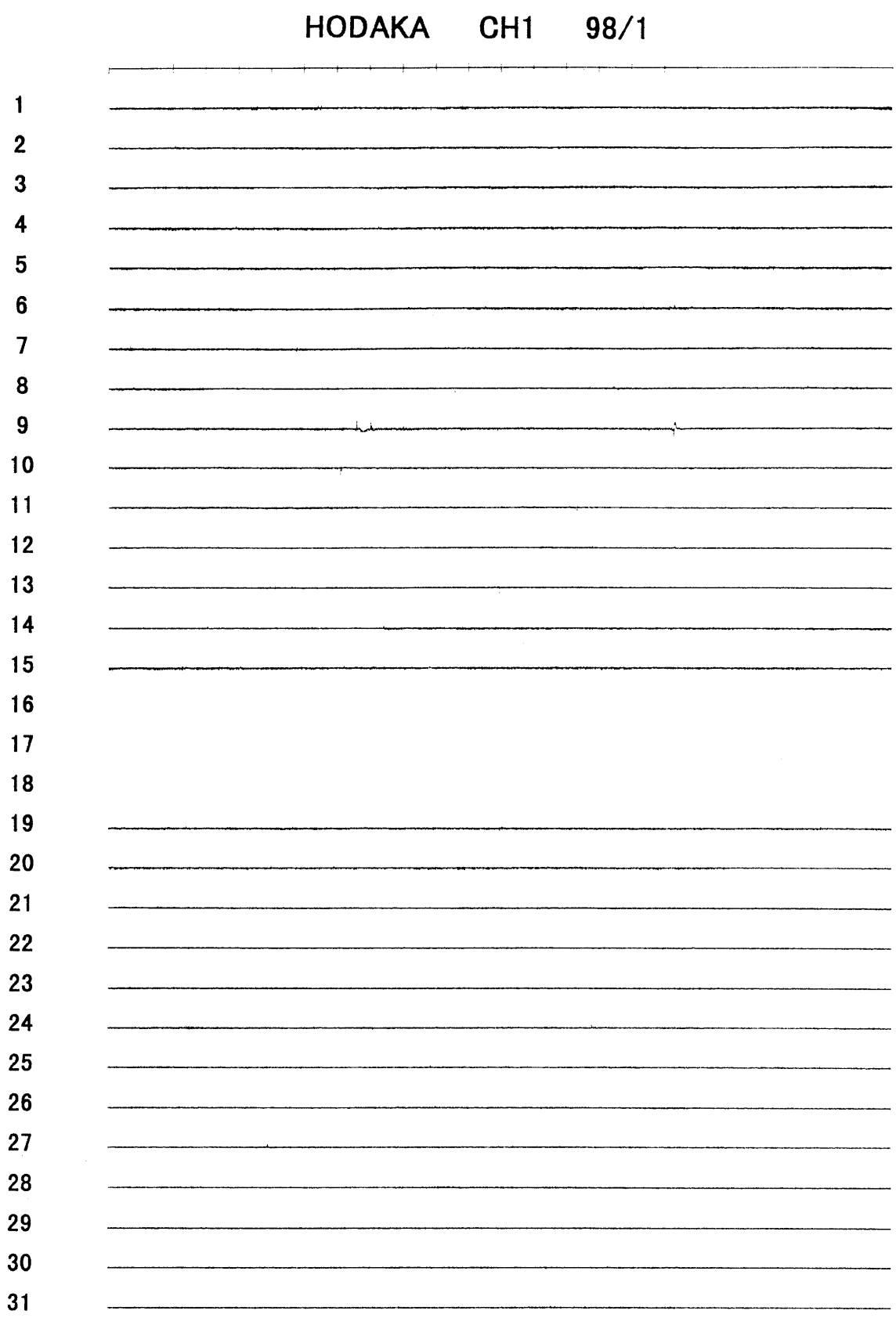
HODAKA CH1 98/1
1
2
3
4
5
6
7
8
9
10
11
12
13
14
15
16
17
18
19
20
21
22
23
24
25
26
27
28
29
30
31

Fig. A-98-1-1

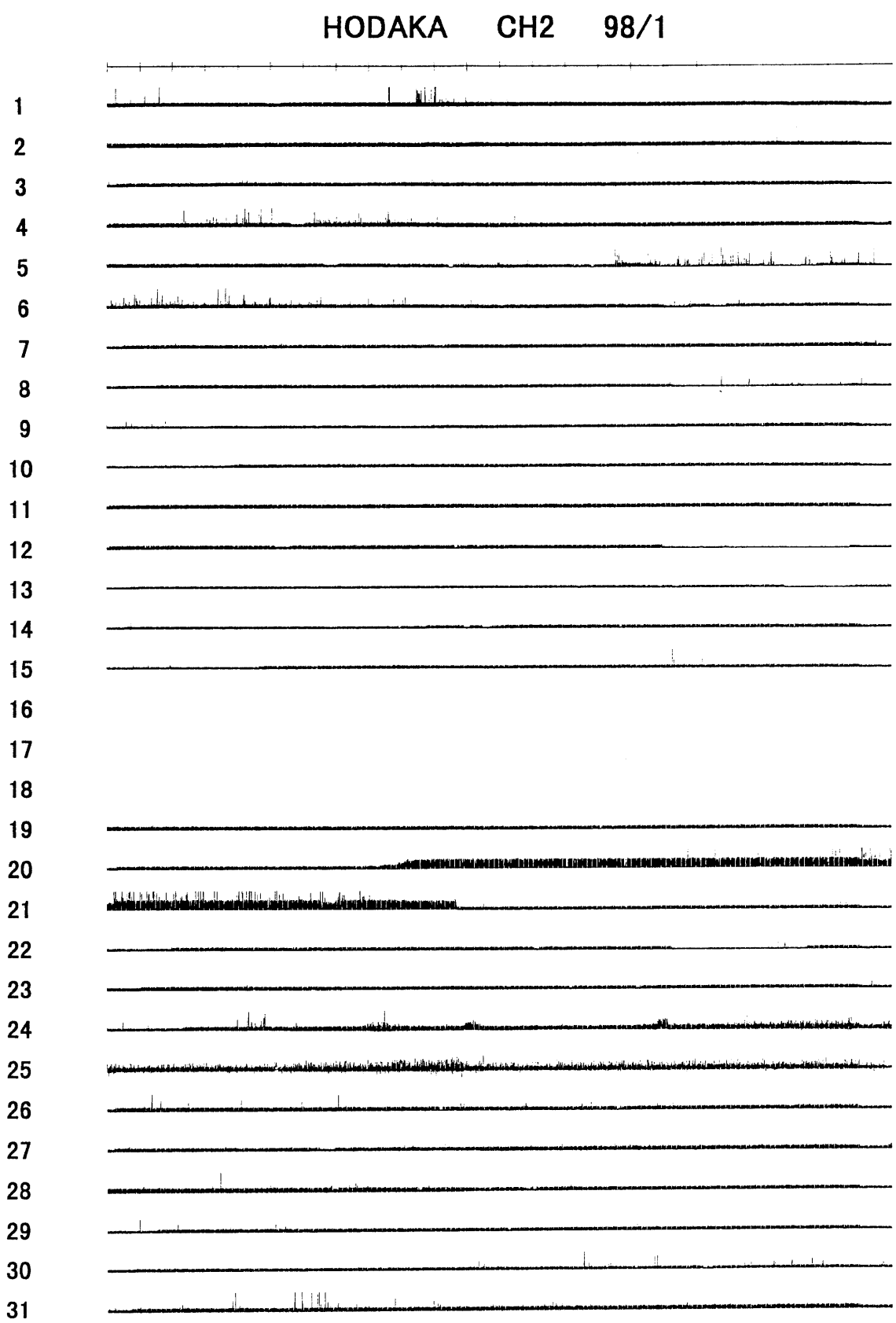
HODAKA CH2 98/1
1
2
3
4
5
6
7
8
9
10
11
12
13
14
15
16
17
18
19
20
21
22
23
24
25
26
27
28
29
30
31

Fig. A-98-1-2

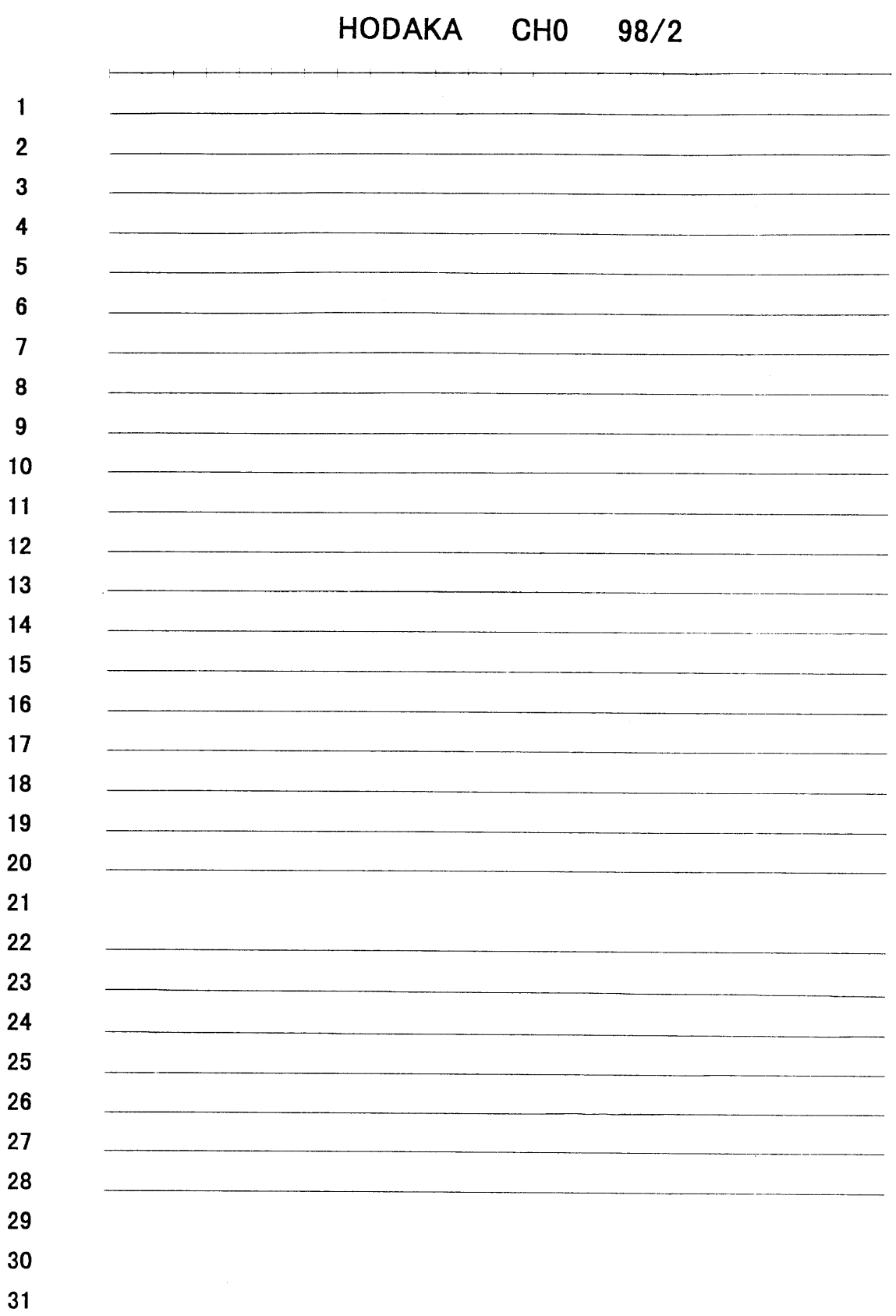
HODAKA CH0 98/2
1
2
3
4
5
6
7
8
9
10
11
12
13
14
15
16
17
18
19
20
21
22
23
24
25
26
27
28
29
30
31

Fig. A-98-2-0

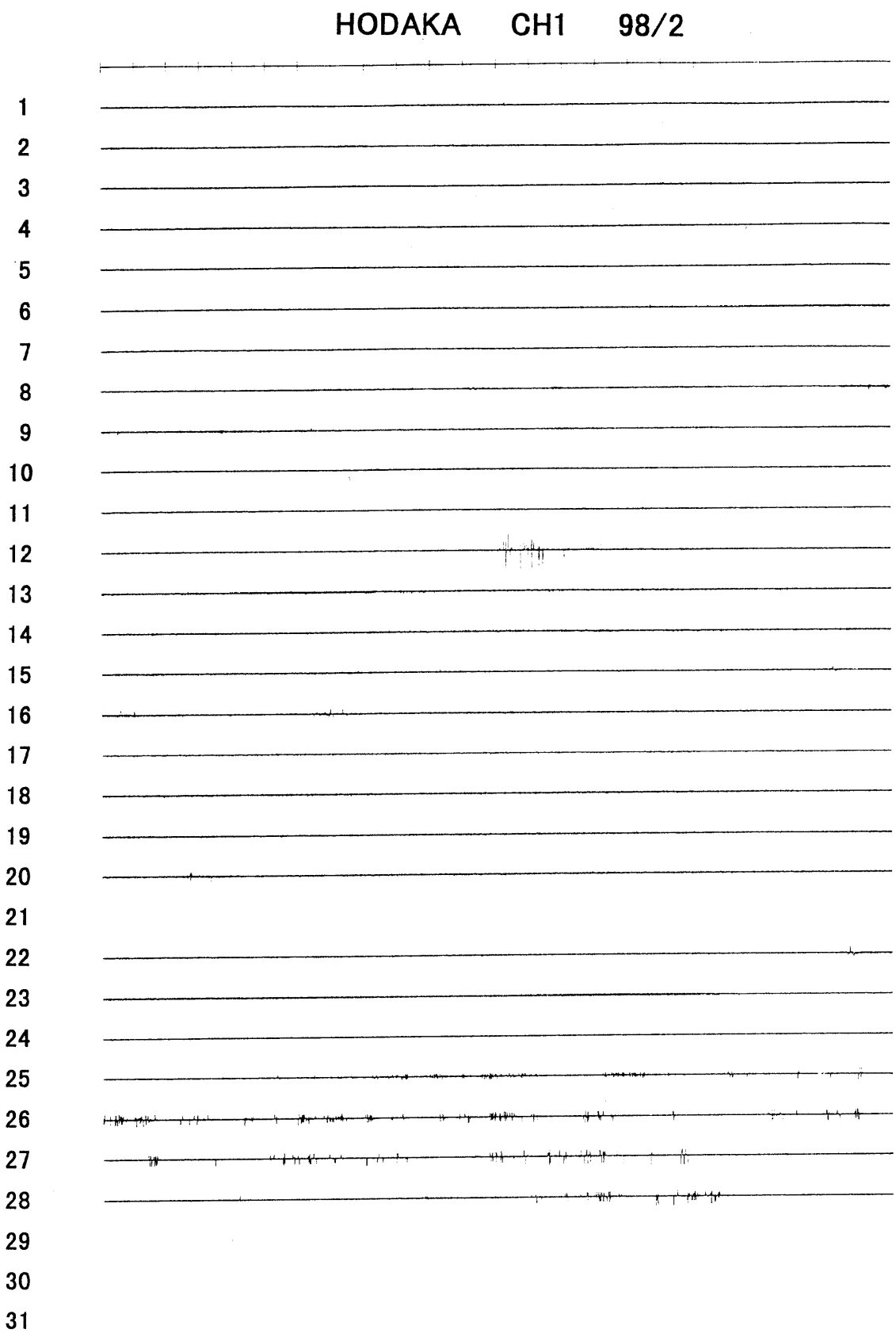
HODAKA CH1 98/2
1
2
3
4
5
6
7
8
9
10
11
12
13
14
15
16
17
18
19
20
21
22
23
24
25
26
27
28
29
30
31

Fig. A-98-2-1

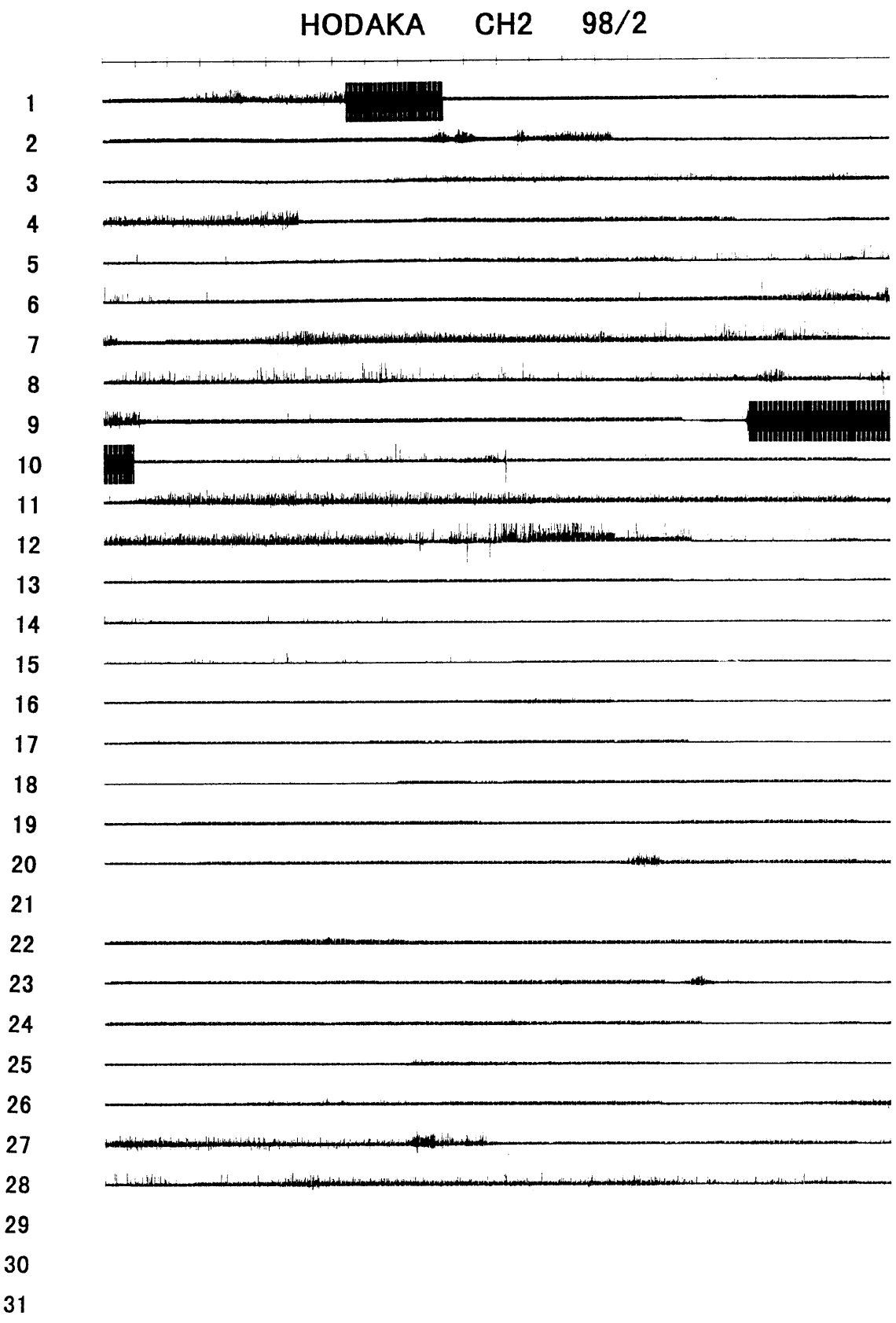
HODAKA CH2 98/2
1
2
3
4
5
6
7
8
9
10
11
12
13
14
15
16
17
18
19
20
21
22
23
24
25
26
27
28
29
30
31

Fig. A-98-2-2

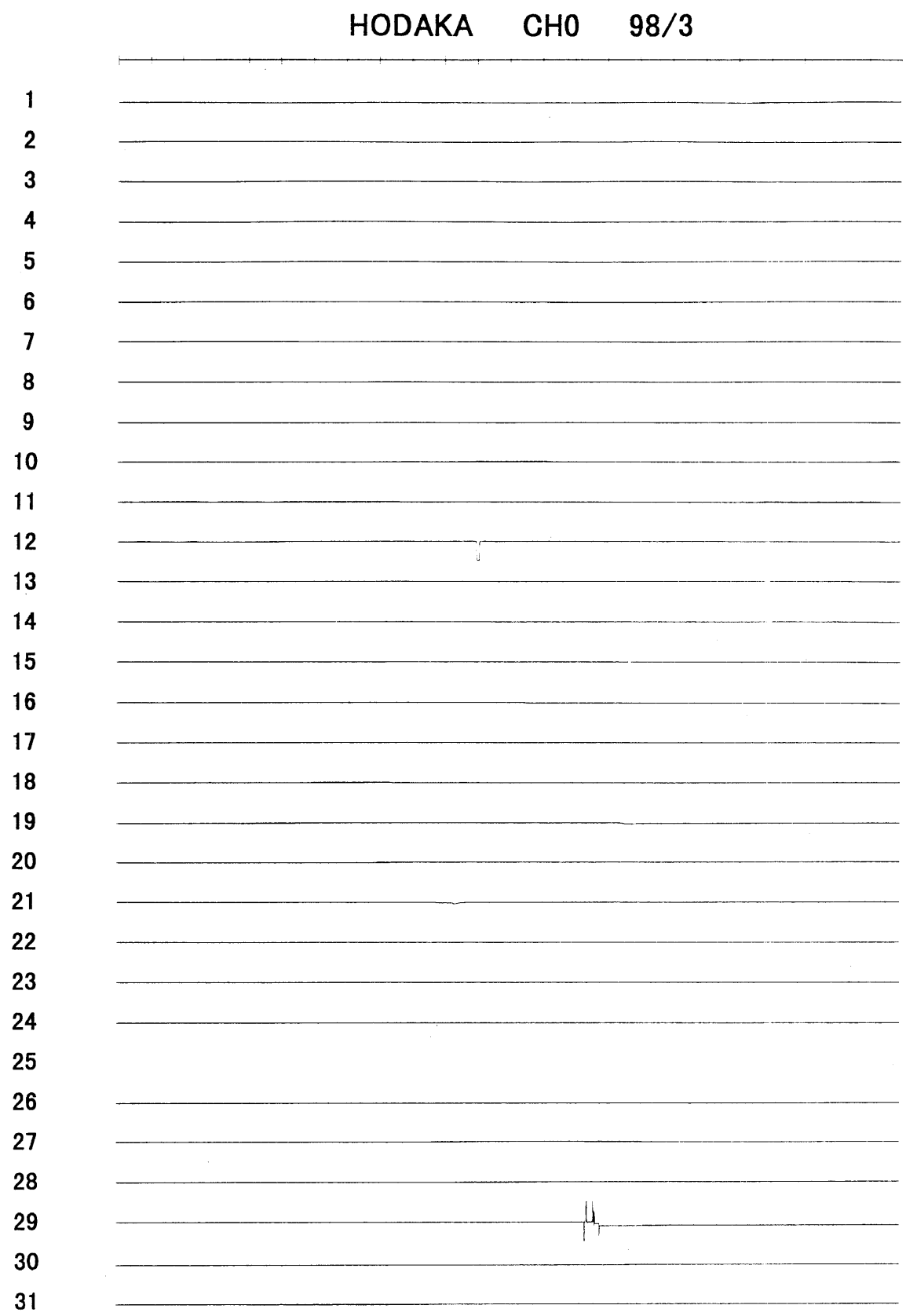
HODAKA CH0 98/3
1
2
3
4
5
6
7
8
9
10
11
12
13
14
15
16
17
18
19
20
21
22
23
24
25
26
27
28
29
30
31

Fig. A-98-3-0

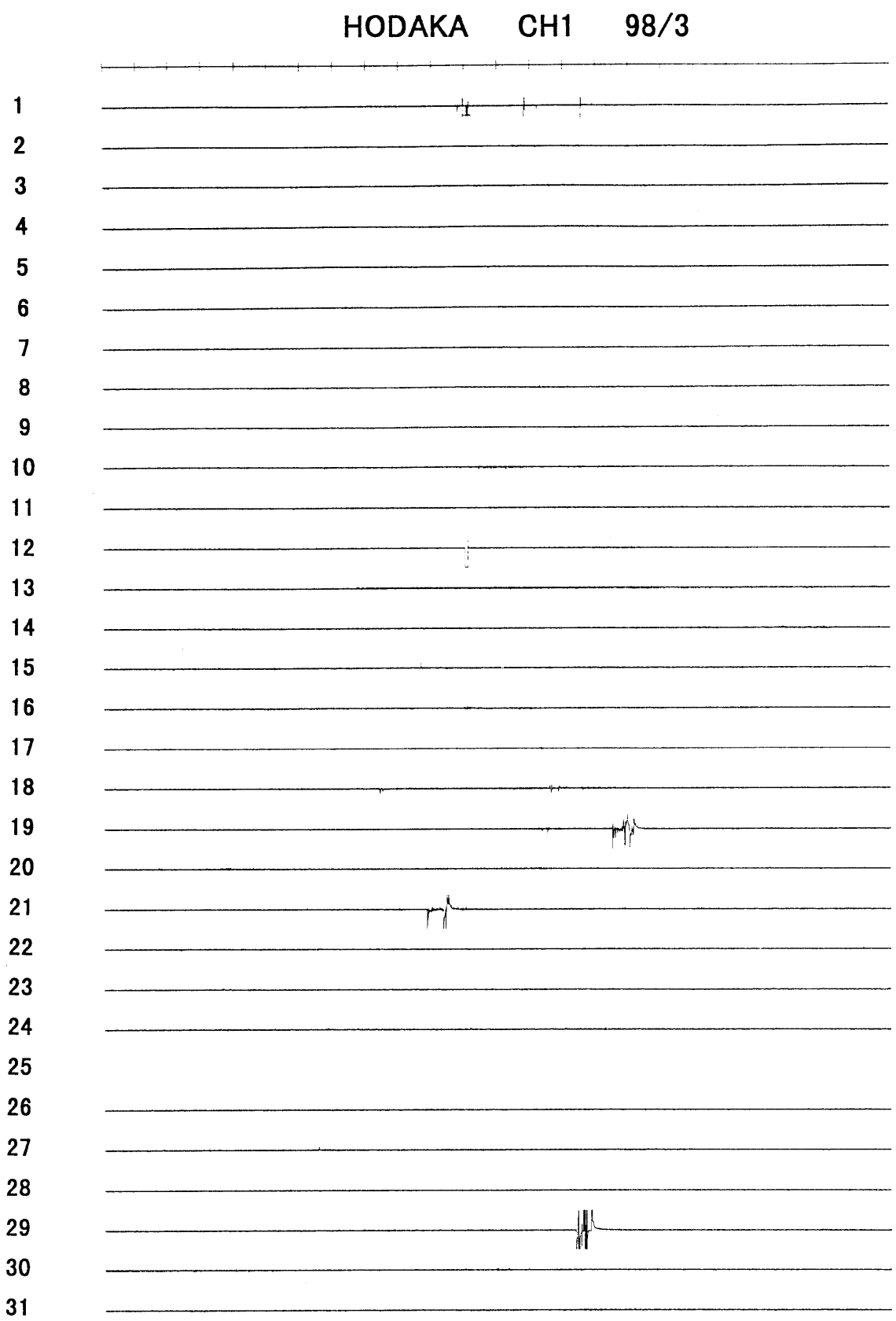
HODAKA CH1 98/3
1
2
3
4
5
6
7
8
9
10
11
12
13
14
15
16
17
18
19
20
21
22
23
24
25
26
27
28
29
30
31

Fig. A-98-3-1

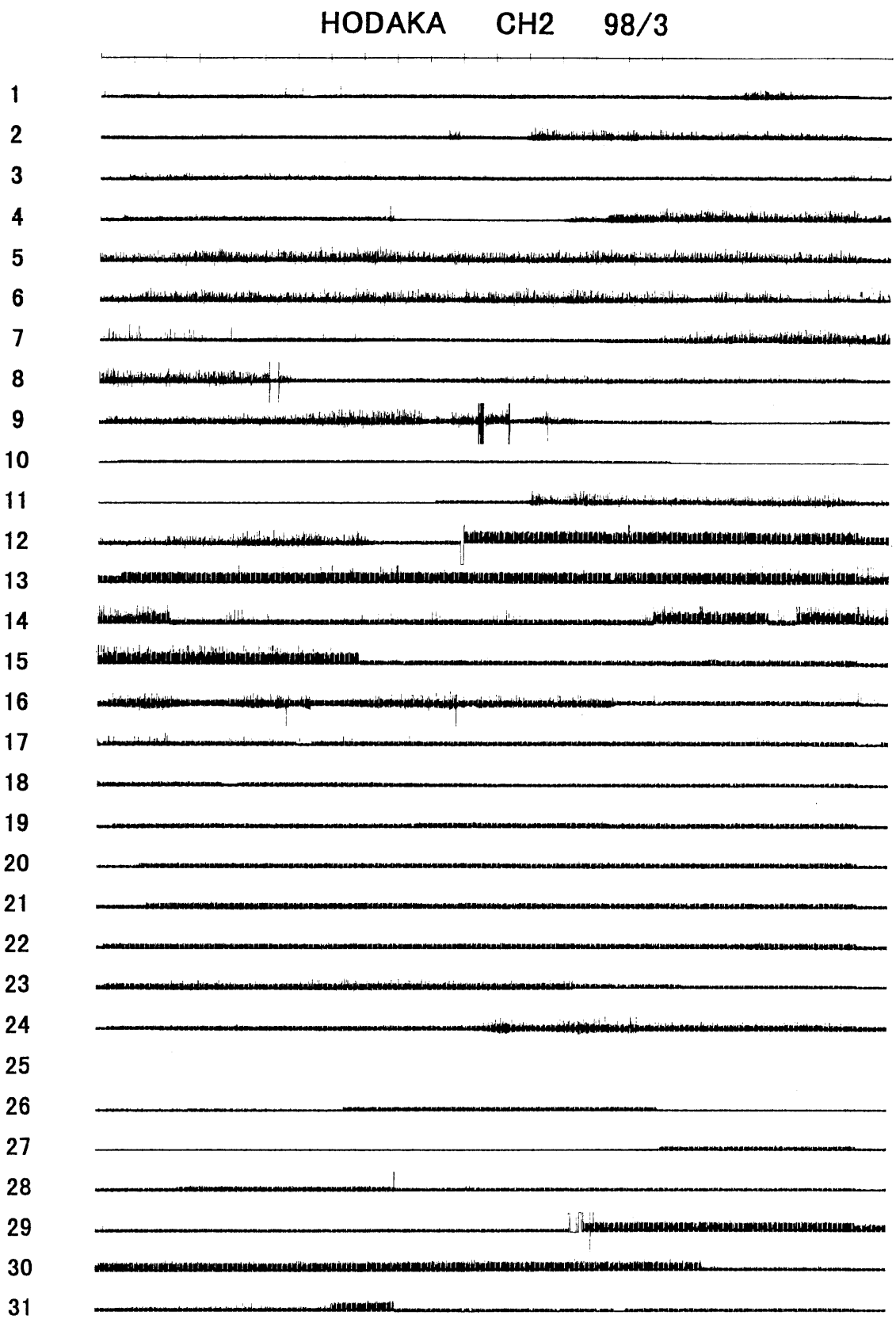
HODAKA CH2 98/3
1
2
3
4
5
6
7
8
9
10
11
12
13
14
15
16
17
18
19
20
21
22
23
24
25
26
27
28
29
30
31

Fig. A-98-3-2

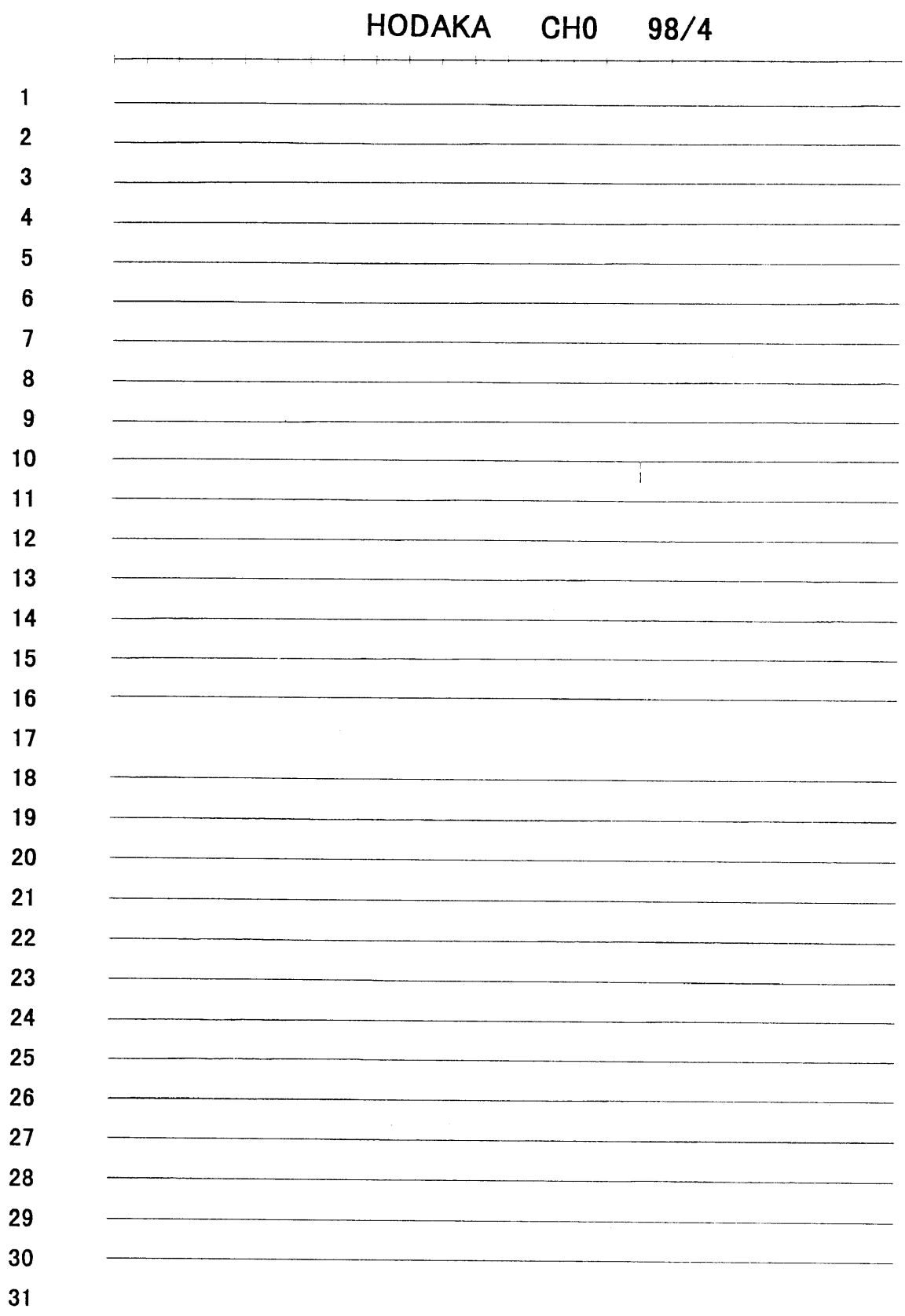
HODAKA CH0 98/4
1
2
3
4
5
6
7
8
9
10
11
12
13
14
15
16
17
18
19
20
21
22
23
24
25
26
27
28
29
30
31

Fig. A-98-4-0

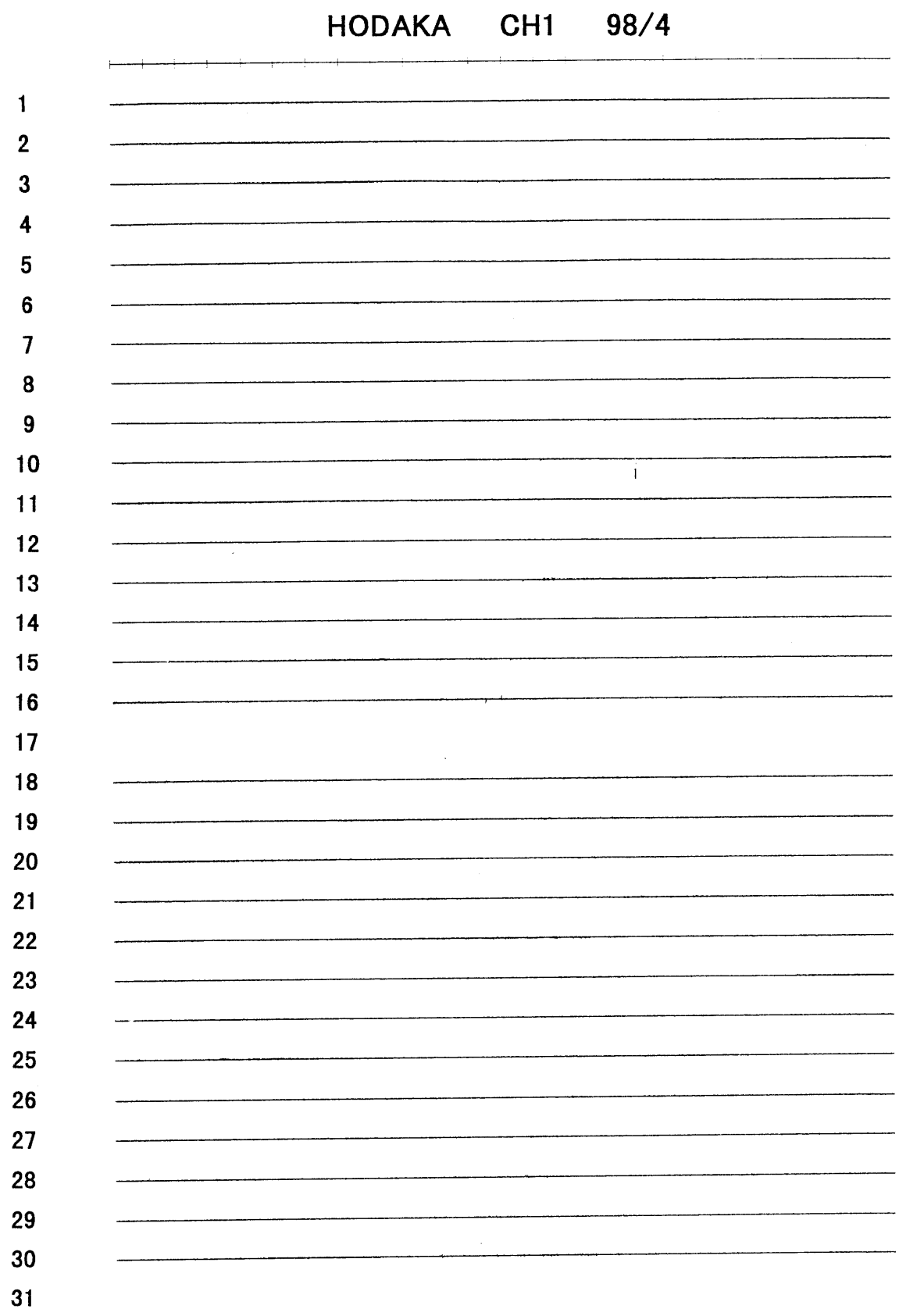
HODAKA CH1 98/4
1
2
3
4
5
6
7
8
9
10
11
12
13
14
15
16
17
18
19
20
21
22
23
24
25
26
27
28
29
30
31

Fig. A-98-4-1

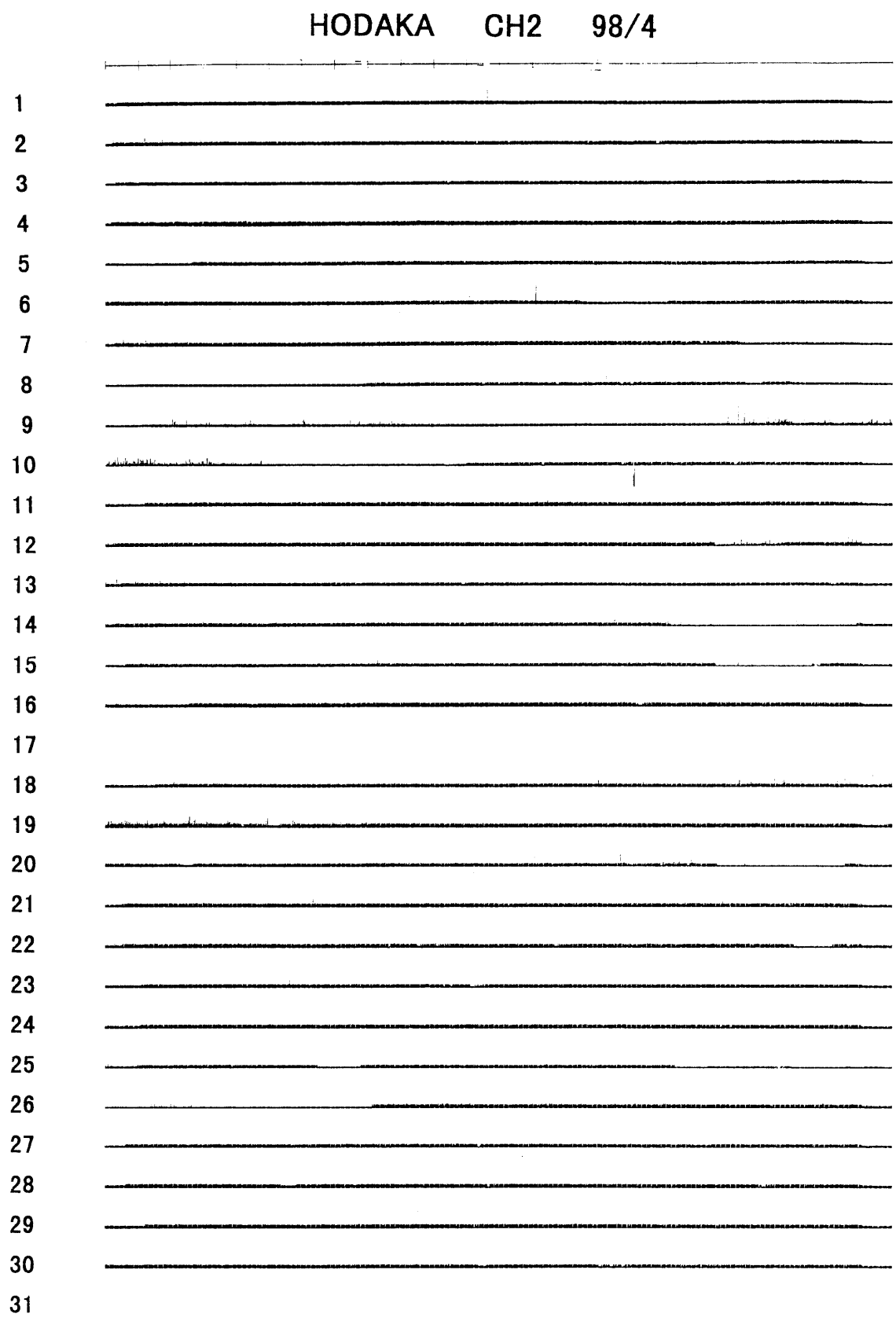
HODAKA CH2 98/4
1
2
3
4
5
6
7
8
9
10
11
12
13
14
15
16
17
18
19
20
21
22
23
24
25
26
27
28
29
30
31

Fig. A-98-4-2

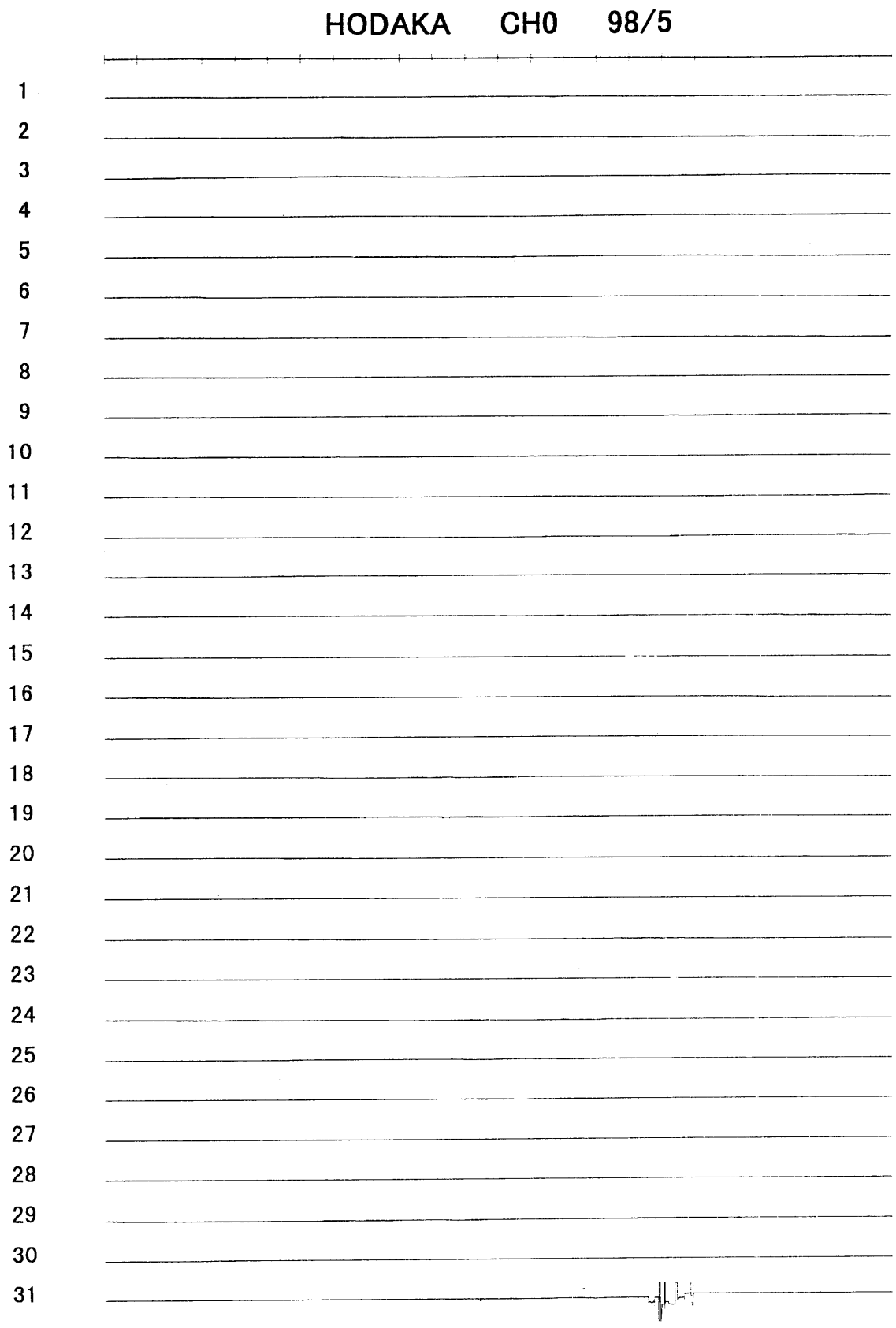
HODAKA CH0 98/5
1
2
3
4
5
6
7
8
9
10
11
12
13
14
15
16
17
18
19
20
21
22
23
24
25
26
27
28
29
30
31

Fig. A-98-5-0

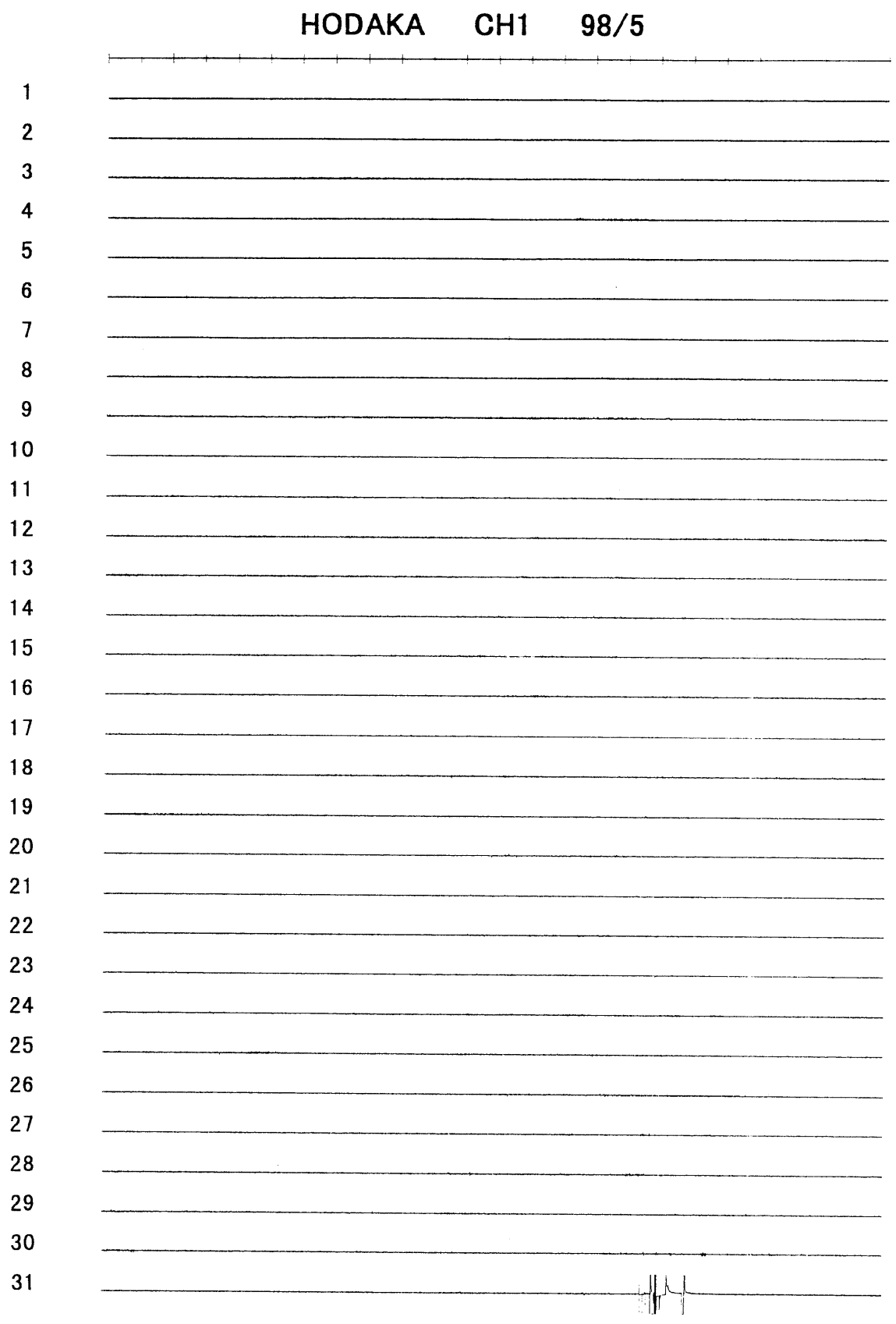
HODAKA CH1 98/5
1
2
3
4
5
6
7
8
9
10
11
12
13
14
15
16
17
18
19
20
21
22
23
24
25
26
27
28
29
30
31

Fig. A-98-5-1

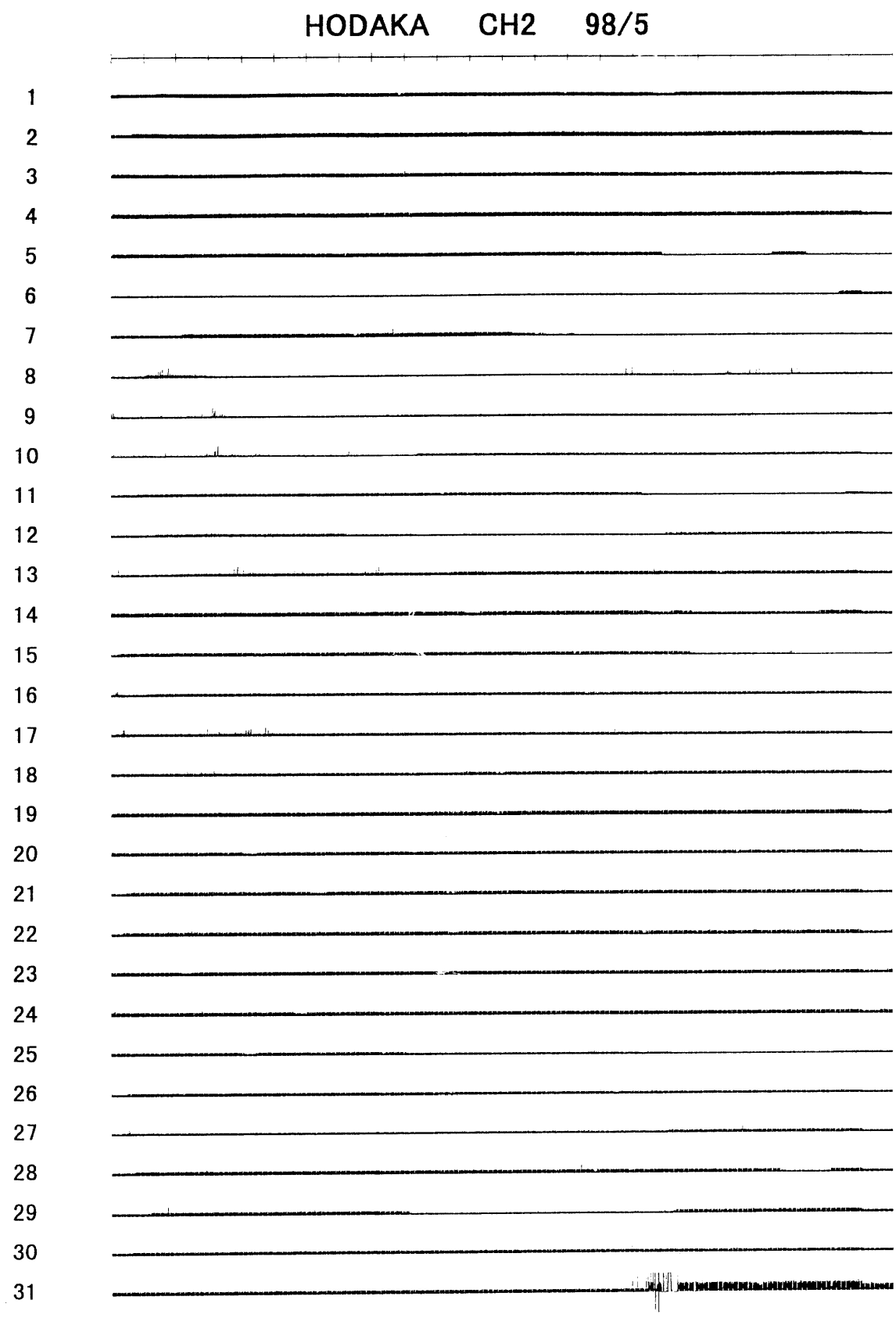
HODAKA CH2 98/5
1
2
3
4
5
6
7
8
9
10
11
12
13
14
15
16
17
18
19
20
21
22
23
24
25
26
27
28
29
30
31

Fig. A-98-5-2

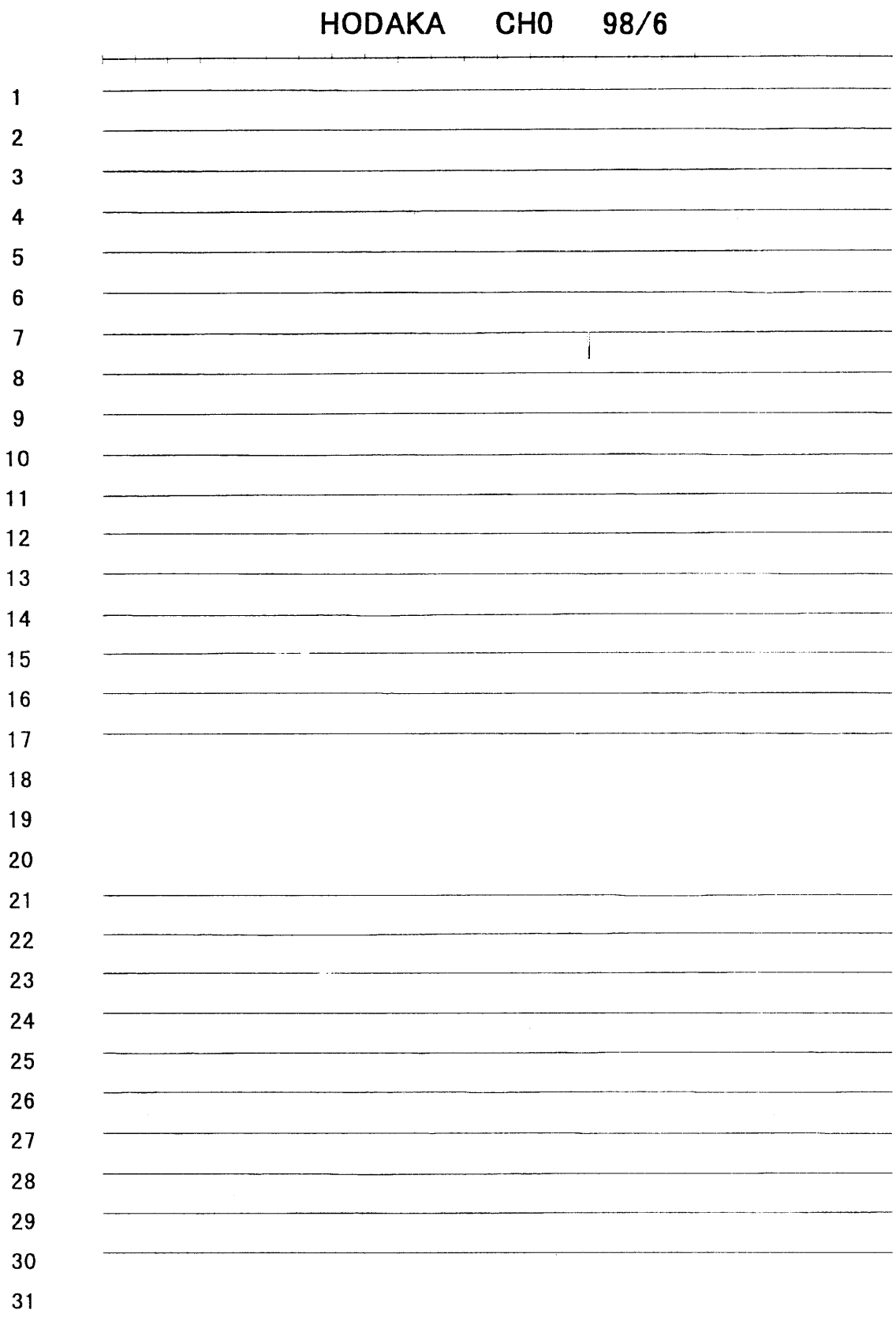
HODAKA CH0 98/6
1
2
3
4
5
6
7
8
9
10
11
12
13
14
15
16
17
18
19
20
21
22
23
24
25
26
27
28
29
30
31

Fig. A-98-6-0

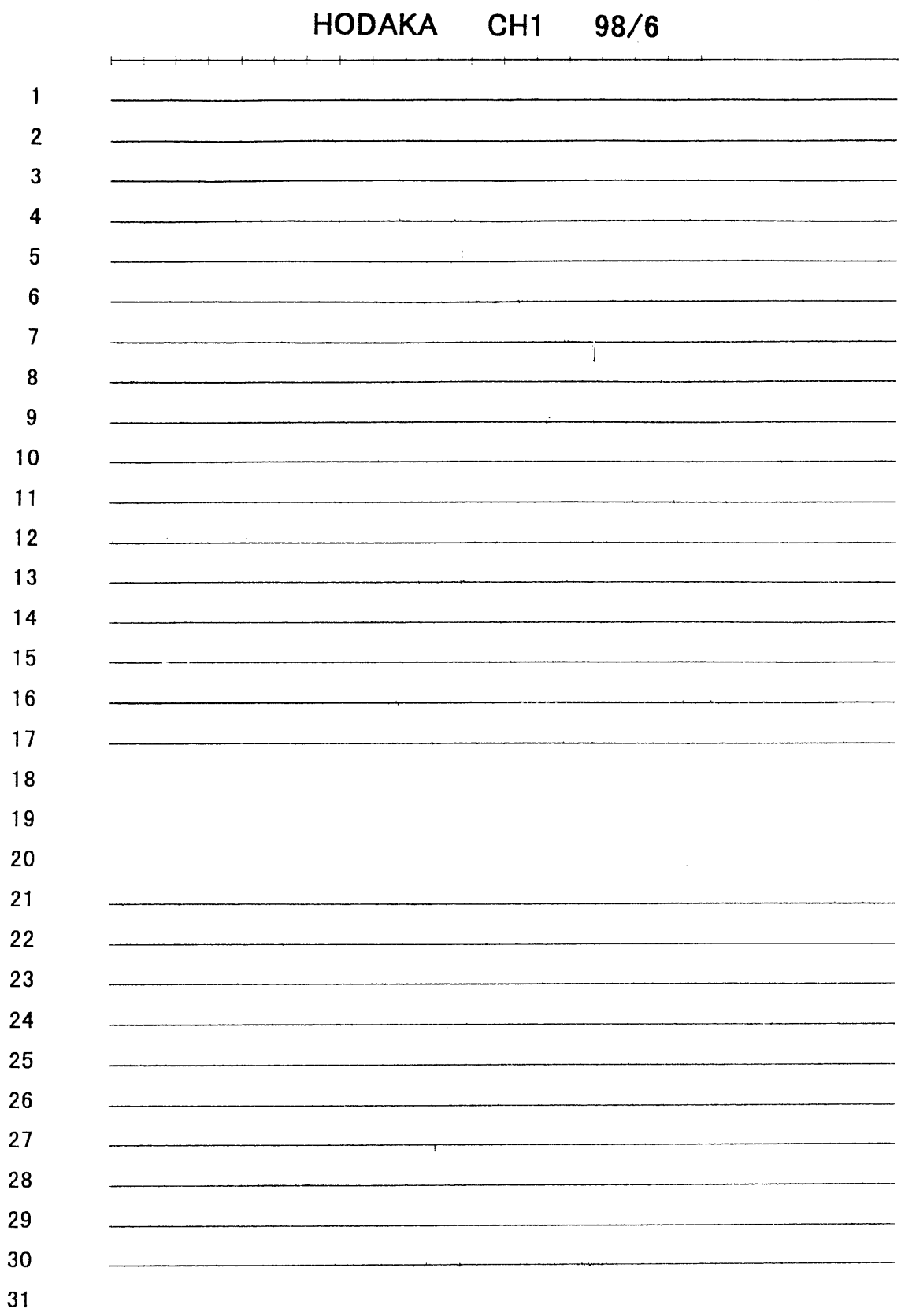
HODAKA CH1 98/6
1
2
3
4
5
6
7
8
9
10
11
12
13
14
15
16
17
18
19
20
21
22
23
24
25
26
27
28
29
30
31

Fig. A-98-6-1

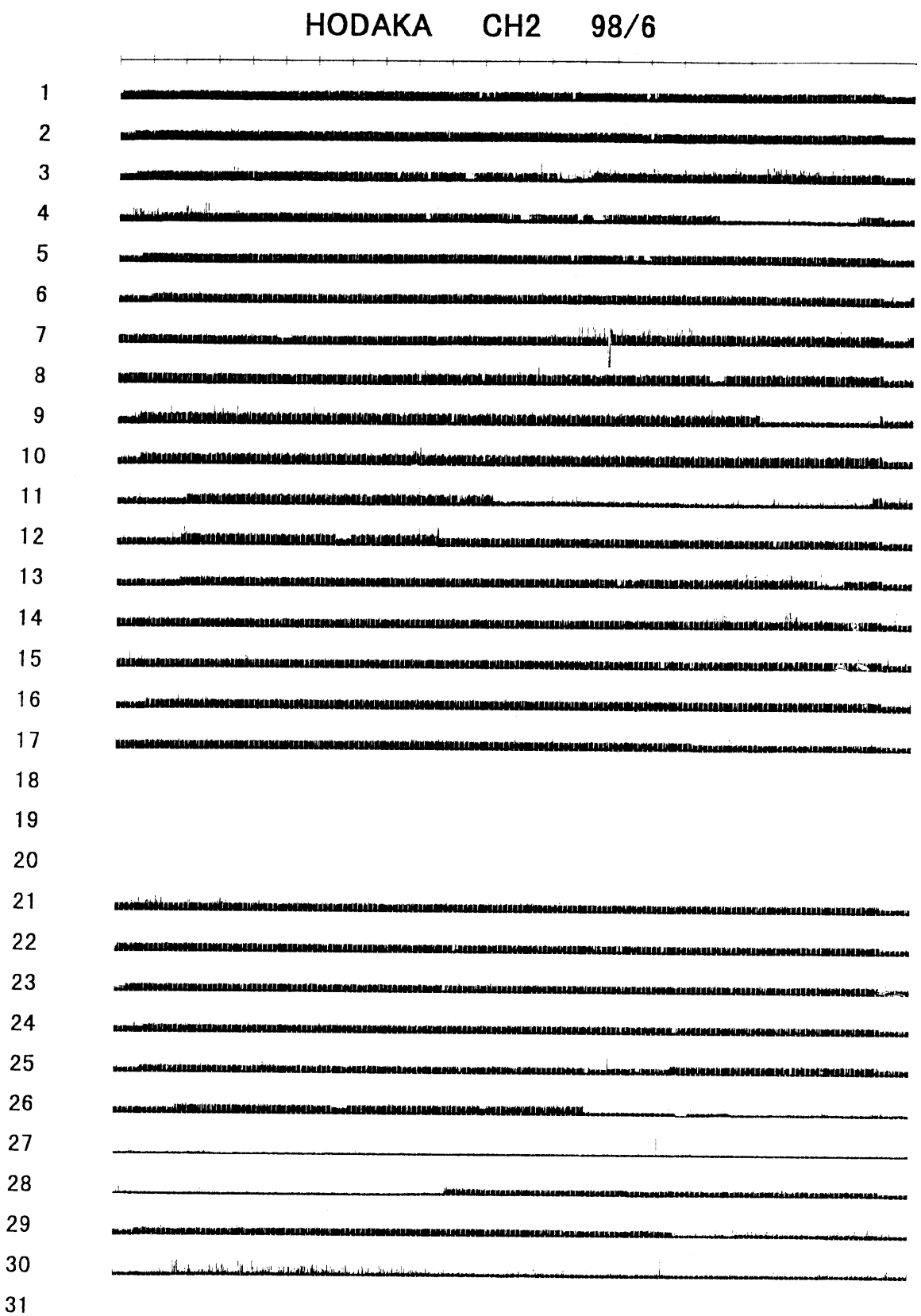
HODAKA CH2 98/6
1
2
3
4
5
6
7
8
9
10
11
12
13
14
15
16
17
18
19
20
21
22
23
24
25
26
27
28
29
30
31

Fig. A-98-6-2

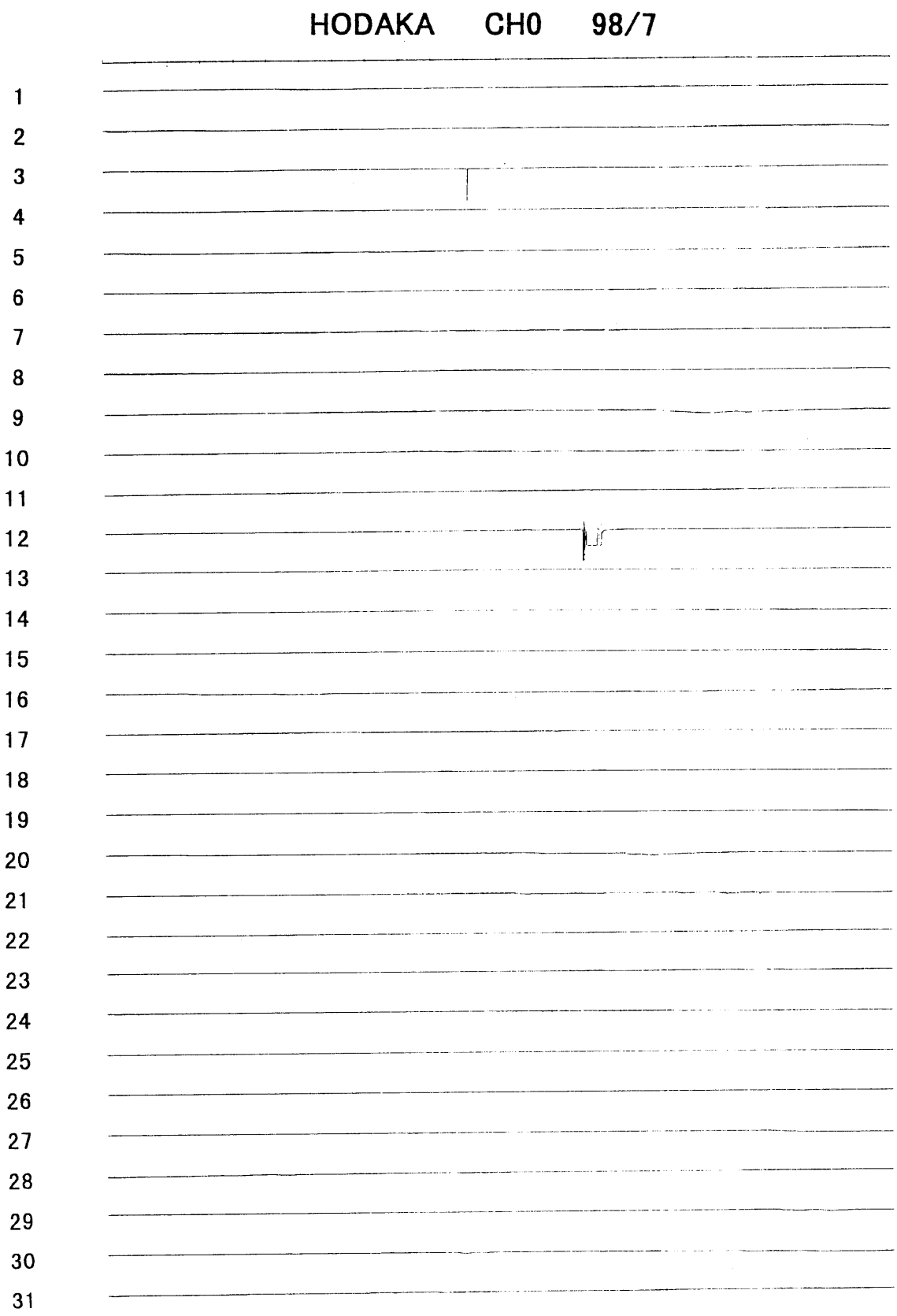
HODAKA CH0 98/7
1
2
3
4
5
6
7
8
9
10
11
12
13
14
15
16
17
18
19
20
21
22
23
24
25
26
27
28
29
30
31

Fig. A-98-7-0

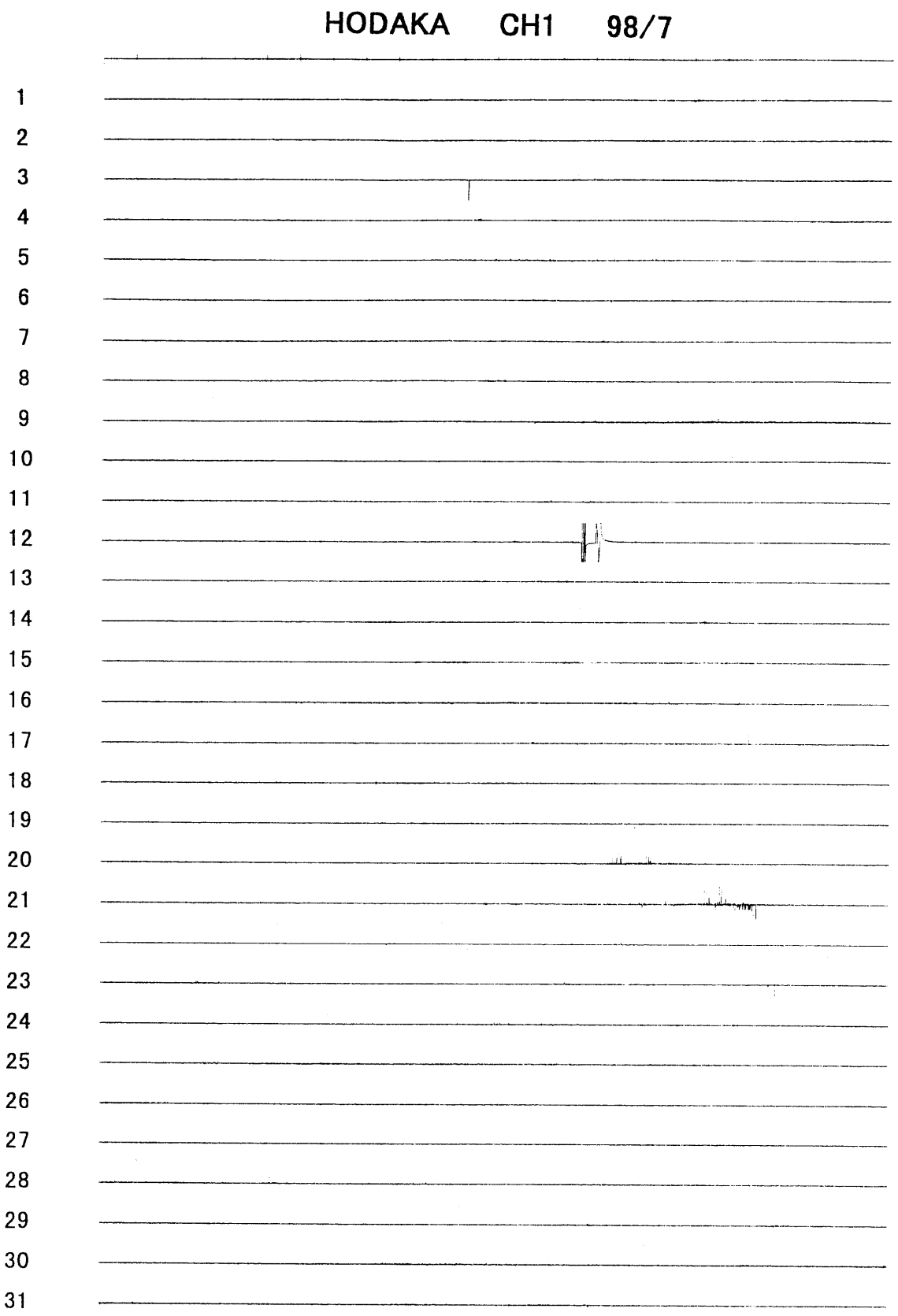
HODAKA CH1 98/7
1
2
3
4
5
6
7
8
9
10
11
12
13
14
15
16
17
18
19
20
21
22
23
24
25
26
27
28
29
30
31

Fig. A-98-7-1

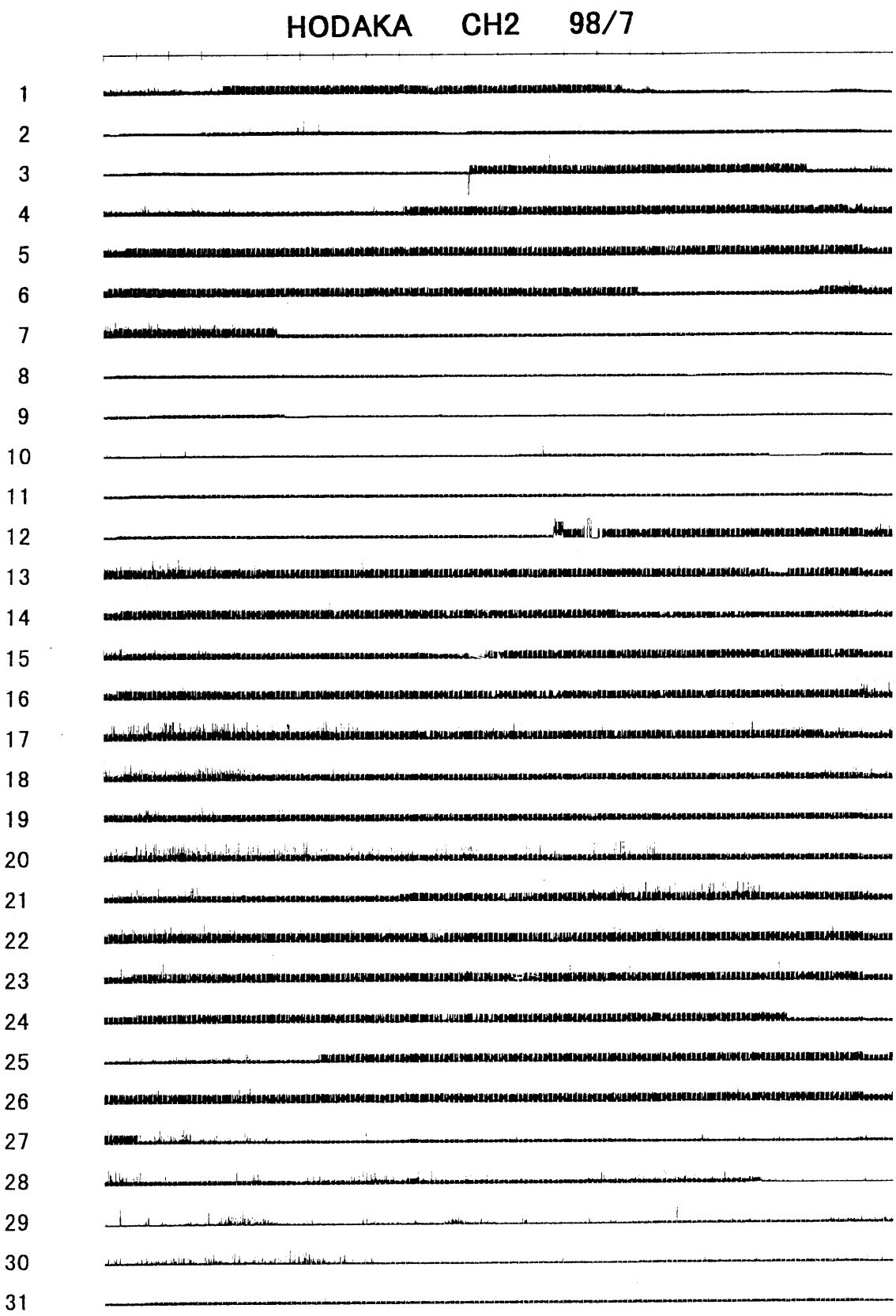
HODAKA CH2 98/7
1
2
3
4
5
6
7
8
9
10
11
12
13
14
15
16
17
18
19
20
21
22
23
24
25
26
27
28
29
30
31

Fig. A-98-7-2

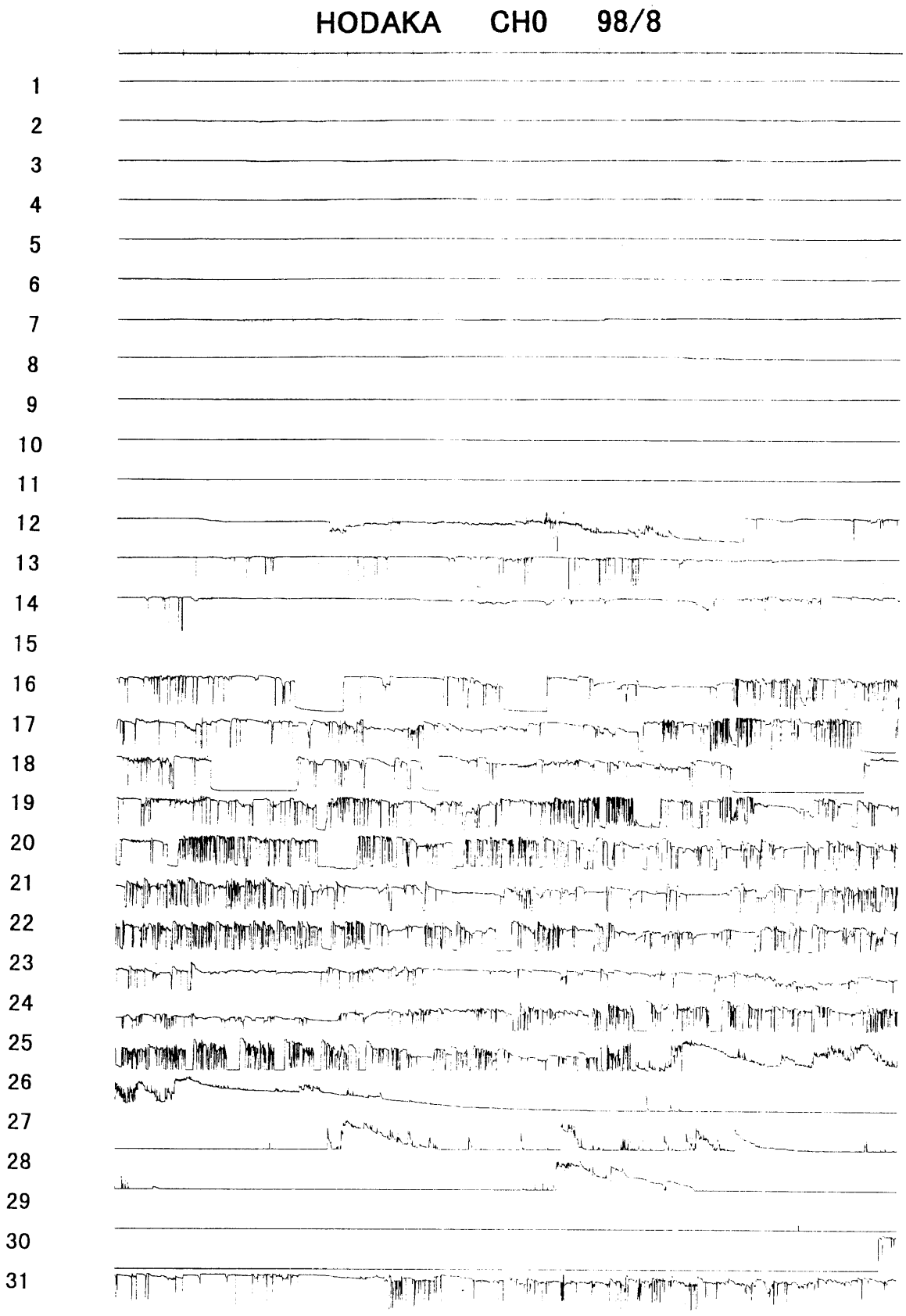
HODAKA CH0 98/8
1
2
3
4
5
6
7
8
9
10
11
12
13
14
15
16
17
18
19
20
21
22
23
24
25
26
27
28
29
30
31

Fig. A-98-8-0

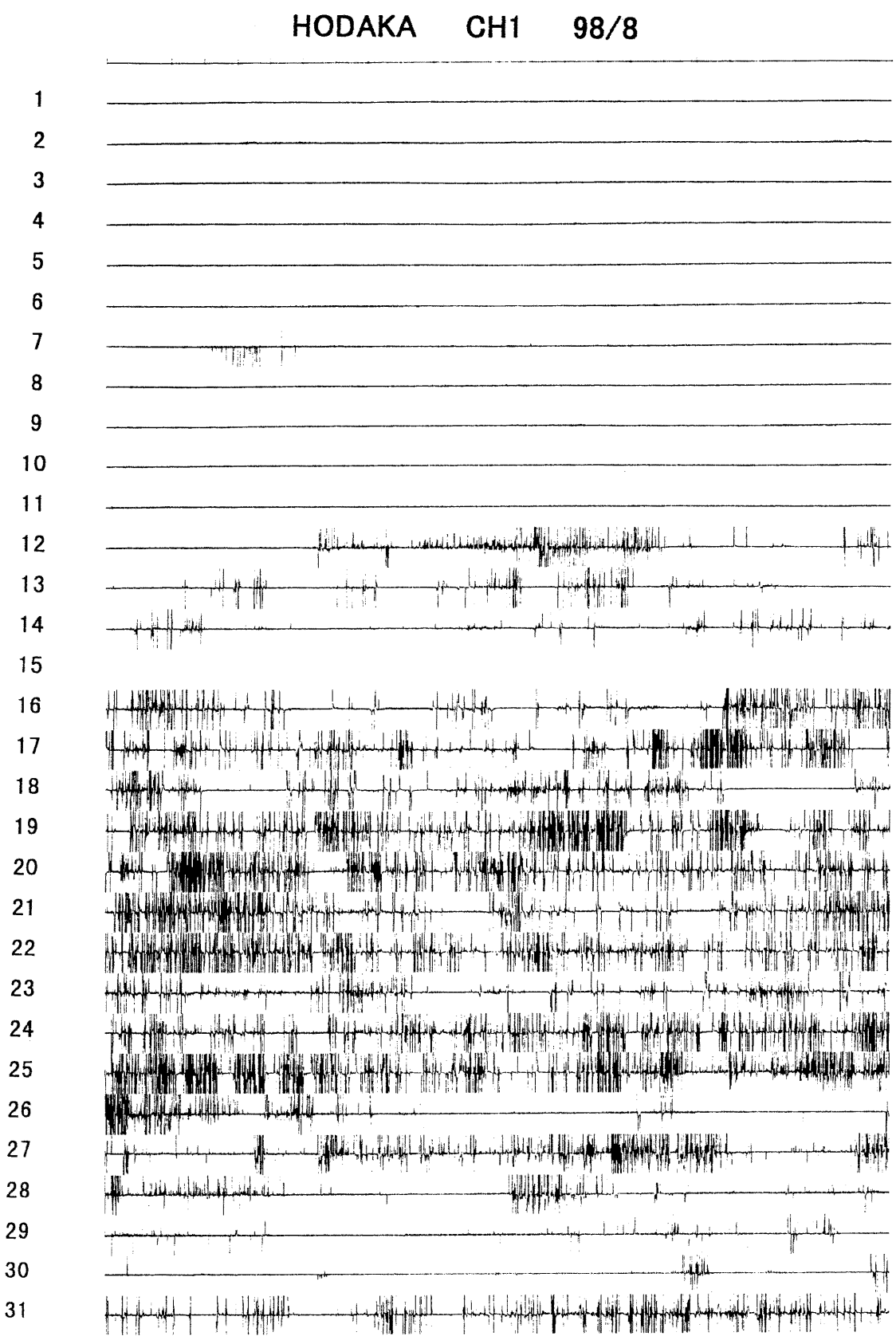
HODAKA CH1 98/8
1
2
3
4
5
6
7
8
9
10
11
12
13
14
15
16
17
18
19
20
21
22
23
24
25
26
27
28
29
30
31

Fig. A-98-8-1

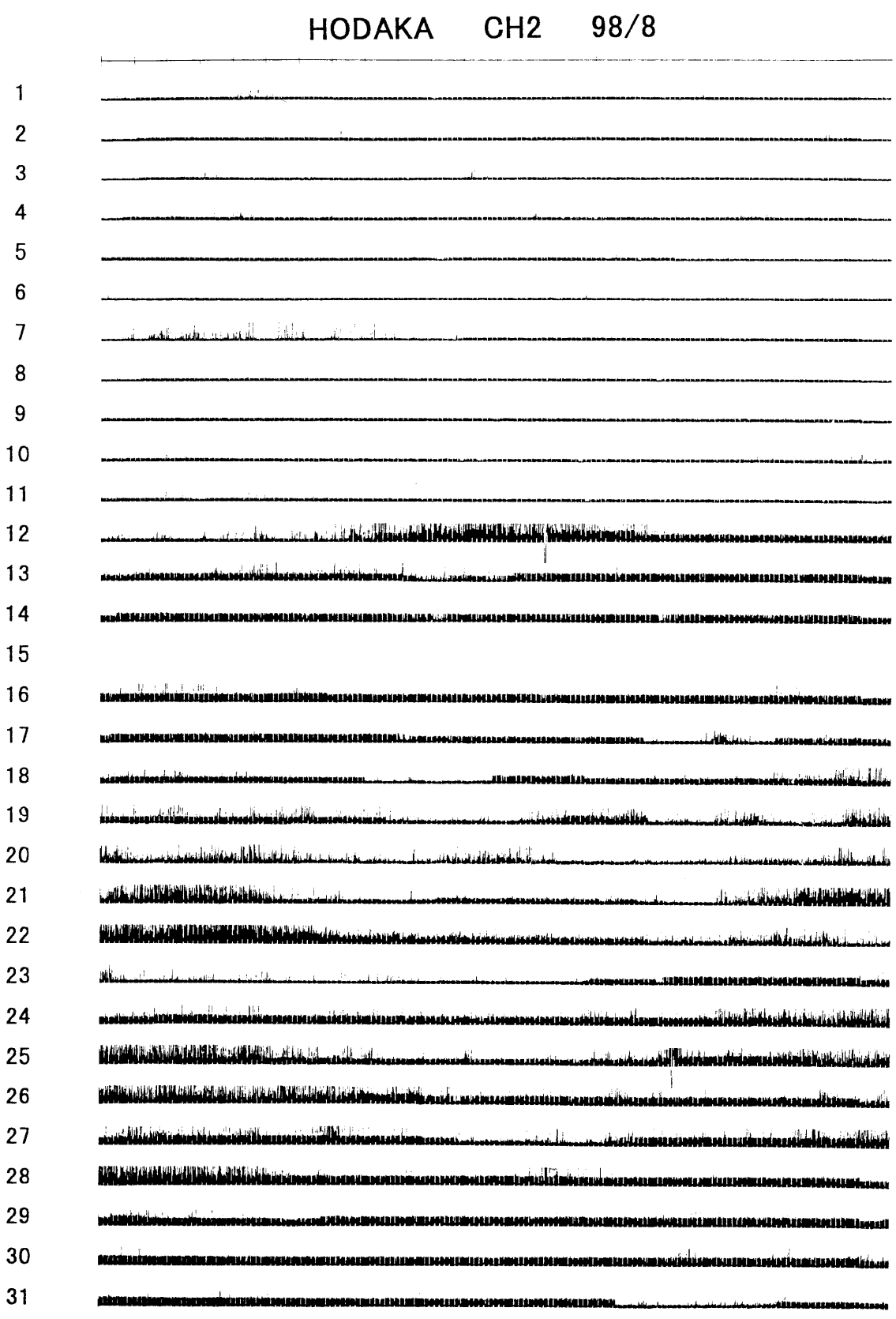
HODAKA CH2 98/8
1
2
3
4
5
6
7
8
9
10
11
12
13
14
15
16
17
18
19
20
21
22
23
24
25
26
27
28
29
30
31

Fig. A-98-8-2

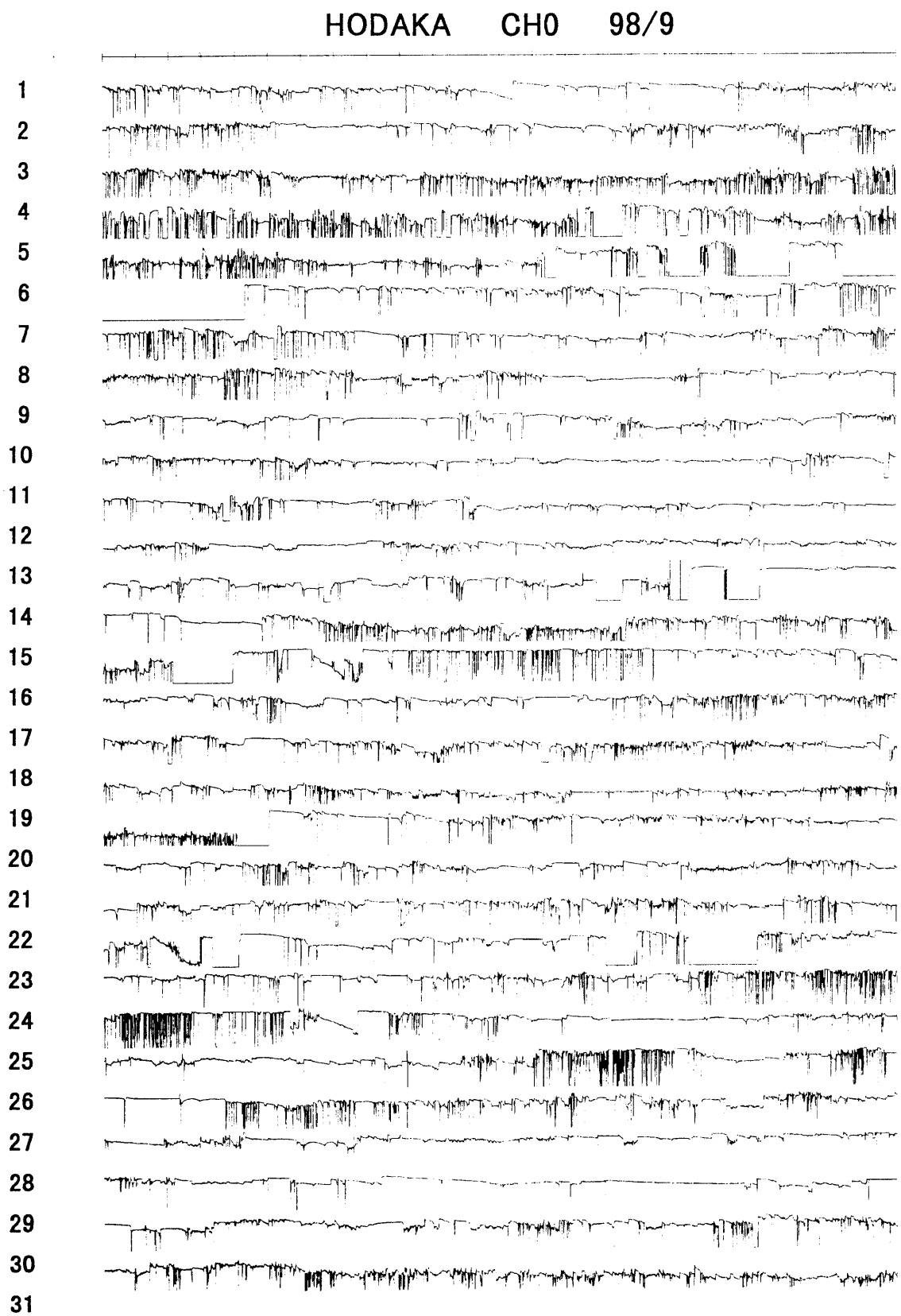
HODAKA CH0 98/9
1
2
3
4
5
6
7
8
9
10
11
12
13
14
15
16
17
18
19
20
21
22
23
24
25
26
27
28
29
30
31

Fig. A-98-9-0

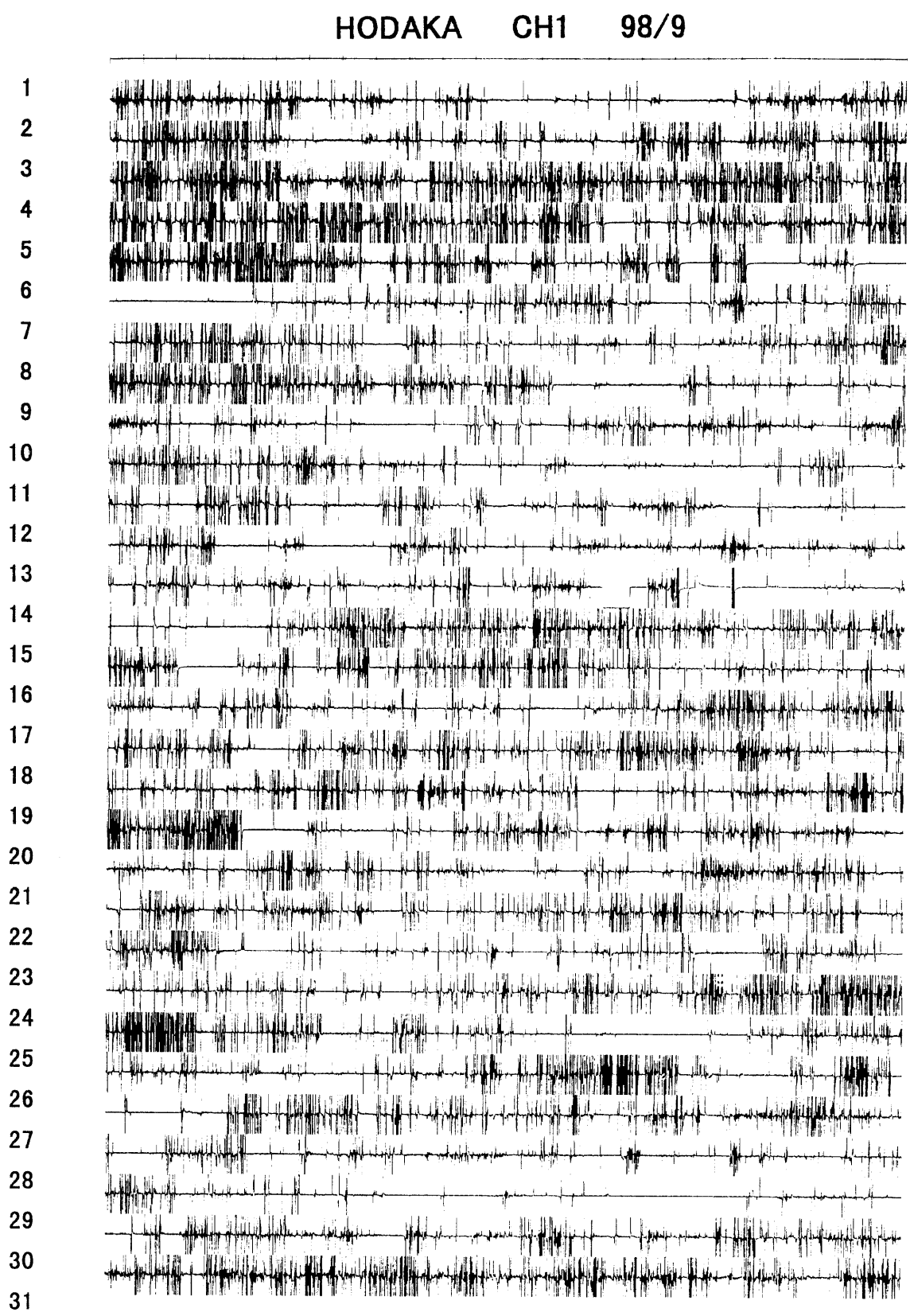
HODAKA CH1 98/9
1
2
3
4
5
6
7
8
9
10
11
12
13
14
15
16
17
18
19
20
21
22
23
24
25
26
27
28
29
30
31

Fig. A-98-9-1

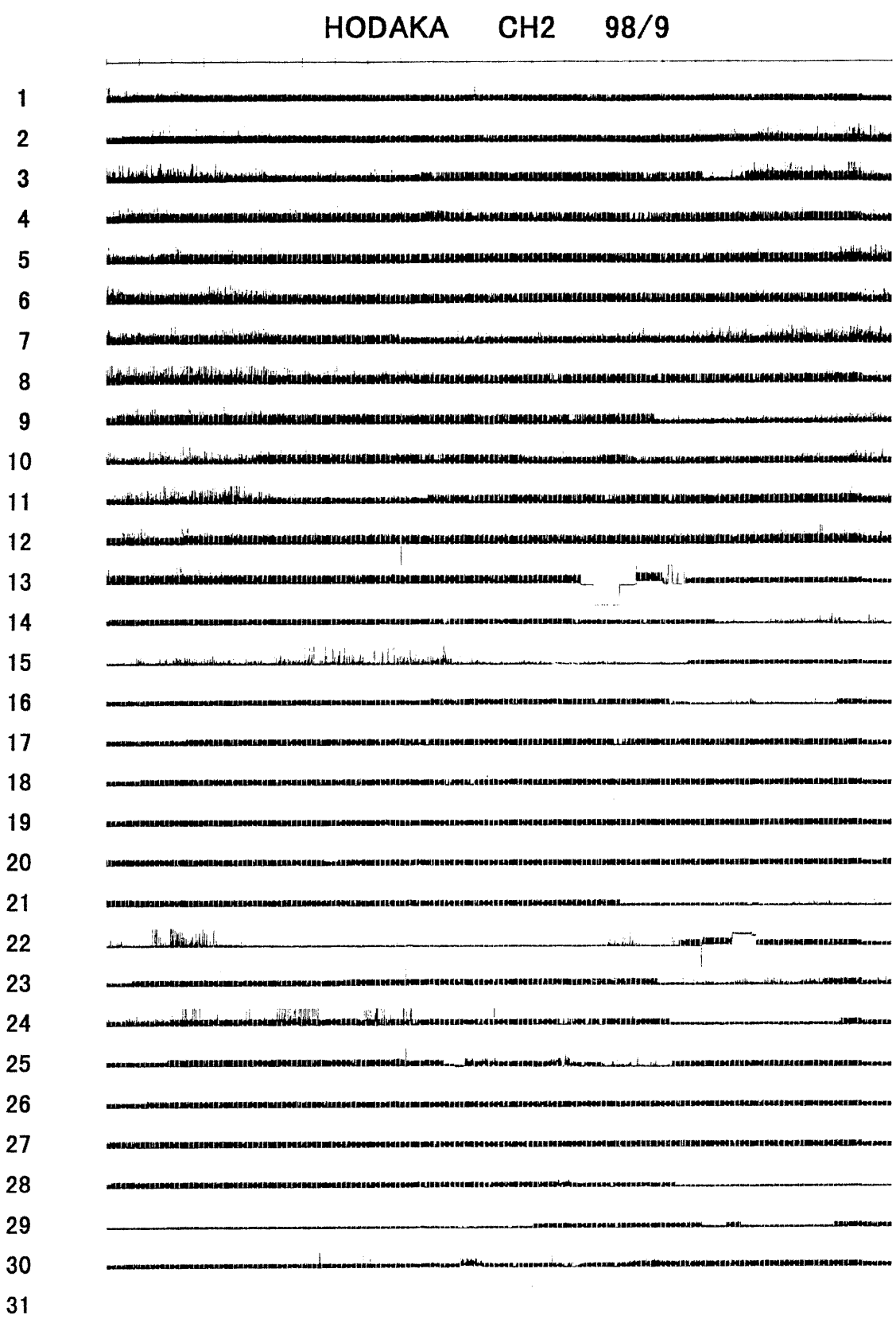
HODAKA CH2 98/9
1
2
3
4
5
6
7
8
9
10
11
12
13
14
15
16
17
18
19
20
21
22
23
24
25
26
27
28
29
30
31

Fig. A-98-9-2

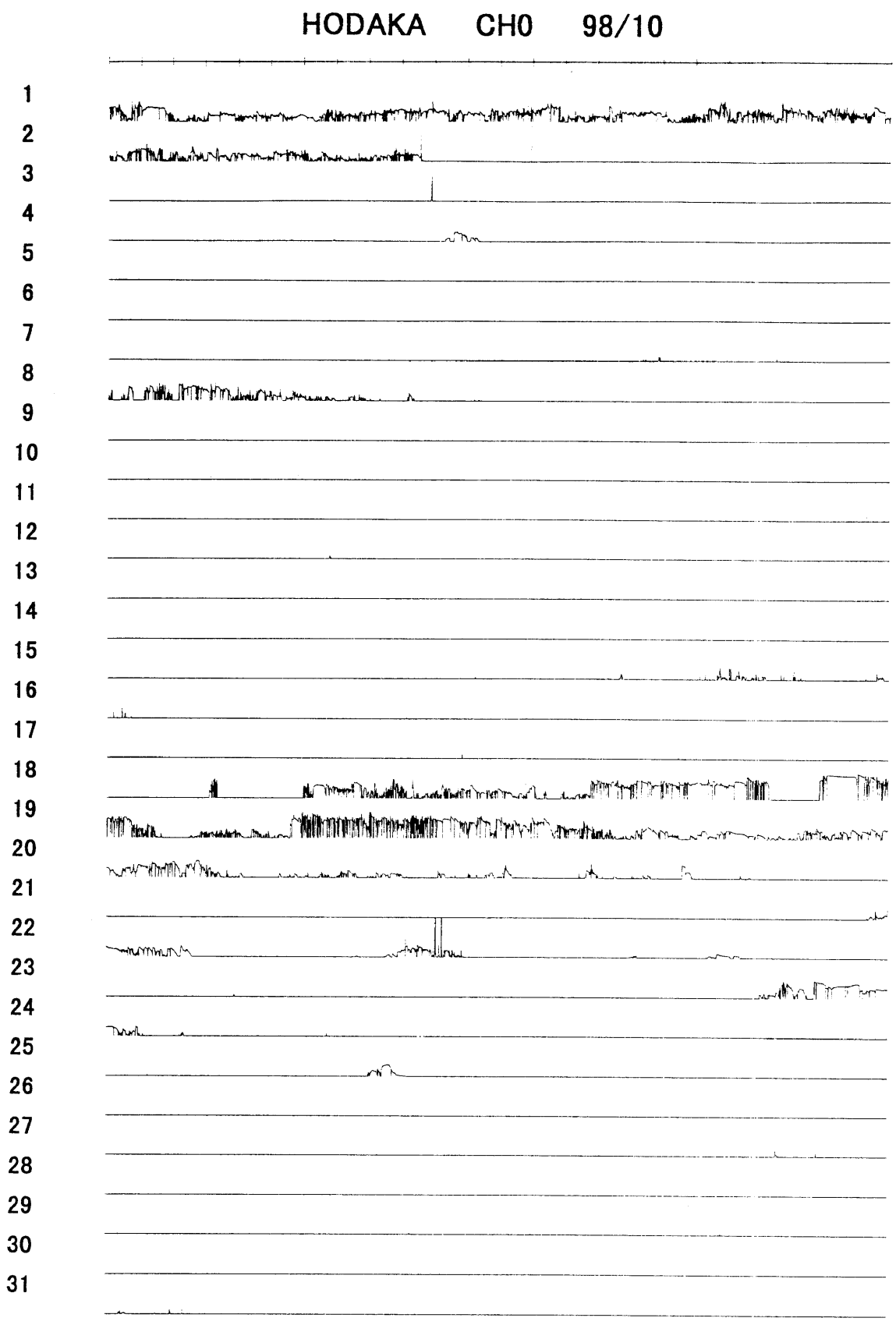
HODAKA CH0 98/10
1
2
3
4
5
6
7
8
9
10
11
12
13
14
15
16
17
18
19
20
21
22
23
24
25
26
27
28
29
30
31

Fig. A-98-10-0

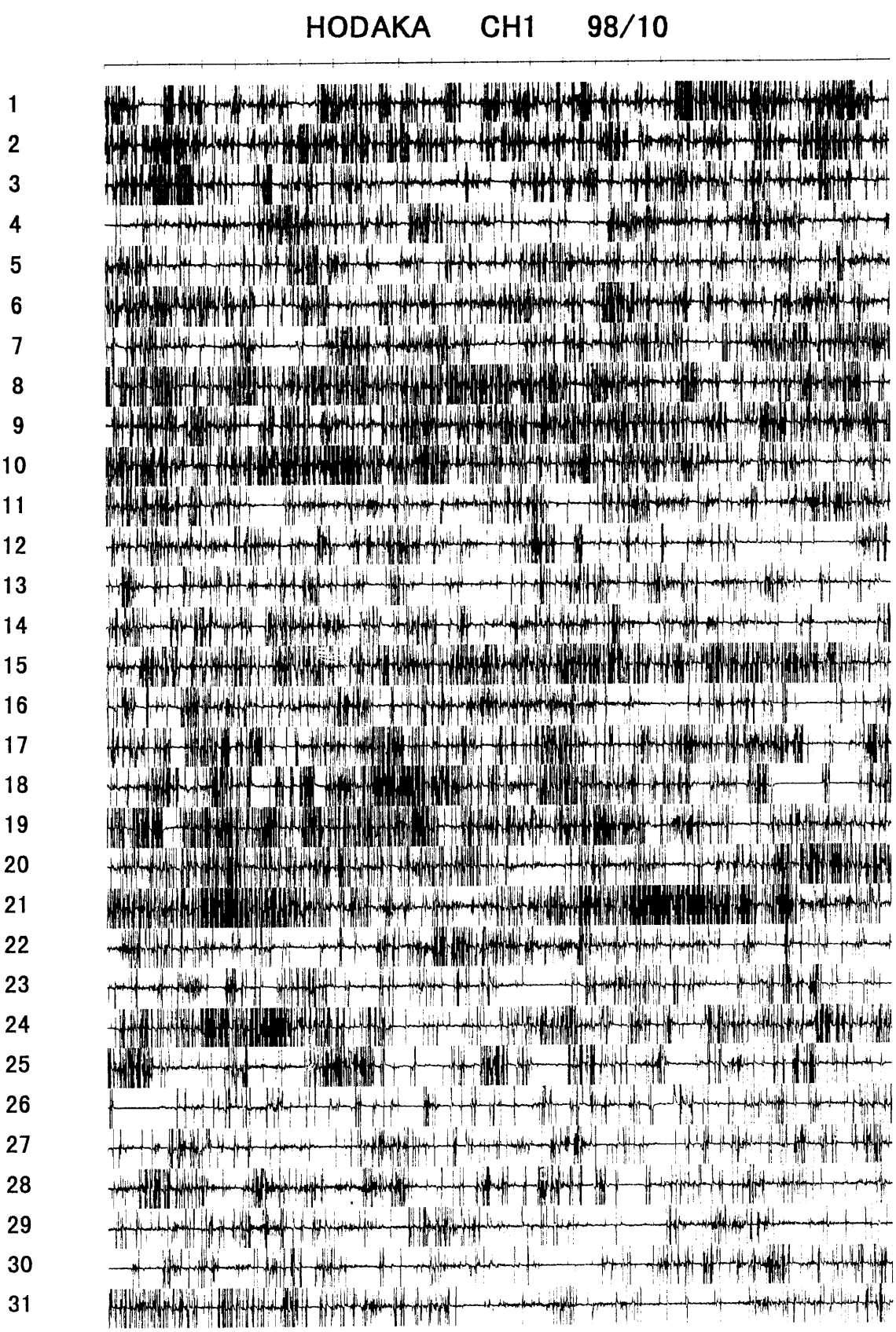
HODAKA CH1 98/10
1
2
3
4
5
6
7
8
9
10
11
12
13
14
15
16
17
18
19
20
21
22
23
24
25
26
27
28
29
30
31

Fig. A-98-10-1

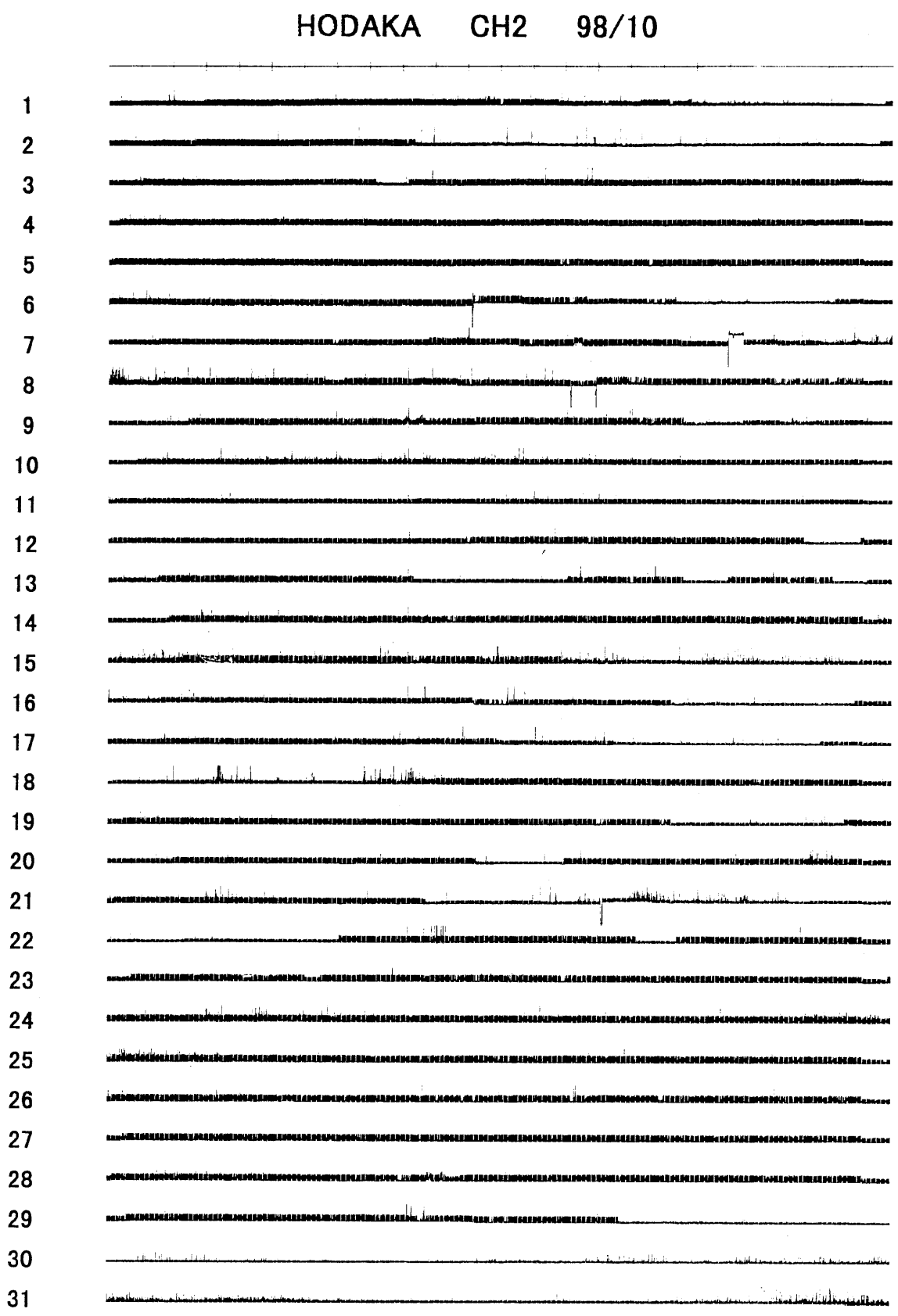
HODAKA CH2 98/10
1
2
3
4
5
6
7
8
9
10
11
12
13
14
15
16
17
18
19
20
21
22
23
24
25
26
27
28
29
30
31

Fig. A-98-10-2

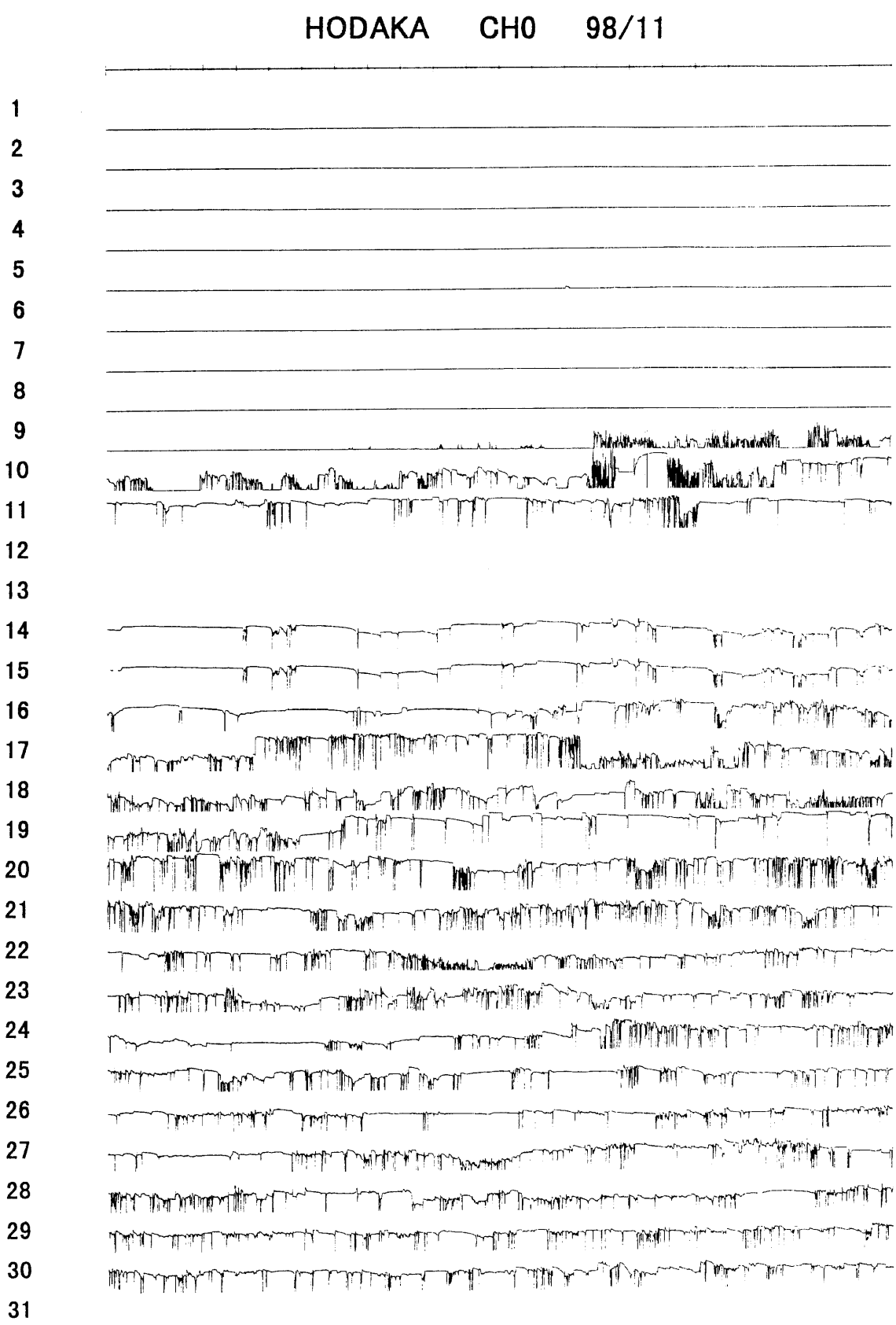
HODAKA CH0 98/11
1
2
3
4
5
6
7
8
9
10
11
12
13
14
15
16
17
18
19
20
21
22
23
24
25
26
27
28
29
30
31

Fig. A-98-11-0

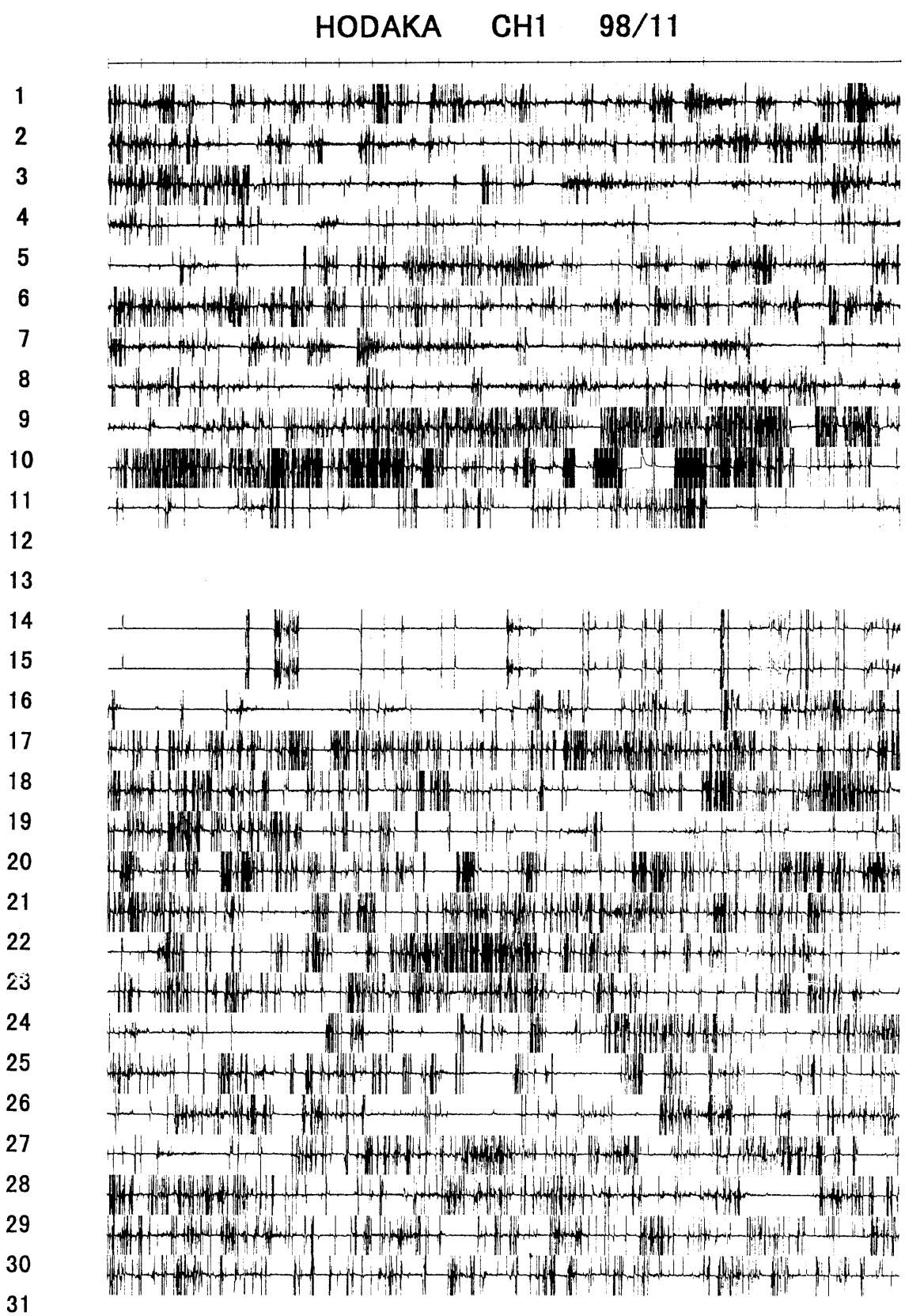
HODAKA CH1 98/11
1
2
3
4
5
6
7
8
9
10
11
12
13
14
15
16
17
18
19
20
21
22
23
24
25
26
27
28
29
30
31

Fig. A-98-11-1

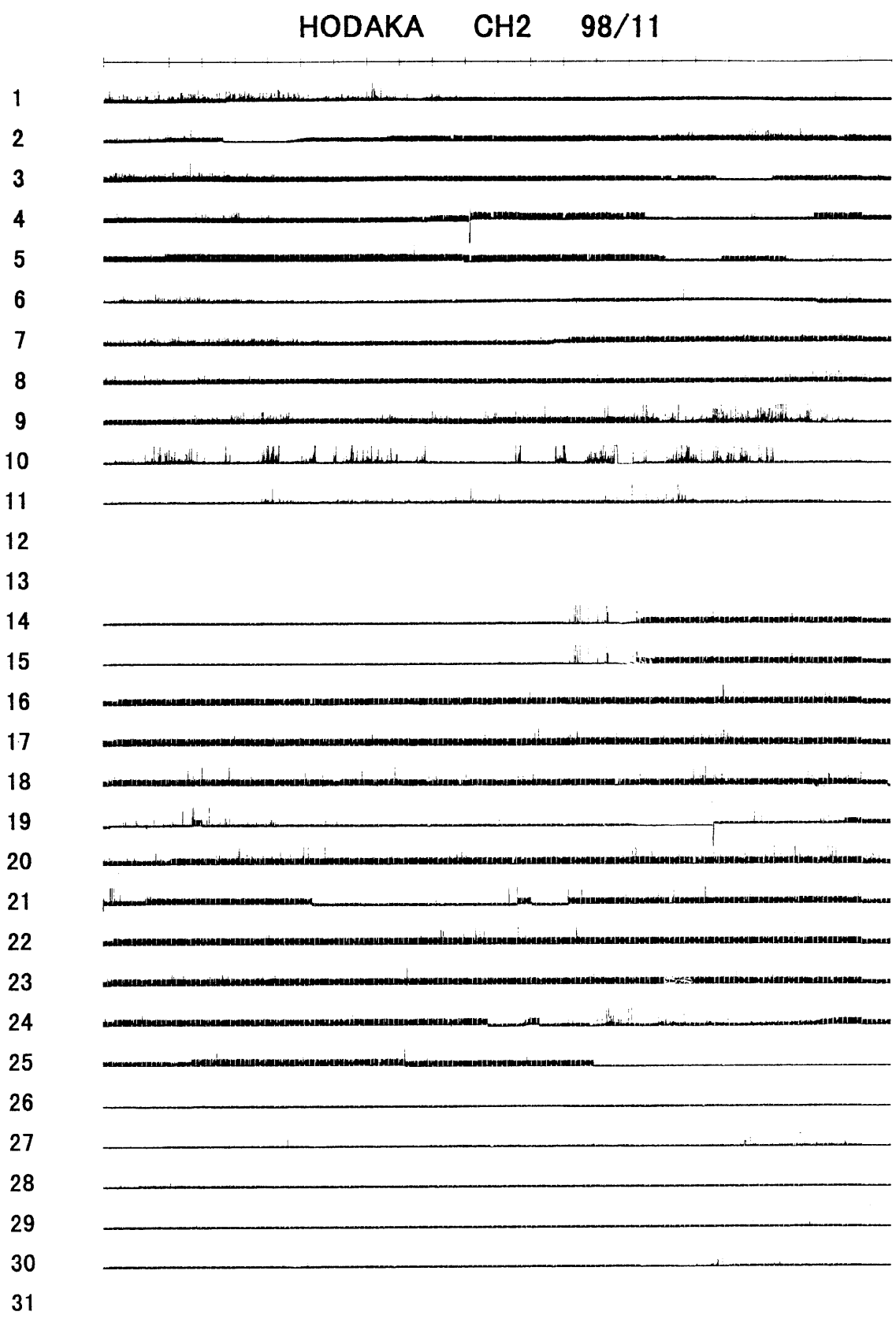
HODAKA CH2 98/11
1
2
3
4
5
6
7
8
9
10
11
12
13
14
15
16
17
18
19
20
21
22
23
24
25
26
27
28
29
30
31

Fig. A-98-11-2

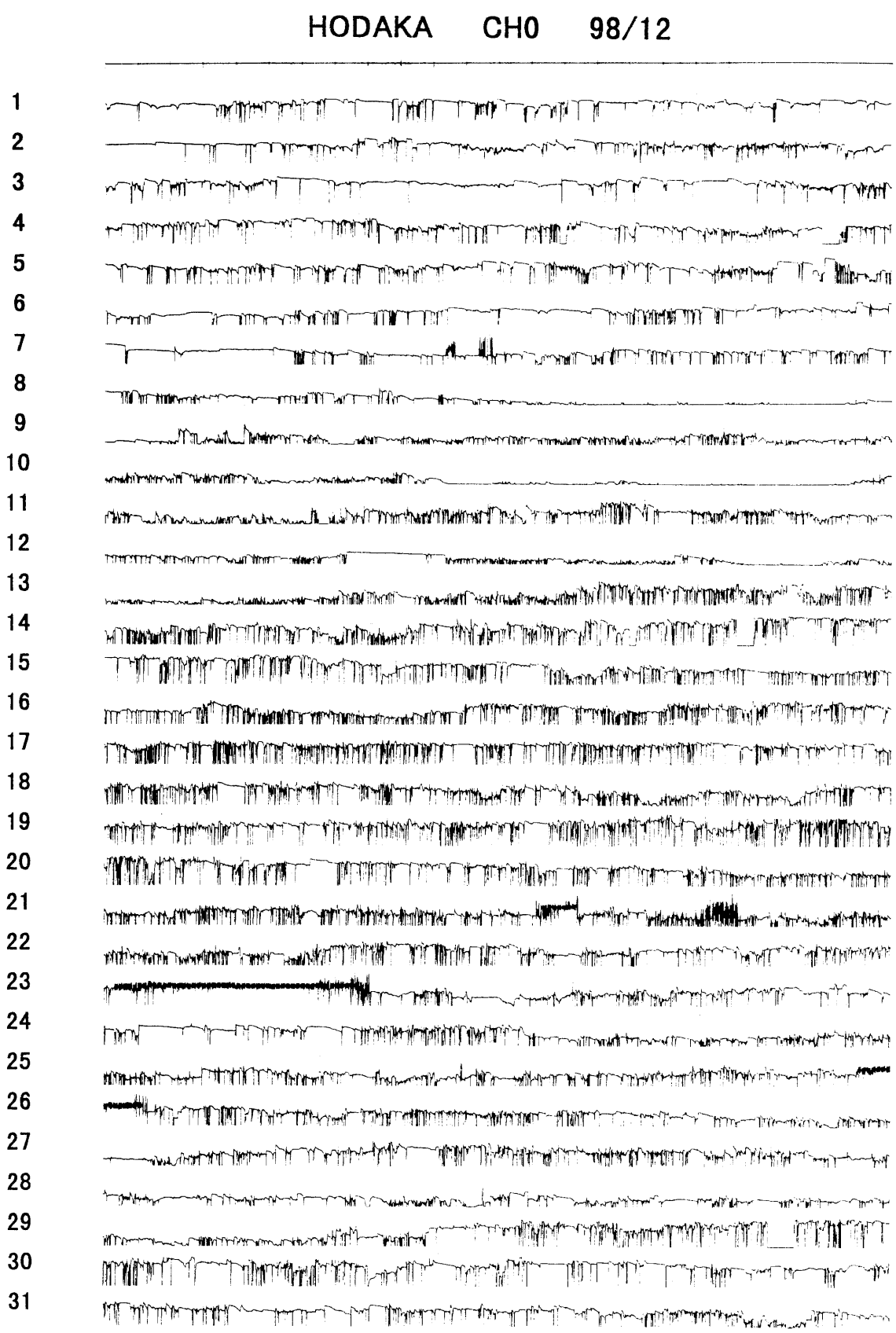
HODAKA CH0 98/12
1
2
3
4
5
6
7
8
9
10
11
12
13
14
15
16
17
18
19
20
21
22
23
24
25
26
27
28
29
30
31

Fig. A-98-12-0

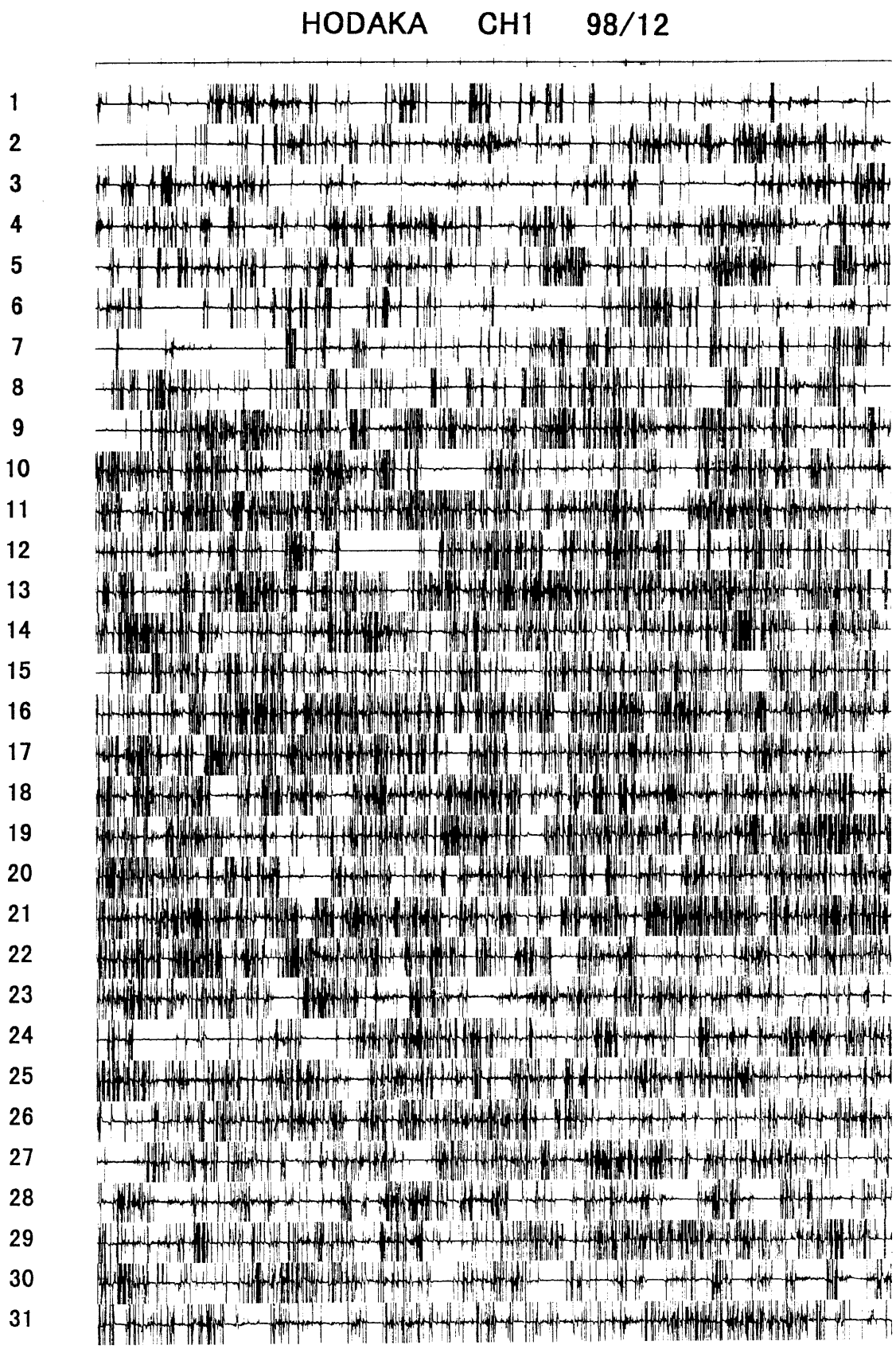
HODAKA CH1 98/12
1
2
3
4
5
6
7
8
9
10
11
12
13
14
15
16
17
18
19
20
21
22
23
24
25
26
27
28
29
30
31

Fig. A-98-12-1

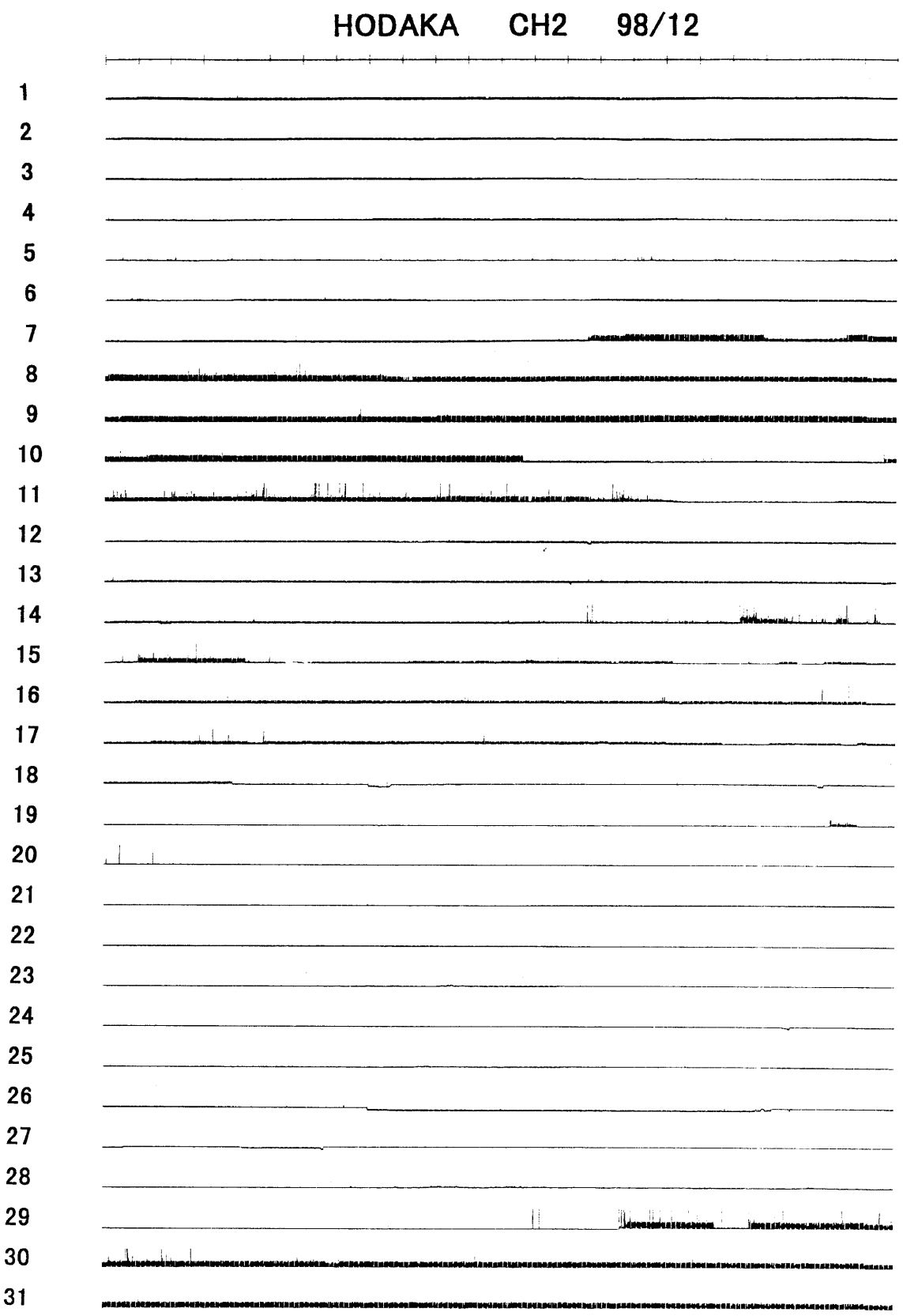
HODAKA CH2 98/12
1
2
3
4
5
6
7
8
9
10
11
12
13
14
15
16
17
18
19
20
21
22
23
24
25
26
27
28
29
30
31

Fig. A-98-12-2

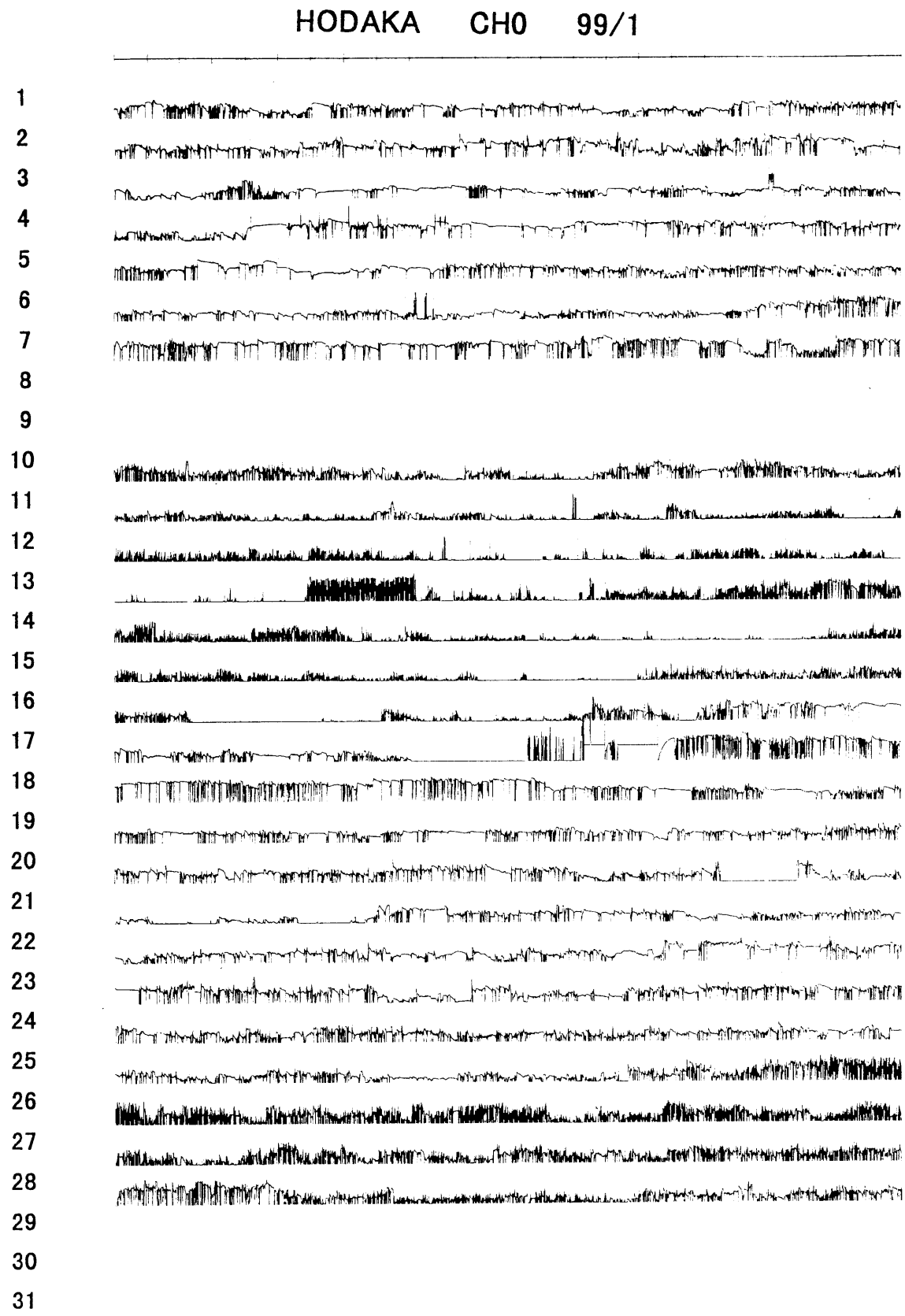
HODAKA CH0 99/1
1
2
3
4
5
6
7
8
9
10
11
12
13
14
15
16
17
18
19
20
21
22
23
24
25
26
27
28
29
30
31

Fig. A-99-1-0

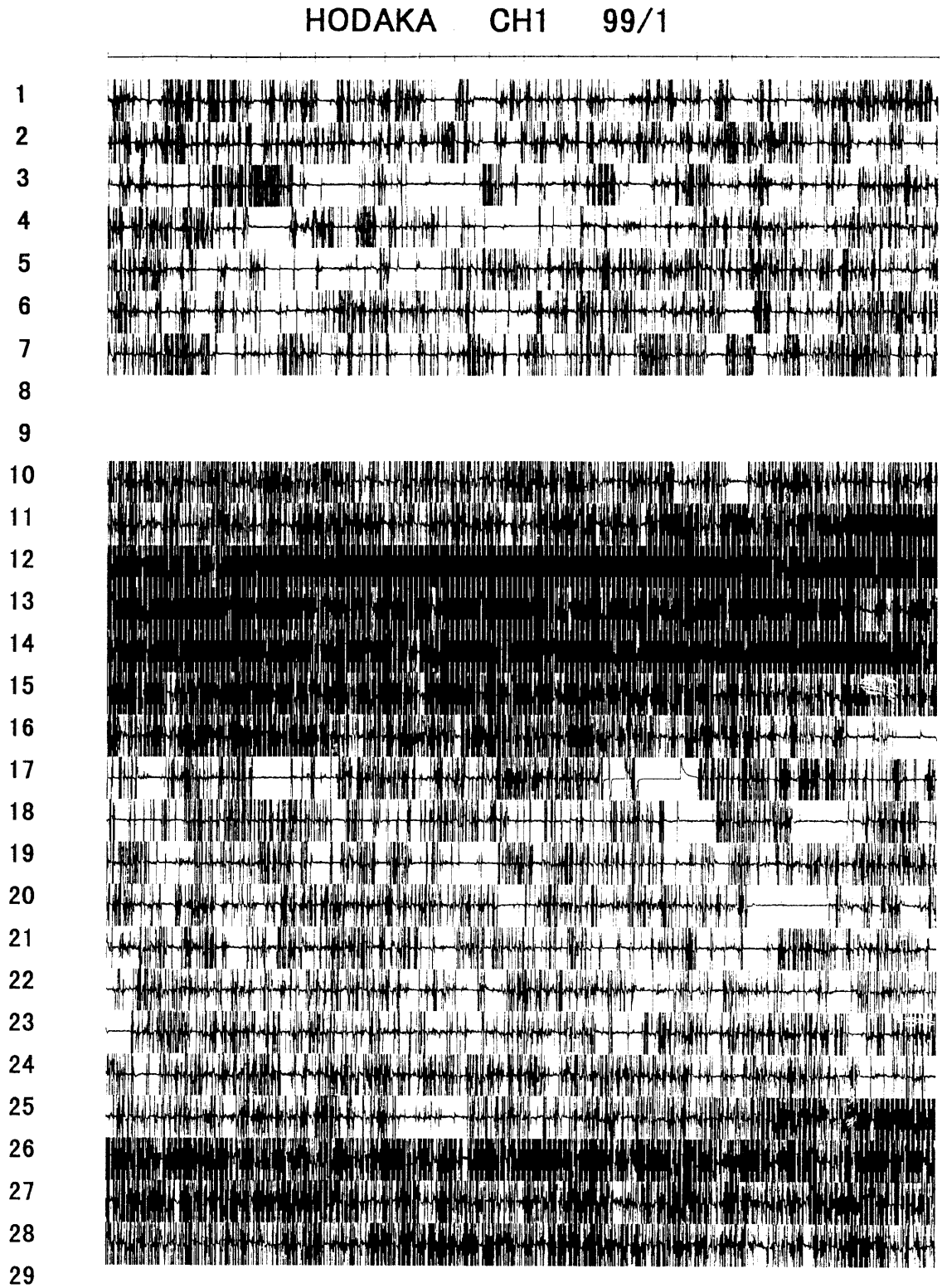
HODAKA CH1 99/1
1
2
3
4
5
6
7
8
9
10
11
12
13
14
15
16
17
18
19
20
21
22
23
24
25
26
27
28
29
30
31

Fig. A-99-1-1

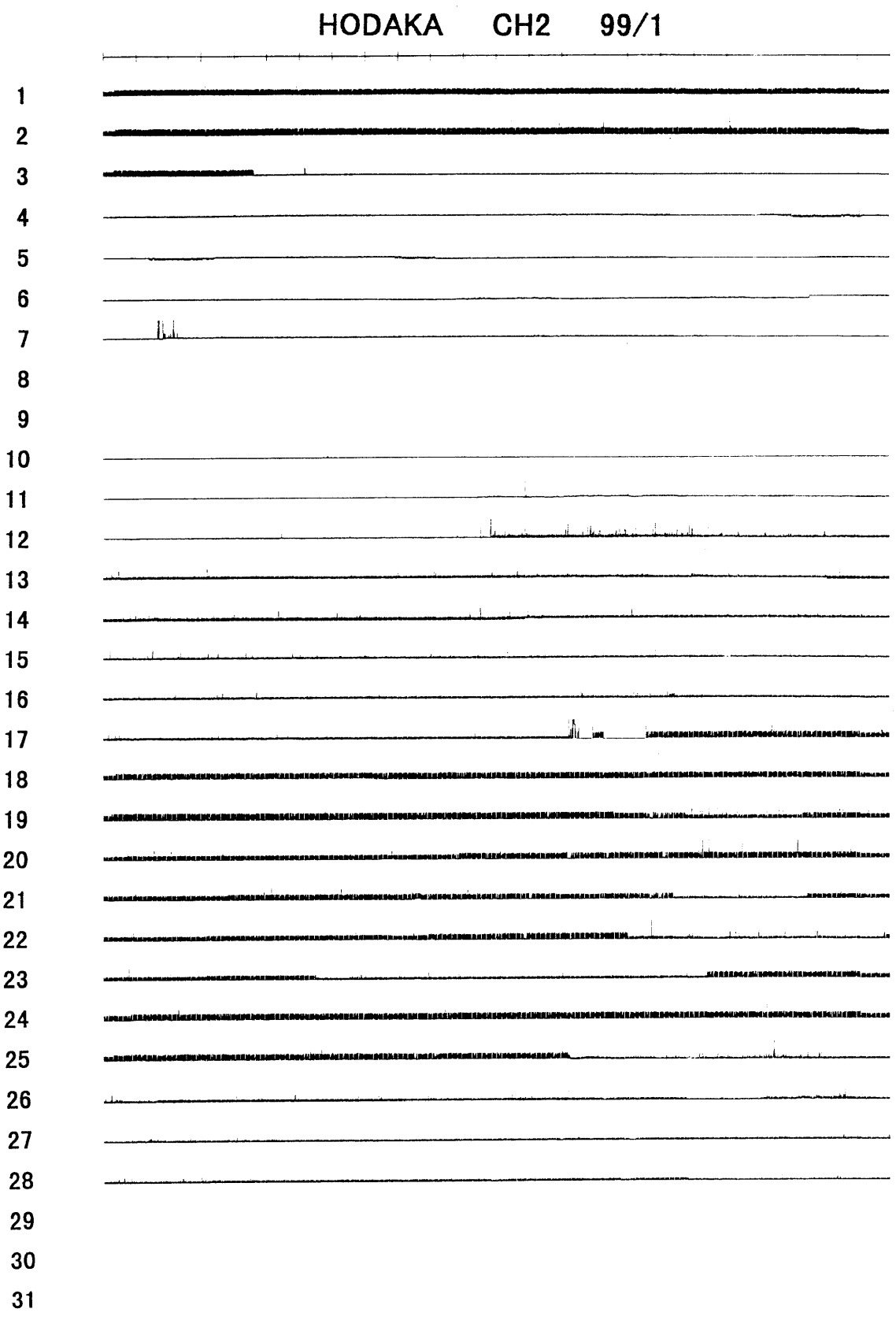
HODAKA CH2 99/1
1
2
3
4
5
6
7
8
9
10
11
12
13
14
15
16
17
18
19
20
21
22
23
24
25
26
27
28
29
30
31

Fig. A-99-1-2

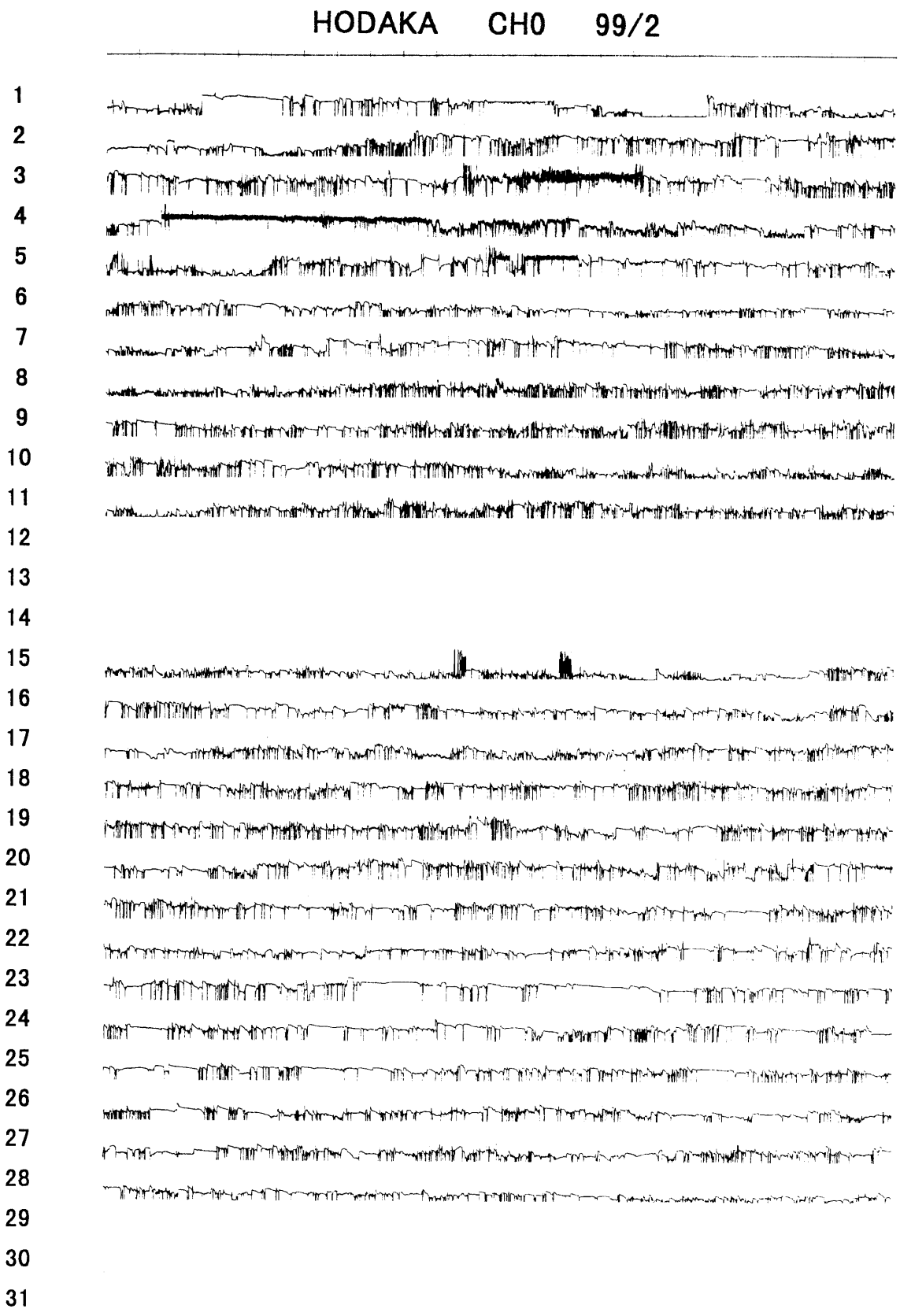
HODAKA CH0 99/2
1
2
3
4
5
6
7
8
9
10
11
12
13
14
15
16
17
18
19
20
21
22
23
24
25
26
27
28
29
30
31

Fig. A-99-2-0

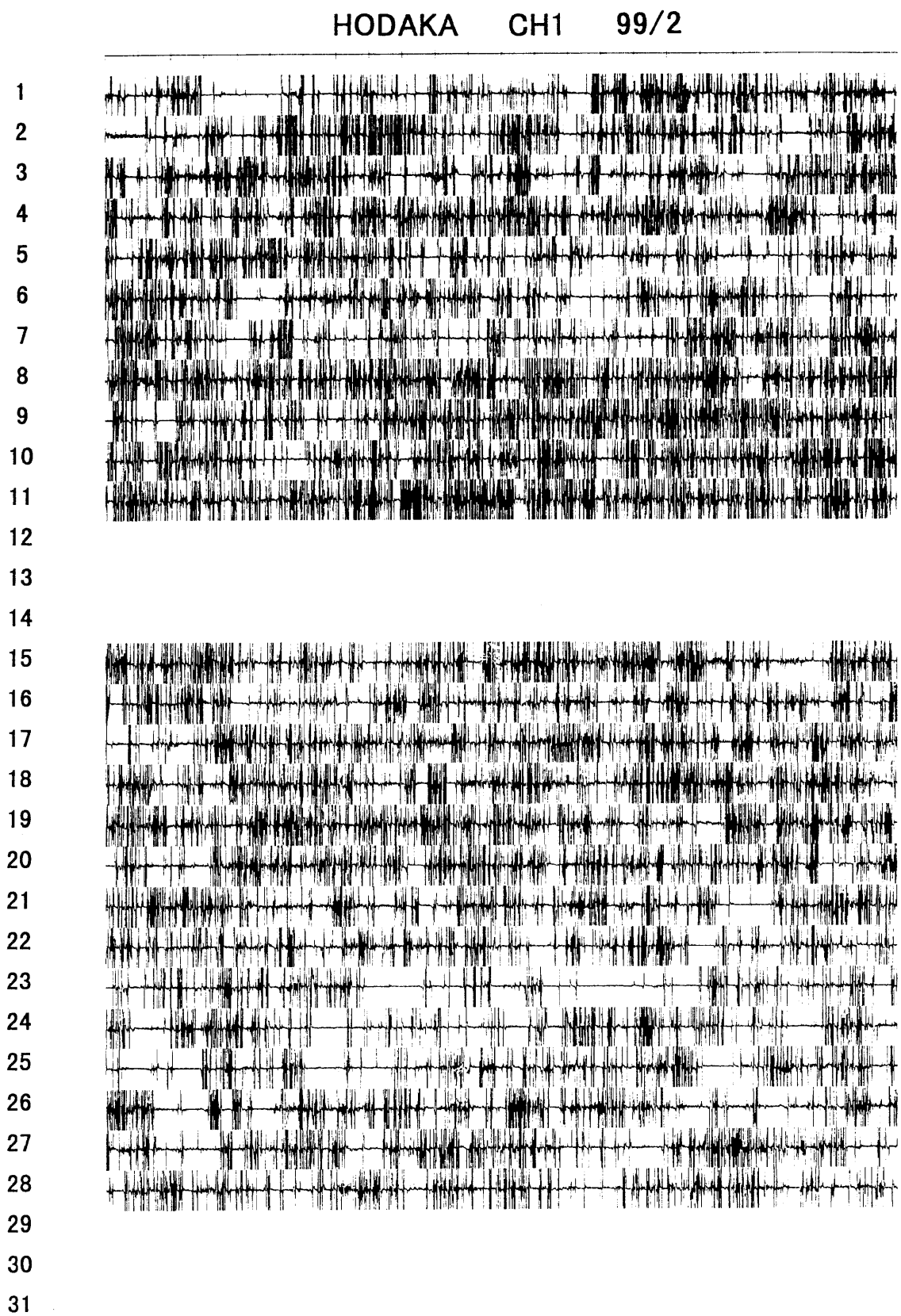
HODAKA CH1 99/2
1
2
3
4
5
6
7
8
9
10
11
12
13
14
15
16
17
18
19
20
21
22
23
24
25
26
27
28
29
30
31

Fig. A-99-2-1

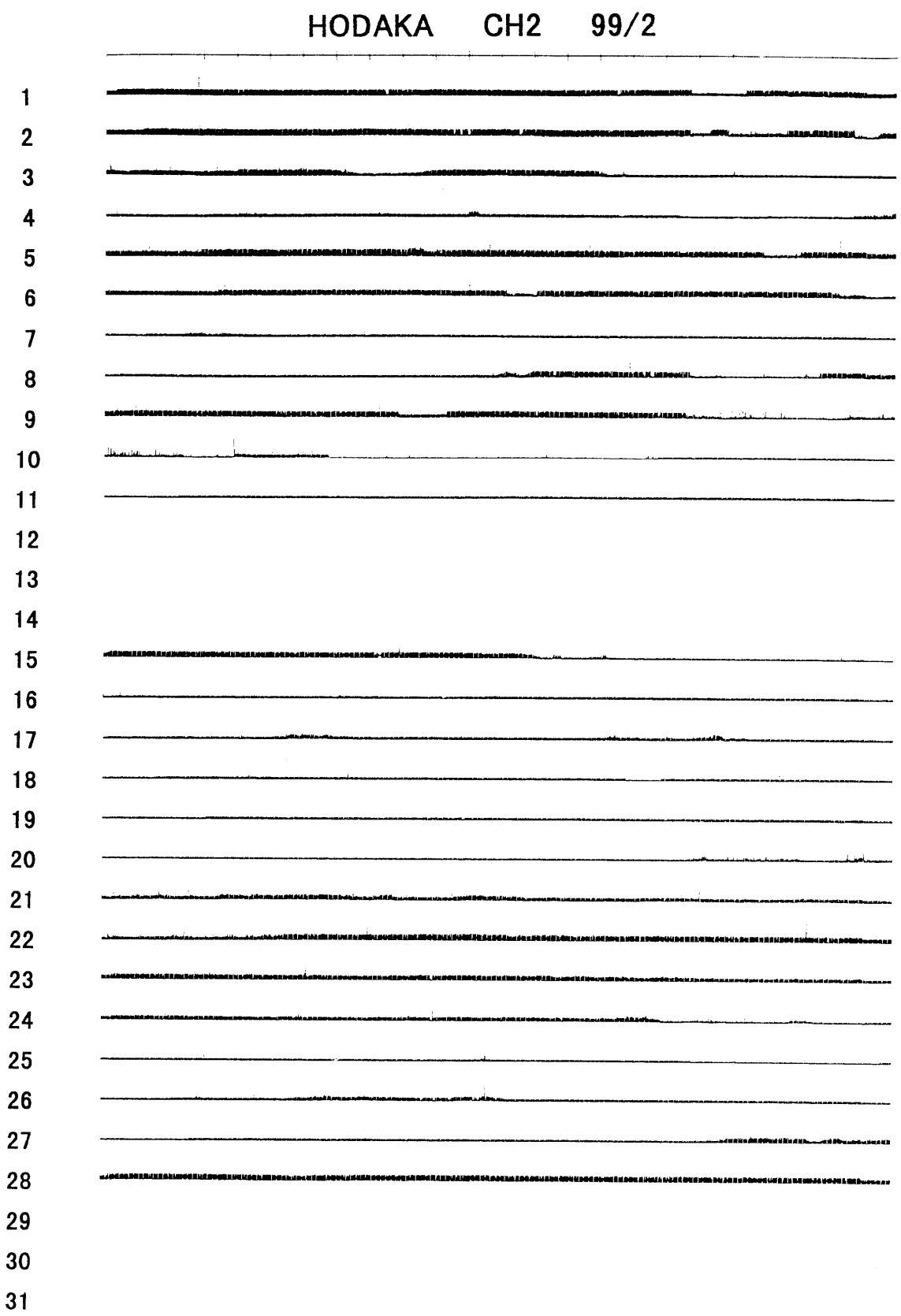
HODAKA CH2 99/2
1
2
3
4
5
6
7
8
9
10
11
12
13
14
15
16
17
18
19
20
21
22
23
24
25
26
27
28
29
30
31

Fig. A-99-2-2

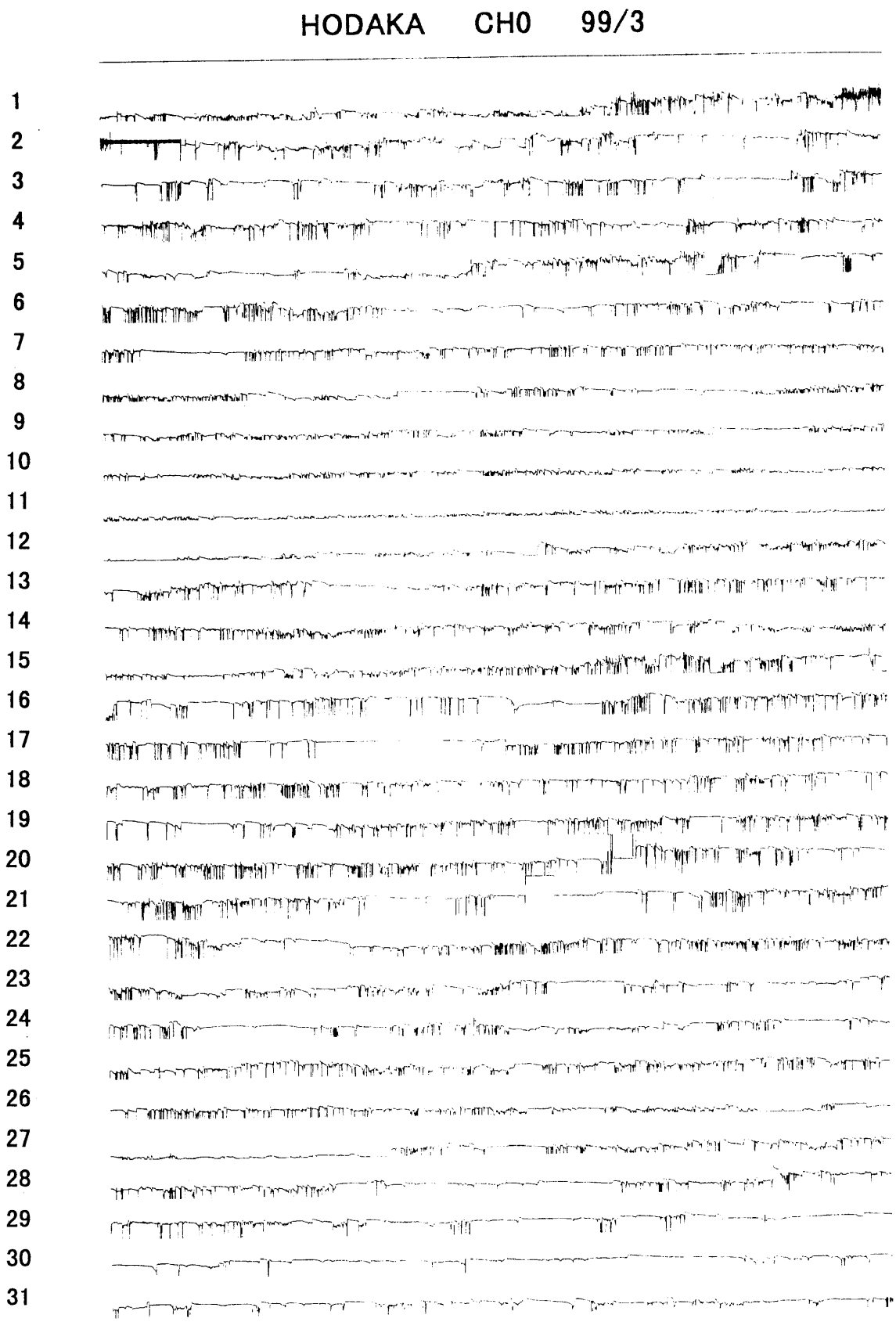
HODAKA CH0 99/3
1
2
3
4
5
6
7
8
9
10
11
12
13
14
15
16
17
18
19
20
21
22
23
24
25
26
27
28
29
30
31

Fig. A-99-3-0

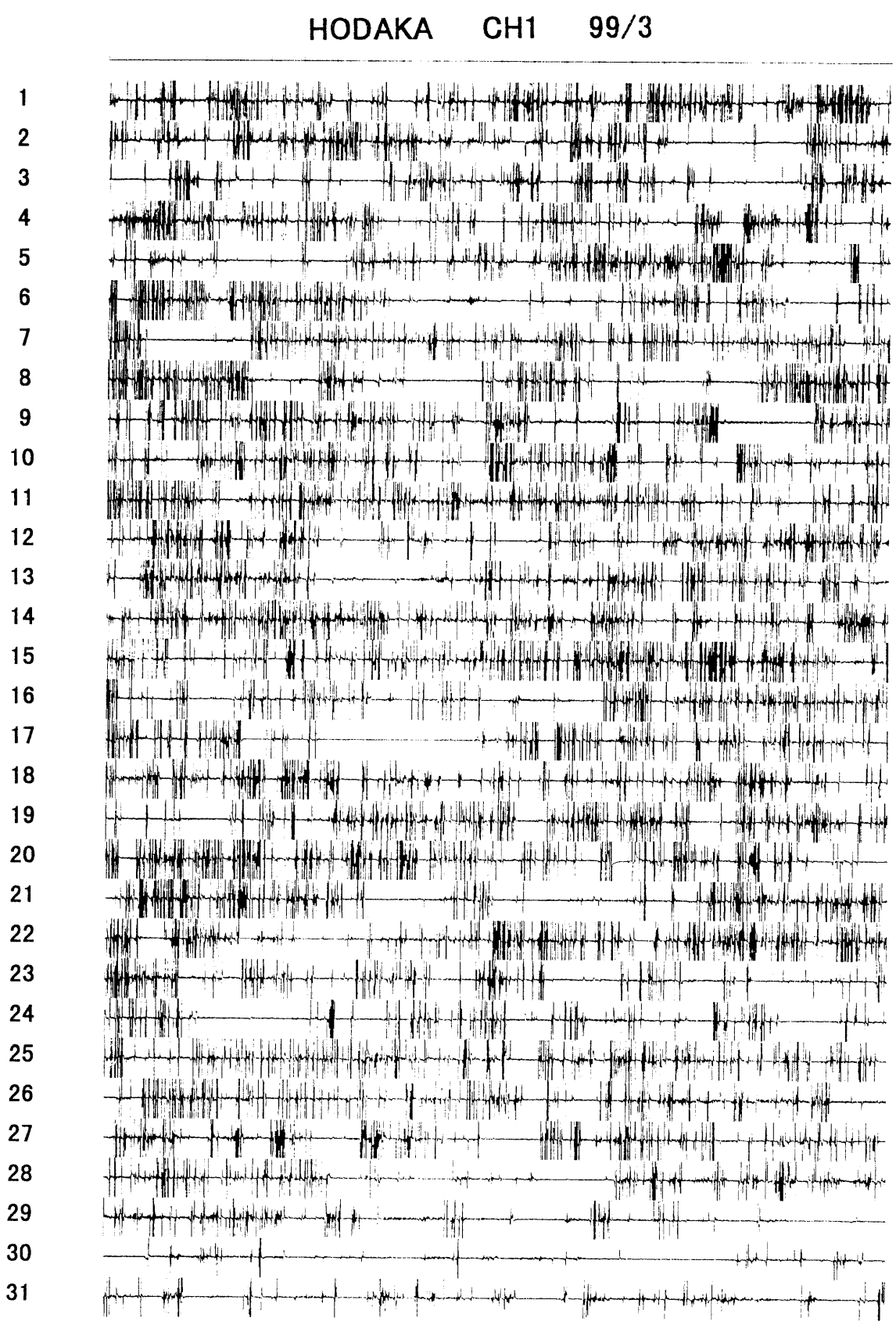
HODAKA CH1 99/3
1
2
3
4
5
6
7
8
9
10
11
12
13
14
15
16
17
18
19
20
21
22
23
24
25
26
27
28
29
30
31

Fig. A-99-3-1

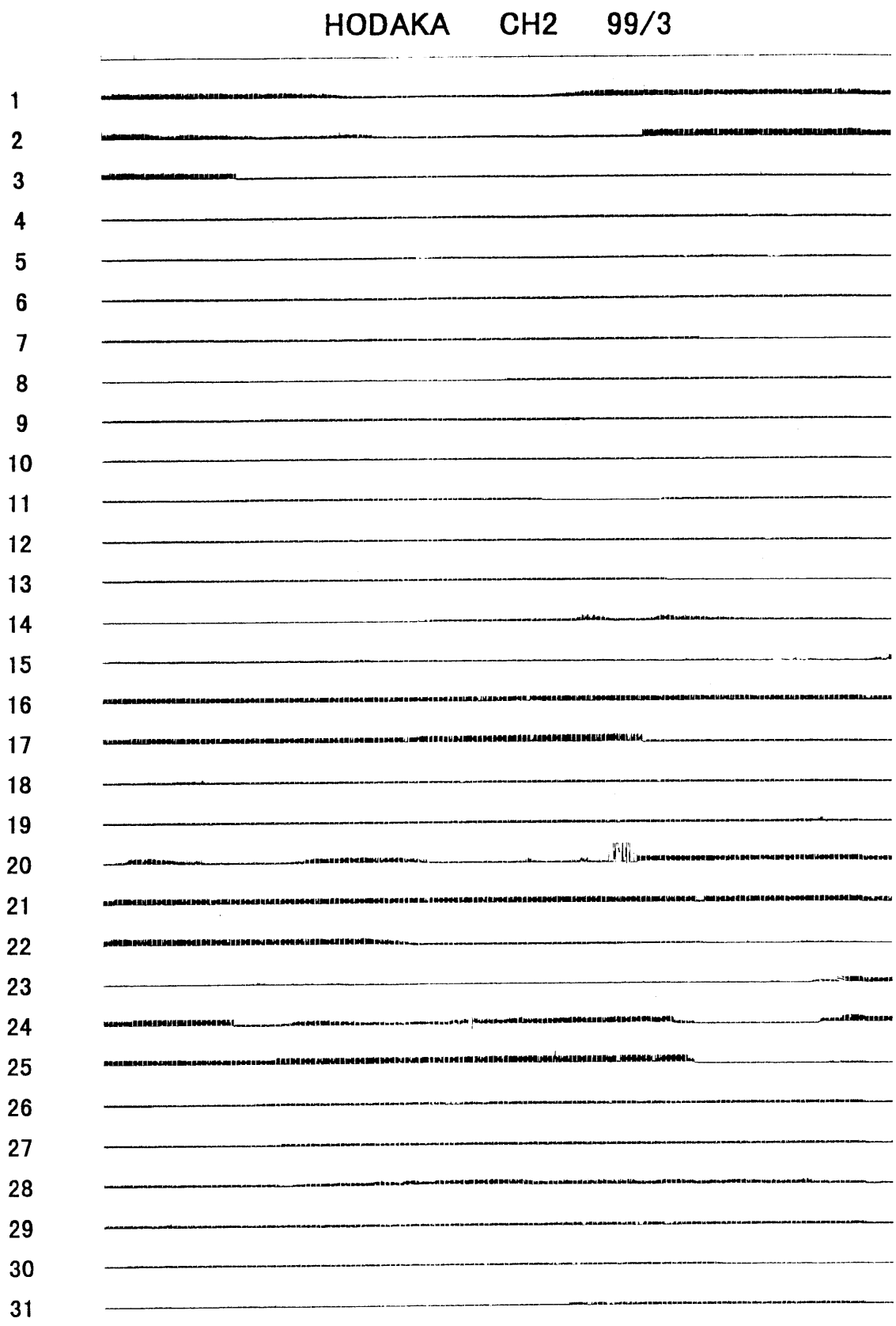
HODAKA CH2 99/3
1
2
3
4
5
6
7
8
9
10
11
12
13
14
15
16
17
18
19
20
21
22
23
24
25
26
27
28
29
30
31

Fig. A-99-3-2

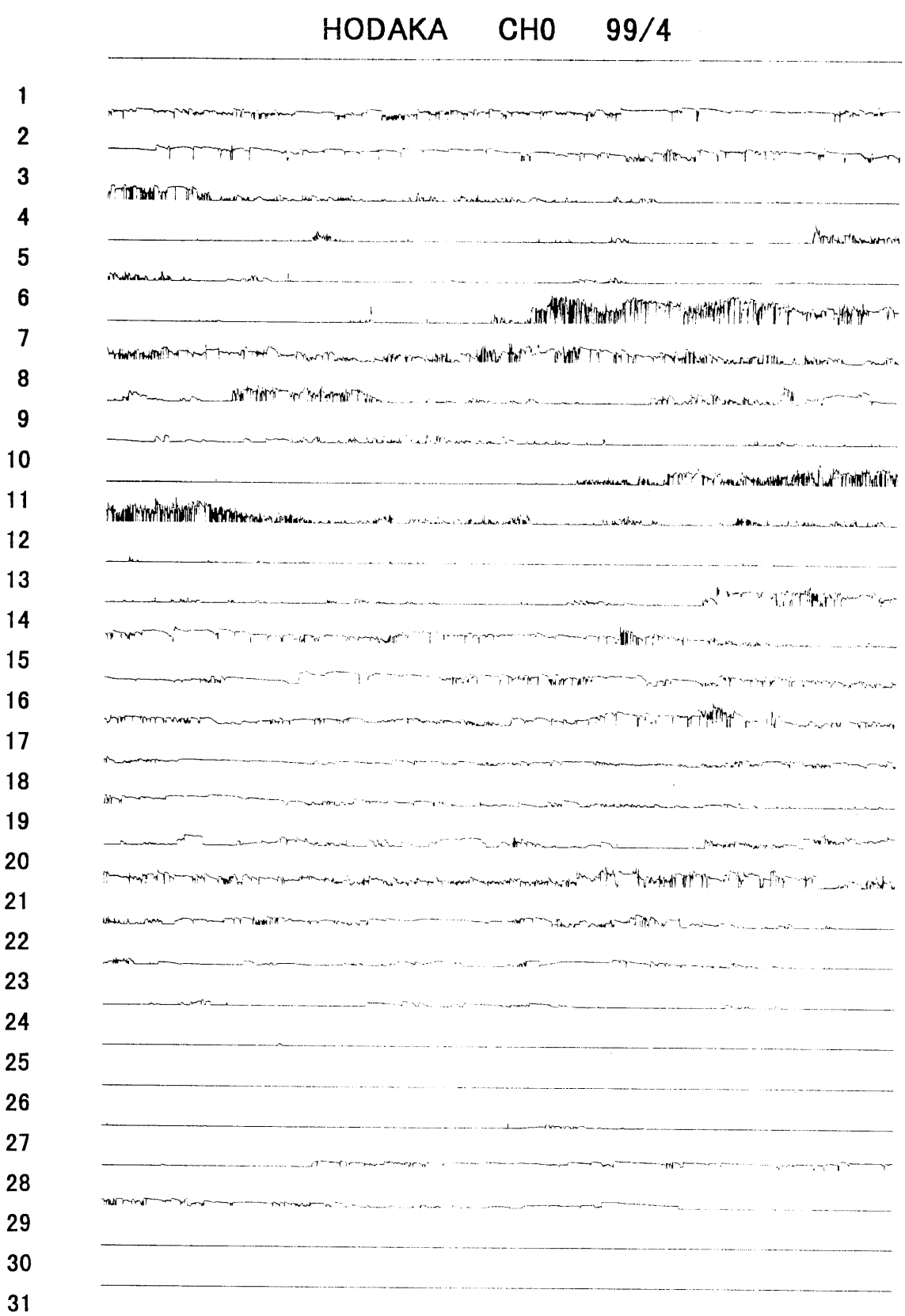
HODAKA CH0 99/4
1
2
3
4
5
6
7
8
9
10
11
12
13
14
15
16
17
18
19
20
21
22
23
24
25
26
27
28
29
30
31

Fig. A-99-4-0

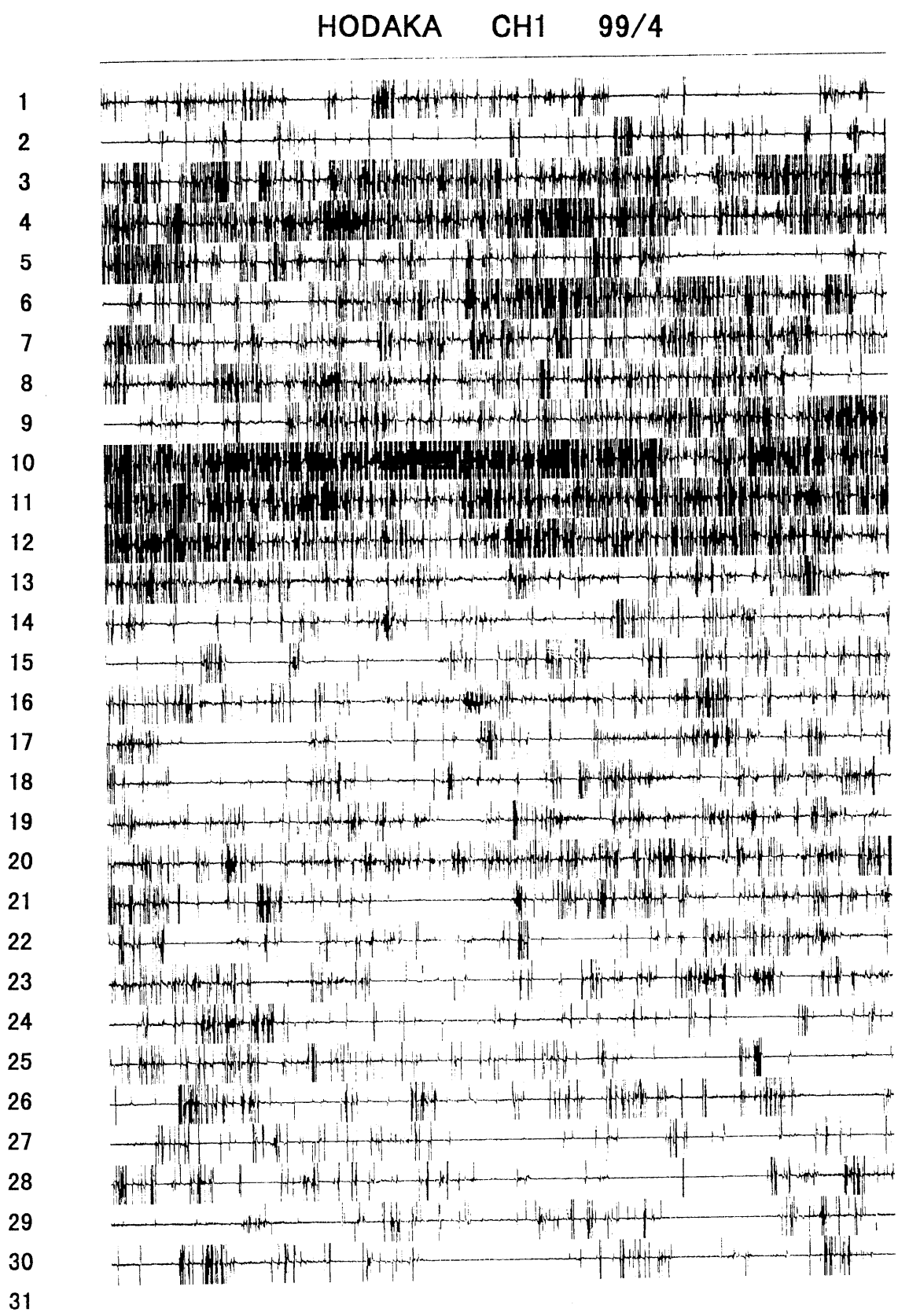
HODAKA CH1 99/4
1
2
3
4
5
6
7
8
9
10
11
12
13
14
15
16
17
18
19
20
21
22
23
24
25
26
27
28
29
30
31

Fig. A-99-4-1

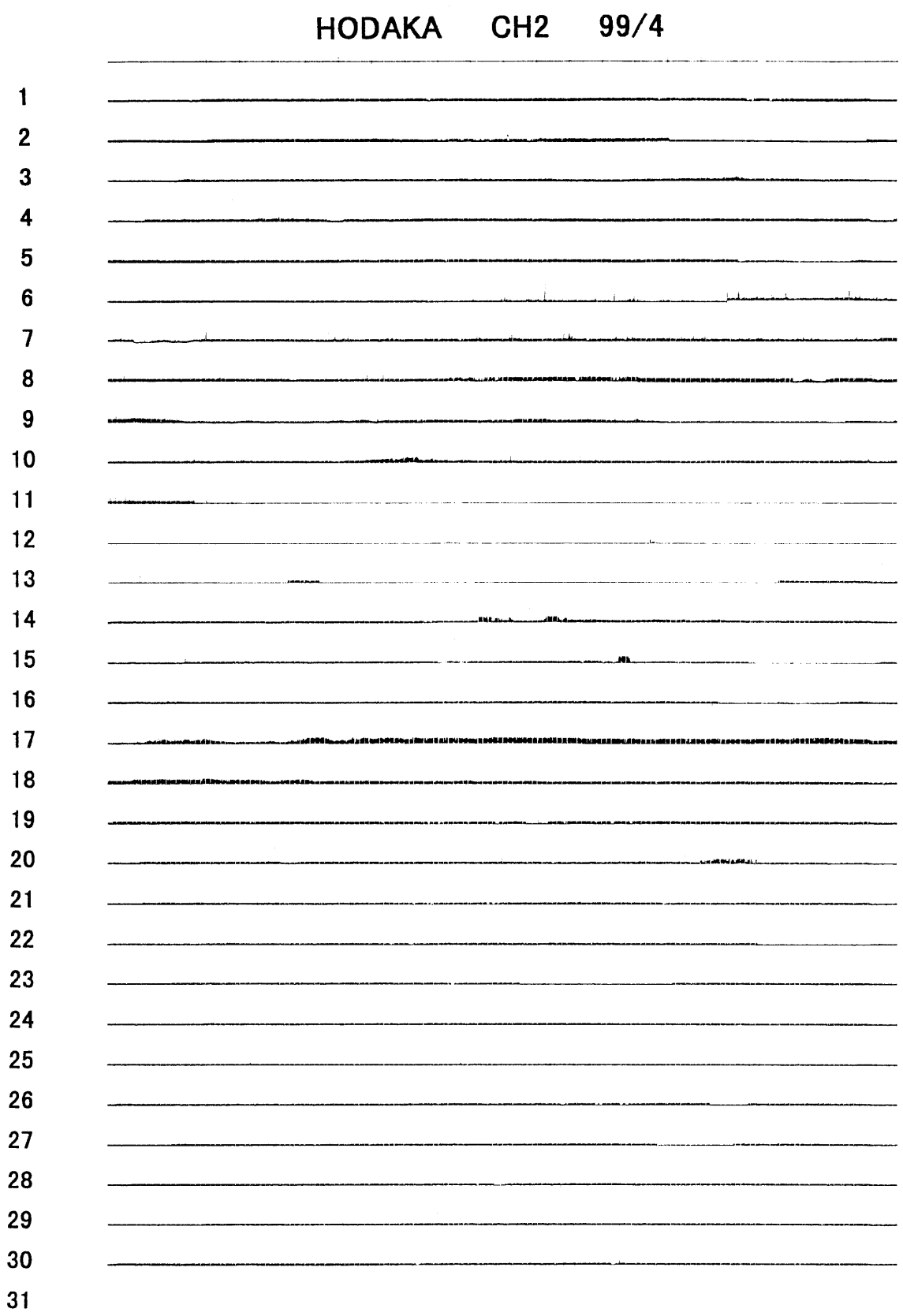
HODAKA CH2 99/4
1
2
3
4
5
6
7
8
9
10
11
12
13
14
15
16
17
18
19
20
21
22
23
24
25
26
27
28
29
30
31

Fig. A-99-4-2

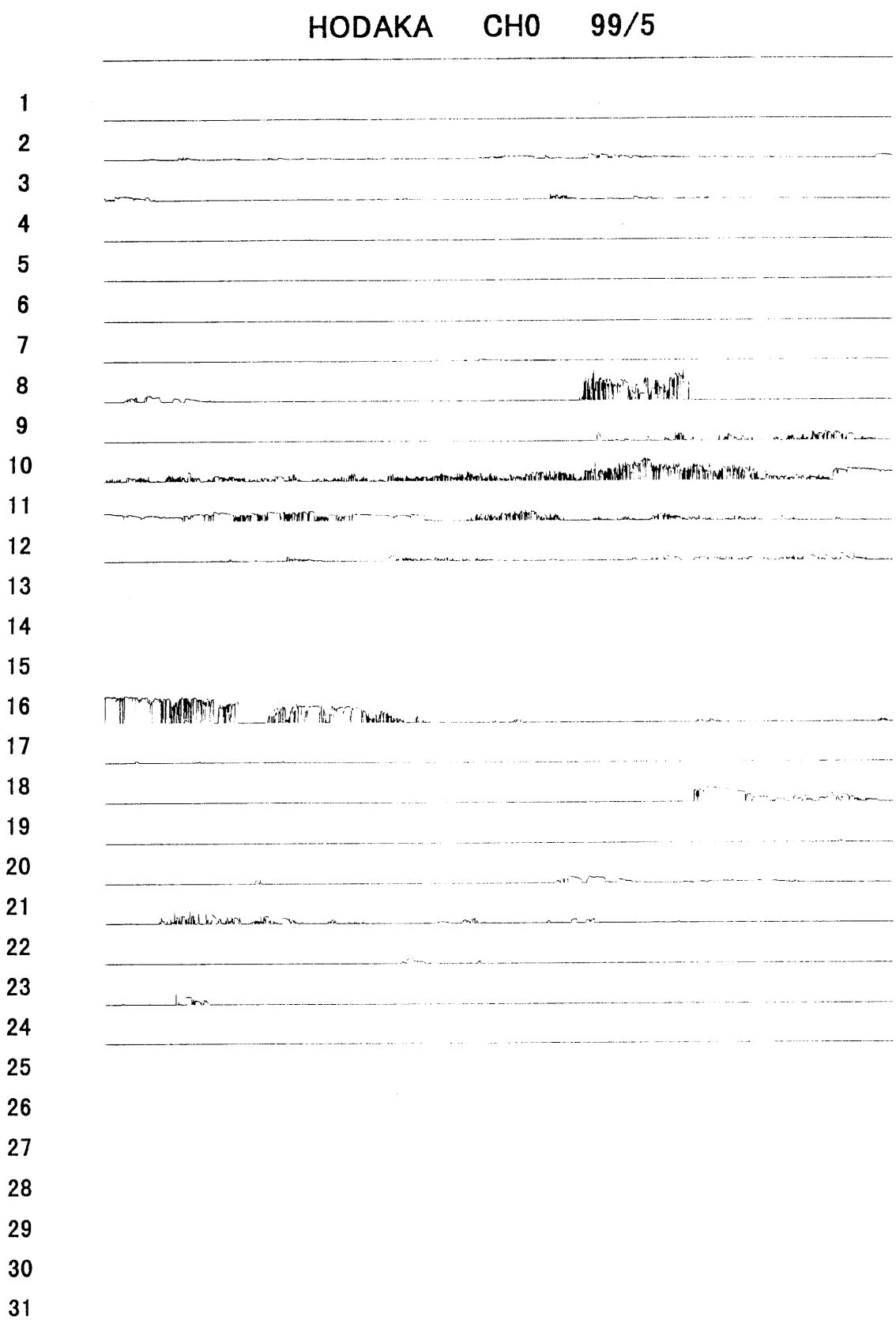
HODAKA CH0 99/5
1
2
3
4
5
6
7
8
9
10
11
12
13
14
15
16
17
18
19
20
21
22
23
24
25
26
27
28
29
30
31

Fig. A-99-5-0

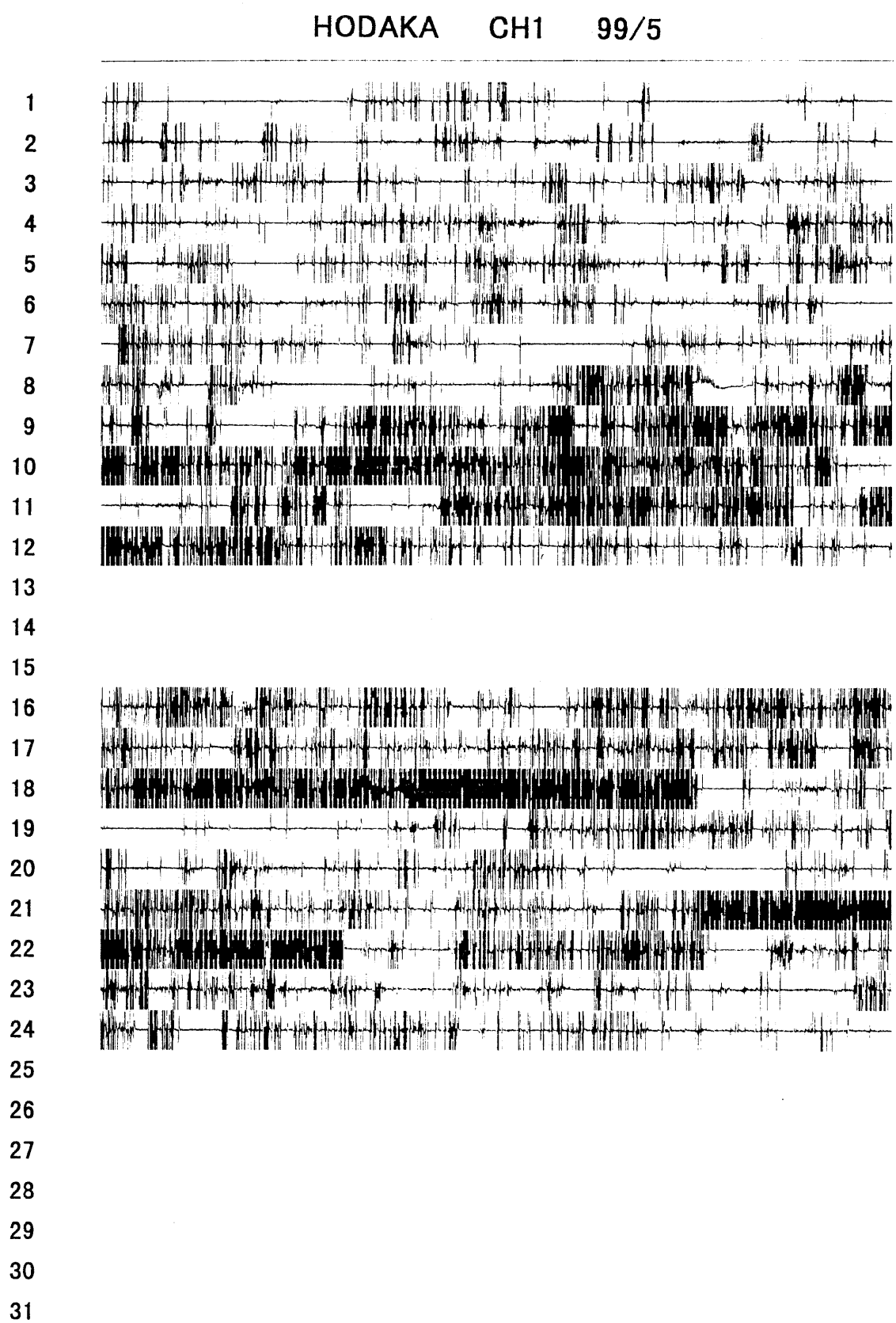
HODAKA CH1 99/5
1
2
3
4
5
6
7
8
9
10
11
12
13
14
15
16
17
18
19
20
21
22
23
24
25
26
27
28
29
30
31

Fig. A-99-5-1

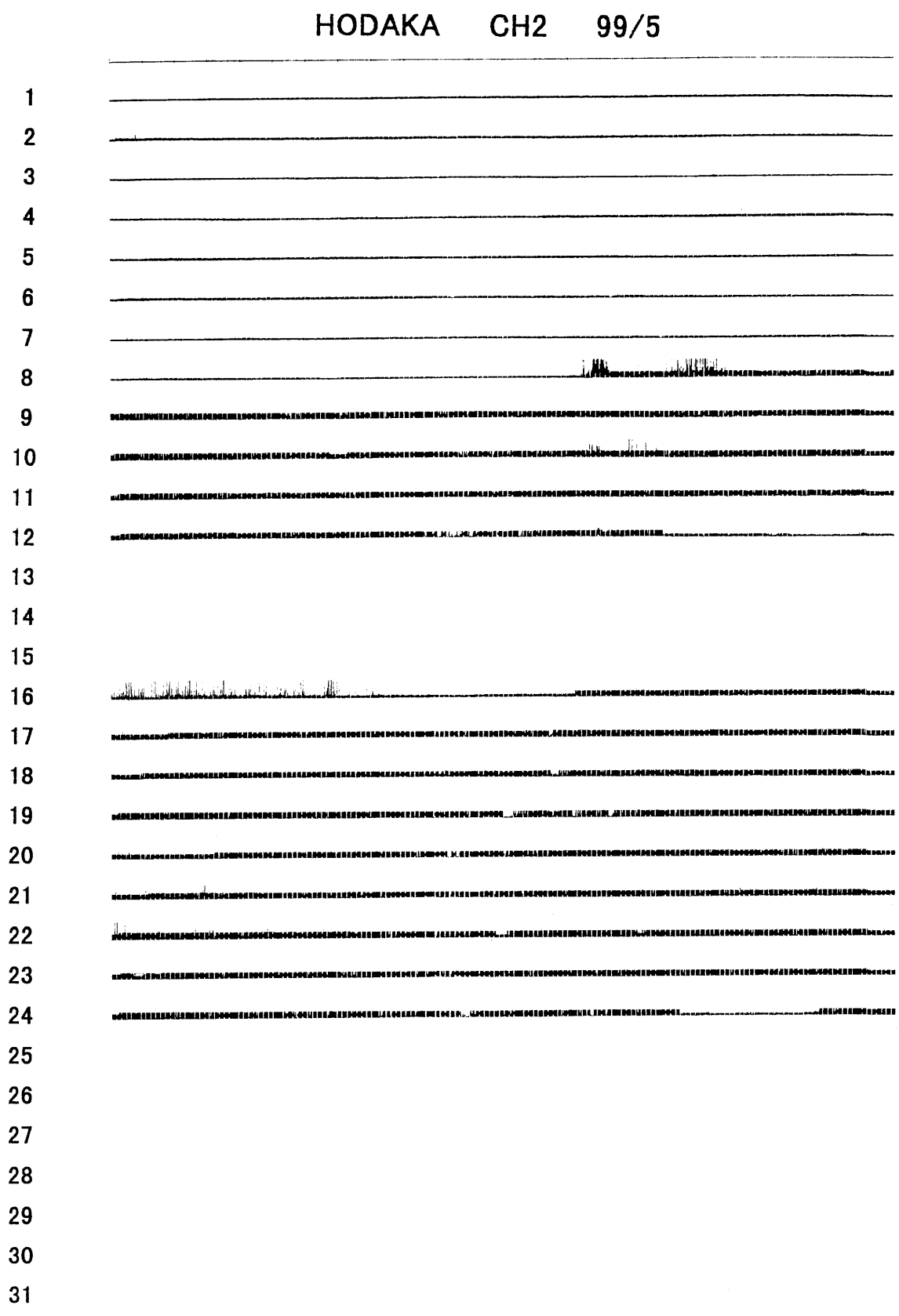
HODAKA CH2 99/5
1
2
3
4
5
6
7
8
9
10
11
12
13
14
15
16
17
18
19
20
21
22
23
24
25
26
27
28
29
30
31

Fig. A-99-5-2

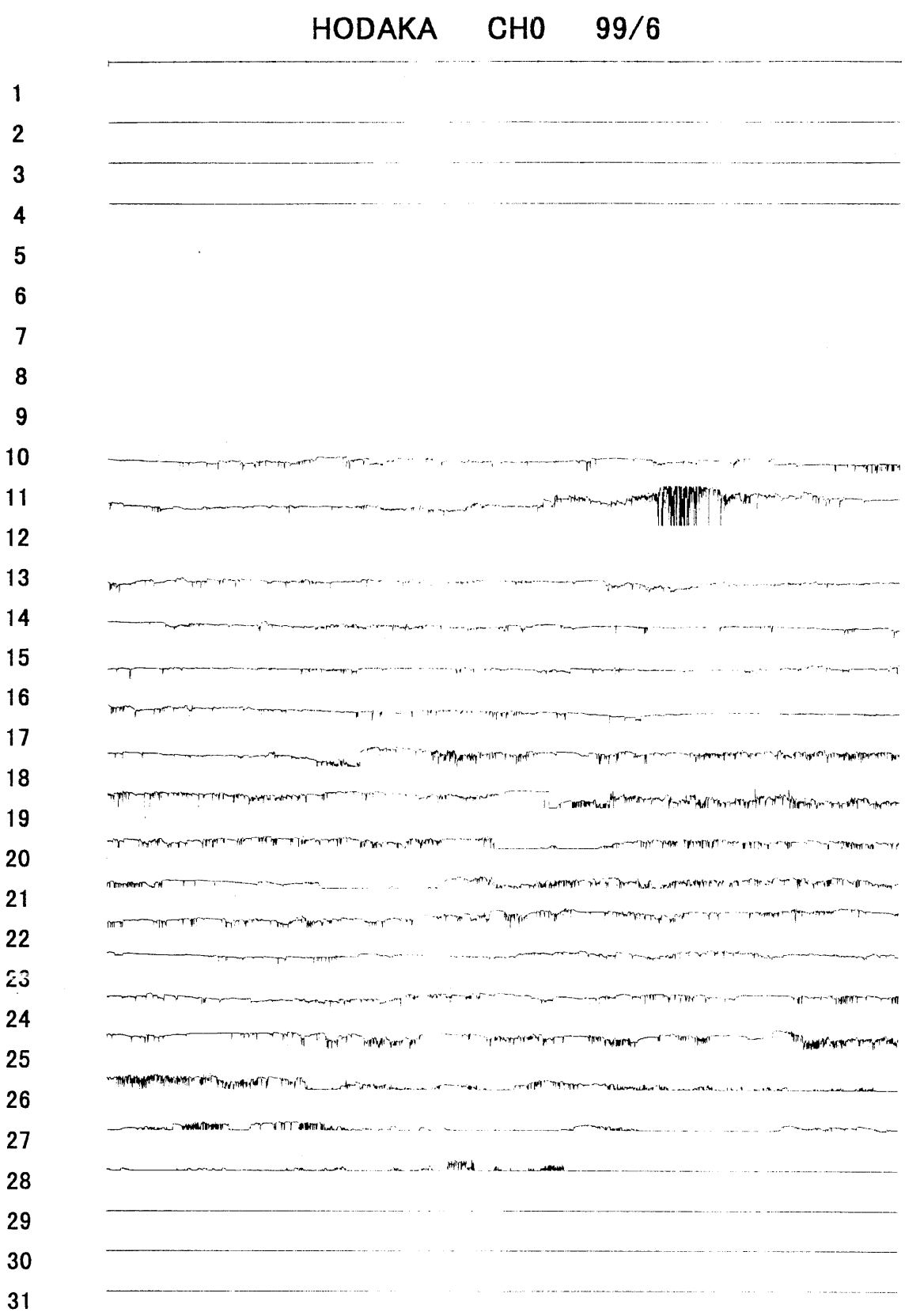
HODAKA CH0 99/6
1
2
3
4
5
6
7
8
9
10
11
12
13
14
15
16
17
18
19
20
21
22
23
24
25
26
27
28
29
30
31

Fig. A-99-6-0

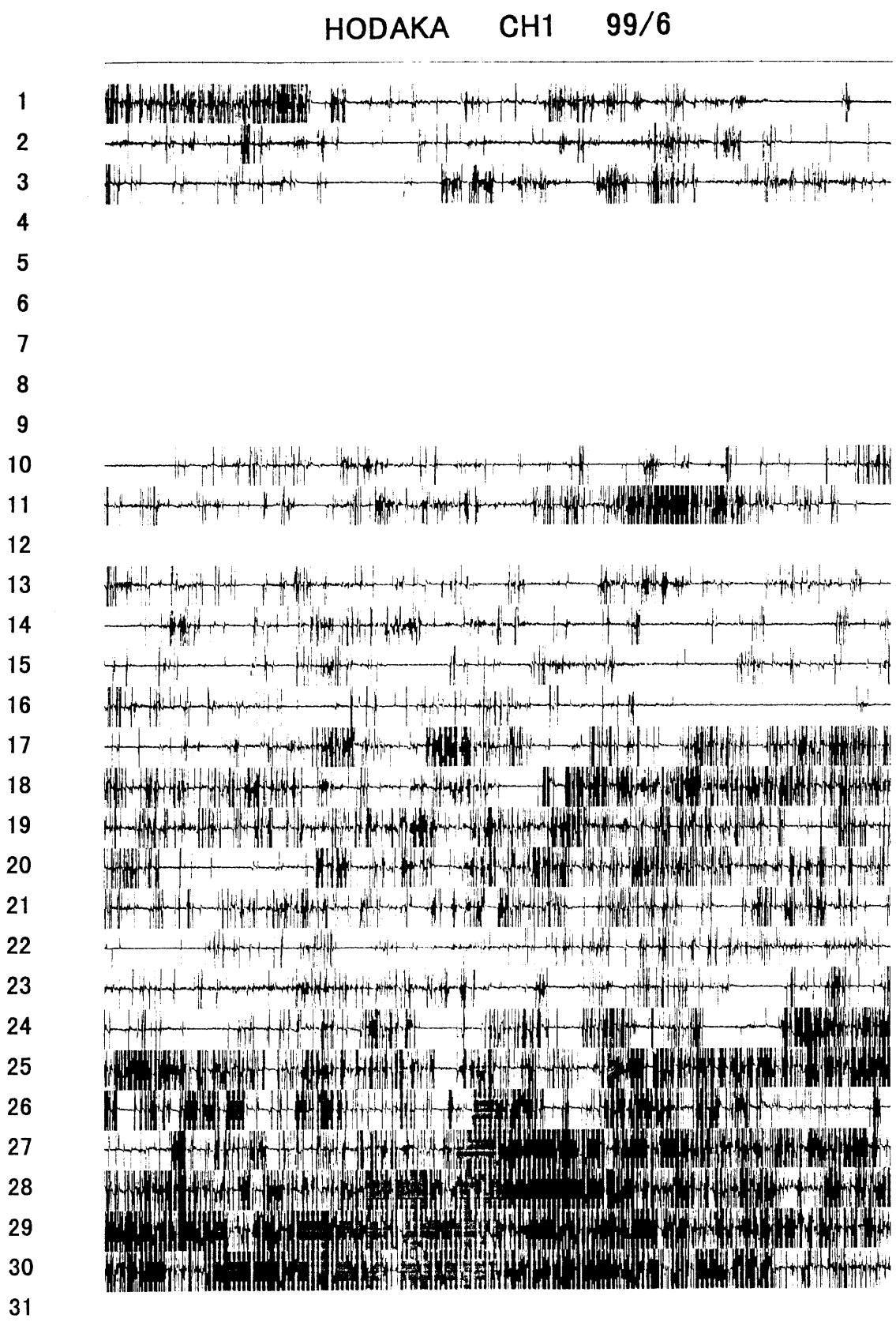
HODAKA CH1 99/6
1
2
3
4
5
6
7
8
9
10
11
12
13
14
15
16
17
18
19
20
21
22
23
24
25
26
27
28
29
30
31

Fig. A-99-6-1

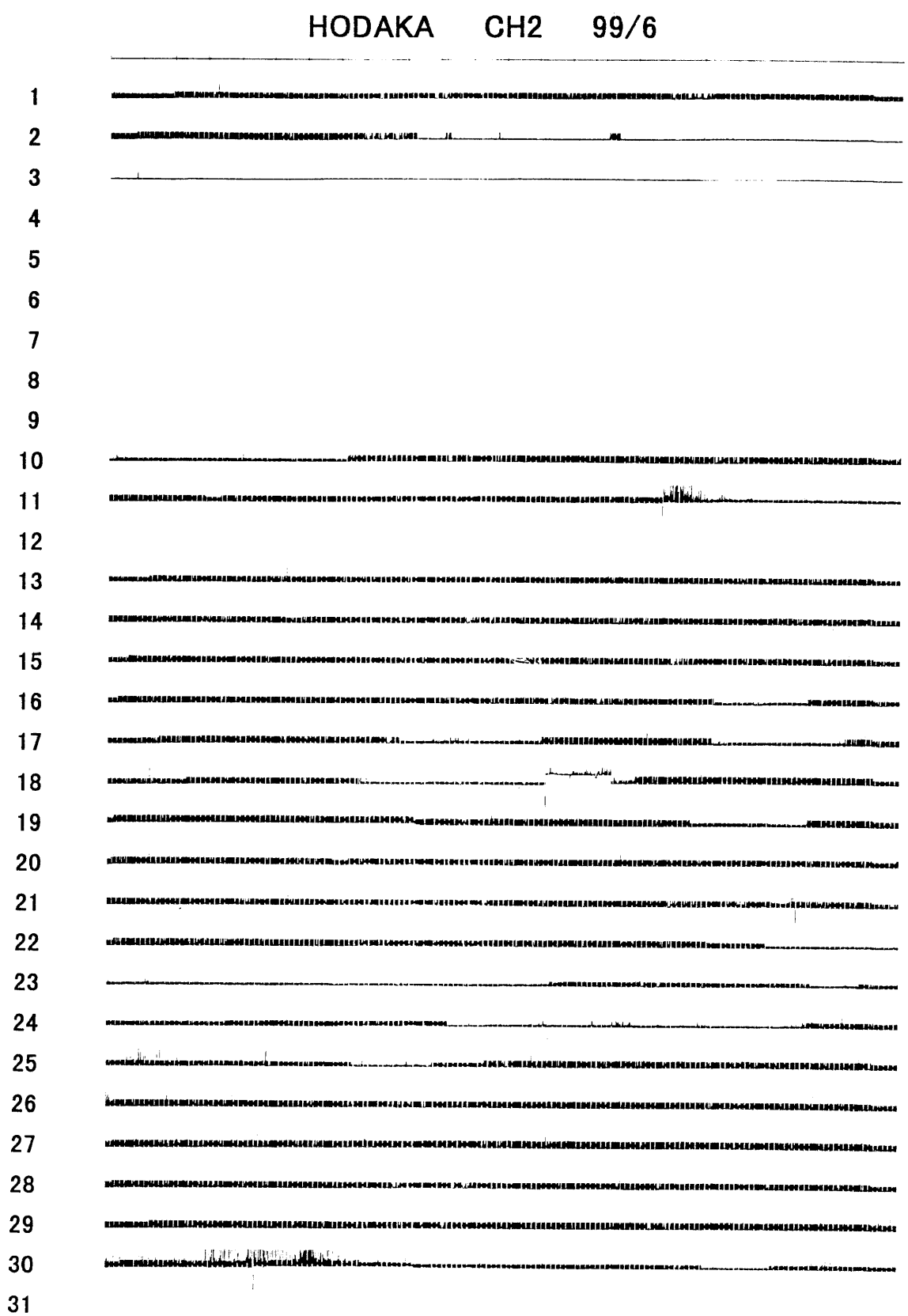
HODAKA CH2 99/6
1
2
3
4
5
6
7
8
9
10
11
12
13
14
15
16
17
18
19
20
21
22
23
24
25
26
27
28
29
30
31

Fig. A-99-6-2

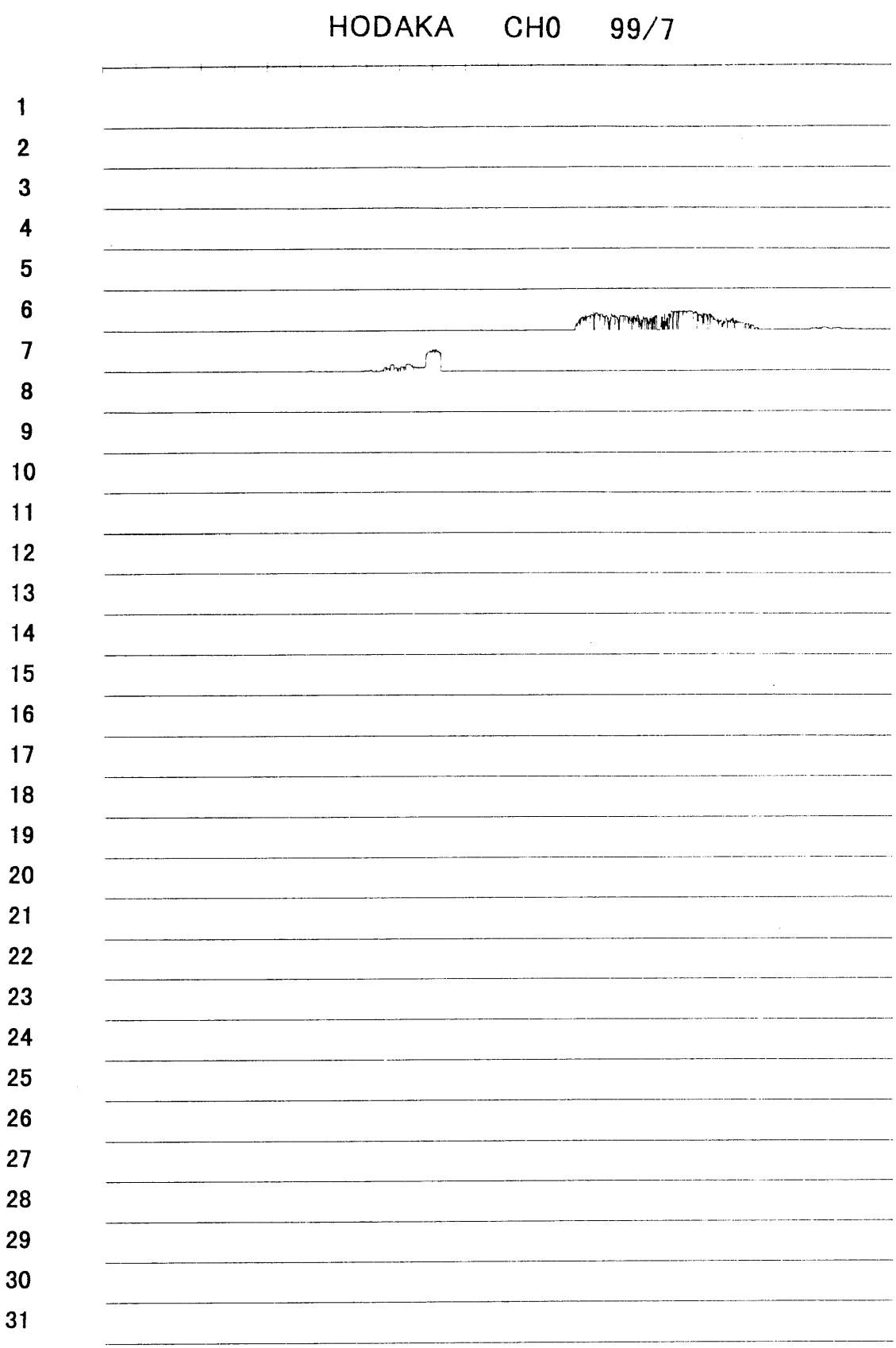
HODAKA CH0 99/7
1
2
3
4
5
6
7
8
9
10
11
12
13
14
15
16
17
18
19
20
21
22
23
24
25
26
27
28
29
30
31

Fig. A-99-7-0

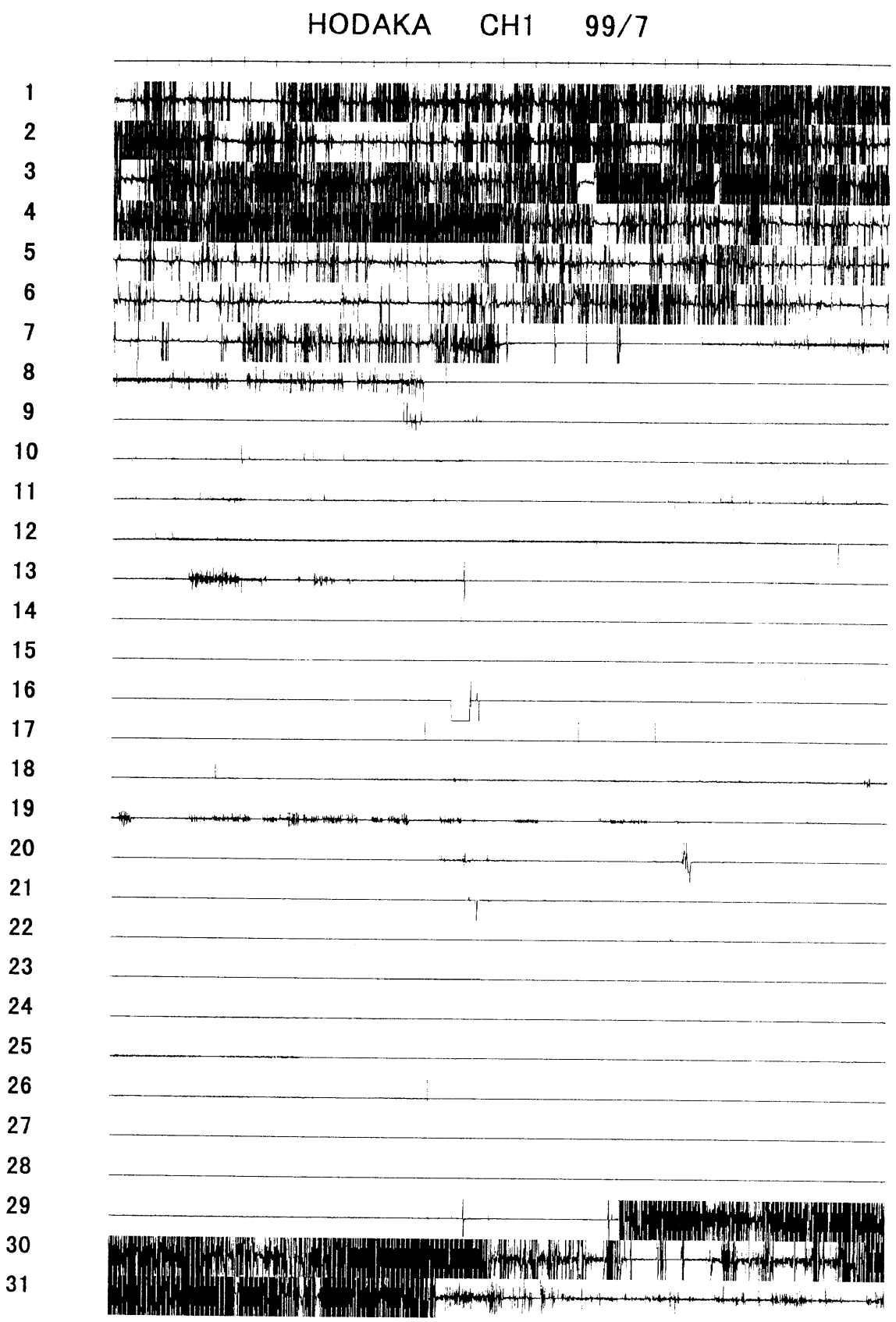
HODAKA CH1 99/7
1
2
3
4
5
6
7
8
9
10
11
12
13
14
15
16
17
18
19
20
21
22
23
24
25
26
27
28
29
30
31

Fig. A-99-7-1

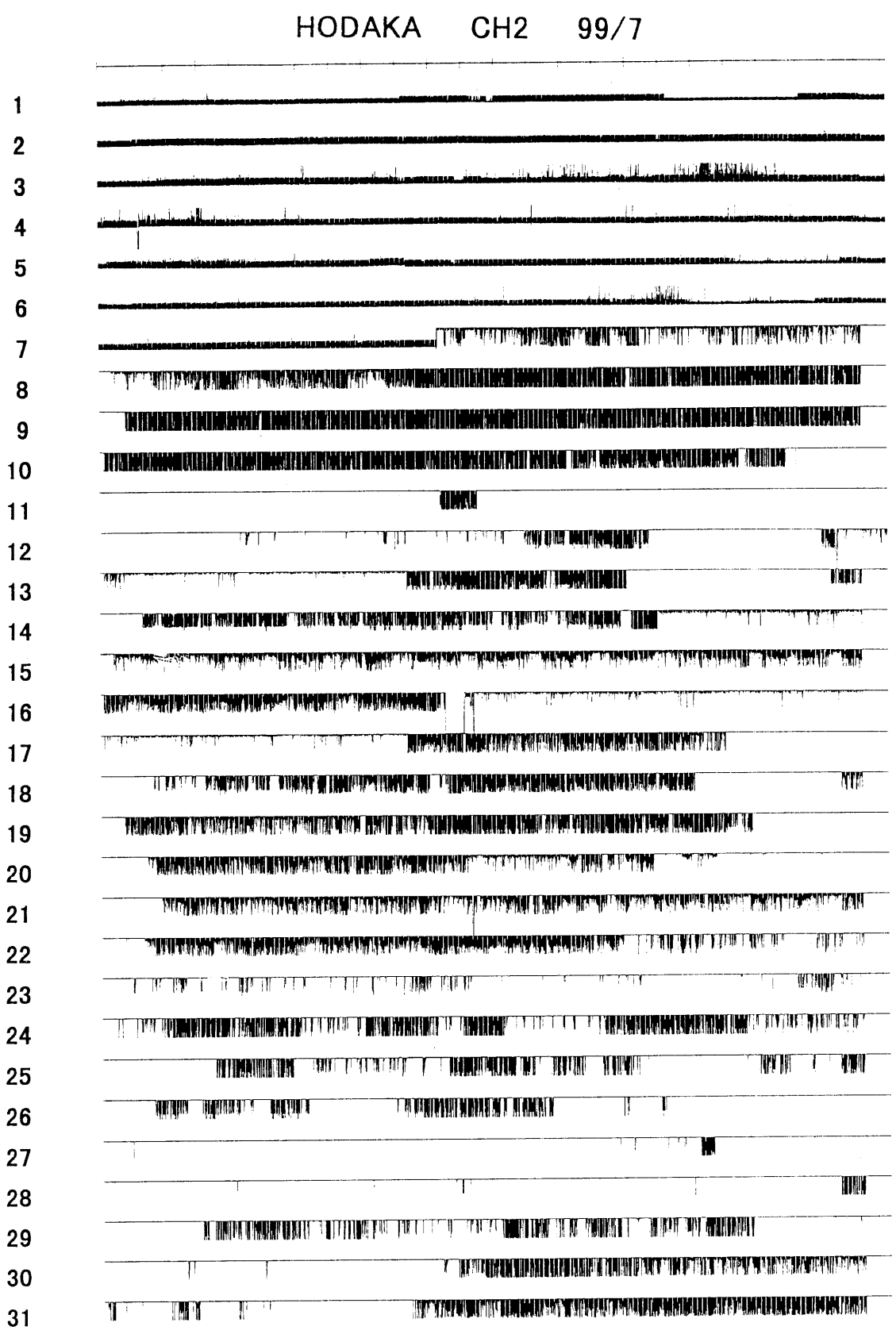
HODAKA CH2 99/7
1
2
3
4
5
6
7
8
9
10
11
12
13
14
15
16
17
18
19
20
21
22
23
24
25
26
27
28
29
30
31

Fig. A-99-7-2

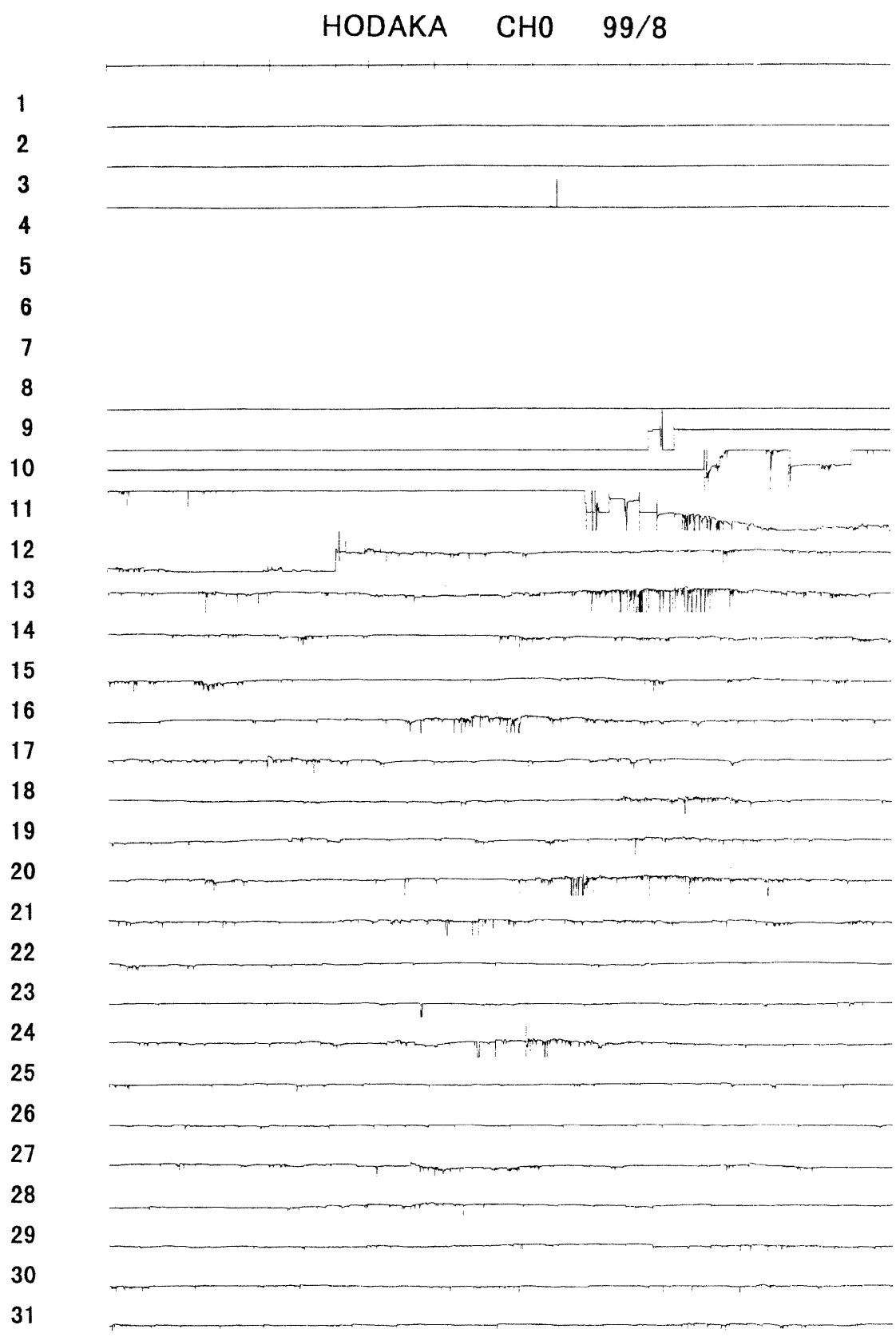
HODAKA CH0 99/8
1
2
3
4
5
6
7
8
9
10
11
12
13
14
15
16
17
18
19
20
21
22
23
24
25
26
27
28
29
30
31

Fig. A-99-8-0

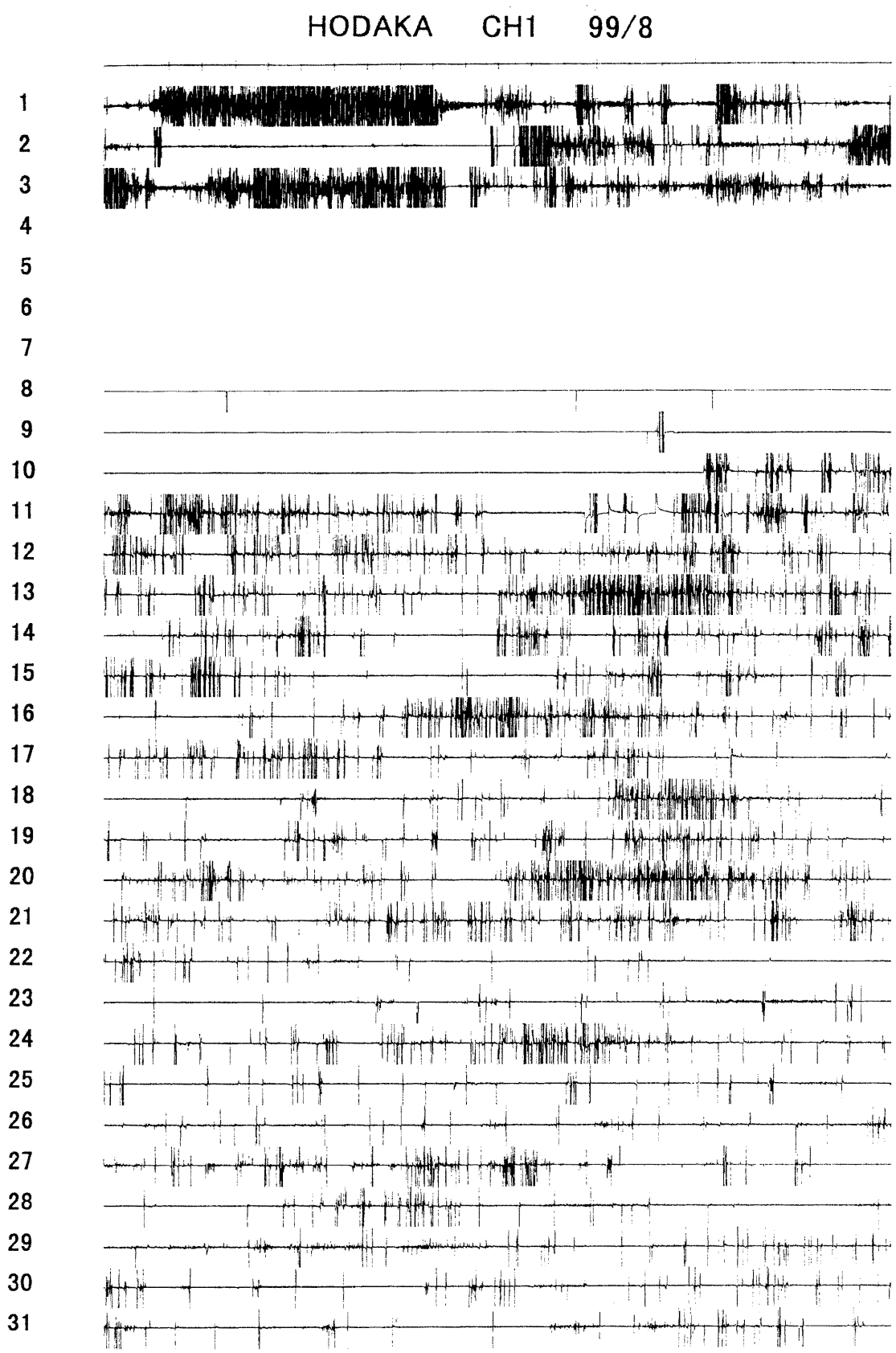
HODAKA CH1 99/8
1
2
3
4
5
6
7
8
9
10
11
12
13
14
15
16
17
18
19
20
21
22
23
24
25
26
27
28
29
30
31

Fig. A-99-8-1

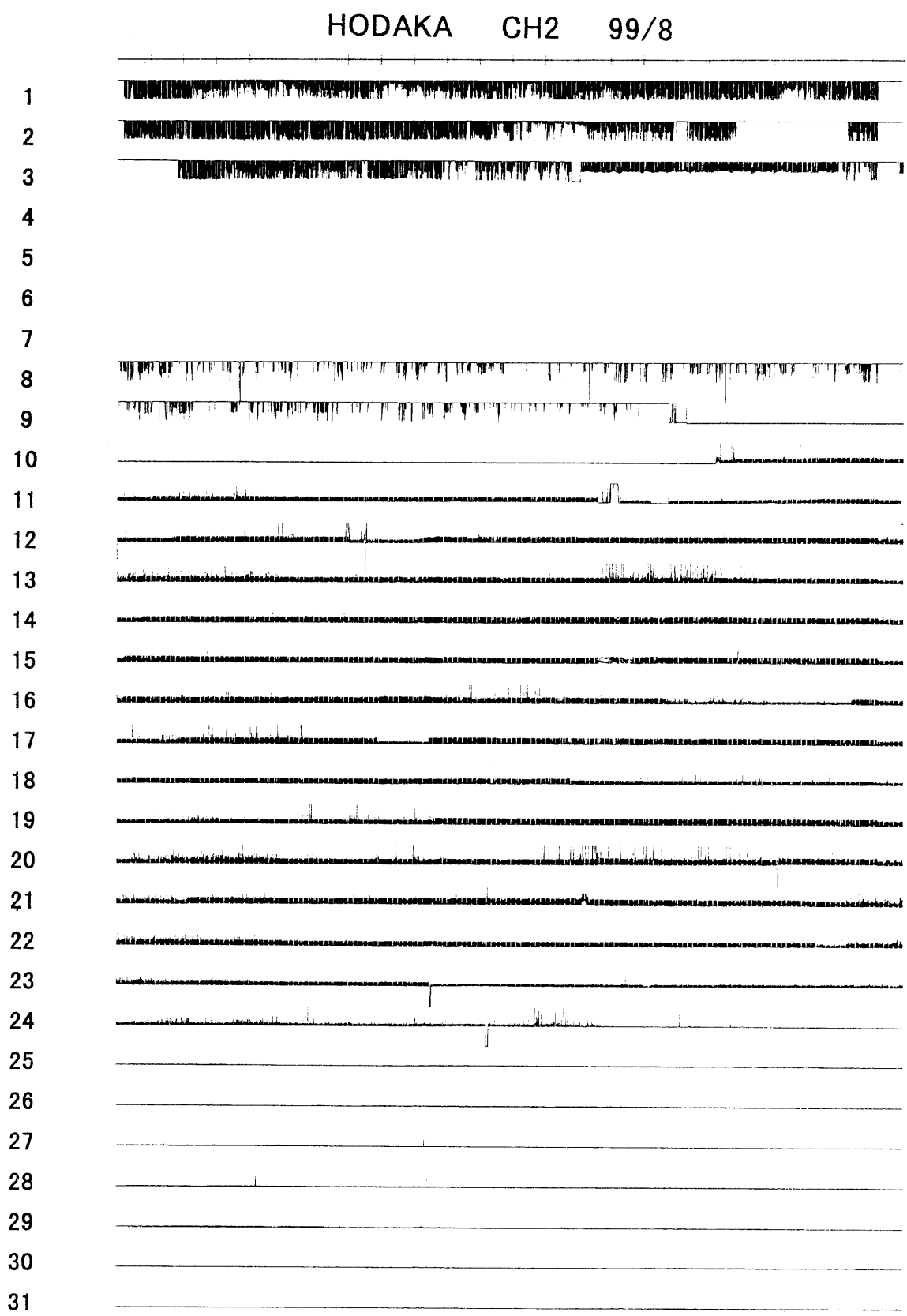
HODAKA CH2 99/8
1
2
3
4
5
6
7
8
9
10
11
12
13
14
15
16
17
18
19
20
21
22
23
24
25
26
27
28
29
30
31

Fig. A-99-8-2

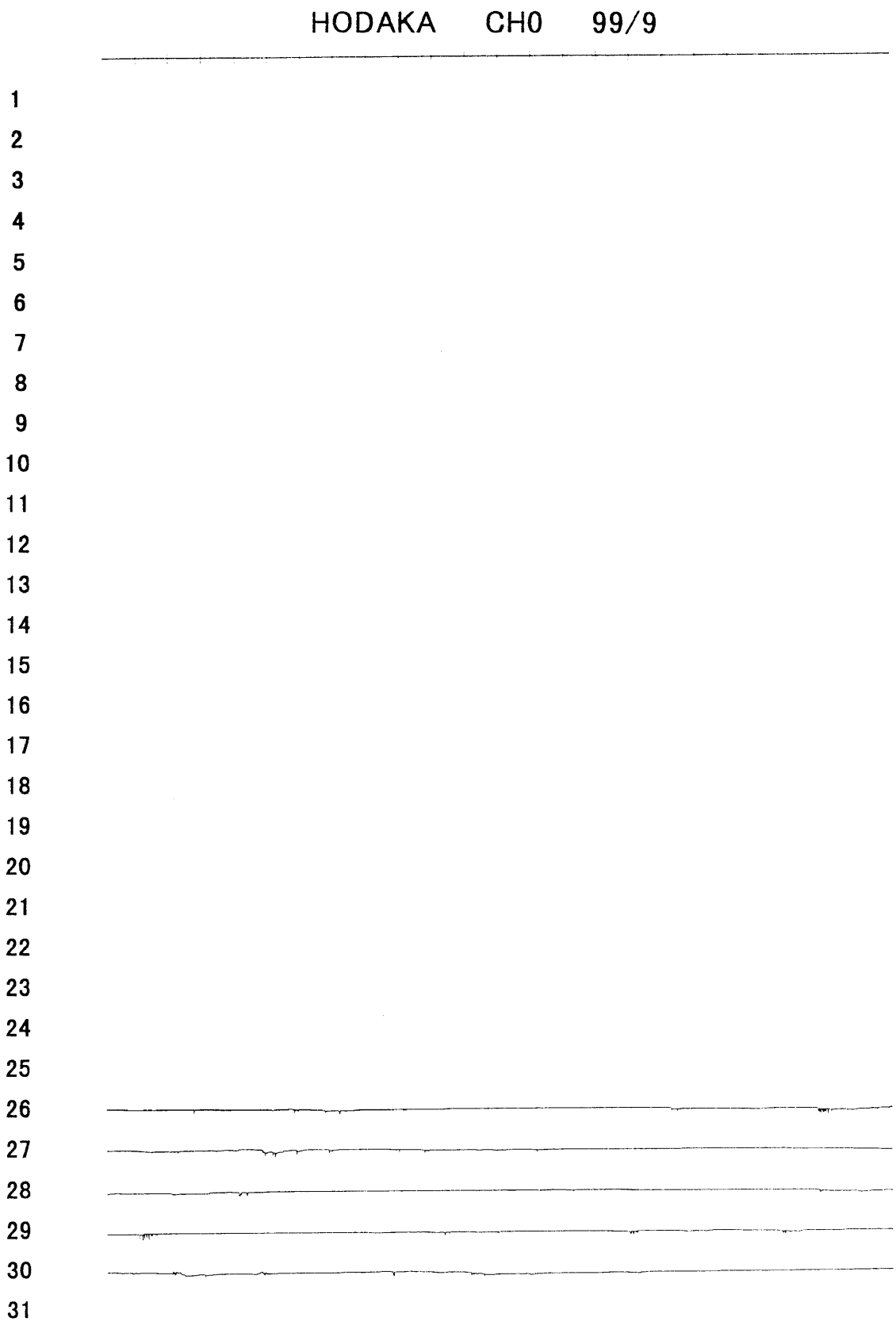
HODAKA CH0 99/9
1
2
3
4
5
6
7
8
9
10
11
12
13
14
15
16
17
18
19
20
21
22
23
24
25
26
27
28
29
30
31

Fig. A-99-9-0

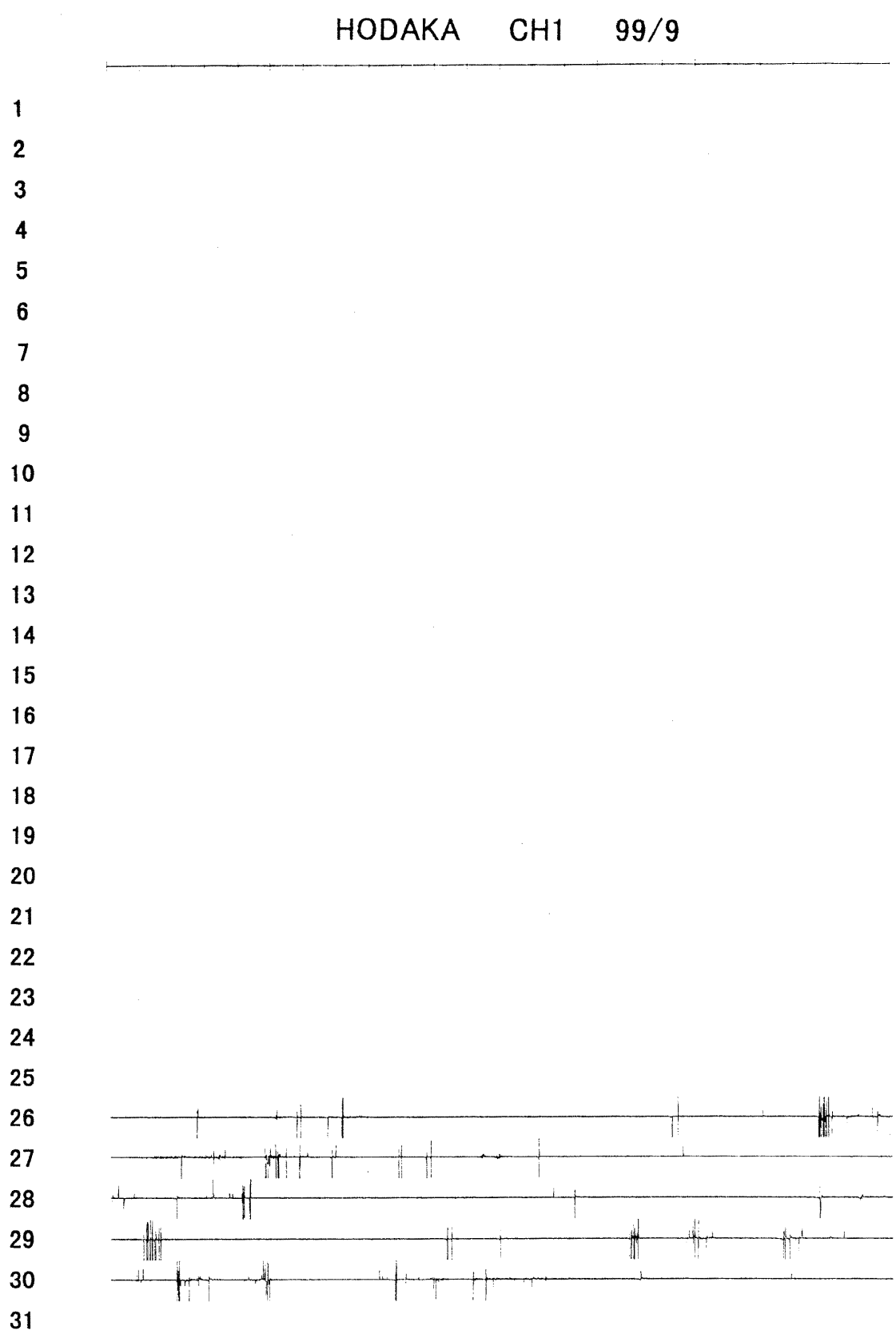
HODAKA CH1 99/9
1
2
3
4
5
6
7
8
9
10
11
12
13
14
15
16
17
18
19
20
21
22
23
24
25
26
27
28
29
30
31

Fig. A-99-9-1

HODAKA CH2 99/9

1
2
3
4
5
6
7
8
9
10
11
12
13
14
15
16
17
18
19
20
21
22
23
24
25
26
27
28
29
30
31

Fig. A-99-9-2

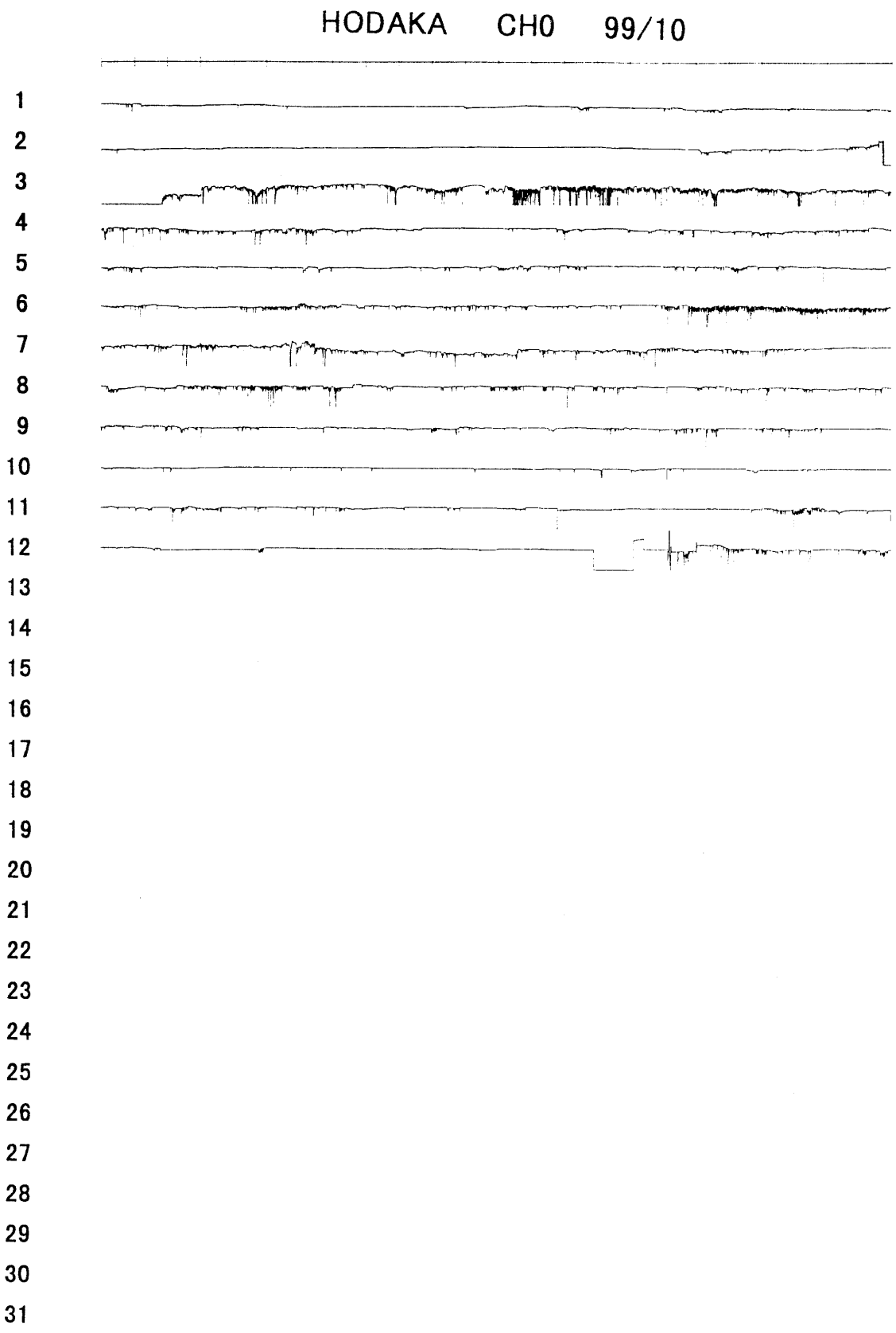
HODAKA CH0 99/10
1
2
3
4
5
6
7
8
9
10
11
12
13
14
15
16
17
18
19
20
21
22
23
24
25
26
27
28
29
30
31

Fig. A-99-10-0

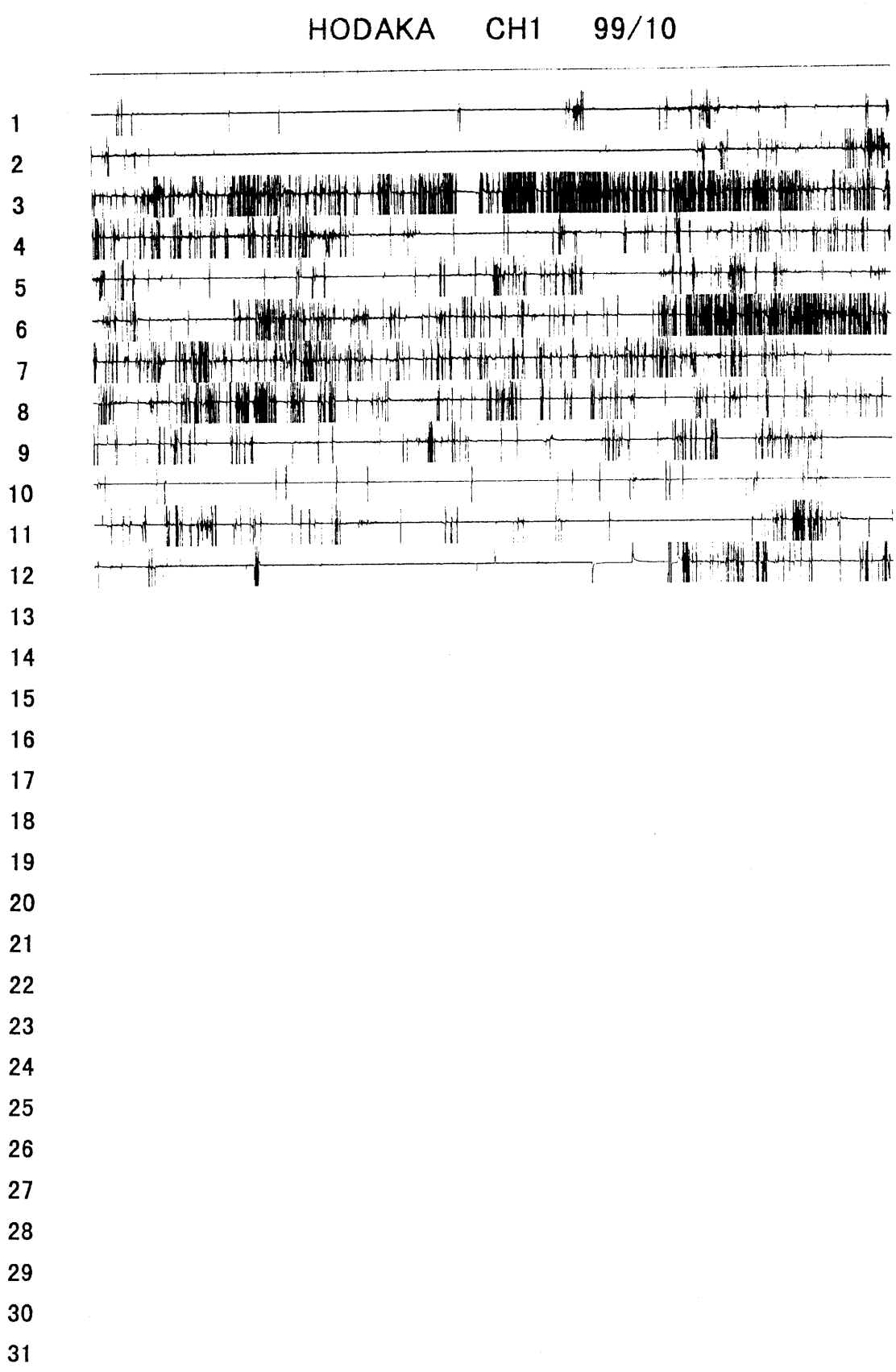
HODAKA CH1 99/10
1
2
3
4
5
6
7
8
9
10
11
12
13
14
15
16
17
18
19
20
21
22
23
24
25
26
27
28
29
30
31

Fig. A-99-10-1

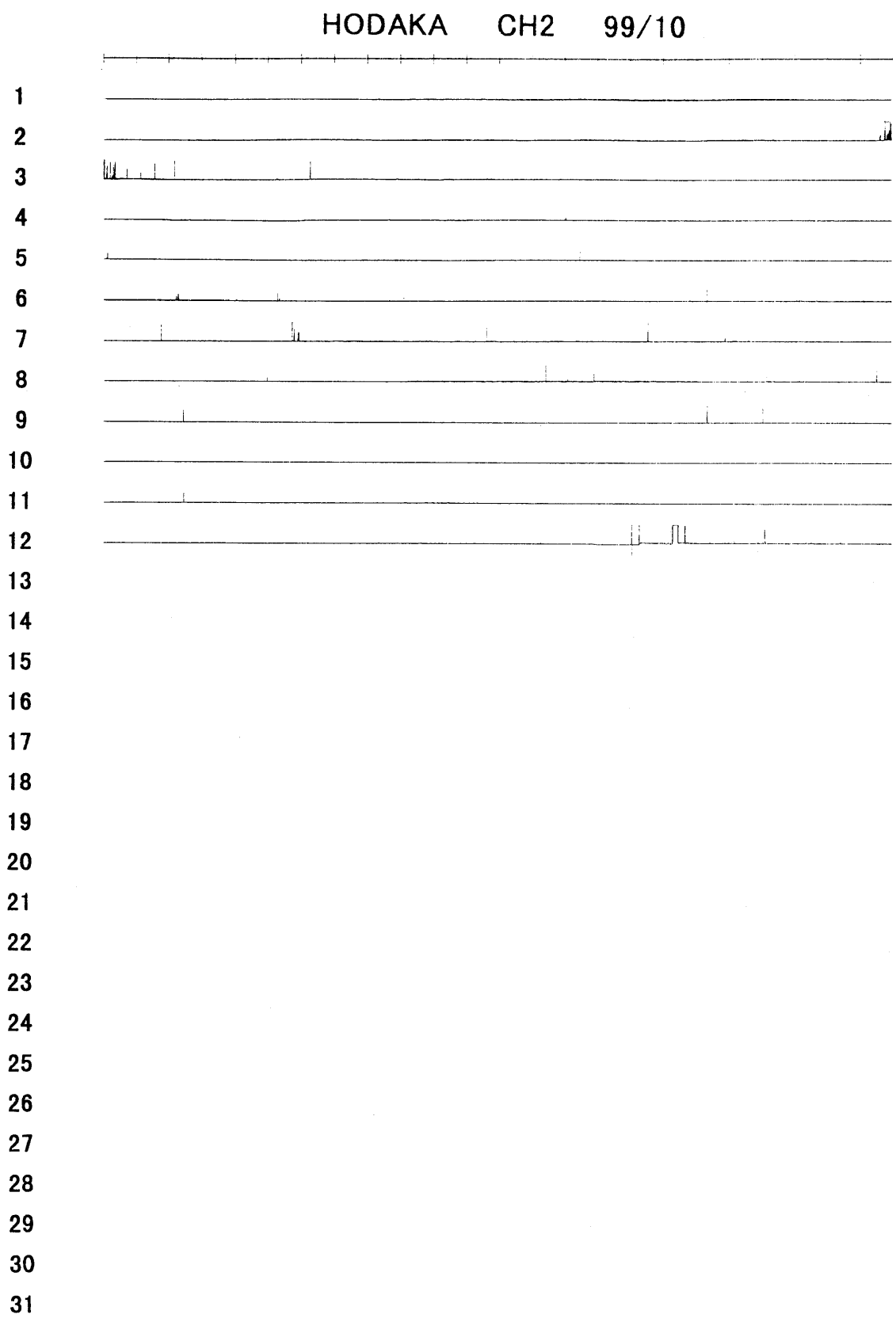
HODAKA CH2 99/10
1
2
3
4
5
6
7
8
9
10
11
12
13
14
15
16
17
18
19
20
21
22
23
24
25
26
27
28
29
30
31

Fig. A-99-10-2

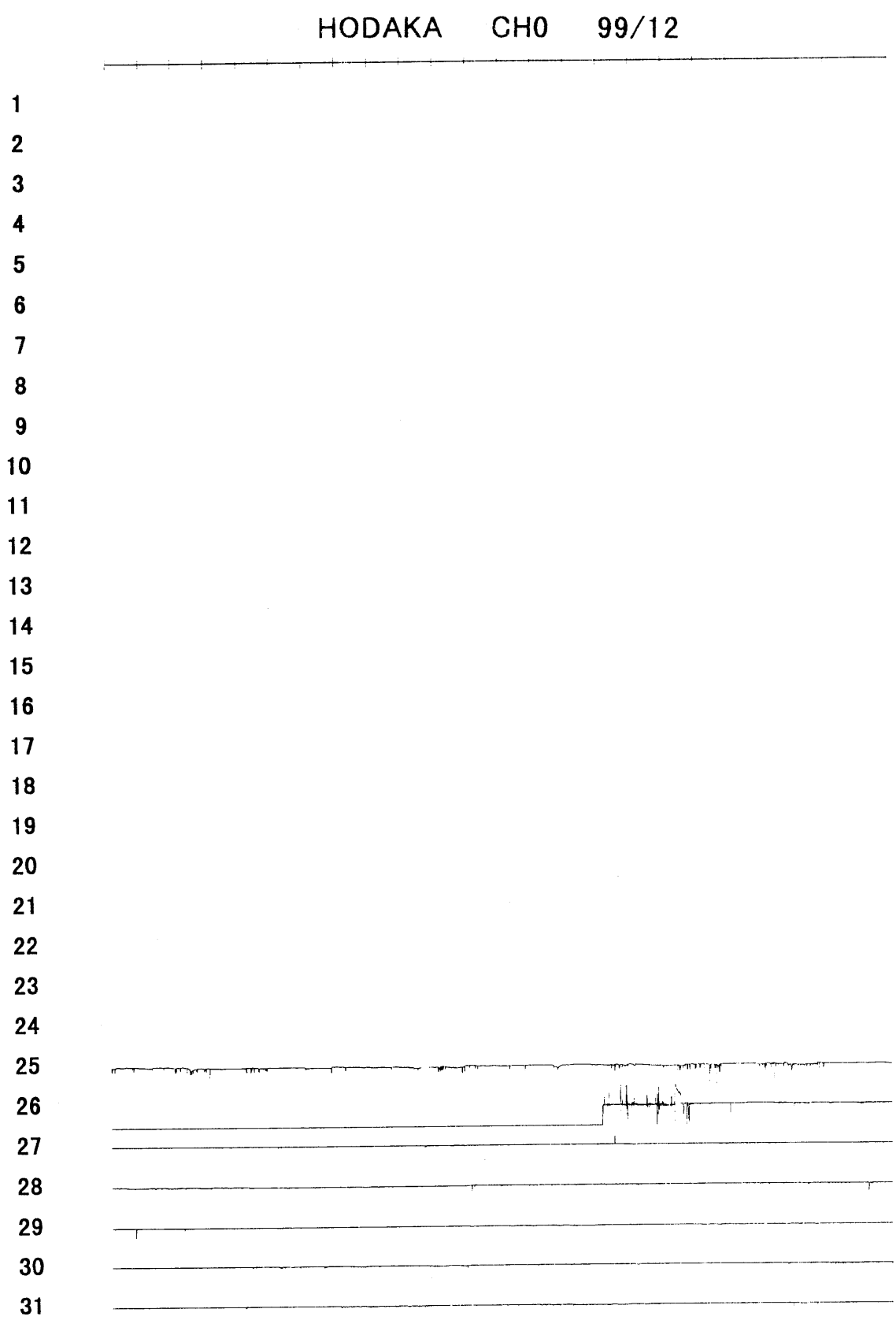
HODAKA CH0 99/12
1
2
3
4
5
6
7
8
9
10
11
12
13
14
15
16
17
18
19
20
21
22
23
24
25
26
27
28
29
30
31

Fig. A-99-12-0

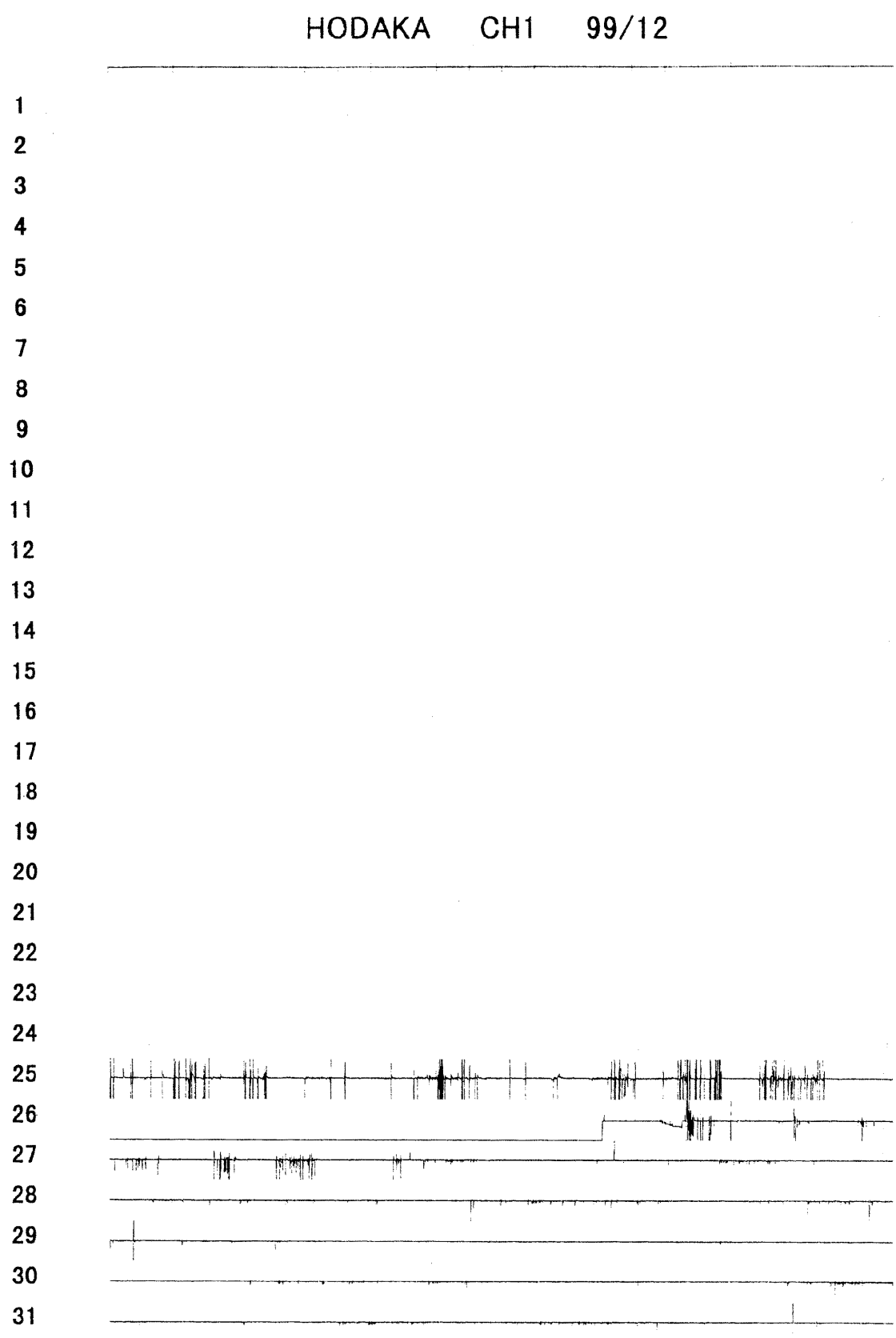
HODAKA CH1 99/12
1
2
3
4
5
6
7
8
9
10
11
12
13
14
15
16
17
18
19
20
21
22
23
24
25
26
27
28
29
30
31

Fig. A-99-12-1

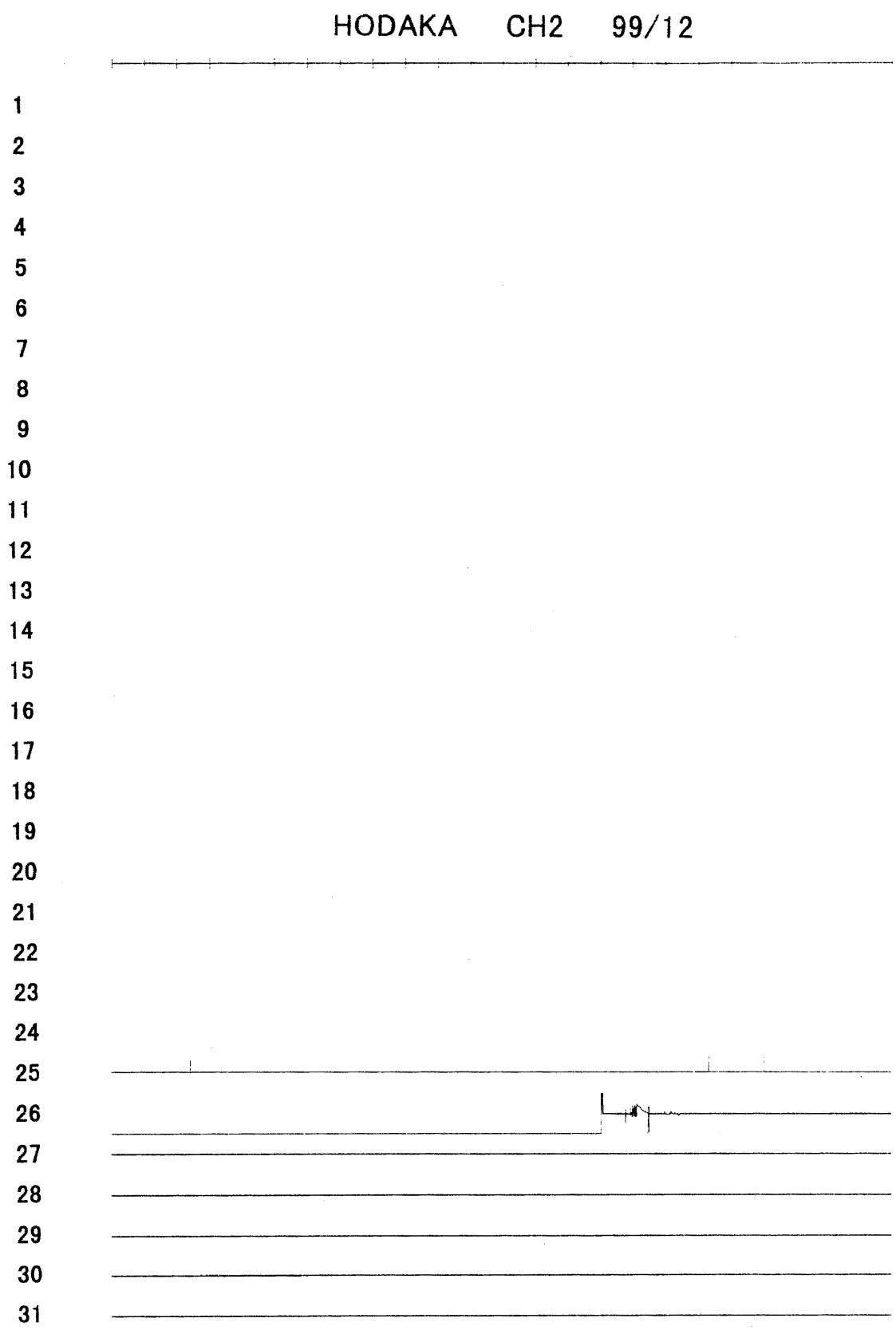
HODAKA CH2 99/12
1
2
3
4
5
6
7
8
9
10
11
12
13
14
15
16
17
18
19
20
21
22
23
24
25
26
27
28
29
30
31

Fig. A-99-12-2